Characterising the role of potential accessory factors that facilitate secretion and gene regulation of the EspC and AaaA autotransporters

---

Mohammad Shakib Alhagh, MSc

Clinical Microbiology

Submitted to the University of Nottingham for

The degree of Doctor of Philosophy

September 2020

Table of content

Declaration

I declare that I have prepared this thesis and not submitted, in whole or in part for the award any degree to the University of Nottingham or other learning research institutions. Except where stated otherwise by reference or acknowledgement, the work presented is entirely my own.

Mohammad Shakib Alhagh

September 2020

Acknowledgements

Firstly, I would like to express my sincerest thanks to my beloved supervisor, Dr Kim Hardie, for the continuous guidance, encouragement, advice, patience, motivation, and immense knowledge she has provided throughout my research project and academic journey. I truly honoured to have such a kind supervisor who cared so much about my higher education and learning novel research skills in Molecular and Clinical Microbiology. Her insight helped me in all the time of research and writing of this thesis. Her enthusiasm and love for teaching and research is contagious and always expected me to think independently about the experiments.

I would also like to take this opportunity to express my deepest gratitude to my co-supervisor Dr Christopher Penfold for all his endless support, kind inspiration during my PhD course.

Besides my supervisors, I would like to thank the rest of my thesis committee: Prof. Robert Layfield (Principal Internal Assessor) and Dr Nicholas Tucker (External Assessor) for their insightful comments and encouragement, but also for the hard question which helped me to widen my research from different perspectives. Special thanks go to my labmates Elena Jordana LIuch, James Brown for their kind advice and support during my laboratory induction sessions. My appreciation goes to all members of Department of Life sciences and Centre for Bimolecular science that kindly support me during this long journey.

My deepest appreciation to Prof. Dlewar Alaadeen, Prof.Miguel Camara, Dr. Karl Woldridge, Dr. Yadolah Zarezadeh, Dr.Jafar Soltani , Dr.shahla Afrasiabian, Dr.Bahram Nikkhoo and Dr.Hassan Rashidi for their kindest motivation and enlightening me the first glance of research.

Last but not the least; I would like to dedicate this thesis to my beloved family especially my mom, dad and lovely sister Sharmin for their moral, financial and spiritual supports during my PhD program. I love you all dearly. A bouquet of British flowers to my close friends and relatives in Sanandaj, Iran for supporting me through sunny and cloudy days of life. Hats off to Molecular Microbiology that widen my horizon into our unseen microbial world. Thank you all for making my life more meaningful.

Abstract

Entropathogenic *Escherichia coli* (EPEC) is one of the major causes of death from infantile diarrheal-related illness in children under 2 years old. EspC, is an Extracellular Serine Protease Autotransporter (AT) belonging to the Enterobacteriaceae (SPATE) superfamily that is highly immunogenic. It is secreted via the type Va classical secretion system which relies on a C-terminal transporter domain that forms a β-barrel in the outer membrane during translocation before being cleaved to release the functional protease (passenger domain). EspC can act as an Enterotoxin, Iron-binding protein and have a cytopathic effect on the host cells. The complete mechanism of EspC secretion, pathogenesis, interaction with the type III secretion system and the role of accessory factors is not completely known. In this study, to better understand the molecular pathway of EspC secretion, plasmids encoding full length native EspC, or EspC fused to mCherry in the presence or absence of the β-barrel transporter were inserted into putative AT secretion accessory factor mutants (Δ*proW*, Δ*slyB*, Δ*sapA*, Δ*ybgC*, Δ*yqjE* and Δ*abrB*). To investigate the resultant localization patterns, immunoblot analysis and fluorescent microscopy were performed. It appears that the β-barrel transporter domain plays an important role in the localization of the EspC secretion pattern since in its absence EspC-mCherry was diffusely distributed, rather than organised at the poles of the bacteria. Analysis of a mutant strain of MG1655 defective in SlyB (Δ*slyB*) showed clear morphological differences to the wild type strain. The Δ*slyB* mutant of MG1655 did not produce any detectable EspC-mCherry when attached to the β-barrel transporter and released more truncated EspC-mCherry compared to parental *E. coli* MG1655. To rule out any pleotropic effects, the Δ*slyB* mutant was genetically complemented by introducing engineered plasmids encoding either native SlyB, or a version of SlyB containing a His-tag. No significant difference was observed in terms of EspC stability and secretion between the mutated and complemented strains, casting doubt about a role of SlyB as an accessory factor in EspC secretion.*Pseudomonas aeruginosa* is an opportunistic pathogen, metabolically adaptable bacterium with diverse antibiotic resistance mechanisms that can cause hospital-associated infections in immunocompromised and cystic fibrosis (CF) patients. The PA0328 autotransporter was identified as a cell-surface tethered autotransporter with arginine-specific aminopeptidase activity and named: arginine-specific

autotransporter of *P. aeruginosa* (AaaA). Previous studies suggested the dynamic spiral localization of EspC during secretion is shared by the autotransporter AaaA. Here, the same investigative approach has been employed to track AT secretion using a fluorescent tagging technology that relies on a small tetracysteine motif (FlAsH) engineered into the AT rather than having a fusion of the AT to the larger mCherry fluorescent protein, to see if this affected the function of SlyB. To do this, immunoblot analysis and confocal microscopy were performed on the parental MG1655 and Δ*slyB* mutant strains producing either AaaA or EspC tagged with FlAsH. EspC and AaaA were identified as large 173 kDa and 80 kDa proteins respectively and were distributed in a similar pattern in both WT and Δ*slyB* MG1655 cells, irrespective of the presence of the β-barrel transporter for both AaaA and EspC.

To investigate the regulation of AaaA, a transcriptional reporter was used that incorporated the native promotor and compared it to one in which a potential regulatory motif was mutated. Analysis of a range of backgrounds containing these reporters revealed a complex network of regulation. The motif disrupted in the *aaaA* promotor had a negative effect on *aaaA* expression independent of RpoN. Observing bioluminescence from the reporters in PA14 Enhancer binding protein (EBP) mutant backgrounds revealed that compared to the parent strain background, P_{aaaA} driven expression was significantly decreased in many mutants when the motif was altered e.g. △*phhR* △*fleQ*, △*ntrC*, △*cbrB, ⊿acoR and* △*dctD.* However, this was not always reflected in reduced *AaaA* activity e.g. △*dctD* displayed more AaaA activity than the PA14 parental strain*.* Mutation of other EBP encoding genes did not alter P_{aaaA} driven expression e.g. *⊿gscR* and *⊿algB* mutants. Further studies using qRT-PCR and site-directed mutagenesis are required to decipher the detail of the regulatory network controlling *aaaA* function.

Whilst this study was not able to confirm the role of specific accessory factors in AT secretion, significant findings were a further uncovering of the complex nature of the regulation of one AT (*P. aeruginosa* AaaA), with specific confirmation of the role of RpoN and a defined subset of EBPs that include MvaT and MvaU.

Abbreviations

%	**percentage**
% (w/v)	**percentage weight per volume**
% (v/v)	**percentage volume per volume**
AT	**autotransporter**
AaaA	**arginine-specific autotransporter of P. aeruginosa**
aa	**amino acid**
ADC	**arginine decarboxylase pathway**
ADI	**arginine deiminase pathway**
APS	**ammonium persulphate**
ATP	**adenosine triphosphate**
ATPase	**adenosine triphosphatase**
Amp	**ampicillin**
ASM	**artificial sputum media (Palmer et al 2007)**
AST	**arginine succyl-transferase pathway**
A22	**S-(3,4-dichlorobenzyl) isothiourea**
AUC	**area under the curve**
BAM	**β-barrel-assembly machinery**
Bp	**base pair**
BAL	**British anti-Lewisite**
˚C	**degrees Celsius**
CCR	**carbon catabolite repression**
CF	**cystic fibrosis**
CFU	**colony forming unit**
c-di-GMP	**bis-(3',5') cyclic di guanylase**
Cm	**chloramphenicol**
CaCl2	**calcium chloride**
CL	**cardiolipin**
dNTP	**deoxynucleotide triphosphate**
DNA	**deoxyribonucleic acid**
Dnase	**deoxyribonuclease**
DTT	**dithiothreitol**

dH2O	**distilled water**
DsRed	**Discosoma sp. Red fluorescent protein**
dSTORM	**direct stochastic optical reconstruction microscopy**
DMSO	**dimethyl sulfoxide**
DAPI	**4',6-diamidino-2-phenylindole**
DIC	**differential interference contrast**
EBP	**Enhancer Binding Protein**
EDT	**1,2-ethanedithiol**
ECL	**enhanced chemiluminescence**
EDTA	**ethylenediaminetetraacetic acid**
EspC	**EPEC secreted protein C**
ESPR	**extended signal peptide region**
EPS	**extracellular polysaccharide**
FlAsH	**fluorescein arsenical hairpin binder**
FeSO4	**ferrous sulphate**
Fig.	**figure**
GTP	**guanosine triphosphate**
GTPase	**guanosine triphosphatase**
GFP	**green fluorescent protein**
G	**gram**
HRP	**horseradish peroxidase**
HEPES	**4-(2-hydroxyethyl)-1-piperazineethanesulfonic acid**
HCl	**hydrochloric acid**
H2O	**water**
Hep-2	**human epithelial cell line 2**
h	**hour**
IgA	**immunoglobulin A**
IgG	**immunoglobulin G**
IPTG	**isopropylthio-β-D-galacto-pyranoside**
IM	**inner membrane**
KH2PO4	**monopotassium phosphate**
Kb	**kilobase**
Km	**kanamycin**

kDa	**kilodalton**
L	**litre**
LPS	**lipopolysaccharides**
LB	**luria Bertani**
M	**molar**
mM	**millimolar**
µM	**micromolar**
µm	**micrometre**
mg	**milligram**
µg	**microgram**
ml	**millilitre**
µl	**microlitre**
min	**minute**
ms	**millisecond**
mA	**milliampere**
MMP	**minimal medium P**
MgSO4	**magnesium sulphate**
MeOH	**methanol**
Nm	**nanometre**
Ng	**nanogram**
NaCl	**sodium chloride**
Na2HPO4	**disodium phosphate**
O/N	**overnight**
OD	**optical density**
OMP	**outer membrane protein**
OM	**outer membrane**
ORF	**open reading frame**
PAI	**pathogenicity island**
PBS	**phosphate buffered saline**
PBST	**phosphate buffered saline 0.5% (v/v) Tween-20**
PCR	**polymerase chain reaction**
POTRA	**polypeptide transport-associated**
PQS	**Pseudomonas quinolones signal**

PIA	**Pseudomonas isolation agar**
QMC	**Queen's Medical Centre**
QS	**quorum sensing**
RLU	**relative luminescence units**
RT	**room temperature**
ReAsH	**resorufin arsenical hairpin binder**
Rpm	**revolutions per minute**
RNA	**ribonucleic acid**
RNase	**ribonuclease**
S/N	**supernatant**
SDS	**sodium dodecyl sulphate**
SDS-PAGE	**sodium dodecyl sulphate polyacrylamide gel electrophoresis**
SR-SIM	**super resolution- structured illumination microscopy**
SIM	**structured illumination microscopy**
SDM	**site-directed mutagenesis**
SOC	**super optimal broth with catabolite repression**
SPATE	**serine protease AT of Enterobacteriaceae**
SRP	**signal recognition particle**
Str	**streptomycin**
TC	**tetracysteine motif**
Tc	**tetracycline**
tRNA	**transfer RNA**
TAE	**tris-acetate-EDTA**
TCA	**trichloroacetic acid**
TEMED	**tetramethylethylenediamine**
Tris	**tris hydroxymethyl aminomethane**
TAM	**translocation and assembly module**
TPase	**transpeptidae**
T1SS	**type 1 secretion system**
T2SS	**type 2 secretion system**
T3SS	**type 3 secretion system**
T4SS	**type 4 secretion system**

T5SS	**type 5 secretion system**
T6SS	**type 6 secretion system**
T7SS	**type 7 secretion system**
T8SS	**type 8 secretion system**
T9SS	**type 9 secretion system**
UV	**ultraviolet**
UAA	**unnatural amino acid**
V	**volts**
WC or wc	**whole cell**
WT or wt	**wild type**

Chapter 1

1. Introduction

1.1 Secretion systems overview

Successful bacterial pathogens manipulate and actively interact with their host. One of the main mechanisms that enable bacterial effective host-pathogen interaction involves Specialised extracellular proteins with different biological functions that include enabling motility, signalling, toxicity and alteration of host cell molecular machineries for the advantage of the invader(1,2). Bacteria have evolved diverse and highly sophisticated macromolecular nanomachines that secrete different substrates to undertake these roles that go beyond proteins to include DNA and small molecules. These substrates are essential for bacteria to respond to their surrounding environment and highly valued as key survival physiological mechanisms. Dependent on the type of secretion system, the bacterial excreted substrates may have any of three possible destinations beyond the cytoplasm where they are synthesized: an intracellular compartment, the cell surface or the external milieu. Another possible fate is the injection of substrates into target prokaryotic or eukaryotic cells(1,3,4).

The remainder of this introduction will focus on proteins produced by Gram negative bacteria which have two membranes within the cell envelope. An inner membrane (IM) that surrounds the cytoplasm, and an outer membrane (OM). Between these is the periplasmic space (Figure 1.1). The most relevant system to this study is the type V secretion system (T5SS), and the others are outlined to provide the context of its current characterization.

1.2 Secretion across the inner cytoplasmic membrane of Gram-negative bacteria

Two translocation machines have been identified for protein translocation from the bacterial cytoplasm into or across the IM: the secretion (Sec) and the twin arginine translocation (Tat) pathways. These two pathways are evolutionarily conserved, and recognized in different domains of life (bacteria, archaea, and eukarya). Most proteins transported by the Sec and Tat pathways will stay within the IM or reside in the bacterial periplasm with a minority of proteins being moved further into the OM or the extracellular space facilitated by other

secretion systems. Sec and Tat pathways have different structures, mechanisms of action and translocate a distinct set of proteins (2,3,5–7).

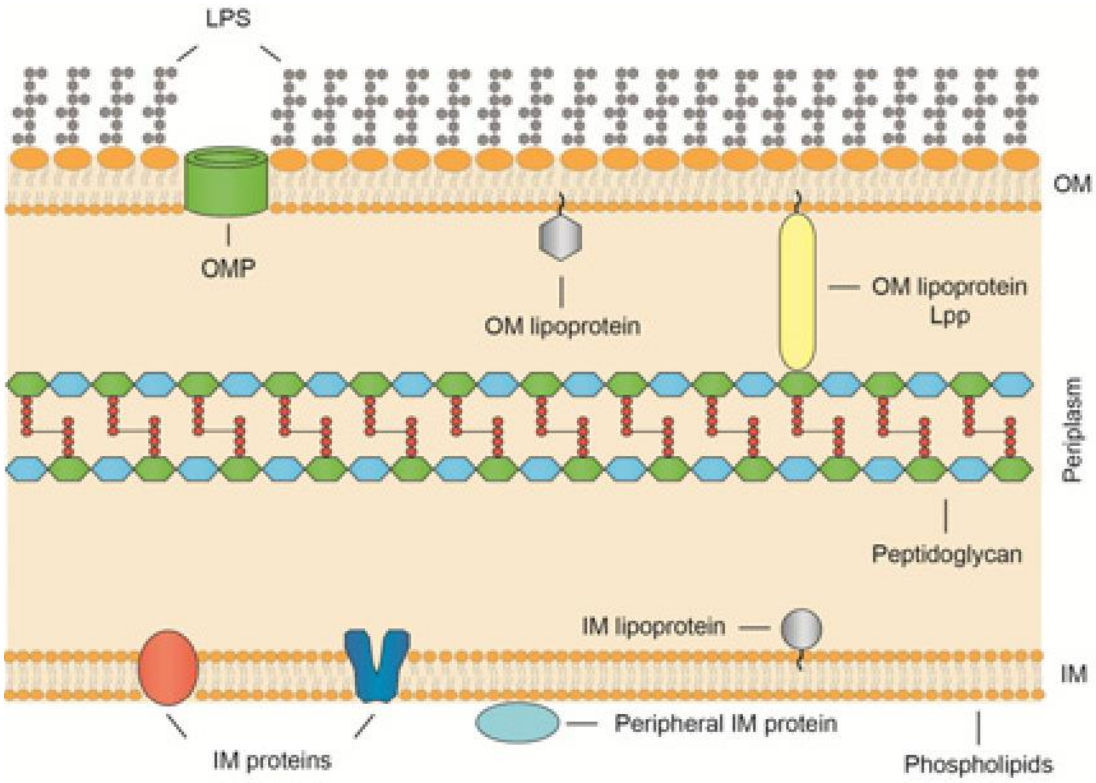

Figure 1.1: The cell envelope of Gram-negative bacteria. The Gram-negative cell envelope is composed of an OM that provides a barrier to the extracellular environment, a periplasmic space which includes a thin layer of peptidoglycan and an IM that divided the periplasmic space from the cytosol. The OM involves lipopolysaccharides (LPS) and different outer membrane proteins (OMPs), which have a unique -barrel structure. The IM consist of integral membrane proteins as well as peripherally attached membrane proteins (8).

1.2.1 The Sec Secretion Pathway

The Sec pathway is mainly responsible for translocation of unfolded proteins (2). Successful translocation by Sec requires a hydrophobic signal sequence at the N-terminus region of the targeted secreted protein that is usually composed of 20 amino acids and possesses segments including a positively charged amino terminal, a hydrophobic centre and polar carboxyl terminal (6). Based on the targeted protein's fate, signal sequences differ (6). For instance, in many Gram-negative bacteria, proteins that are destined for the periplasm or extracellular space have SecB-specific signal sequences (9). SecB acts like a chaperone,

attaching to pre-secretory proteins and inhibiting protein folding(9). Substrates are then delivered from SecB to the multifunctional protein SecA. The SecA ATPase powers translocation through the SecYEG channel (10). Before substrate translocation, a protease cuts off the signal sequence and the secreted protein is folded in the periplasm from where it may be translocated to the extracellular space by the Type II or Type V secretion systems(2,11).

Inner membrane proteins contain another form of Sec-dependent signal sequence that is recognized by the signal recognition particle (SRP)(2). Such substrate proteins usually have hydrophobic domains and are not fully stable in the cytoplasmic environment(2). SRP-dependent preproteins translocate through the membrane co-translationally directly from the ribosome attached state(3,12). SRP particles are composed of 4.5S RNA attached to a protein called Ffh(12). At first, SRP releases from ribosome and binds the transmembrane domain of proteins(13). SRP then attaches to the docking protein FtsY, which facilitates delivery of the ribosome-protein complex to the SecYEG translocation channel(6). Translation of the target protein will provide driving force and energy requirement of developing protein through the channel(2,14). Finally, the transmembrane domain of the protein will pass through the channel and remain attached to the IM (Figure 1.2)(14).

1.2.2 The Twin-Arginine translocation (Tat) Pathway

The Tat secretion pathway is another inner membrane protein translocation system in bacteria and Archaea (Figure 1.3). Tat is mainly responsible for export of proteins in their complete folded conformation (7). This secretion pathway is important because some proteins undergo post-translational modification in the cytoplasm(2). These modification elements such as redox factors are not available in the periplasm and extracellular space and therefore, the folding process and modification need to occur in the cytoplasm before translocation(15).

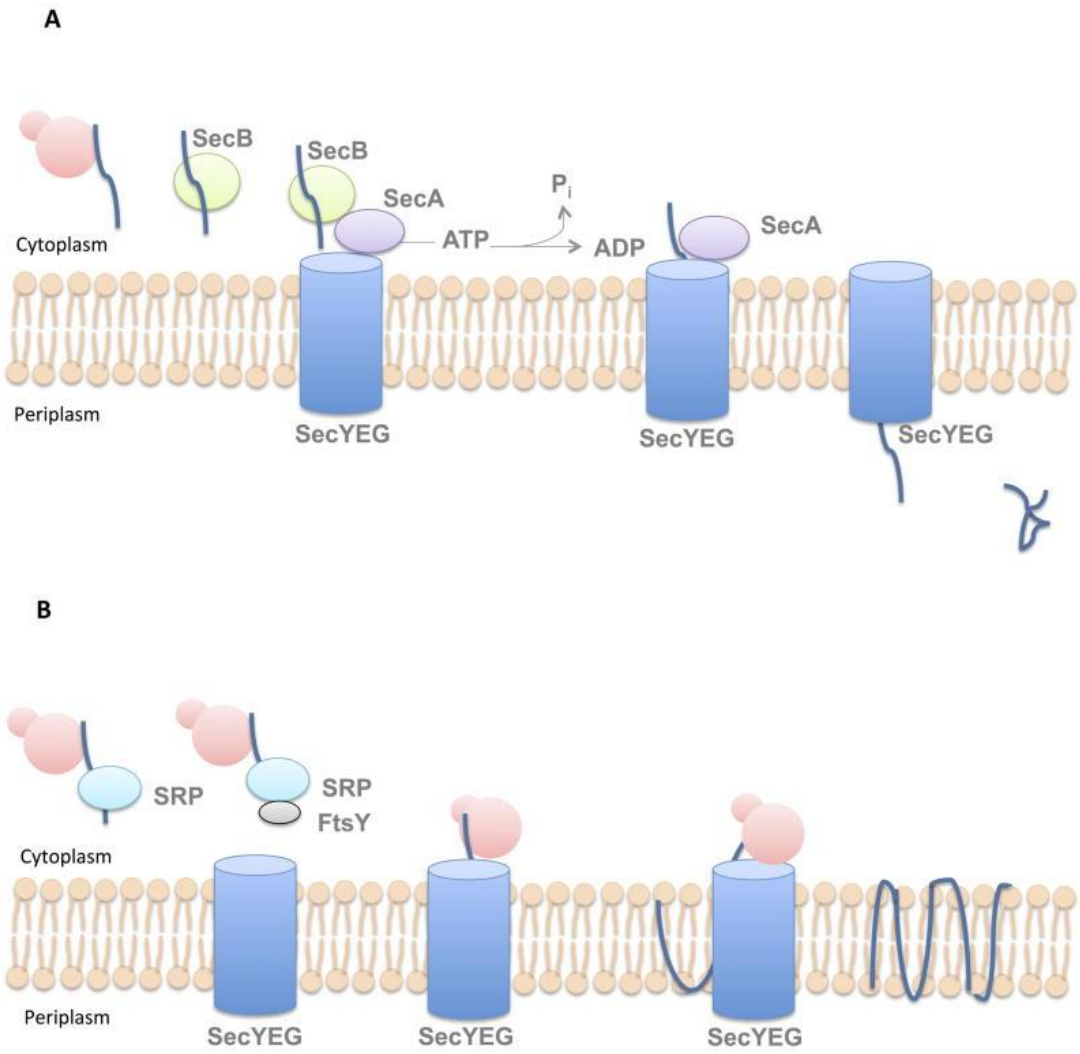

Figure 1.2: Overview of inner membrane Sec pathways secretion systems. (2). In bacteria, the Sec pathway transports unfolded proteins across the cytoplasmic membrane with two different specific SecB (A) and SRP (B) signal sequences based on target protein destination. In bacteria, the Sec pathway translocates unfolded proteins across the cytoplasmic membrane. Proteins secreted by this pathway may either become embedded in the inner membrane or will be released into the periplasm. In Gram-negative organisms, these periplasmic proteins may be released extracellularly with the help of another secretion system. (A) Proteins destined for the periplasm (or extracellular release) are translocated by a posttranslational mechanism and contain a removable signal sequence recognized by the SecB protein. SecB binds presecretory proteins and inhibits folding while also delivering its substrates to SecA. SecA both leads proteins to the SecYEG channel and act as the ATPase that provides the energy source for protein translocation. Following transport through the SecYEG channel, proteins are folded in the periplasm. (B) The Sec

pathway utilizes a cotranslational mechanism of export to secrete proteins destined for the inner membrane. These proteins include a signal sequence identified by the signal recognition particle (SRP). During translation, the SRP binds target proteins as they release from the ribosome and attracts the docking protein FtsY. FtsY delivers the ribosome-protein complex to the SecYEG channel, which translocates the nascent protein across the cytoplasmic membrane. During translocation across the channel, the transmembrane domain can escape through the side of the channel into the membrane, where the protein remains attached.

The Tat translocation pathway is composed of 2 or 3 subunits TatA, TatB, and TatC combined in a multi-functional protein structure(16,17). In Gram-positive bacteria, TatA and TatB form the complex while in *E. coli*; TatB and TatC first attach to the specific signal peptide of Tat-targeted proteins, and then bind to another subunit TatA that ultimately forms the membrane channel complex(18). The specific Tat signal sequence has a unique pair of "twin" arginines in the motif S-R-R at the N-terminus of the target folded protein(18). The destination of most proteins translocated by the Tat secretion pathway in Gram-positive bacteria is the extracellular space, while in Gram-negative bacteria substrates can either remain in the periplasmic space or be translocated outside of the cell facilitated by the Type II Secretion System(2). In pathogenic bacteria such as *Pseudomonas aeruginosa*, *Yersinia pseudotuberculosis* and *E. coli* O157:H7, the Tat secretion pathway is essential for full clinical manifestation in animal infection models(19–21). For instance, Phospholipase C is a typical example of Tat-secreted protein virulence factor that helps bacteria evade the immune system and promotes intracellular competency(19,22,23). Phospholipase C is a protease that hydrolyses phospholipids in host cells. Phospholipase C is produced by pathogenic bacteria such as *P. aeruginosa*, *Legionella pneumophila* and *Mycobacterium tuberculosis*(24).

E. coli produces different Tat-targeted proteins that their main function identified as cofactor with enzymatic activity(25). The trimethylamine Noxide (TMAO) reductase (TorA) is found in *E. coli* classified as Tat-targeted enzyme that binds bis-molybdopterin guanine dinucleotide (MGD) as its single cofactor(25). (TorA) as Tat signal peptide can facilitate protein export and act as a binding site for the TorD biosynthetic chaperone(25). TorD involves in cofactor loading, Tat proofreading function and inhibits premature targeting of TorA(25).

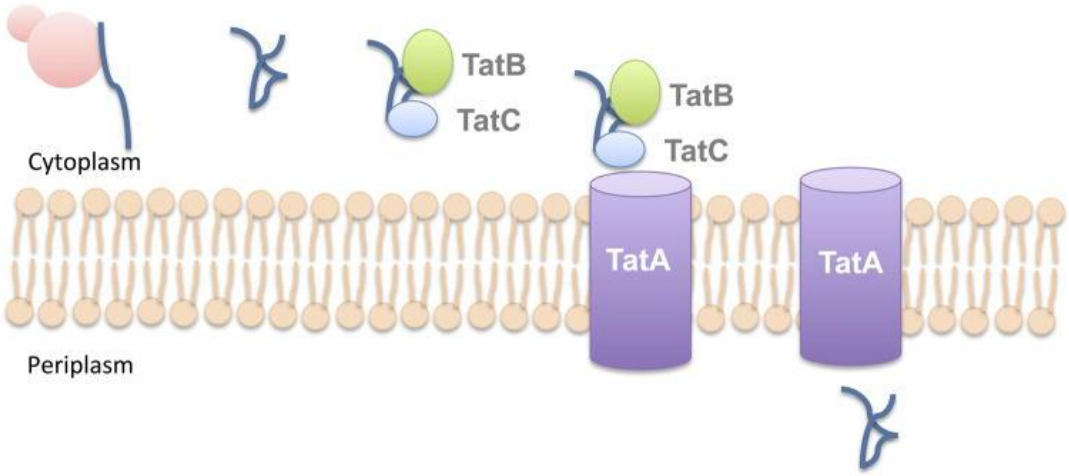

Figure 1.3: Overview of inner membrane Tat pathways secretion systems. This pathway is composed of 2–3 subunits (TatA, TatB, and TatC). In Gram-positive bacteria, TatB and TatC bind a specific N-terminal signal peptide including a "twin" arginine motif on folded Tat secretion substrates. TatB and TatC then attract TatA to the cytoplasmic membrane, where it forms a multifunctional channel. Secretion of Folded proteins across the channel follows. In Gram-negative bacteria, these proteins may stay in the periplasm, or can be exported out of the cell by the T2SS(2).

1.3 Protein secretion systems beyond the IM of Gram-negative bacteria

Some Gram-negative bacteria have Sec- or Tat dependent two-step pathways or independent one step protein secretion pathways. In Sec- or Tat dependent secretion pathways, proteins are first translocated to the periplasm by the Sec or Tat secretion systems as described in previous sections, and then delivered to extracellular environment or injected into host target cells through a second translocation system.

In Sec- or Tat independent secretion pathways, target proteins are translocated by specific channels that stretched across both the inner and outer bacterial membranes of bacteria. The specialized secretion systems in Gram-negative bacteria are numbered Type I through Type VI, and each one of these systems secretes a specific subset of proteins(2,3,26,27). These secretion systems are different from each other in their complexity, structural design and mechanism of secretion (Figure 1.4)(28–31).

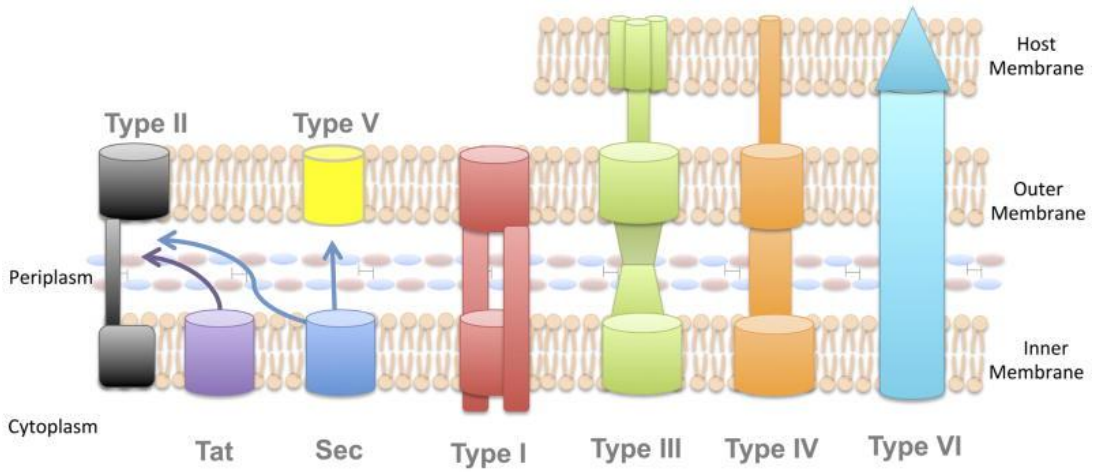

Figure 1.4: Overview of Secretion systems in Gram-negative bacteria. (2) Virulence proteins in Gram-negative bacteria pass through different layers of phospholipid membranes facilitated by specific protein translocation pathways. Some virulence proteins are released by a two-step, Sec- or Tat-dependent mechanism. These proteins cross the inner membrane with the help of either the Sec or Tat translocation pathways and are then secreted across the outer membrane using a second secretion system. The T2SSs and T5SSs secrete proteins in these conditions. For Folded substrates, successful translocation though inner membrane and into the periplasm will occur first, and then the target protein will be delivered to the T2SS. By contrast, autotransporters of the T5SS must be in unfolded state before outer membrane translocation will happen and therefore substrates first translocated across the inner membrane by the Sec pathway. Moreover, several Gram-negative protein secretion systems transport their substrates across both bacterial membranes in a one-step, Sec- or Tat-independent process. These are composed of the T1SSs, T3SSs, T4SSs, and T6SSs. All these pathways include periplasm-spanning channels and translocate proteins from the cytoplasm to the outside the cell, although, their protein secretion pathways are different. Three of these secretion systems, the T3SS, T4SS, and T6SS can also secrete proteins across an additional host cell membrane, delivering translocated target proteins directly to the cytosol of a host cell. Also present, but not shown are: The extracellular nucleation-precipitation (ENP) pathway or Type VIII secretion system (T8SS) is found in Gram-negative *Enterobacteriaceae* mainly among *Salmonella spp* for the secretion and aggregation of prepilins for fimbiae biosynthesis including the prototypical amyloid fibers (curli) that play an important role in biofilm. The T8SS, found in the outer membrane includes three protein components that help curli fibers aggregation in the extracellular space(32). In addition, the newly

identified type IX secretion system (T9SS) is a complex translocon found only in some species of the Bacteroidetes phylum. This secretion system plays an important role in gliding motility for commensal microorganism and can also act as a virulence factor across the outer membrane (OM) in pathogenic bacteria. In recent studies, major essential genes of this secretion system were identified(33).

1.3.1 The Type I Secretion System

Type I secretion systems (T1SSs) have been identified in diverse group of Gram-negative bacteria that cause infections in animals and plants(2,34). The main features of this secretion pathway are the one-step translocation process and incorporate a large assembly of proteins incorporating ATP-binding cassette (ABC) transporters. T1SSs translocate antibiotics and toxins to the extracellular environment(35). To do so, this secretion system stretches from the inner to outer membrane(2). Some bacteria may possess multiple T1SSs, each of one of them allocated for translocation of one or a few unfolded substrates(36). In terms of function, these substrates have different roles such as proteases and lipases(2). In addition, adhesins, heme-binding proteins, and proteins with repeats-in-toxin (RTX) motifs are translocated by this secretion pathway(2,34). T1SS substrates are typically Sec-independent and usually have an uncleaved C-terminal signal sequence (2,34)

T1SSs have three main structural elements: an ABC transporter protein in the inner membrane, a membrane fusion protein (MFP) that passes through the inner membrane and creates a channel to the outer membrane factor (OMF) (34). The ABC transporter hydrolyses ATP to obtain the energy for substrate translocation, MFP interaction and substrate identification(37). The N-terminus of the MFP is located in cytoplasm and plays an important role in substrate selection(38,39) After substrate selection, OMF creates a pore in the outer membrane that facilitates unfolded state substrate translocation(36). In T1SSs, the multifunctional protein TolC is usually used instead of OMF, and is not only involved in pore formation but also in helping substrate translocation (2,36,39)

1.3.2 The Type II Secretion System

Type II secretion systems (T2SSs) are identified and reported in most of Gram-negative bacteria. This secretion system is composed of a channel located in

outer membrane and their primary role is translocation of folded proteins from the periplasm to the outer milieu after successful secretion of substrate protein by Sec or Tat translocation pathways as described in previous sections(40,41). Type II secretion system substrates must contain a Sec- or Tat-type separable specific signal sequence at their N termini region and are in a periplasmic folded state before translocation through the outer membrane channel(2,40).Diversity and specificity among substrate proteins translocated by Type II secretion system to extracellular environment have been recognized(2,40). In some groups of bacteria, T2SS is essential for the translocation of different substrates, while for others, it is only required for single protein export(42). Proteases, lipases, and phosphatases are among the most important biological enzymes that are secreted by this system (2,40).

T2SSs are composed of 15 different proteins, which can classified into 4 sub-functional units including the outer-membrane complex, the inner-membrane platform, the secretion ATPase, and the pseudopilus(40). As the name implies, the outer-membrane complex situated in the outer membrane, where it acts as the channel gate through which folded periplasmic T2SS substrates are secreted(43). This channel consists of a multimeric protein called the secretin. The secretin has an extended N- terminal region in its structure that stretches the whole periplasm and connects with different T2SS proteins in the inner membrane(43). The inner membrane platform, which is comprised of different copies of at least 4 proteins, is situated in the inner membrane and reaches into the periplasm(40). This platform plays an important role in the translocation process, by connecting with the secretin, pseudopilus, and the ATPase to regulate and manage substrate secretion(40). The ATPase unit provides the energy of the system and is situated in the cytoplasm(2). In terms of evolution and structure, the T2SS pseudopilus bears anatomical resemblance to proteins that shape type IV pili on bacterial cell surfaces(44). The piston secretion model suggests that these pseudopili pull back in order to facilitate T2SS folded substrate translocation through the outer membrane channel(40,45,46). To do so, "secretion-competent" proteins in the periplasm first join the periplasmic domain of the secretin that ultimately trigger the cytoplasmic ATPase to initiate retraction of the T2SS pseudopili that gives the substrate energy and mobility to pass through the secretin channel(2).

Different pathogenic bacteria utilize T2SSs for their virulence factor transport to extracellular environment(2). Common examples of virulence protein substrates are toxins such as cholera toxin of *V. cholera* that causes watery diarrhea and exotoxin A of *P. aeruginosa* that inhibits protein synthesis in host cells(47,48). Other pathogenic bacteria like *Legionella pneumophila, enterotoxigenic and enterohemorrhagic E. coli (ETEC and EHEC), K. pneumonia, Aeromonas hydrophila and Dickeya dadantii* translocate vital enzymes for environmental adaptability with their host cells and enhance evolution competency(49–55).

1.3.3 The Type III Secretion System

Type III secretion systems (T3SSs) also known as injectisomes are an export mechanism found in diverse groups of Gram-negative bacterial pathogens to secrete target virulence substrates (effector proteins) directly into the eukaryotic host cell. The T3SS substrates pass through inner and outer bacterial membrane in one step process in order to evade the immune system(2,3). In pathogens such as *Pseudomonas* and *Yersinia* only a handful of effector proteins are translocated by this needle and syringe like complex, while in other bacteria like *Shigella* and EHEC many different substrates are secreted in this manner(2). N-termini region of T3SS substrates contain inseparable Secretion signals(2). Some of the effector proteins are equipped with specific chaperones that lead the substrate toward the T3SS base segment for translocation in an unfolded state and ATP-dependent manner(2). Type 3 secretion systems (T3SSs) are a key integral part of two sophisticated bacterial machineries: the flagellum, which facilitate cell motility, and the non-flagellar T3SS (NF-T3SS), which translocates effectors into eukaryotic cells(56). Phylogenomic and comparative analyses suggested that flagellum was primordial and first evolved to transport extracellular flagellar components. Variants of the flagellar T3SS have also been identified that transport virulence factors in *Campylobacter jejuni* and *Y. enterocolitica*(56). The NF-T3SS protein delivery function arose from part of flagellum structure(56).

The T3SS is composed of 9 conserved core proteins and around 20 essential functional proteins(57,58). The structural elements of this secretion system are commonly encoded in operons located in pathogenicity islands of the bacterial chromosome or on plasmids and bacteria obtain T3SS through horizontal gene transfer(2,59). The secretion pathway found in *Shigella* is very similar to its evolutionary distinct species *Salmonella* and different to *E. coli* pathotypes EHEC

and EPEC(59–61). The T3SS can be classified into three main elements: base complex or basal body, the needle component, and the translocon(57,62). The base complex contains 15 proteins in cytoplasmic compartments or stretched through the entire inner and outer membrane with different central rod rings(62,63). The needle section is a filamentous structure with a wide hollow inside the core that spans through the secretin into the extracellular environment. T3SSs translocate unfolded effector substrates(57,58,63). The T3SS tip complex is situated at the top of the needle, and is essential for host sensing, interaction and effector substrate regulation(64,65). Moreover, it is vital for injection of the translocon into host cell membranes(65,66). The T3SS translocon acts as a bridge and forms a pore structure between effector proteins and host cell membrane(66–68). The Translocon is assembled after the T3SS apparatus binds to host cells(66). A two-step secretion model is also proposed for the T3SS by which effector substrates and translocon elements are first secreted and remain in structures like lipid vesicles before host cell attachment(69). After host cell connection, the needle may facilitate pore formation by sensing the translocon and tip proteins that ultimately release the effector proteins(70).

T3SS effectors share similar strategies to target host cell functions and key cellular pathways(71). During infection, these effectors may also cause antagonistic effects on regulatory pathways(71). These diverse strategies include targeting of the host cell cytoskeleton in *Shigella* and *Salmonella*(71). Another strategy is targeting of host cell trafficking pathways to regulate host cell surface receptors, immunomodulatory molecules, and bacterial persistence in *Shigella*, *Salmonella*, and EPEC/EHEC(71). Disruption of epithelium integrity can be caused by T3SS effectors targeting the cytoskeleton and host cell trafficking(71). In addition, T3SS-expressing enterobacteria can target host cell death/survival pathways and modulate critical NF-$_K$B and MAPK signaling cascades to regulate host inflammatory signals(71).

1.3.4 The Type IV Secretion System

Type IV secretion systems (T4SSs) in terms of evolution and structure is very similar to the bacterial DNA conjugation systems (2,72). This secretion pathway is mainly found in Gram-negative bacteria and can translocate a diverse group of substrates such as single proteins, protein-protein and DNA-protein complexes through inner and outer membranes and inject them into another bacterial or

eukaryotic cells(72). Like T3SSs, this secretion system can also stretch into host cell membranes, enabling secretion of substrates into target cells(2).

One example T4SS multiprotein complex is the VirB/D system of *Agrobacterium tumefaciens* that translocate oncogenic T-DNA into plant cells(73).This secretion pathway is composed of 12 proteins, entitled VirB1-VirB11 and VirD4(74). Most of these protein subunits are embedded in membrane and actively interact with each other(74). The VirB6-10 proteins span from inner to outer membranes and create translocation channel(74). VirB4, VirB11, and VirD4 are found in the inner base membrane and provide the energy requirement by ATP hydrolysis (75). VirD4 also acts as a chaperone protein, binding substrates before translocation through the channel(74,75). Major VirB2 and minor VirB5 subunits form the extracellular pilus (74). The role of the T4SS pilus in the secretion process is still unknown. It seems like that the pilus is vital for bacterial host attachment or acts as a channel for protein secretion(74,76).

1.3.5 The Type VI Secretion System

Type VI secretion systems (T6SSs) are conserved in most of Gram-negative bacteria to translocate effector proteins into prokaryotic (contact dependent manner) and eukaryotic cells(77,78). Our understanding about structure and function of this secretion system is still limited and it seems like this pathway is designed for bacterial cell-to-cell communication and adaptive interaction with their surrounding environment(2,78,79), or competing with rival bacteria for environmental host colonization(79–81).

In terms of structure, T6SSs are complex and comprise a large apparatus composed of 21 proteins that include 13 structural conserved proteins which resembles Phage tails(78). One study suggested that T6SSs might be derived from inverted phage tails that secrete target effector proteins outside of the bacterial cell(81). In addition to identified T6SS effector proteins, it has been suggested that some structural compartments of the T6SS complex may also act as effector proteins. These effectors have many different shapes and diverse functions. Most of them involved against the bacterial cell wall and membrane, which contributes a role for this secretion apparatus in enhancing interspecies bacterial competition (78,79). The T6SS effector proteins are encoded near a gene that confers immunity and protection to the producing bacterium, therefore preventing self-destruction from toxins(78).

T6SSs provide a diverse modular toolkit to deliver anti-eukaryotic and antibacterial toxic effectors directly into target cells(82). T6SS effectors can be grouped into peptidoglycan hydrolyzing effectors with amidase or muraminidase activity such as the Tae superfamily (type VI amidase effector) that cleaves peptidoglycan within cross-links(82). Another broad superfamily of T6SS effectors includes the cell wall effector Tge (type VI glycoside hydrolase effector) which splits open the glycoside bond between MurNAc and GlcNAc by conserved catalytic glutamate residue(82).

DNase Nucleic acids are another set of T6SS effectors that include toxin domains of the HNH (histidine, asparagine, histidine)-endonuclease superfamily such as Hcp-fused effectors of *E. coli* and the PAAR-containing P. aeruginosa effector Tse7(82).

Pore-forming toxins such as VasX from *V. cholerae*, phospholipases, and effectors such as *P. aeruginosa* Tse6 which manipulates the energy balance are other groups of proteins released by this secretion system(82).

1.3.6 Type V Secretion System

The type V secretion system (T5SS) appears at first sight to be the simplest mechanism of secretion and most of the protein substrate members of this diverse group are virulence factors for pathogenic bacteria(2). Previously discussed bacterial secretion systems were multi-subunit and their unique translocation mechanism designed in the way for crossing over the membranes by complex channel-like Nano-machines. By contrast, T5SS effector proteins appear peculiar as mainly consist of one polypeptide chain containing a characteristic β-barrel domain specialized for channel formation and insertion in bacterial outer membranes to effect successful translocation of the remaining part of secreted protein or a separately encoded protein(28,83). Type V secretion systems are much smaller in size and only found among the Gram-negatives(30). As secretion in T5SS happens in outer membrane, effector substrate must first pass through inner membrane in an unfolded condition by the Sec pathway. Their N-terminal Sec signal sequence is then cleaved off during translocation(2,84). The energy source for Type V secretion systems is not completely clear and there is no ATPase as a driving force or ATP source in the periplasm or OM(85,86). Effector Proteins of the Type V secretion system also

known as autotransporters (ATs) due to the potential self-sufficient nature of secretion(87).

Type V secretion is divided into subgroups based on their structure, domain arrangements and function of the passenger domains(87): type Va through type Ve, and recently identified type Vf (Figure 1.5)(88).

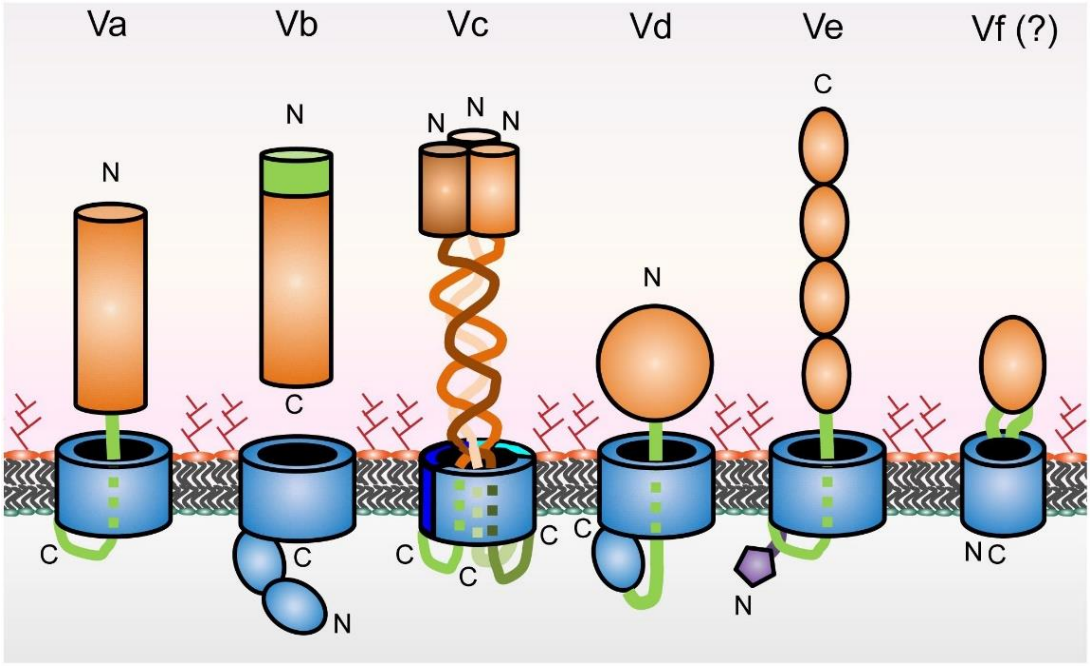

Figure 1.5: Schematic of type V secretion system subgroups based on their topology and transport domain. β-barrels and Polypeptide-transport-associated (POTRA) domains for recognition of its corresponding passenger TpsA are shown in blue, linkers and TPS domains in green, and passengers in orange. The periplasmic extension of type Ve proteins are in purple. The positions of the N- and C-termini are indicated. Type Vf is not fully understood as part of the type V secretion scheme; this is shown by the question mark(87).

Table 1.1. Diverse functions of type V secretion system passenger domains(87).

Function	Mode of action	Example	AT-Type	Reference
Enzyme	SPATE Protease Group I	EspC (*Escherichia coli*)	Type Va	Stein et al., 1996
Enzyme	SPATE Protease Group I	EspP (*Escherichia coli*)	Type Va	Roman-Hernandez et al., 2014
Enzyme	SPATE Protease Group II	Hbp (*Escherichia coli*)	Type Va	Soprova et al., 2010
Enzyme	SPATE Protease Group II	Pic (*Escherichia coli*)	Type Va	Abreu et al., 2016
Enzyme	SPATE-like	IgA protease (*N. gonorrhoeae)*	Type Va	Diebel et al., 2004
Enzyme	Non-SPATE	NalP protease (*N. meningitidis*)	Type Va	Arenas et al., 2013
Enzyme	Non-SPATE	Ssp1 and Ssp2 (*Serratia marcescens*)	Type Va	Ohnishi et al., 2001 Kida et al.,2008
Enzyme	Non-SPATE	LepA (*P. aeruginosa*)	Type Vb	Ohnishi and Horinouchi, 2009
Enzyme	Lipase/esterase	EstA (*P. aeruginosa*)	Type Va	Wilhelm et al., 2007
Enzyme	Lipase/esterase	McaP (*M.catarrhalis*)	Type Va	Timpe et al., 2003 Lipski et al.,2007
Enzyme	Lipase/esterase	EstA (S. liquefaciens)	Type Va	Riedel et al., 2003
Enzyme	Lipase/esterase	ApeE (*S. typhimurium*)	Type Va	Carinato et al., 1998
Enzyme	Lipase/esterase	PlpD **(** *P.aeruginosa*)	Type Vd	Salacha et al., 2010 da Mata Madeira et al., 2016
Enzyme	Lipase/esterase	FplA *Fusobacterium nucleatum*	Type Vd	Casasanta et al., 2017
CDI	Growth inhibition of competing bacteria	CdiB-CdiA Enterobacteriaceae	Type Vb	Diner et al., 2012
CDI	Growth inhibition of competing bacteria	BcpA/B *B. pseudomallei*	Type Vb	Garcia et al., 2013
Metabolism	Alteration of host cell processes	BadA *Bartonella henselae*	Type Vb	Riess et al., 2004

Metabolism	Alteration of host cell processes	InvD *Y. pseudotuberculosis*	Type Ve	Sadana et al., 2018
Immune Evasion	Circumventing host immune response	IgA protease (*Escherichia coli)*	Type Va	Zinchenko et al., 2018
Function	**Mode of action**	**Example**	**AT-Type**	**Reference**
Immune Evasion	Circumventing host immune response	EtpA (*Escherichia coli)*	Type Vb	Roy et al., 2009
Immune Evasion	Circumventing host immune response	YadA (*Yersinia spp.)*	Type Vc	Schindler et al., 2012
Immune Evasion	Circumventing host immune response	Eib (*Escherichia coli*)	Type Vc	Leo and Goldman, 2009; Leo et al., 2011
Cyto- /Hemolysis	…….	VacA (*Helicobacterpylori*)	Type Va	Cover and Blanke, 2005
Cyto- /Hemolysis	…….	ShlA (*Serratia marcescens*)	Type Vb	Reboud et al., 2017
Cyto- /Hemolysis	……	ExlA (*P. aeruginosa*)	Type Vb	Yang and Braun, 2000
Adhesin	Adhesion to surfaces/receptors	AIDA-I (*Escherichia coli*)	Type Va	Laarmann and Schmidt, 2003;
Adhesin	Adhesion to surfaces/receptors	EhaA (*Escherichia coli*)	Type Va	Charbonneau et al., 2006
Adhesin	Adhesion to surfaces/receptors	Pertactin (*Bordetella pertussis*)	Type Va	Aricò et al., 1993
Adhesin	Adhesion to surfaces/receptors	FHA (*Bordetella pertussis*)	Type Vb	Serra et al., 2011
Adhesin	Adhesion to surfaces/receptors	HMW1/2 (*H. influenzae*)	Type Vb	Buscher et al., 2006
Adhesin	Adhesion to surfaces/receptors	YadA (*Yersinia spp.*)	Type Vc	Tertti et al., 1992; Mühlenkamp et al.,2017
Adhesin	Adhesion to surfaces/receptors	Eib (*Escherichia coli*)	Type Vc	Leo and Goldman, 2009
Adhesin	Adhesion to surfaces/receptors	Intimin (*Escherichia coli*)	Type Ve	Kenny et al., 1997
Adhesin	Adhesion to surfaces/receptors	InvA (*Yersinia spp*.)	Type Ve	Isberg et al., 2000
Adhesin	Auto-Agglutination and biofilm formation	Ag43 (*Escherichia coli*)	Type Va	Sherlock et al., 2006
Adhesin	Auto-Agglutination and biofilm	FHA (*Bordetella pertussis*)	Type Vb	Serra et al., 2011

	formation			
Adhesin	Auto-Agglutination and biofilm formation	EtpA (*Escherichia coli*)	Type Vb	Roy et al., 2009
Function	**Mode of action**	**Example**	**AT-Type**	**Reference**
Adhesin	Auto-Agglutination and biofilm formation	YadA (*Y.enterocolitica*)	Type Vc	Trunk et al., 2018
Adhesin	Auto-Agglutination and biofilm formation	Eib (*Escherichia coli*)	Type Vc	Leo and Goldman, 2009
Intracellular motility	Activation of actin polymerases	IcsA (*Shigella flexneri*)	Type Va	Goldberg and Theriot, 1995
Intracellular motility	Activation of actin polymerases	YapV (*Yersinia spp*.)	Type Va	Besingi et al., 2013
Intracellular motility	Activation of actin polymerases	BimA (*Burkholderia spp.)*	Type Vc	Benanti et al., 2015

1.4 Classical Autotransporters (Type Va) biogenesis

Autotransporters are a family of secreted proteins with a conserved sequence that forms a domain that generates a β -barrel in the outer membrane to aid secretion(89). Originally this was proposed to undertake the role of secretion on its own, but now it is becoming clear that other proteins are probably also involved, but it is not clear how the whole mechanism functions(89). Type Va autotransporters are also known as classical ATs, and the family has been extensively reviewed in recent years(87). According to evolution biology, it appears that all members of the AT family known so far originated from speciation and late gene bacterial duplication events and to a lesser extent horizontal gene transfer (90,91). The complete mechanism of translocation in this superfamily of proteins is not fully elucidated, and the term "Autotransporter" remains debatable as more components of the pathway are identified. In recent years, diverse groups of periplasmic chaperones and outer membrane proteins have been identified that might associate with this translocation process(30). However, unlike the type I to IV secretion systems, it was first argued, as the name implies, that Autotransporter system requires no energy or accessory protein for substrate translocation. Instead it was postulated that secretion was due to the covalently bound β- barrel domain(92).

After the identification of first Autotransporter IgA1 protease in *N. gonorrhoeae* that targets human antibodies, similar functional virulence proteins have been

found in other Gram negative bacteria such as EstA, a lipase from *Pseudomonas aeruginosa* (93,94). In all of the Autotransporter proteins, the basic structure is the same and comprises 3-4 important domains including signal sequence, passenger domain, linker domain and the translocation unit (Figure 1.6)(95). ATs are first translated in the cytosol where the polypeptide chain remains in an unfolded state facilitated by chaperones, and is translocated across the inner membrane (IM) into the periplasm by the SecYEG translocon(13,96). The signal sequence or leader sequence located in the N-terminal region of the Autotransporter proteins enables target protein substrates to find their way to the inner membrane via recognition by SecB and sometimes alternative SRP pathway, which allow translocation of the preprotein by targeting the ribosome-SRP complex directly to the translocon(6,97,98). The passenger domain (also called α domain or N-domain), carries the functional unit of the autotransporter(99,100). There are numerous examples of AT passenger domains with a protease activity. Classical AT proteases are divided into three groups: SPATE (serine protease autotransporters of *Enterobacteriaceae*), SPATE-like, and non-SPATE proteases(90,101). Classical ATs can have other functions as well e.g. adhesin factor *in* diffuse adherence (AIDA)-I *from E.coli, Pertactin from Bordetella pertussis* and extracellular virulence factors such as lipases, serum resistance factors and cytotoxins(3,30,94). A β- domain or helper domain is located at the C-Terminal of Autotransporters(100,102). This domain forms a 12-stranded β barrel while located in outer membrane, and the main function of this domain is channel formation and translocation of the N-terminal passenger domain to the extracellular space(99,103,104). Sometimes the passenger domain is cleaved off after OM translocation(105–107), and this may be mediated by the passenger domain of the AT e.g. the passenger domains of the *H. influenzae* Hap and *B. pertussis* SphB1 proteins are cleaved in an intermolecular autocatalytic manner by an internal endogenous serine protease(108,109), or sometimes by a separate protease e.g. *Shigella* IcsA protein is cleaved by a dedicated accessory protease of the omptin family called IcsP(110,111). In addition, the passenger domains of different *N. meningitidis* ATs including App, Aus I, MspA and the IgA protease are cleaved by NalP, which encodes a serine protease(3,112). By contrast, the SPATE proteins are not processed by their internal endogenous serine protease activities. Instead, the unique cleavage step of passenger or functional domains in these proteins occurs inside the pore generated by the β domain(3,112).

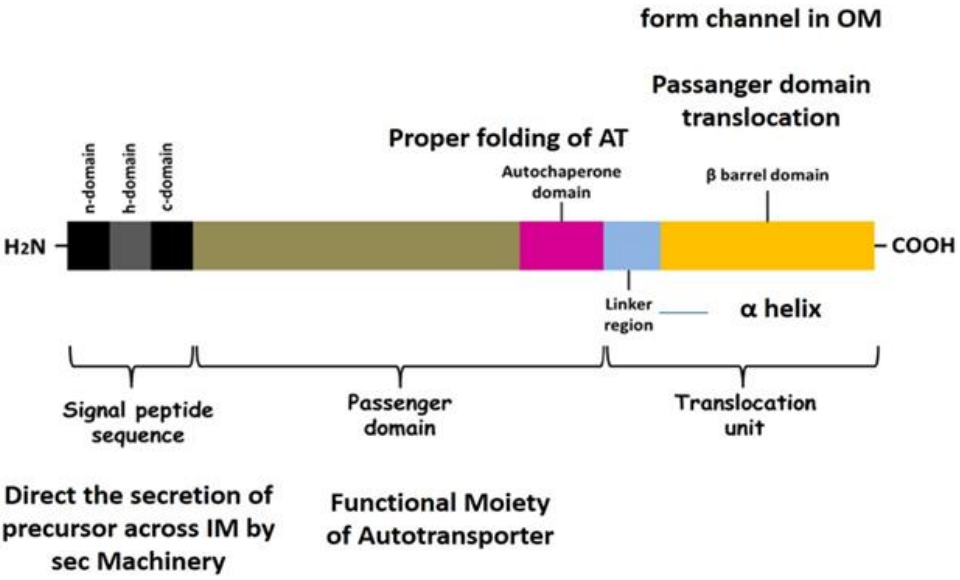

Figure 1.6: Different characteristic domains of Autotransporter proteins, and their function for secretion. (113)

In the periplasm, ATs stay unfolded, and are protected from aggregation by periplasmic chaperones like SurA, Skp and DegP(114–118). Insertion and integration of the β-barrel domain into the OM is mediated by the β-barrel assembly machinery (BAM) complex(30,119). The BAM complex in *E.coli* is composed of BamA and four additional helper proteins (BamB to BamE)(120). This complex integrates most integral OM β-barrel proteins into the OM(121) . An additional segment in subgroups of autotransporters, called the Intramolecular chaperone domain (also known as the autochaperone domain) was identified in recent years located between the C-terminal of the passenger domain and the linker region(94,122,123). This domain mainly influences proper folding of passenger functional domain of the autotransporter during and after secretion across the outer membrane(94,122,123). Once the AT passenger domain has reached the channel in the outer membrane, the linker domain will support translocation of the passenger domain to the extracellular space(28).

1.5 The diverse models proposed to explain AT Passenger secretion

Autotransporter secretion to the bacterial cell surface depends on the AT subtype (Figure 1.5) (30,88). One reasonable suggestion hypothesises that ATs provide energy from innate folding to drive secretion. Another explanation proposes a

Brownian ratchet model is once the export has occurred, the passenger domain cannot return back into the periplasm, and therefore the passenger is pushed into extracellular space where it folds(94,124). As an alternative, the presence of asymmetric charge within the passenger domain structure was also suggested as an effective energy provision for this secretion system(125).

1.5.1 Passenger hairpin Secretion Pathway (Type Va)

In this proposed secretion pathway (Figure 1.7), the AT passenger domain is translocated by a C-terminus-first mechanism, and a hairpin-loop is shaped in this region of the passenger domain in the internal section of the β-barrel. This is followed by a continuous folding process of the functional domain on the cell surface, initiating from the C-terminus region(126–129).

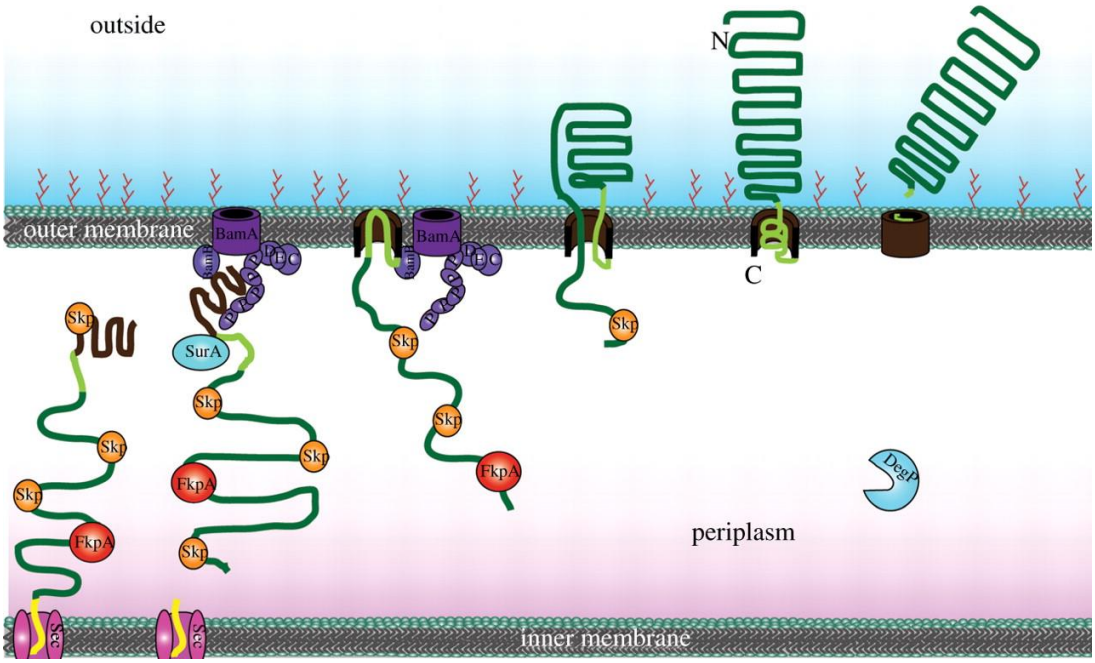

Figure 1.7: Type Va autotransporter hairpin model.(30) The autotransporter polypeptide is passed through the inner membrane (IM) by the general Sec pathway. Signal peptide extensions (in yellow) are not detached from Sec machine after successful translocation of autotransporter functional units to the periplasmic space regulate Sec translocon movement. In the periplasmic space, chaperone proteins such as Skp (orange), FkpA (red) and SurA (in blue) and DegP (in blue) attach to the autotransporter and keep the substrate in a competent unfolded state. The chaperone DegP acts as a protease

and quality control assessor. The signal peptide is cleaved by signal peptidase (not shown), presenting the functional parts to the periplasm. The C-terminal membrane anchor (in brown) is identified by the POTRA (P) domains of BamA (in purple); the Bam complex facilitates binding of the β-barrel membrane anchor into the outer membrane (OM). The linker region (light green) produces a hairpin structure within the channel. The passenger domain (dark green) covers the hole surrounding the passenger domain. Translocation energy may be provided by passenger domain folding. After successful translocation, the linker domain that is composed of an α-helical conformation will block the outer membrane inside the channel. Proteolytic enzymes may contribute to passenger domain release to outside of the cell.

1.5.2 Two-partner secretion pathway (Type Vb)

The type Vb secretion pathway is also known as the two-partner secretion system (TPSS). It is composed of two separate polypeptide chains encoded in one operon (Figure 1.8). An example is the filamentous hemagglutinin FHA found in *Bordetella* or adhesion proteins of *Haemophilus influenza* (93,94,130,131). This secretion pathway is often utilized for translocation of large effector proteins(94). One of the two TPSSs proteins is the translocator channel (TpsB), while the other one is a specialized passenger (TpsA)(87). TpsB consist of a 16-stranded, OM integral β-barrel protein with two periplasmic POTRA (polypeptide transport-associated) domains(132). As there are two distinct polypeptide chains, no proteolytic enzymatic activity is needed to release the passenger into the extracellular environment(87). The secretion model proposed for Type Vb is different as the TpsB transporter is first integrated into the outer membrane by the BAM complex, and then TpsA will identify, bind and interact with TpsB through the TpsB POTRAs and the N-terminal TPS conserved signal of TpsA. The TpsA signal remains unfolded in the periplasm and during translocation through the TpsB barrel(114). Dynamic interaction of the TpsA signal and TpsB POTRA domains and the pulling force within the barrel facilitate release of TpsA substrate from its transporter and refolding after translocation has been confirmed by surface Plasmon resonance, NMR and crosslinking experiments(133–136). The first model for Type Vb secretion suggested that a hairpin like structure formed inside the barrel facilitating folding of the main part of TpsA in a C-to-N direction (117,134,137). A second model proposed that the

N-terminal domain first folded and was secreted independently, and then the rest of the protein followed in a N-to-C direction(138–140).

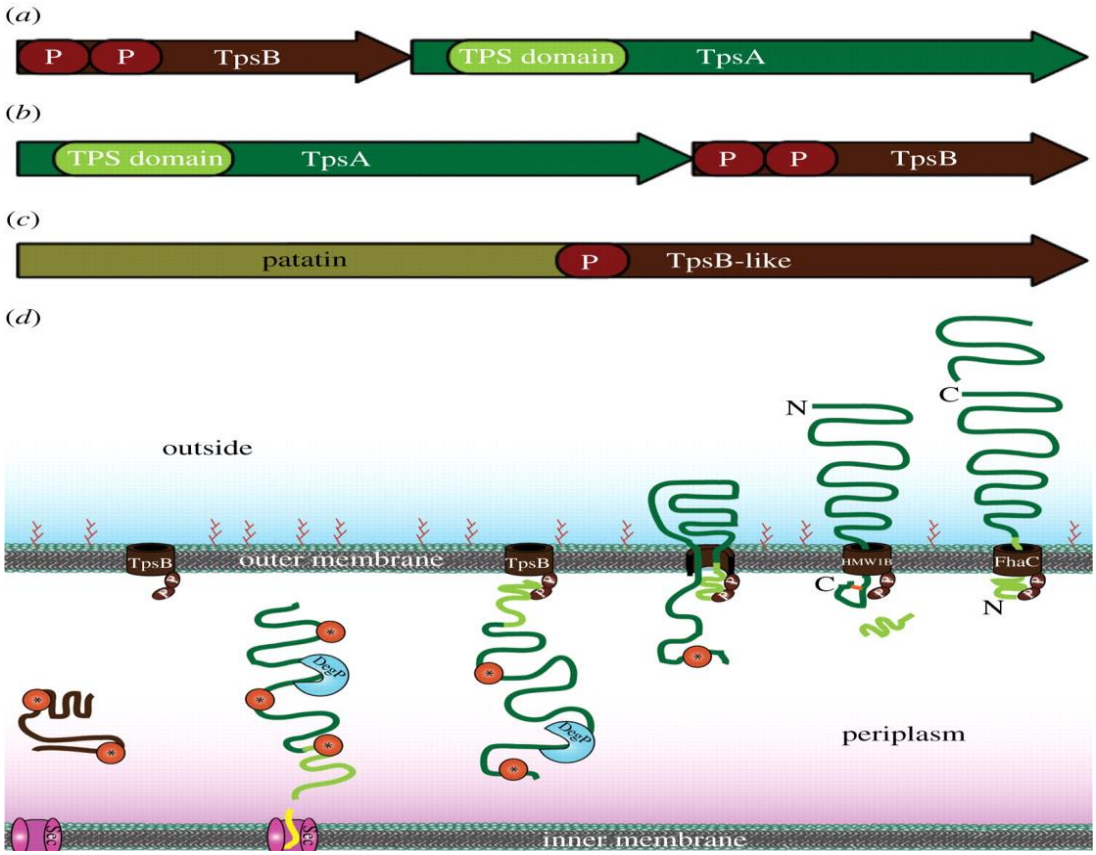

Figure 1.8: Type Vb two-partner secretion model and genomic organization. (30) Panel A-C show the different genomic organizations for the TPSS encoding genes. Panel D shows that the TpsB protein first folds into a β-barrel configuration in the OM, with two periplasmic POTRA domains. Another polypeptide, TpsA, is translocated by Sec to the periplasm, interacts with chaperones and delivers the passenger domain for translocation across the OM into the extracellular space.

1.5.3 Chaperone-usher secretion pathway (Type Vc)

Type Vc secretion system is very similar to type Va classical AT system (Figure 1.9), however due to presence of many intertwined trimeric structures in this system and their main adhesin function, the proteins are also known as trimeric autotransporter adhesins (TAAs). An example would be YadA, the Yersinia adhesin A from *Yersinia enterocolitica* and *Yersinia pseudotuberculosis*(141). These secretion pathway is composed of three similar polypeptide chains and in

their last folded form they consist of a C-terminal 12 stranded β-barrel (4 β-strands per monomer), and a trimeric passenger that usually folds into a marshmallow-like configuration with a coiled spiral stalk and a round head domain containing the N-terminus region of the protein(142–144). Due to the trimeric structure of these ATs, passenger secretion is more complicated(87). Three passenger polypeptide chains must pass through narrow β-barrel domain(87). First step locates the 12-stranded β-barrel to the OM. Then the passenger makes a hairpin loop for each of the three domains after folding that ultimately leads the protein to extracellular translocation(143,145–147). Periplasmic chaperone proteins prepare a competent folding protein state before substrate delivery to the translocation channel in the outer membrane(148). This proposed model is reminiscent uropathogenic *E. coli* pilin assembly (Chaperone-usher secretion pathway) and Hia adhesin from *Haemophilus influenza*(148–150).

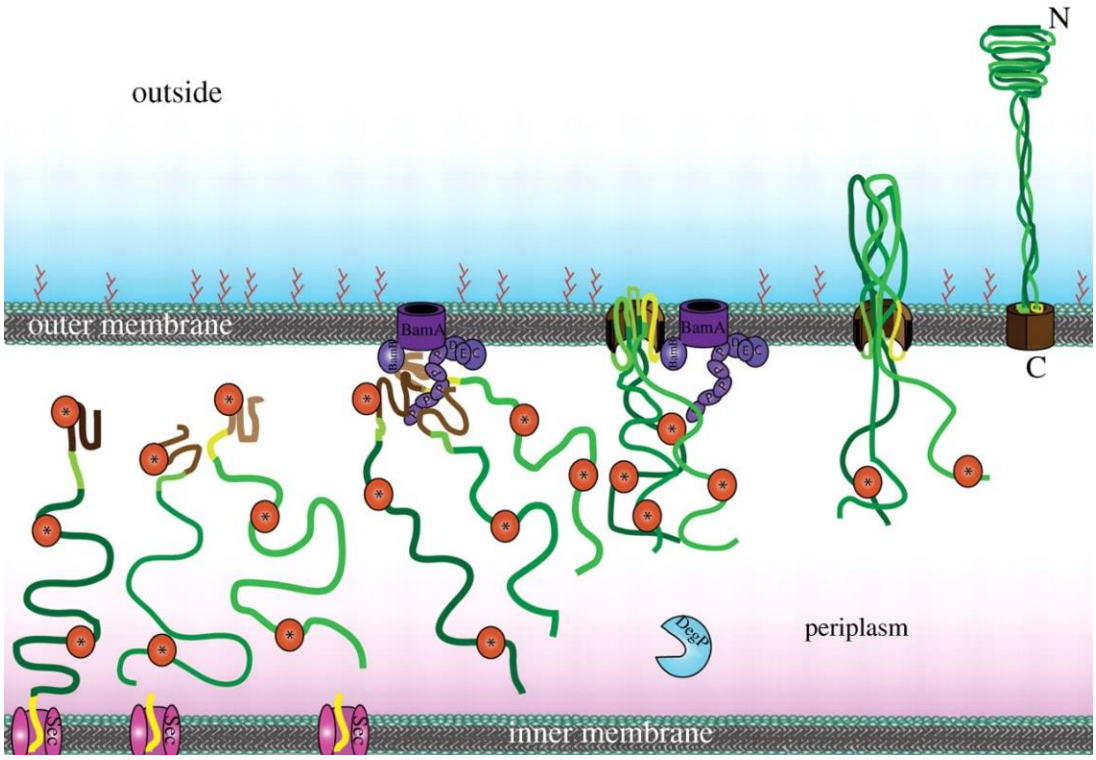

Figure 1.9: Type Vc model of autotransporter. (30) The protein substrate is first translocated to the periplasmic space by the Sec-dependent pathway, trimeric autotransporters are preserved in an unfolded state in the periplasm with the help of chaperones and the intrinsic low tendency of substrates to fold. Three monomers associate, and their β-domains associate,

and integrate in the OM as a 12-strand barrel, through which the passenger domain is translocated with the aid of the Bam complex.

1.5.4 Type Vd secretion pathway

The type Vd are newly identified autotransporters that overlap main features of both type Va and type Vb systems within their structure with minor differences(87). Common prototypical examples of this hybrid group are PlpD from *P. aeruginosa* and FplA from *Fusobacterium nucleatum*(151,152). The C-terminal β-barrel domain of type Vd ATs resemble type Vb systems. Both contain 16 β-strands but only one POTRA domain is found in type Vd for TpsA substrate binding before translocation(30). The passenger domain in type Vd is configured as a α/β-hydrolase fold, and their main functions are lipases/esterases in contrast, the passenger domain of type Va ATs exhibit more diverse functions, and usually fold into a β-helical structure(152–154). The passenger secretion model for type Vd is not completely understood, but it appears that POTRA domain found in this system may involve chaperone protection, protease and cleavage or secretion activity(151,152).

1.5.5 Type Ve (Inverse Autotransporters)

Type Ve ATs have a structure and biogenesis very similar to type Va classical autotransporters, with their 12-stranded β-barrel domain and monomeric passenger domain staying connected after secretion(30,87,155). The only main difference found with classical ATs is inversion of β-barrel and passenger domain such that they are positioned in a N-to-C configuration, and therefore proteins using this secretion system are also known as inverse autotransporters(156). Additional unique long repetitive Ig-like or lectin-like domains found in Type Ve passenger regions may be involved in providing energy for translocation and passenger secretion(155,157). Moreover, a periplasmic domain has also been identified in Type Ve ATs that may help stability and protection during host pathogen interaction(158). Intimin and invasin from *Escherichia coli* and *Y. enterocolitica* are common examples for the Type Ve secretion system(30,155).

1.5.6 Type Vf is it an autotransporter?

The type Vf secretion pathway are a fairly recently classified autotransporter superfamily after identification of BapA which is unique to *Helicobacter pylori*(159). In terms of structure, this class of autotransporter is composed of

only 8-stranded β-barrel domain and surface exposed region that is integrated into the N-terminal domain (159). It seems likely that their passenger domain is a continuous loop of the β-barrel domain however, their complete topology and mechanism of secretion is still in early stage discovery(87).

1.6 Evolution and infection biology of Enteropathogenic *Escherichia coli* (EPEC)

An example of a Gram-negative pathogen that uses a number of different secreted proteins as virulence factors is Enteropathogenic *Escherichia coli* (EPEC). The Gram-negative bacterium *E. coli* may have coexisted as a colonizer in the intestinal mucosa through a commensal or symbiotic ecological relationship with the human host. Most *E. coli* strains in the human body are harmless, beneficial and non-pathogenic that even enable the human host to develop resistance against colonization by dangerous pathogens(160,161). On the negative side of the story, prototypic *E. coli* bacteria can also act as a multipotent pathogen that are capable of causing a wide range of clinical diseases that may be different in terms of root cause and etiology, disease duration, and clinical manifestation in susceptible populations(162,163). In human hosts, gastrointestinal tract, urinary tract, CNS and hematic system are more susceptible to pathogenic *E. coli* colonisation. The different clinical presentations range from typical diarrhoea and dysentery to more severe extra-intestinal complications such as haemolytic uremic syndrome (HUS), sepsis or even renal failure and death(162–164). Most *E. coli* Pathovars are associated with outbreaks and sometimes epidemics in both developing and developed counties due to its low infectivity dose and easy transmission (163,165,166). In addition, *E. coli* is subject to gene alteration and mutation due to horizontal gene transfer mechanisms such as transformation (uptake of free or Plasmid DNA), conjugation (plasmid or transposon-mediated transfer), and transduction (phage-mediated transfer) that occur frequently in this bacterium. These dynamic genetic mechanisms provide diversity, adaptability and an evolutionary platform for commensal strains to transform into pathogenic forms(162,167–171). For these reasons, *E. coli* Pathotypes are considered as a public health concern, and it appears that concrete surveillance strategies need to be implemented in developing countries as diarrheal illness and in particular pathogenic *E. coli* are responsible for the majority of death related diarrhoea in children less than 5 years of age in Africa and South Asia (163,172).

Most commensal *E. coli* belong to phylogroup A (173,174). Pathotypes of *E. coli* contain around 1 million extra base pairs in their genome compared to the commensal strains (163). This genetic material includes transposons, bacteriophages, pathogenicity Islands (PAIs) and virulence plasmids (encoding colonization factors and toxins) that facilitate adaptation, integration and essential survival traits such as antibiotic resistance, competence and virulence (174–177).

A pathotype is simply defined as a group of strains in a particular species of bacteria that share and acquired the same virulence factors through genetic transfer, and each can cause a common disease(162,178). In immunocompetent individuals, *E. coli* Pathotypes must obtain a combination of stable virulence factors to initiate the infection process (162,179).

Pathotypes of *E. coli* can be divided into enteric / diarrheal and extra-intestinal infectious diseases(162,180). In general, important clinical presentations including enteritis with diarrhea, urinary tract infections (UTI) and sepsis/meningitis are associated with different *E. coli* Pathovars (162).

The diarrheagenic *E. coli* (DEC) pathogens are more diverse compared to extra-intestinal strains. The most important enteric pathovars are Entropathogenic *E. coli* (EPEC), Entroaggregative *E. coli* (EAEC), Entrotoxigenic *E. coli* (ETEC), Entrohemorragic *E. coli* (EHEC), Entroinvasive *E. coli* (EIEC), diffuse adherent *E. coli* (DAEC), adherent invasive *E. coli* (AIEC) and shiga like toxin producing enteroaggregative *E. coli* (STEAEC) (Figure 1.10)(160,162,178). Moreover, extra- intestinal pathogenic *E. coli* (ExPEC) strains are divided into uropathogenic *E. coli* (UPEC), neonatal Meningitis *E. coli* (NMEC) and sepsis related *E. coli* (SEPEC) (160,163,179,181–183).

One of the major causes of death from infantile diarrheal-related illness in children under 2 years old and probably the first identified Pathotypes of *E. coli* is EPEC(184–187). EPEC was first described in 1955 following different outbreaks of summer infantile diarrheal disease (163,188–190). Population, age, diagnostic techniques, social and economic level of society and geographical region in developing countries are associated with prevalence and reported incidence rates of EPEC (186,191,192). EPEC does not produce enterotoxin or shiga-like toxin (non-invasive) and it appears that despite invasive characteristics *in vitro*, it does not invade tissue cells *in vivo* (185,193–195). EPEC has the *eae* gene

located in a Pathogenicity Island. This gene is responsible for encoding the intimin receptor(196). Pathogenicity and initiation of infection of EPEC begins with formation of attaching and effacing (A/E) lesions (Figure 1.10) which help the bacteria become closely attached to the host plasma membrane resulting in microvilli destruction or removal and twisting of the enterocyte plasma membrane(197,198). This interaction between host and pathogen greatly effects cytoskeletal arrangements in the host cell forming actin-rich bases to which the bacteria attach (199). Thus, EPEC are called attaching and Effacing (A/E) pathogens (163,181).

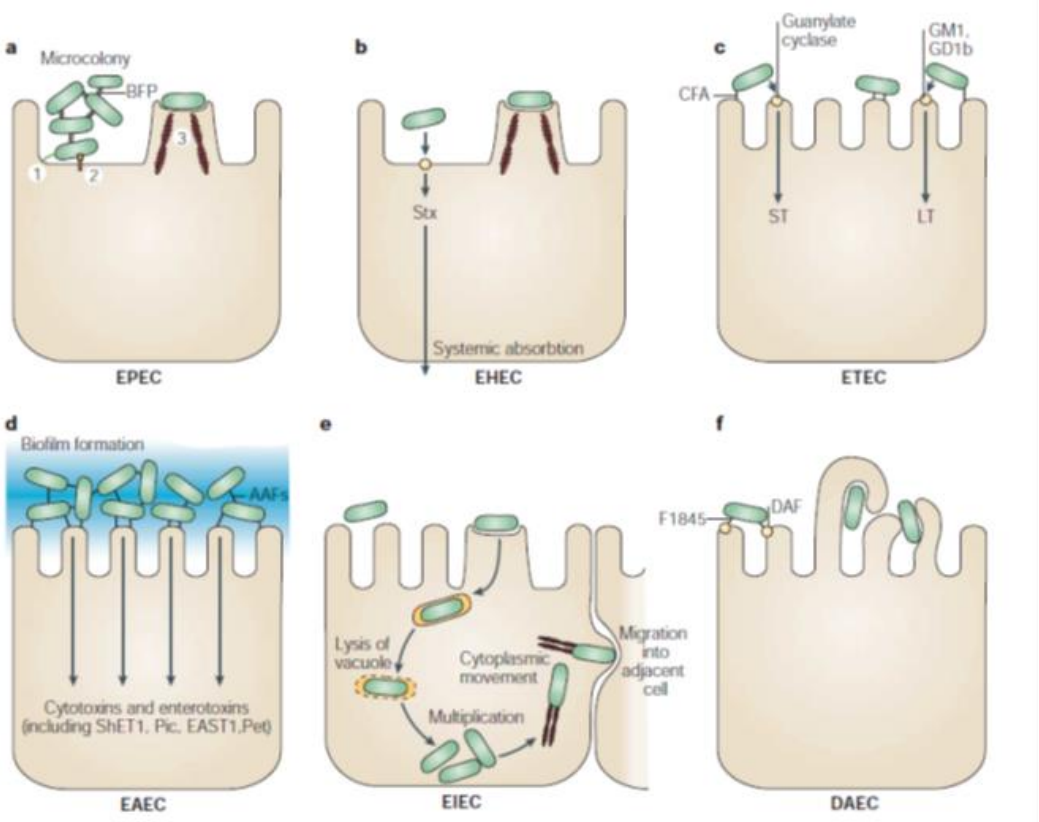

Figure 1.10 : Host pathogen interactions of pathogenic *E. coli.* (162) The six identified categories of diarrhoeagenic *E. coli* each have unique characteristics in their pathogenicity with eukaryotic cells. Here, the interaction of each category with a typical target cell is schematically represented. These schematic representations are mainly the result of *in vitro* studies and might not totally reflect the phenomena that happens in infected humans. a | EPEC attach to small bowel enterocytes, but destroy the normal microvillar architecture, inducing the characteristic attaching and effacing lesion. Cytoskeletal derangements are accompanied by an inflammatory response and diarrhoea. 1.

Initial adhesion, 2. Protein translocation by type III secretion, 3. Pedestal formation. b | EHEC also induce the attaching and effacing lesion, but in the colon. The distinguishing feature of EHEC is the elaboration of Shiga toxin (Stx), systemic absorption of which leads to potentially serious clinical complications. c | Similarly, ETEC adhere to small bowel enterocytes and induce watery diarrhoea by the secretion of heat-labile (LT) and/or heat-stable (ST) enterotoxins. d | EAEC adheres to small and large bowel epithelia in a thick biofilm and elaborates secretory enterotoxins and cytotoxins. e | EIEC invades the colonic epithelial cell, lyses the phagosome and moves through the cell by nucleating actin microfilaments. The bacteria might move laterally through the epithelium by direct cell-to-cell spread or might exit and re-enter the baso-lateral plasma membrane. f | DAEC elicits a characteristic signal transduction effect in small bowel enterocytes that manifests as the growth of long finger-like cellular projections, which wrap around the bacteria. AAF, aggregative adherence fimbriae; BFP, bundle-forming pilus; CFA, colonization factor antigen; DAF, decay-accelerating factor; EAST1, enteroaggregative *E. coli* ST1; LT, heat-labile enterotoxin; ShET1, Shigella enterotoxin 1; ST, heat-stable enterotoxin.

Formation of A/E lesions in the intestinal cells of both typical and atypical EPECs are encoded by the large Pathogenicity island region called the Locus of Enterocyte Effacement (LEE) (162,195,200). LEE was first identified in EPEC strains in 1995 by McDaniel and his colleagues (201–203). The infectivity and virulence ability of EPEC depends on successful transcription, translation and translocation of LEE genes (176,204,205). Effacement of enterocyte microvilli and signal induction of pedestal formation is coordinated after successful translocation of LEE effector proteins(206–208). Translocation of 7 effector proteins including Tir, Map, EspB, EspF, EspH, EspZ and EspG by the Type III secretion system encoded by LEE occurs, and other essential protein genes encoded in the non-LEE-encoded effector (NLE) regions dispersed throughout the chromosome contribute to EPEC pathogenicity(202,208–211). Moreover, genes responsible for Bundle Forming Pilus (BFP), are encoded in Plasmids among Typical EPEC are also located in the LEE region(212,213). Horizontal gene transfer of the LEE region to nonpathogenic strain of *E. coli*, results in the clinical presentation of A/E lesions *in vitro*(200,201,214). The 35-kbp LEE region is composed of 41 Open Reading Frame (ORF) that are grouped into 5 polycistronic operons and 3 important domains (Figure 1.11)(211,215,216). Core LEE is mainly conserved—especially among genes coding for the type 3 secretion

system—whereas genes encoding effector proteins are more variable(217). In previous studies, significant difference were also found between the 5′- and 3′-associated flanking regions that show diverse lines of evolution(217).

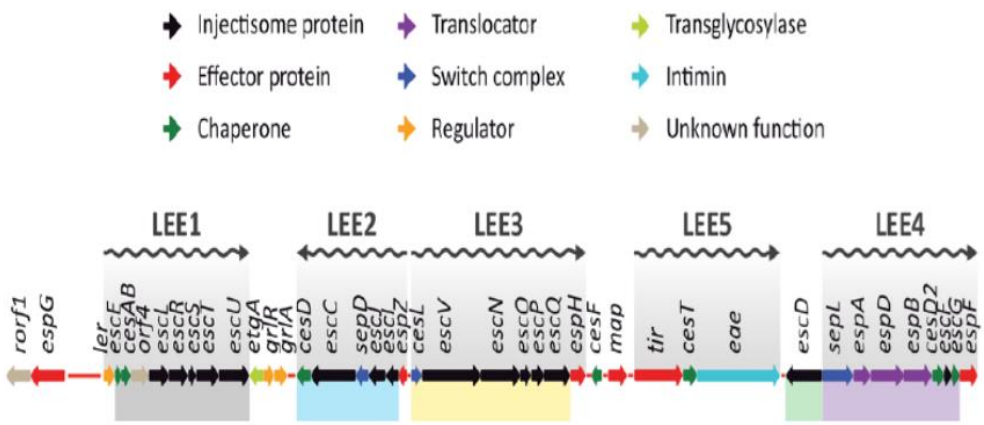

Figure 1.11: The LEE PAI is composed of five polycistronic operons and shorter transcriptional units. (113)

The pathogenesis of EPEC depends on the ability to cross over the gastric protective barrier and form close attachment to the mucosal layer of the small intestine and colon (162,181). In general, the infection biology and host-pathogen interaction of EPEC comprises of colonization of the intestinal mucosa, an escape strategy and subversion of the host immune system along with multiplication, exploitation and enterocyte destruction (162,218). According to Donnenberg and Kaper, the colonization and pathogenesis process in EPEC may occur in three important phases including micro-colony localized adherence or initial loose attachment mediated by BFP and flagella, second stage signal transduction and finally close attachment mediated by type III secretion effector proteins including EspA, EspB, and EspD. Collectively, these interactions cause actin cytoskeletal rearrangement and formation of a pedestal structure below the bacterial attachment site on the infected host cell (162,167,169,212). Intimin, a 94-kDa outer membrane protein, is another important adhesion factor that plays an important role in EPEC close attachment to host epithelial cells and cytoskeletal rearrangement(219,220). This protein is encoded by the *eae* gene within LEE (221). The conserved N-Terminal region of Intimin is located in the bacterial outer membrane while the variable and diverse adhesive C- Terminal region that contains 280 amino acids is located outside of bacterial cell in the extracellular space (222). According to different arrangement of nucleotide

sequences in C-Terminal region of intimin protein, around 30 subtypes have been identified (201,223–227). The C-Terminal region of intimin binds to its specific 90-kDa receptor protein Tir (Translocated intimin receptor) that facilitates translocation of intimin protein into the cytosol of host cell via the Type III secretion system (T3SS) (228). After successful translocation of intimin, Tir receptor will be placed in the plasma membrane and present its middle section at the host cell surface in order to create loop shape structure (229). This translocation facilitates intimin interaction with the Tir receptor loop region (228–231). After successful attachment, the C -Terminal domain of Tir protein stimulates actin polymerization and tight junction destruction that ultimately can causes diarrhea in human host (Figure 1.12 , 1.13 and 1.14)(228–232).

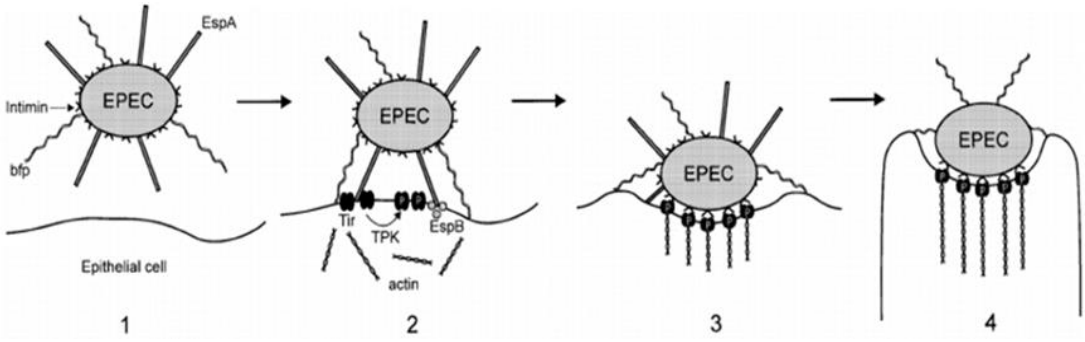

Figure 1.12: Different stages of EPEC pathogenesis composed of localized adherence, intimate attachment, and signal transduction that results in diarrhoea in the host. (218)

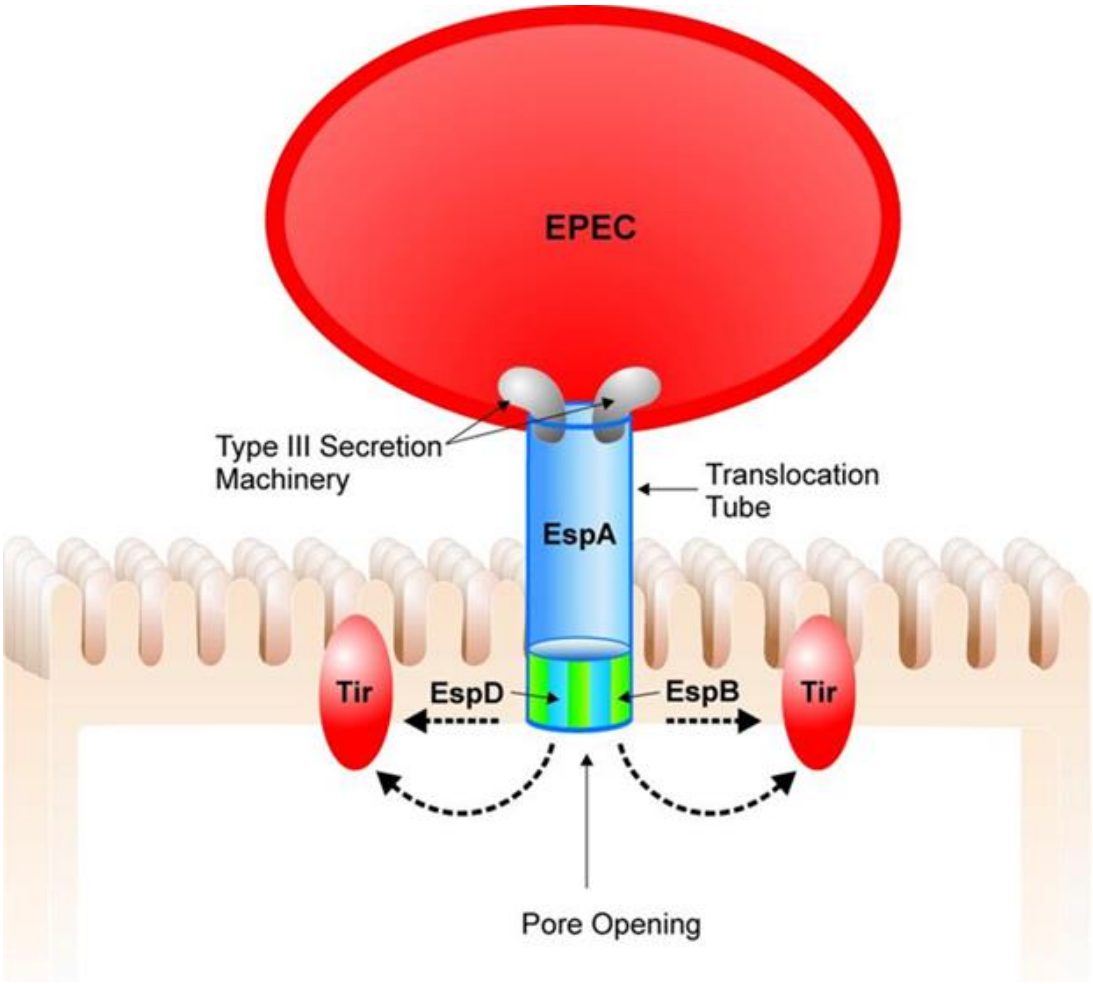

Figure 1.13: Translocation of EPEC-secreted proteins (Esps) and virulence factors occurs through type III secretion system. EspA forms a filamentous structure protruding from the bacterium and provides interaction with the host cell. EspB is transferred into the host cytosol and plasma membrane. EspD integrates in the host membrane and in collaboration with EspB facilitates pore formation in host cell(221).

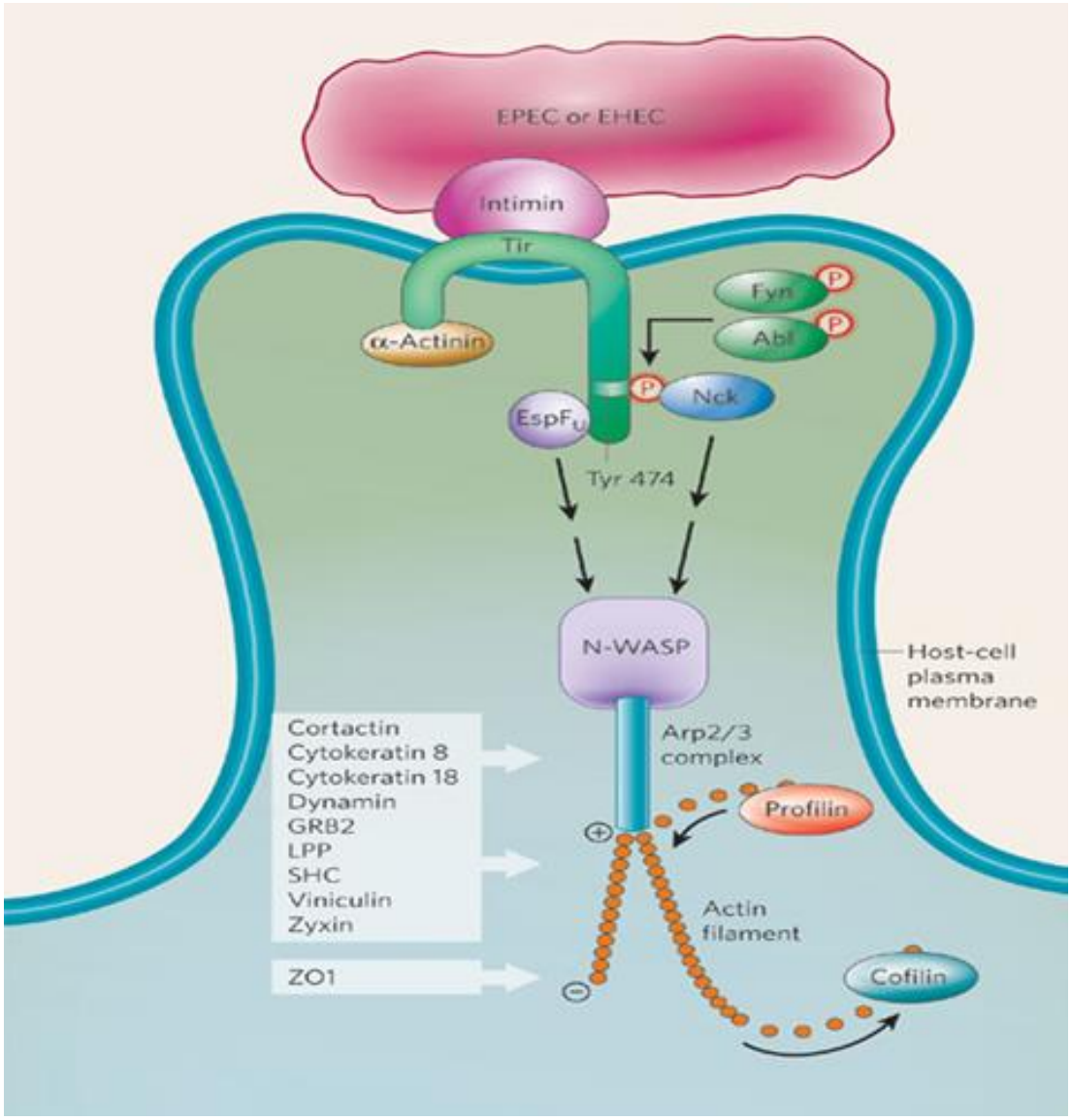
EPEC or EHEC
Intimin
Tir
α-Actinin
Fyn
Abl
Nck
EspF
Tyr 474
N-WASP
Host-cell plasma membrane
Cortactin
Cytokeratin 8
Cytokeratin 18
Dynamin
GRB2
LPP
SHC
Viniculin
Zyxin
ZO1
Arp2/3 complex
Profilin
Actin filament
Cofilin

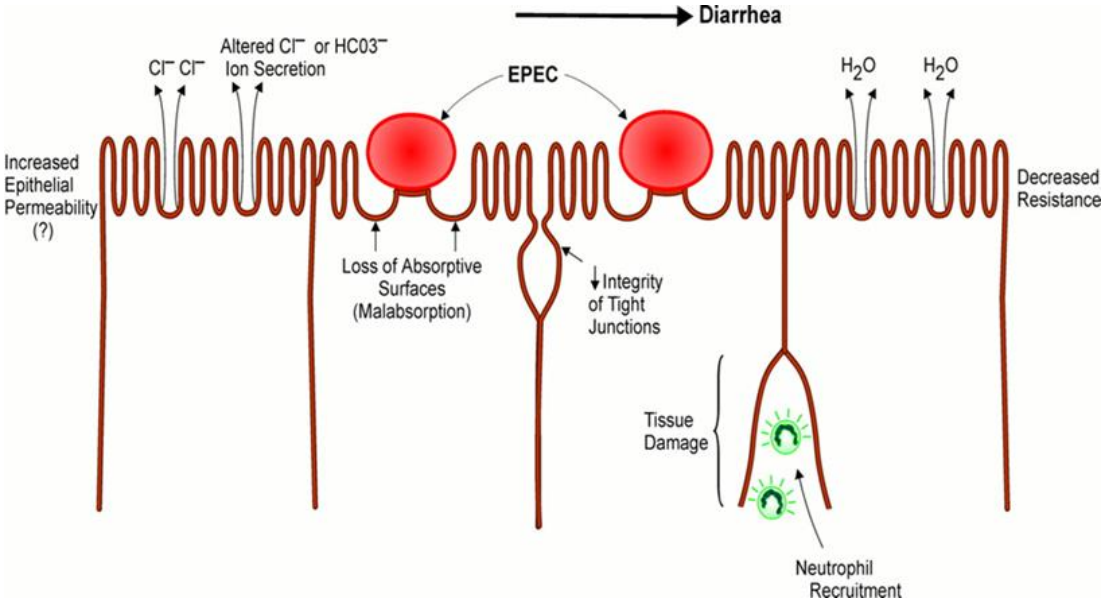
Diarrhea
Cl⁻ Cl⁻
Altered Cl⁻ or HC03⁻ Ion Secretion
EPEC
H2O
H2O
Increased Epithelial Permeability (?)
Decreased Resistance
Loss of Absorptive Surfaces (Malabsorption)
Integrity of Tight Junctions
Tissue Damage
Neutrophil Recruitment

Figure 1.14: EPEC intimate attachment triggers signal transduction and loss of tight junction. (a) EPEC intimate attachment to the host cell by intimin-Tir binding. Host cell cytoskeletal rearrangements stimulate formation of cuplike pedestal under bacterial attachment site and activate actin polymerization cascade through signal transduction. (b) Different factors including reduced tight junction, tissue damage, and loss of absorption surface due to pedestal formation and alteration of epithelial permeability are associated with diarrhea caused by EPEC (221).

1.7 EspC, The serine protease autotransporter of EPEC

Extensive studies found different autotransporter encoding genes in diarrheagenic *E. coli* pathotypes including EPEC(113). EspC was the most common and active protease AT identified among tEPEC and aEPEC groups(233). EspC is a SPATE (94,234). EspC is not significantly involved during attachment or invasion of tissue culture cells(234). EspC, like other members of the SPATE superfamily is a highly immunogenic protein(235). Serological studies suggested that EspC is strongly detected in infected individual's serum 28 days after infection and serum negativity was also reported before infection(149,236). EspC is not encoded within LEE region and is thus classified as a NLEE autotransporter(237). The *espC* gene is located within a second EPEC pathogenicity island at 60 min on the chromosome of *E. coli*. Recent study revealed DNA sequences located at 59.35 min in the EHEC1, EPEC2, and EHEC2 strains were not similar to the same location of the chromosome in *E. coli* K-12 strain MG1655(237). Although EspC is a non-LEE-encoded protein, the regulation of *espC* is influenced by the global regulator Ler encoded in LEE that controls virulence gene expression during EPEC pathogenesis such as genes encoding the T3SS, secreted Esp proteins, Tir, and intimin(238).

This protease AT first utilizes the classical type Va secretion system to reach the extracellular space, and then may exploit the type III secretion system for host epithelial cell interaction and final injection into the target cell(239,240).

Like other classical monomeric autotransporters, EspC is composed of 3 domains. First, the leader peptides located in the N-terminal region that enables the protein secretion process across the inner membrane(113). Next, the Passenger domain composed of conserved serine protease motif GDSGS acts as the functional unit of the autotransporter and finally the COOH terminal domain

that inserts into the outer membrane to facilitate mature protein translocation to the target cell(113,236). EspC has a specific sequence motif composed of amino acids Gly-Phe-Ser (termed as GFS motif) which one study found by site-directed mutagenesis (SDM) is necessary for successful translocation of EspC(149). Although *espC* is located in a second pathogenicity island on the EPEC chromosome, the role and function of EspC and its pathway of secretion is not completely known(237). In general, the *espC* open reading frame (ORF) encodes a protein of approximately 140 kDa (1,306 amino acids) however, the secreted version identified in culture supernatants has a size of approximately ~110 kDa which represents the passenger domain between amino acids 54 to 1,030. The secreted 110-kDa form of EspC lacks the first 53 amino acid signal sequence and potentially the C-terminal β-barrel domain is located between amino acids 1,031 to 1,306(234,241).

In recent years, preliminary studies on rat intestinal tissues identified the role and relationship of EspC with enterotoxin activity when potential and current differences increased in Ussing chambers(237). In addition, incubation of a high concentration of EspC with HEp-2 cells (a specific epithelial cell line) *in vitro* suggested that this autotransporter can produce and induce cytopathic and cytotoxic effects (235,237,238). Studies also suggested that the cytotoxicity effect of EPEC depends on complete fusion of EspC with Epithelial host cell membranes and translocation of the serine protease motif (passenger domain) into the target site(238). Another study proposed that injection of EspC protein into the target cells could produce unique cytopathic effect by generating abnormal round cells, cell separation and contraction of the actin cytoskeleton(238,239). This cytopathic effect was explained by EspC protease activity cleaving cytoskeletal factors such as fodrin, paxillin and focal adhesion kinase during infection(238,242). In terms of infection biology, it appears that EspC involvement with epithelial cell damage occurs during attachment and actin polymerization steps(242). Moreover, cytopathic studies also indicated that EspC is associated with pepsin factor V and spectrin proteolysis in human cells(236,242). It is widely accepted that Iron uptake systems from the environment and human host are necessary for survival of pathogenic bacteria(243). Recent studies on different EPEC strains revealed the proteolysis of haemoglobin by EspC, and acquisition of Iron from heme containing proteins *in vitro*. It is argued that EspC acts as an Iron-binding protein during infection (236). As for other AT's the molecular details of the secretion pathway followed

by EspC are unclear. Interestingly, previous study in our laboratory suggested that EspC follows a spiral pattern of localization as it exits the bacterial cell producing it(113,244). It is possible that this is mediated by accessory factors and elucidating the details would shed light on secretion of the AT family or identify potential novel targets for antimicrobials. Different periplasmic and OM accessory factors like the BAM complex and TAM have been proposed to facilitate AT translocation(245,246). It remains unclear if any of these mediate the spiral distribution of EspC during secretion. New therapeutic targets are needed due to the rise in AMR, and in order for a new drug to be released its mechanism of action and target need to be understood. This information is also important to undertake the development from lead hit molecule to the most effective and efficacious drug.

1.8 Arginine-specific AT of *P. aeruginosa* (AaaA)

Pseudomonas aeruginosa is a common Gram-negative opportunistic rod shape pathogen that is widely distributed in nature(247,248). Due to its dynamic metabolic pathways, this bacterium survives and adapts in different environmental conditions including the human body and clinical hospital settings(249). In the human population, it is responsible for around 10% of nosocomial infections with high mortality and morbidity worldwide(250,251). A broad range of illness, from UTI to burn and respiratory infection, are linked to this microbe and severe forms are usually reported in immunocompromised and Cystic fibrosis (CF) patients(252–254). Cystic Fibrosis is a multisystem inheritable genetic disorder where patients suffer from a defect in the CF transmembrane conductance regulator (CFTR) gene(253). The CFTR regulator controls electrolytes and chloride transport across the cell membrane and is involved in homeostasis. In the absence of this regulatory protein, mucus layers in the lung become thick and sticky(253). However, bacterial infection in CF patient mucus layers can also cause mortality and morbidity and are mainly prone to *Pseudomonas aeruginosa* respiratory infections from early childhood(248).

P. aeruginosa has a natural resistance to different types of antibiotics and diverse virulence that is encoded by its large, 6.3 mega Bases (MB), genome and susceptible to high genetic rearrangement and acquisition(255). *P. aeruginosa* Multi-drug and pan-drug resistant strains are increasing worldwide and are

becoming difficult to treat as these strains are resistant to most used antibiotics including aminoglycosides, cephalosporins, fluoroquinolones, and carbapenems(248). In general, the main mechanisms *P. aeruginosa* uses to confront antibiotic empirical treatment can be divided into intrinsic, acquired and adaptive resistance(256). The intrinsic resistance of *P. aeruginosa* is composed of different mechanisms such as reducing Outer membrane permeability, expression of efflux pumps that return antibiotics out of the cell and the production of specific enzymes that inactive antibiotics(256). The acquired resistance of *P. aeruginosa* happens through horizontal transfer of resistance genes or mutational changes(256). The adaptive resistance of *P. aeruginosa* involves biofilm formation in the lungs of chronically infected patients that prevents antibiotic access to the bacterial cells(256).

Complex genotypic processes help bacterial survival during infection and antibiotic treatment(248). In the early stages of infection, different virulence factors and innate antibiotic resistance mechanisms facilitate bacterial survival(248). Treatment with antibiotics and host inflammatory immune responses create oxidative stress(248). This environmental stress condition activates expression of different genes that enable adaption and a switch to persistent and resistant phenotypes(248).

In early stage of acute infection, host and pathogen interaction is mutually harmful as bacterial cytotoxic molecules damage the host natural cell metabolic process and on the other hand, the host immune response creates antimicrobial agents and induces phagocytosis for bacteria(248). In this condition, motile *P. aeruginosa* are better adapted and more pathogenic phenotype(248).

In chronic infection, *P. aeruginosa* can switch to an immobile lifestyle with less pathogenicity to enable adaptation and bacterial persistence under harsh environmental condition(248). In this protective mechanism, bacteria attach to abiotic and biotic surfaces and create microcolonies through cellular aggregations after losing motility(248). These structures are so called biofilms and provide protection against oxidative stresses, metabolic waste, nutrient restriction, antibiotics and microbial competition(248). The bacterial cells in biofilms are embedded in a self-produced matrix of extracellular polymeric substances (EPS) that form their surrounding environment(253). The matrix creates a favourable

condition for biofilm mechanical stability and bacterial cell to cell communication(248).

Due to metabolic diversity, *P. aeruginosa* strains generate different secondary metabolites and polymers and utilize different carbon sources(248). *P. aeruginosa* stains PAO1, PA14 and PA7 are recognized by the International *Pseudomonas aeruginosa* Consortium based on single nucleotide polymorphisms (SNPs) within the core genome comparison (257).

In *P. aeruginosa*, three classical autotransporter proteins (Va) were identified from the PA01 genome(255). These have now been known as EstA (Wilhelm *et al* 1999), EprS (Kida *et al* 2013) and AaaA (Luckett *et al* 2012). In addition, Proteins belonging to the TPS system (Vb) (Kida *et al* 2008) and the patatin-like autotransporters (Vd) (da Mata Madeira *et al* 2016) secretion system have also been reported.

PA0328 autotransporter was first recognized as a cell-surface tethered autotransporter with arginine-specific aminopeptidase activity (AaaA)(258). This important virulence factor autotransporter is a Va classical AT (259). AaaA cleaves and releases L-arginine from the N-terminus of peptides or proteins, although these have not been specifically identified. AaaA may also enable nitrogen uptake under low oxygen conditions such as those found during biofilm formation by providing arginine as an energy source in microaerophilic pockets (253,258,260). It has not been ruled out that AaaA may activate a bacterial protein, or inactivate a host protein to aid virulence, but it has been shown that it is required for chronic rather than acute infections of the skin and lungs(258).

Like EspC, AaaA has been localized to a spiral within the bacterium that produces it (homogenously in *P. aeruginosa*, or heterologously in *E. coli*). FRET has shown that the spiral structure is dynamic, ie that EspC and AaaA do not remain in the same position in the cell for very long, and this provides a potential mechanism of secretion that pushes the nascent AT from the centre of the bacterium to the poles as it exits the cell(113,244). The molecular interactions and mechanistic steps occurring during this translocation are not yet understood.

AaaA is not released into the extracellular environment. Instead it is tethered to the bacterial outer membrane so that only the passenger domain interacts with medium (253,258). This feature of AaaA provides an ideal target for novel

synthetic antimicrobial agents due to its surface exposure and easy accessibility. It is therefore important to understand its role in pathogenicity and to characterize the network of regulation that controls its production so that potential novel treatments can be used effectively.

1.9 Aims and objectives

Since it has become evident recently that ATs do not entirely undertake secretion in isolation, but likely interact with accessory factors during their export to the bacterial surface, the following areas of interest were investigated in this study:

- Characterisation of the potential of putative accessory factors to facilitate secretion of the EspC and AaaA autotransporters
- Interrogation of the promoter of *aaaA* to identify potential regulators

Chapter 2

2. Materials and Methods

2.1 General Chemicals

Chemicals used in this study were provided by Sigma bioscience (UK) unless otherwise mentioned, and biosafety protocols followed according to manufacturer's instructions.

2.2 Bacterial Growth Media

Bacterial strains used in this study were cultured in Lysogeny broth (LB) media. The LB broth (Oxoid Ltd) was prepared in 1L batches by dissolving 10 g tryptone, 5 g yeast extract and 10 g NaCl in 950 mL deionized water. pH adjustment to 7.0 was performed using 1N NaOH before bringing volume up to 1 L as described by Sambrook et al., 1989(261). To prepare LB agar, 0.8% (w/v) technical agar No. 3 (Oxoid Ltd) was added. Media was sterilized by autoclaving at 121°C on liquid cycle for 20 min at 15 psi. After cooling in a water bath to 55°C for 5-10 min, antibiotic was added if required (see table 2.1). LB media were stored at room temperature or 4°C for future use. *Pseudomonas* Isolation Agar (PIA) was prepared according to Sigma bioscience (UK) manufacturer's instructions. Freshly plated *P. aeruginosa* and *E.coli* strains containing plasmids were always used for plasmid extraction and other DNA analysis to avoid mutation.

2.3 Growth and storage Conditions

Bacterial strain colonies were obtained after overnight incubation at 37°C on LB agar. For LB broth, inoculated strains were propagated overnight at 37°C shaking with 200 rpm. Frozen stocks were prepared by adding 1ml of 50% v/v Glycerol into the same volume of an overnight LB broth culture to give a 25% final concentration of glycerol for general storage. Strains were kept frozen in special cryovial Eppendorf tubes at -80°C for future use. Glycerol stocks for the School of Life Sciences, Nottingham University main strain collection were also prepared by mixing overnight culture and sterile 80% v/v glycerol in a 1:1 ratio.

2.4 Antibiotics

Antibiotics used in this study added to selective media when necessary, according to table 2.1. Storage aliquots kept at -20°C for future use.

Table 2.1: List of antibiotics and concentration used for selective media preparation.

Antibiotic	Stock Concentration	Working Concentration
Ampicillin	100 mg/mL	100 µg/mL
Chloramphenicol	25 mg/mL (in ethanol)	*E. coli* 25 µg/mL *P. aeruginosa* 400ug/ml
Gentamycin	10 mg/mL	10 µg/mL
Kanamycin	50 mg/mL	50 µg/mL
Tetracycline	10 mg/mL (in 50% ethanol)	*E. coli* 10 µg/mL *P. aeruginosa* 200ug/ml

2.5 Optical density (OD_{600nm})

The spectrophotometer (Thermo Scientific) was used in all experiments to measure cell density prior to normalisation. A volume of 1 ml was placed into a cuvette (Fischer Scientific) and the readings compared to a blank medium sample. Cultures with readings greater than 1.0 OD_{600nm} were diluted to fall within the range of accuracy of the spectrometer.

2.6 Gene Expression and induction condition

The pBAD vector system was used in this study for expressing recombinant proteins in bacteria. This system is based on the *araBAD* operon, which controls *E. coli* L-arabinose metabolism. The gene of interest is placed into the pBAD vector downstream of the *araBAD* promoter, which drives expression of the gene of interest in response to L-arabinose and is inhibited by glucose.

For gene expression of pBAD vectors under the control of *araBAD* promotor, L-Arabinose was used for induction prior to protein sample preparation. 20% (w/v)

L-arabinose stock solution prepared and 0.22 µm filters provided by Sartorius Stedim Biotech (Minisart®) were used before storage. 0.2% final concentration (w/v) of prepared L-arabinose stock solution was added to each sample for gene expression.

For recombinant protein expression, bacterial overnight cultures were diluted 1:100 in fresh LB broth. Growth of bacterial cells was measured by absorbance readings at a wavelength of OD_{600nm}, using a Thermo Biomate 3 Spectrophotometer until it reached 0.5, when the arabinose was added and then cultures were incubated for 2 hour more with shaking at 37 °C.

2.7 Plasmids used to investigate *aaaA* expression and regulation

Mini CTX-Pkan-lux (constitutive control) and mini CTX-PaaaA-lux plasmids (WT) were previously constructed by other PhD students in our group. Mini CTX PaaaA△rpoNmotif -lux was constructed in this study. All plasmids for *aaaA* expression and regulation listed in Supplementary Table 1.

2.8 Plasmids used for AT localization experiments

All plasmids in this study for localization listed in Table 2.2.

Table 2.2: List of Plasmids used in this study for characterizing the Localisation of fluorescently labelled EspC and AaaA.

Plasmid	Description	Construct depiction	Protein Size	Antibiotic	Ref.
pLA33C1	pBAD33 containing native *espC* gene under the control of an *araBAD* promoter.	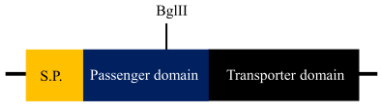	140 kDa	Cm^r	(244)
pLA33C1mc	pBAD33 encoding EspC-mCherry fusion (mCherry ORF was inserted at the *BglI*I site approximately in the middle of passenger domain of EspC) under the control of an *araBAD* promoter.		174 kDa	Cm^r	(244)
pMAC33	pBAD33 encoding truncated EspC-mCherry (a stop codon introduced at the end of *mCherry* gene causes a frameshift to truncate translation before the transporter domain) under the control of an *araBAD* promoter	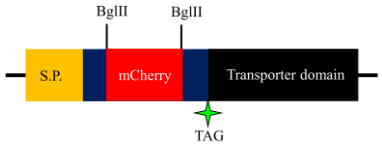	~70 kDa	Cm^r	(244)

Plasmid	Description	Construct depiction	Protein Size	Antibiotic	Ref.
pbadSlyBhis(A)	*slyB* + his tag in C-term cloned into pBad24 under the control of an *araBAD* promoter.	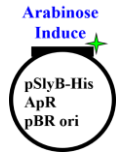	28KDa	Amp	(262)
pbadSlyB	*slyB* gene cloned into pBad24 under the control of an *araBAD* promoter.		25KDa	Amp	(262)
pLA33AaaA	pBAD33 containing native *aaaA* gene under the control of an *araBAD* promoter.		80 kDa	Cm^r	(244)
pLA33C1-TC 531aa	*espC* gene tagged with FlAsH tag CCPGCC at position 531aa	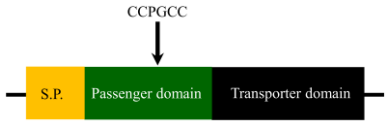	80 kDa	Cm^r	(244)
pLA33AaaA-TC-TAG343aa	*aaaA* tagged with CCPGCC at 292aa and further inserted with amber stop codon at position 343aa to generate AaaA truncated version	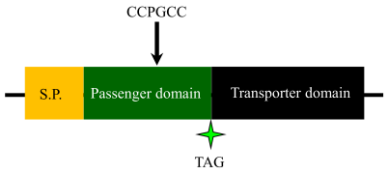	80 kDa	Cm^r	(244)

2.9 Bacterial Strains

The bacterial strains used in this study are listed in Supplementary Table 2.

2.10 Molecular DNA Analysis and DNA manipulation

2.10.1 DNA preparation

GenElute™ plasmid miniprep kits (Sigma) were used for extraction of plasmids according to manufacturer's instruction. Elution was performed with water rather than the provided elution buffer.

Chromosomal DNA was extracted using a genomic DNA kit (Promega wizard) according to the manufacturer's instructions. Purification of DNA was achieved by using the DNA clean up kit (Qiagen).

Concentration and absorbance characteristics of extracted DNA were measured by the NanoDrap® ND-1000 (Nanodrop Technologies). 1.5ul of samples was applied for measure purity.

2.10.2 Restriction enzyme digestion of DNA

Restriction enzymes used in this study were provided by New England Biolabs (UK) and Promega (UK). These enzymes were used according to the manufacturer's instruction. In general, a 25-50µl total volume reaction was prepared from 500-1000ng plasmid DNA, 2.5-5 µl of 10x suitable restriction buffer and molecular biology grade H_2O (Fisher Scientific, UK) added up to desired final reaction volume. A volume of 0.5-1µl restriction enzyme was mixed into the reaction last for effective digestion. Samples then incubated in 37°C for 1-2 h and analysed by agarose gel electrophoresis.

2.10.3 DNA analysis on gel electrophoresis

A DNA sample of 5µl was combined with 2µl of New England Biolabs (UK) loading dye before being loaded onto a 0.8% (W/V) agarose gel. Agarose gels were prepared using agarose BioReagent for molecular biology (sigma) mixed with 1x tris-acetate-ethylenediaminetetraacetic acid (TAE) buffer(263). An aliquot of 5 µl SYBR® Safe DNA Gel Stain concentrate was used before loading the samples on the prepared gel. The gel was then transferred in 1× TAE buffer and electrophoresis conducted at 100V for 50min. DNA fragments were visualized on Biorad Gel DOC™ XR+ with image Lab™ Software.

2.10.4 Molecular Weight Marker

4-5 µl of 1kb DNA ladder (New England Biolabs (N3232S), UK) were used for estimation and measurement of DNA fragments.

2.10.5 Oligonucleotide primers

Primers used in this study are listed In table 2.5 .

Table 2.3: list of all primers used in this study for plasmid confirmation and sequencing. Bold part are restriction digestion sequences.

Primer Name	Primer sequence (5'→3')	Restriction sites	Gene Ref (Plasmid)
FslyB	ACG GTT **TCT AGA** TCA ATG ATT AAA CGC GTA TT	*xbaI*	Louise Arnold: hybridises from 3bp upstream of *slyB* atg
RslyB	CGT AAC **GAG CTC** TAT TTA GCG CGG AGA AACGG	*sacI*	Louise Arnold: hybridises over stop codon plus 3bp downstream *slyb*
FproU	GGT TAC **GAG CTC** ATA ATG GCT GAT CAA AAT AA	*sacI*	Louise Arnold: hybridises from 3bp upstream of *proW* atg
RproU	ATT GCA **TCT AGA** GTG CAG AGT TAC TTAATGAAT	*xbaI*	Louise Arnold: hybridizes over stop codon plus 9bp of *proW*
RyqjE	TAT GGT **GAG CTC** ACT TTA CTG CTC ACG GGA CT	*sacI*	Louise Arnold: hybridises over stop codon plus 3bp of *yqjE*
FyqjE	ATG GCT **TCT AGA** TAA TAC CGC CTG TGA GTA GT	*xbaI*	Louise Arnold: Zebrafish and listeria
RybgC	GCA TGC **GAG CTC** GTG AAT ACA ACG CTG TTT CG	*sacI*	Louise Arnold: hybridizes over stop codon plus 3bp upstream of *ybgC* (gene backwards)
FybgC	TAT CGT **TCT AGA** AGT CAC TGC TTA AAC TCC GC	*xbaI*	Louise Arnold: hybridizes from 2bp downstream of *ybgC* atg
Rnei	ACT GGA **GAG CTC** ACC ATG CCT GAA GGC CCG GA	*sacI*	Louise Arnold: hybridises from 5 bp upstream of atg of *nei*
Fnei	GCT TAG **TCT AGA** GGC CTA GTG CTG GCA GCC AG	*xbaI*	Louise Arnold: hybridises over stop codon of *nei*
yqjEF*2	AGC CTA **GAA TTC** ATG GCG GAC ACT CAT CAC	*ecoRI*	Louise Arnold: hybridises over start codon of u*qjE*
yqjER*2	GCA TCA **TCT AGA** TTA CTG CTC AGG GGA CTC	*xbaI*	Louise Arnold: human chromosome
slyBF*2	TCT AGC **GAA TTC** ATG ATT AAA CGC GTA TTG	*ecoRI*	Louise Arnold: hybridises from 3bp upstream of *slyB* atg

Continued from previous page...

Primer Name	Primer sequence (5'→3')	*Restriction sites*	Gene Ref (Plasmid)
slyBR*2	CTG AAT **TCT AGA** TTA GCG CGG AGA AAC GGT	*xbaI*	Louise Arnold: hybridises over stop codon plus 3bp downstream *slyb*
FsapA	ACT GTG GGT GC no hits on blast	…….	Louise Arnold: thesis acg ctg aaa ctg tgg gtg c hybridizes in middle of *sapA*, 400bp from stop codon
RsapA	GTT CGC **GAG CTC** TAA TCA TGG TTT TTT CAC CT	*sacI*	Louise Arnold: hybridises over stop codon plus 3bp of *sapA* (gene backwards)
F-espC	TTTATCGCAACTCTCTACTGTTT	…….	Designed by Mahmoud M. Ashawesh
R-ApaI-espC	TGCATGCCTGCA**GGGCCC**GGTCGACTCTAGG	*ApaI*	Designed by Mahmoud M. Ashawesh
RpoN SDM Forward II	ATCCTAATTT**CCGCGG**CGCGAGCAT	*SacII*	Designed by Frances Smith
RpoN SDM Reverse II	GCGGATTGTTTCATGTCTCTGGAGCACGAATTGAC	…….	Designed by Frances Smith
SA1 Forward	TCCTGAGTATTATTTCACAAATACC	…….	In this study
SA2 reverse	GCGTAATACGACTCACTATAGG	…….	In this study
PDM4 Forward	CACAGGAACACTTAACGGCTG	…….	In this study
PDM4-Reverse	GGGTGATGCTGCCAACTTAC	…….	In this study
Forward AaaA PAO1 Primer	CATGCACGGCCTGAAGCG	…….	In this study
Reverse PAO1 AaaA primer	CGCGAGCATCATTCGATGC	…….	In this study
rpon-FW PAO1 Primer	GTTTCGCAACCACGAGTGC	…….	In this study
rpon Reverse PAO1 primer	CAGTTTCTCGCCGACATAGTC	…….	In this study

2.10.6 Q5 Site-Directed Mutagenesis Kit (NEB) and KOD DNA Polymerase

The primers for site-directed mutagenesis were designed using the web-based NEBaseChanger® tool (http://nebasechanger.neb.com). Substitution mutations were made in the 500bp upstream promoter region using site directed mutagenesis according to the recommendations in the Q5 SDM protocol. Briefly, PCR amplification was carried out based on following KOD Xtreme standard reaction setup and step-down cycling conditions (tables 2.6, 2.7). The PCR reaction product was then dialysed to remove excess salts and then treated with Kinase (phosphorylation), ligase (intramolecular ligation/circularization) and DpnI (template removal) to leave only the synthesised plasmid. Together, these enzymes allow for rapid circularization of the PCR product and removal of the template DNA. KLD reaction was incubated for 5 minutes at RT. This was then transformed into chemically competent *E. coli* NEB5α by heat shock Procedure and the cells were grown on tetracycline 30 µg/ml LB agar overnight at 37°C(264).

Table 2.4: Q5 SDM recommended conditions used in this study.

Component	Volume	Final Concentration
2X Xtreme Buffer	25 µl	1X
dNTPs (2 mM each)	10 µl	0.4 mM (each)
PCR Grade Water	X µl	
Sense (5') Primer (10 µM)	1.5 µl	0.3 µM
Anti-Sense (3') Primer (10 µM)	1.5 µl	0.3 µM
Template DNA[a]	Y µl	
KOD Xtreme™ Hot Start DNA Polymerase (1 U/µl)	1 µl	0.02 U/µl
Total reaction volume	**50 µl**	

Table 2.5: Step down cycling PCR conditions for site directed mutagenesis used in this study. Annealing temperature modified based on the nature of primers.

Step-down cycling	
1. Polymerase activation	94°C for 2 min
2. Denature	98°C for 10 s[b]
3. Annealing/Extension	74°C for 1 min/kbp
Perform Steps 2 and 3 for 5 cycles	
4. Denature	98°C for 10 s[b]
5. Annealing/Extension	72°C for 1 min/kbp
Perform Steps 4 and 5 for 5 cycles	
6. Denature	98°C for 10 s[b]
7. Annealing/Extension	70°C for 1 min/kbp
Perform Steps 6 and 7 for 6 cycles	
8. Denature	98°C for 10 s[b]
9. Annealing/Extensions	68°C for 1 min/kbp

2.10.7 Conventional PCR Amplification

For standard or conventional PCR, 25 µl total volume reaction prepared from Q5® High-fidelity PCR Kit (New England BioLabs (E0555S/L), UK) was use according to manufacturer's instructions(265) . Prepared reactions were then transferred into the SensoQuest Labcycler (SensoQuest GmbH) for 35-cycle heat reaction.

2.10.8 DNA Sequencing

DNA sequencing was performed by Source BioScience, Nottingham using Sanger sequencing services and ABI3730XL sequencer. Prepared sequence data were downloaded via Source BioScience SpeedREAD automated data delivery system and analysed using the SnapGene® software. Alignment of DNA or protein

sequences to identify homology was achieved using the Basic Local Alignment Search Tool 'BLAST' provided by NCBI (http://blast.ncbi.nlm.nih.gov/Blast.cgi). The Sequences of the pre-determined DNA and protein were obtained from the NCBI (http://www.ncbi.nlm.nih.gov/) using gene and protein databases, respectively.

Table 2.6: Conventional PCR condition used in this study. Annealing temperature modified based on the nature of primers.

PCR Mix		
Components	**Volumes**	**Final concentration**
Q5 High-Fidelity 2X Master Mix	12.5 µl	1X
10 µM Forward primer	1.25 µl	0.5 µM
10 µM Reverse primer	1.25 µl	0.5 µM
DNA template	variable	25 ng-75 ng
Nuclease-Free Water	to 25 µl	
Thermocycling conditions		
Cycle Stage	**Temperature**	**Time and Repetitions**
Initial denaturation	98°C	30 sec / one cycle
Denaturation	98°C	10 sec
Annealing	55°C *	30 sec
Extension	72°C	30 sec every 1kb
Final Extension	72°C	2 min / one cycle
Hold	4°C	Pause

35 cycles

2.11 Transfer of genetic material into bacteria

The plasmids used in this study were either conjugated or transformed into *P. aeruginosa* or *E. coli* strains as is described in Sambrook et al (1989) molecular cloning laboratory manual(263).

2.11.1 Conjugation

The *E. coli* strain S17-1 λpir (table 2.4) was used in conjugation reactions as the donor strain. Conjugations were performed based on Westfall et al (2004). Single colonies of *E. coli* S17-1 λpir and the recipient *P. aeruginosa* strain were

grown overnight in 10 ml of LB at 200 rpm. *E. coli* S17-1 λpir was grown at 37°C while *P. aeruginosa* was grown at 42°C to reduce the effect of the restriction/modification system. An aliquot of 1ml from each of the overnight cultures was transferred into Eppendorf tubes and subsequently washed twice with LB using a microfuge to centrifuge the cells (Biofuge Pico Heraeus) for 5 min at 2571 X g. The pellet was then resuspended in 50µl of LB. The donor and recipient strains were combined at a ratio of 1:1. The cells were plated onto well dried LB agar plates and incubated for 6 hours at 30°C. Following this, the cells were scraped off using a sterile loop and placed into an Eppendorf tube containing 1 ml of LB. 50µl suspension was plated onto PIA plates containing the appropriate antibiotic for selection.

2.11.2 Chemical bacterial transformation

Competent mutant *E. coli* cells were first prepared from 1:100 dilution of 1ml overnight *E. coli* culture into 99ml of sterile LB broth in 500ml flasks. Second, the flasks were incubated at 37°C with shaking at 200 rpm for around 2 hours until they obtained OD_{600nm} of 0.4-0.6. Bacterial cells were harvested by transferring 100ml of LB into centrifuge tubes and spun (Allegra™X-22R centrifuge, Beckman Coulter) at 3000 rpm for 10min at 4°C and the supernatant discarded. The cells were resuspended in 25ml 100mM $MgCl_2$ (Sigma-Aldrich, UK) at 3000 rpm for 10min at 4°C and the supernatant discarded. Afterwards, bacterial cells were resuspended with 50ml 100mM Cacl2 (Sigma-Aldrich, UK). Incubate on ice for 60min and then supernatant discarded after spin at 3000 rpm for 10min at 4°C for harvesting the cells. The pelleted cells were resuspended on ice with 5 ml 100 mM $CaCl_2$ (Sigma-Aldrich, UK). Finally, competent cells were transferred into pre-chilled Eppendorf tubes and aliquots of 300µl of competent cells used for heat shock transformation. For longer storage, competent cells were stored in -80°C in 10% glycerol.

2.11.3 Heat shock Transformation

Heat shock transformation was conducted by transferring 100ng (1-2ul) to 300ul $CaCl_2$ prepared competent cells. Next, *E. coli* cells were incubated on ice for 45 min before 1-2 min heat shock following 2 min incubation on ice. 500 µl of LB liquid was added to recipient cells and incubated at 37 °C for 60 min with shaking. After incubation, cells were centrifuged for 2 min at 5500 rpm and the supernatant discarded. Cells were then resuspended with 60µl sterile LB broth.

Volumes of 10ul or 50ul of cells were applied to LB plates containing appropriate antibiotics. Plates for further investigation and colony observation were incubated overnight at 37°C. For each batch of competent cells, a negative control of heat-shocked cells without plasmid were prepared and for each transformation a separate plate lacking antibiotics was inoculated to verify viability.

2.11.4 Transformation by electroporation

The *E. coli* strains DH5α were used in transformation reactions. electroporation was also the transformation method of choice.

2.11.5 Preparation of electrocompetent cells

Electroporation was used for transformation of plasmid DNA into *E. coli* electrocompetent cells. Bacterial cultures were grown overnight with appropriate antibiotics in LB, diluted 1/100 into 200ml of LB and grown to OD_{600nm} = 0.3 at 37°C. Cells were harvested at 3000 rpm (Allegra™X-22R centrifuge, Beckman Coulter) for 20 mins at 4°C. Washed three times in 20ml of cold dH_2O and then washed one time in sterile 10% v/v/ glycerol. Final pellets were resuspended in 500 µl 10% glycerol. Aliquots of 100 µl were frozen at -80°C immediately for future use.

2.11.6 Electroporation

Electroporation Gene Pulser®/MicroPulser™ Cuvettes (Equibio) were chilled on ice for 15 mins before use. 50µl of competent cells were mixed with 10-100ng (1.5µl) of plasmid DNA. The cuvettes were dried and immediately electroporated using a Bio-Rad Gene Pulser set at EC2 for 2ml and 2.4kV. A volume of 500ul of prewarmed LB broth was added to the cuvettes immediately after electroporation, and cells were incubated shaking at 37°C for 1 hours. Cells were then incubated overnight on selective LB agar plates. Cells with the addition of 1µl of nuclease-free water were used as a negative control.

2.11.7 Screening of colonies following transfer of DNA

In the case of the miniCTX-*lux* vector, post-conjugation and post-transformation plates were viewed under the light camera (Hamamatsus, Wasabi software) and colonies selected which produced light.

2.12 Gene replacement using pDM4

Colonies from pDM4 double mutant plates were grown in LB overnight at 37°C with shaking at 200 RPM with 20 ul of these cultures used to inoculate 5 ml of LB broth containing 5% (w/v) sucrose (Sigma). These were grown for 24 hrs at 37°C with shaking at 200 RPM. After around 5 hours, recombinant cultures were seen to slow in the rate of growth in comparison to wild type and these were maintained and grown for 24 hours. Subsequently, these cultures were used to inoculate LB agar plates containing 5% sucrose (w/v) (Sigma), and incubated overnight at 37°C.

2.13 P-nitroanilide degradation assay

To measure AaaA activity, a colourimetric assay using the molecule L-arginine-P-nitroanilide was utilised. When P-nitroanilide was released from L-arginine, a yellow colour was observed and the concentration of this quantified using an automated plate reader (Anthos LUCY). Strains were assayed in minimal media P (MMP) prepared according to Haas, D *et al* (1997) containing Na_2HPO_4 10.4 mM, KH_2PO_4 4.8 mM, $MgSO_4$ 1.7 mM, $FeSO_4$ 6.6 µM (Sigma). L-arginine- P-nitroanilide was added at a final concentration of 0.5mM. Overnight cultures were normalized to 0.25 OD_{600nm}. The cells were then washed 2 times in MMP with centrifugation at 3707 Xg for 5 minutes to separate the pellet from supernatant. Following the final centrifugation, the supernatant was discarded, and the pellet resuspended in 1 ml of MMP. For each bacterial strain, 3 wells in a sterile clear bottomed 96 well plate (Greiner bio1 F bottom) were prepared with 150µl of the 1 mM working solution of arginine-p-nitroanilide and 150µl of the OD_{600nm} 0.25 bacterial suspensions. The degradation of arginine-p-nitroanilide was determined by 1h measurements of OD_{405nm} for 24 h at 37^{o}C in an automated plate reader.

2.14 Tecan assay to measure gene expression using the miniCTX-lux transcriptional reporter

Mini CTX-lux was chosen as the reporter for this study. This luciferase reporter provides rapid and quantitative measurements of gene expression. 500bp upstream region of *aaaA* containing the promoter was cloned into a plasmid next to the *lux* operon that encodes for enzymes that generate light (Mini CTX-PaaaA-lux reporter). As a control: the constitutive promoter of the kanamycin

resistance cassette was also cloned next to the *lux* operon to monitor whether the production of light altered independently of the aaaA promoter (Mini CTX-Pkan-lux). The CTX-lux reporters were introduced into mutants of regulators hypothesized to play a role in regulation of *aaaA* expression and light production was measured during growth over 24 hours.

Minimal media P (MMP) was prepared including M9 salt, 1M $CaCl_2$, 1M $MgSO_4$ and 1M Glucose. The O/N cultures were normalised to an OD_{600nm} of 0.05. A volume of 200 µl was added in triplicate to Greiner 96 well flat black microtitre plates. To prevent evaporation wells surrounding the samples were always inoculated with LB media.

Cell density (OD_{600nm}) and Bioluminescence were measured in an Infinite 200 (Tecan). Readings were taken every 30 minutes during the run, temperature of 37°C was maintained and no shaking was included.

2.15 Statistical analysis

Statistical analyses Paired Student's t tests were performed using the GraphPad Prism 6 Software and General ANOVA summary test analysis also measured. A non-significant result is indicated by 'ns', a P value of <0.05 by 1 asterisk, <0.01 by 2 asterisks, <0.001 by 3 asterisks and <0.0001 by 4 asterisks.

2.16 Protein analysis

2.16.1 *E. coli* whole cell and secretory protein preparation

For protein analysis, *E. coli* stains were first cultured in LB broth overnight. After finishing the induction time, the OD_{600nm} of the culture was measured and 1 ml aliquots removed from the culture and used to prepare the samples. Supernatants and pellets were obtained by centrifugation for 1-2 min at 13,000 rpm (Eppendorf™ Benchtop Microcentrifuge).

E. coli whole cell preparation was undertaken by resuspension of pallet with 200 µL of 1 X sodium dodecyl sulphate-polyacrylamide gel electrophoresis (SDS-PAGE) loading buffer (50 mM Tris-HCl, pH 6.8, 100 mM dithiothreitol (DTT), 2% (w/v) sodium dodecyl sulphate (SDS), 0.1% (w/v) bromophenol blue and 10% (v/v) sterile Glycerol).

Secretory proteins of *E. coli* strains were obtained by TCA precipitation of supernatant. Supernatants were first separated from pallet as previously described and precipitated with 10 % (v/v) trichloroacetic acid (TCA) for 30 min on ice. Next, the samples were centrifuged for 15min at 13,000 rpm (Eppendorf™ Benchtop Microcentrifuge) and discard the supernatant. Afterwards, the pellet was washed with 500ul ice-cold acetone and centrifuged for 5min at 13,000 rpm (Eppendorf™ Benchtop Microcentrifuge) before the supernatant discarded and tubes air dried for 15min. Dried pellets were finally resuspended with 200ul 1X SDS loading buffer. Both whole cell and secretory proteins were boiled in 100°C for 5min before loading on SDS-PAGE gel for analysis.

2.16.2 SDS gel preparation

For SDS gel and protein profile analysis, 9% polyacrylamide separating gels and 3% stacking gel was prepared in this study(266).

Prepared SDS gels were kept overnight in the cold room covered with wet tissue and aluminium foil. Samples were loaded the next day into wells of the stacking gel and the gels transferred into Bio-Rad Mini-Protein® Tetra Cells system filled with 1X electrophoresis running buffer (0.025 M Tris base, 0.19 M Glycine and 0.08% (w/v) SDS) using a PowerPac™ HC power 16 mA per gel were applied until the loading dye reached the top of the running gel. Afterwards, 40 mA per gel were applied for sample protein separation. 5 µl of ColorPlus Prestained Protein Marker, Broad Range (7-175 kDa) (New England Biolabs, P7709V) was loaded for protein molecular weight measurement.

Table 2.7: A separating and stacking gel preparation for SDS protein analysis (*Stacking Gel Buffer 3% contains 0.5M Tris PH 6.8 + 0.4% SDS; **Separating Gel Buffer 9% contains 1.5M Tris PH 8.8 + 0.4% SDS).

Preparation of Stacking gel (3%)	Quantity	Preparation of Separating gel (9%)	Quantity
Stacking Gel Buffer*	2ml	Stacking Gel Buffer**	2.5ml
Acrylamide	400µl	Acrylamide	3ml
Water	1.45ml	Water	4.44ml
TEMED	5 µL	TEMED	5 µL
APS	50 µL	APS	50 µL

2.16.3 Immunoblotting

Protein profiles of each sample was first separated by SDS page gel (section 2.9). Next, the SDS gel was transferred into nitrocellulose membrane by Mini Trans-Blot® Electrophoretic Transfer Cell (BioRad, UK). Blotting was performed in cold 1x transfer buffer (20 mM Tris base, 150 mM Glycine and 20% (v/v) MeOH) at 150 mA for 60 min. Then, nitrocellulose membrane was separated from the SDS gel and blocked in PBS supplemented with 0.5% (v/v) Tween-20 (PBST) and 5% (w/v) dried skimmed milk powder at 4°C overnight. Next day, nitrocellulose membrane was incubated with primary antibody, which was diluted in blocking solution as mentioned in the table below at room temperature for 60 min for specific protein detection. Then, the membrane was washed (3 x 5 min) with 0.5% PBST before incubation with Anti-rabbit IgG horseradish peroxidase (HRP) secondary antibody (1:10000 dilution in 0.5% PBST) under the same conditions as described for primary antibody. Finally, immunoblotting was revealed by using Pierce® ECL Western Blotting substrate (ThermoFisher Scientific, UK) and the Amersham Hyperfilm™ chemiluminescence film (GE Healthcare Limited, UK) according to the manufacturer's instructions.

Table 2.8: Primary antibodies used for immunoblotting in this study.

Rabbit primary antibody	Dilution	Reference
α-EspC	1:1000	(149)
α-dsRed	1:10,000	Source Bioscience
α-AaaA	1:2000	(258)
α -Histag	1:1000	Sigma

2.17 Fluorescence Microscopy and imaging

Microscopy images were observed on a Nikon Eclipse 50i using a 100X oil lens fitted with Nikon intensilight C-HGFI for light illumination. For microscopy cell preparation, colonies of bacterial culture were inoculated and propagated in 4 ml fresh LB broth in appropriate selective antibiotics. Next day, Fresh overnight cultures were diluted to $OD_{600nm} \approx 0.02$ into the same medium and grown at 37°C in a shaking water bath to $OD_{600nm} = 0.1$ to 0.2. Afterward, 0.2% final concentration of 20% arabinose was added for protein induction. Cell growth was continued with shaking for an additional 2 hours. To prevent bacteria motility under the cover slip, a 1.2% (w/v) agarose pad was prepared and 1.5µl of bacterial cells covered with cover slip. Images were captured by using Nikon Digital Sight DS-U3 connected to Nikon NIS-Elements F4.00.06 software and image analysis were processed by Image J software.

2.18 FlAsH labelling tetracysteine-tagged recombinant proteins

AaaA fluorescent tags were created via the small tetracysteine tag technology. The tetracysteine TC-Tag (Cys-Cys-Pro-Gly-Cys-Cys) was fused within the gene of interest. The encoded fusion protein can then be specifically recognized by a biarsenical labelling reagent (FlAsH-EDT2). The labelling reagent finally becomes fluorescent upon binding to recombinant proteins containing the TC-Tag.

For identification of recombinant proteins including tetracysteine motif, the membrane-permeable biarsenical dye, FlAsH-EDT2 (Invitrogen), was used.

Strains of bacteria were cultured, inoculated for overnight and induced by 0.02% arabinose as previously described unless otherwise stated. Cells producing TC-tagged protein were harvested by centrifugation at 5500 rpm (Eppendorf™ Benchtop Microcentrifuge)

for 2 min and washed once with 1x HEPES buffered saline BioUltra (Sigma), ice cold, and resuspended in 1 ml to 1.0 of OD_{600nm} using the same buffer. The cells were centrifuged once more, and the pellet was resuspended (slowly) in 500 µl 1x HEPES buffer containing 3-5 µM (final concentration) FlAsH-EDT_2 substrate followed by incubation for 35-45 min in darkness at RT. After incubation, cells were harvested by centrifuging as before and the supernatant discarded according to the University of Nottingham guidelines. Subsequently, cells were washed twice with 1 ml 1x British Anti-Lewisite (BAL) wash buffer at final concertation of 0.25 mM as recommended by the manufacturer (added twice volume of wash buffer to the volume of added substrate). Finally, cells were further washed once again with the 1x HEPES buffered saline, ice cold and resuspended to approximately 0.5 of OD_{600nm}. An aliquot of 2 µl of washed cells were mounted on microscope slides with a 1.2% agarose pad, covered with a coverslip, sealed with transparent nail polish and examined under fluorescent confocal microscope.

Table 2.9: The fluorescent excitation and emission spectra for the FlAsH and ReAsH reagents

Labeling Reagent	Excitation Maximum	Emission Maximum
FlAsH reagent	508 nm	528 nm
ReAsH reagent	593 nm	608 nm

2.19 Confocal fluorescence microscope

To generate more specific images, a Zeiss LSM 700 compact confocal laser scanning microscope was used fitted with HXP 120C lamp for light illumination and a Zeiss alpha-Plan-Apochromat 60x/1.46 Oil objective lens. Images were captured by using AxioCam digital microscopecamera connected to ZEN software and analysed using image J software.

Chapter 3

Localization of EspC and AaaA in mutants deficient of putative secretion accessory factors.

3.1. Introduction

3.1.1. Diverse localization patterns of autotransporter secretion

ATs are large proteins (90 to 200 kDa) with a characteristic C-terminal transporter domain produced by Gram-negative bacteria (113). Their secretion journey and localization during translocation has not yet been fully elucidated and may require currently uncharacterized accessory factors. Two different distribution patterns have been reported for ATs: polar and spiral.

3.1.2. Polar localization of autotransporters

A polar localization pattern has been reported for IcsA, SepA, AIDA-I and BrkA (113,267). The polar localisation of *Shigella* IcsA AT was observed by following the production of translational fusions with green fluorescent protein (GFP). Constructions of IcsA-GFP that lacked either the amino signal peptide sequence or the carboxyl β-barrel domain revealed that polar localization still occurred(268), leading to the conclusion that neither domain was essential for polar localization(268). In addition, this study also highlighted the need of two nonadjacent regions (amino acids 58–103 and amino acids 507–729) within IcsA for localization of IcsA-GFP in order place in the old poles(268). A similar pattern of IcsA-GFP localization to old poles was detected for *Enterobacteriacae* and *Vibrio*(268). Interestingly, IcsA localized in a similar manner when produced in a △SecA strain of *E. coli* and polar localization happened independently in the cytoplasm prior to SecA ATPase and the SecYEG membrane channel (translocon) facilitated secretion(269). A cytoplasmic chaperone (DnaK) was postulated as being an important factor for IcsA polar localization and secretion after screening of a genomic library of polar putative secreted *E. coli* proteins and it appears that this accessory factor is important for chaperoning of autotransporters for polar localization in the cytoplasm(270). The cell division protein FtsQ was also essential for localization of IcsA and other autotransporters to the pole (271).

Probing of intact wild-type *S. flexneri* with antiserum to SepA another autotransporter with 150-kDa serine protease indicated punctate foci at the bacterial pole similar to the pattern seen for IcsA, which localizes more favourably to the older pole(267). AIDA-I, a 132-kDa autotransporter which is involved in adhesion to human cells by pathogenic diffusely adherent *E. coli* (DAEC) strains was found in a polar localization on the surface of wild-type *E. coli* when expressed from plasmid pIB264(267). In the same study, localization of the *Bordetella* 103-kDa autotransporter BrkA was examined from plasmid pDO6935 in wild-type *E. coli* and similar polar localization was found on the surface of 96% ± 5% of intact organisms(267).

Non-autotransporter proteins with different functions in processes such as motility, attachment and cell communication, plus cell division factors and toxins have a polar localization(272,273). Recent studies suggested that polar localization could be driven by an interaction with the bacterial cytoskeleton actin homologue, MreB. To support this claim, one study perturbed MreB in *P. aeruginosa* with A22 (S-3,4-dichlorobenzyl isothiourea). This A22 treatment altered the polar localization of the type IV pilus retraction ATPase (PilT) and weakened twitching motility(274). Moreover, production of IcsA-GFP and GFP-EpsM (a polar IM protein from *Vibrio cholerae*, tagged with GFP at the N-terminus) in *mreB* deficient cells resulted in asymmetrical distribution on the whole cell surface and scattered several fluorescent foci(275). These findings suggest that MreB could be involved in a mechanism that enables protein distribution with cell polarity and structural organization of polar positioning(276–278).

3.1.3. Spiral localization of autotransporters

Helical localization of the autotransporter EspC has been observed in our research group(244). EspC was fluorescently tagged by fusion with mCherry, and with an intact β-barrel it was localized in a spiral pattern reminiscent of the cytoskeleton (113). To verify that this observation was not an artefact of insertion of the sizeable mCherry into EspC, and to determine if the spiral localization was a feature of more than one autotransporter, the study was extended to incorporate AaaA and fluorescent tags were created via the small tetracysteine tag technology(113,244). The tetracysteine TC-Tag (Cys-Cys-Pro-Gly-Cys-Cys) when fused to a gene of interest allows the encoded fusion protein to be specifically recognized by a biarsenical labelling reagent. A biarsenical

labelling reagent, FlAsH-EDT2, becomes fluorescent upon binding to recombinant proteins containing the TC-Tag(113). Using this approach it was revealed that EspC and AaaA share a spiral localization dependent on their β-barrel transporter domains(113,244).

In separate studies in our group (Louise Arnold thesis), a random transposon screen identified a number of genes that appeared to encode proteins that facilitate EspC secretion(149). The proteins encoded by the mutated genes had not previously been implicated in autotransporter secretion.

3.1.4. ProW

ProW is an inner membrane permease involved in the function of the osmoregulation transporter ProU that has a 100-residues long periplasmic N-terminal tail followed by seven transmembrane segments(279,280). The ProU transport system, encoded in the *proVWX* operon is composed of 3 functional elements: ProV, an ATPase protein, ProW, an inner membrane protein, and ProX, a periplasmic substrate binding component, that collectively contribute to transport betaine and proline betaine into the *Shigella* cytoplasm(281).The *Shigella* ProU osmosensing system plays an important role in enhancing the growth, replication, and survival of *Shigella* within the cytosol of infected cells(281).Previous studies found that transcriptional activity of the *proVWX* operon is significantly increased upon infection of both epithelial cells and macrophages(282). In addition, *in vitro* studies found that the ProU system senses the ionic strength of the environment(281).

3.1.5. SlyB or PCP (PAL *c*ross-reactive *p*rotein)

SlyB or PCP (PAL *c*ross-reactive *p*rotein) is a tiny lipoprotein consist of 158 amino acids which is conserved in a diverse group of Gram-negative bacteria(262). In recent studies, the *slyB* gene of *Pasteurella multocida* has been found to be upregulated during infection; however, its main protein function remains unknown(283). In *E. coli* and *Salmonella enterica, slyB* is downregulated by high Mg2+ concentration, mediated by the PhoP/PhoQ two-component system(284,285). SlyB may be involved in outer membrane stability by reducing cell dependency to Mg2+ as a counterion(284,285). Comprehensive study conducted by Brokx et al. based on microarray and RT-PCR analysis revealed that *slyB* is highly expressed in *E. coli*(286). Another study suggested that the

production of virulence factors in *Serratia marcescens* is unaffected by *ΔslyB* and it appears that SlyB is not associated with regulatory function(287). In *P. aeruginosa*, *slyB* expression is highly dependent on sigma factor AlgU that regulates alginate production and is involved in adaptive response to periplasmic stress(288,289). Proteome analysis of a fraction enriched for membrane proteins in *Burkholderia multivorans* suggested that SlyB is associated with cell envelope integrity and found as a major protein of the OM(262).

3.1.6. SapA

Host-derived antimicrobial peptides (AMPs) are mainly amphipathic, cationic nonspecific immune system molecules that attack bacterial membranes, change transmembrane potential, and stimulate cytoplasmic leakage resulting in apoptosis(290,291). Sap transporters have been found as important virulence factors involved in antimicrobial peptide resistance in different Gram-negative pathogens of both animal and plant hosts(292). The *sap* (sensitivity to antimicrobial peptides) operon encodes an inner membrane ABC-transporter, found actively involved in resist killing against AMPs and acts as a virulence factor in *Haemophilus ducreyi* (292). Previous study found that SapA in Nontypeable *Haemophilus influenzae* (NTHI), which is periplasmic substrate binding protein of the Sap transporter, binds to AMPs(293). In addition, other studies found that SapA is essential for virulence and persistence of infection in a middle ear of a mammalian host model of otitis media (293,294). However, the complete mechanism by which the Sap transporter complex can provide AMP resistance is still unknown. Recent study found SapA contributes to bacterial virulence and is required for *Haemophilus influenzae* by directly providing protection from AMP lethality *in vivo*(295). recent data also suggested that *ΔsapA* was unable to obtain heme for growth after iron starvation(296). SapA was found essential for iron translocation across the *Haemophilus influenzae* inner membrane, however, the exact mechanism of Iron uptake system for this pathogen remains unknown(296). It appears that SapA consists of a shared substrate binding site for heme and AMPs within the host cell microenvironments and this multifunctional role for the *Haemophilus influenzae* Sap transporter is necessary for both metabolic iron needs and resistance to host immune response effector(295,296).

3.1.7. YbgC

The Thioesterase superfamily plays an important role in metabolism, membrane biosynthesis, signal transduction, and gene regulation(297). The Tol-Pal system is found in many different Gram-negative bacteria, and composed of five core proteins (TolQ, TolR, TolA, TolB and Pal) with accessory genes for YbgC and YbgF proteins located in the cluster operon(298,299). This Tol-Pal system stretches across the cell envelope and most proteins encoded by this system are involved in keeping cell envelope integrity and the cell division process(298). However, the complete physiological and metabolic role of YbgC is still unknown. A proteomics analysis of the YbgC protein in *Salmonella enterica* serovar Enteritidis identified that the *ybgC* gene as essential for growth and cell survival in the presence of whole egg white(300). In addition, expression of *tolR* and *tolA* was reduced in the *ΔybgC* mutant strain indicating relationship between the Tol-Pal system and YbgC AF protein(300). Another study highlights the role of *ybgC* gene in lysozyme resistance in egg white filtrate of *Salmonella enterica*(301). The outer membrane permeability, cellular structure and morphology, along with fatty acid composition of *Salmonella enterica* exposed to lysozyme are all changed in *ΔybgC* mutant(301).

YbgC involvement in phospholipid metabolism and a main thioesterase activity have been found in *E. coli, H. influenzae, and H. pylori*(302,303). Acyl carrier protein (ACP) is an important cofactor that mediates fatty acid and phospholipid synthesis(304). In this metabolic reactions ACP interacts with a diverse group of enzymes, which includes the thioesterase YbgC(304). Another novel finding suggested the role of thioesterase YbgC affects motility by modulating c-di-GMP levels in *Shewanella oneidensis*(297).

3.1.8. YqjE

YqjE, conserved inner membrane protein is another accessory factor utilized in this study. Previous studies suggested a possible role of this protein in inhibition of translation in an unknown mechanism and may also contribute to enhance a dormant or latent state in *E. coli* following prolonged exposure to nitrogen starvation(305,306). Most bacterial cells are stressed, and therefore, some become resistant to antibiotics by initiating a latent phase known as persistence. recent studies found YqjE can increase bacterial antibiotic tolerance, mainly by reducing cell growth(307,308).

3.1.9. AbrB

abrB is putative regulator in *E. coli* and in previous study was predicted to be involved in transport across membranes(149). The *E. coli* aidB gene is controlled by two different mechanisms, an ada-dependent pathway stimulated by methyl damage to DNA and an ada-independent pathway triggered when cells are grown without oxygen(309). In previous studies, *ΔabrB* causes an unstable phenotype with respect to anaerobic, Ada-independent expression of the aidB gene(309).

Using the strains and plasmids from these previous studies, the aim of the work presented in this chapter was to ascertain whether the putative secretion accessory factors played a role in the spiral localisation of autotansporters. Towards this aim, plasmids producing fluorescent versions of EspC were inserted into the AT accessory factor secretory mutants (*ΔproW, ΔslyB, ΔsapA, ΔybgC, ΔyqjE* and *ΔabrB*), and EspC localisation tracked by immunobloting and microscopy. This analysis revealed that SlyB did affect EspC secretion. To better understand the role of SlyB, genetic complementation was attempted with plasmids producing SlyB with or without a His tag. In addition, the study was expanded to incorporate another autotransporter, AaaA. To do this, plasmids encoding AaaA were introduced into the Δ*slyB* mutant. Moreover, to discount the possibility that the large mCherry was influencing the observations, AaaA was labelled with FlAsH and compared to similarly tagged EspC.

The aim of this chapter was based on previous studies conducted by Louise Arnold, Stephanie Pommier and Mahmoud Ashawesh. Initially Louis Arnold identified transposon mutants deficient in EspC secretion. Following this study, Dr Stephanie Pommier constructed defined clean mutants, using lambda red. The strategy used to create clean mutant accessory factors was to amplify 1000bp before and after the genes of interest followed by cloning the PCR product in pBluescript for sequencing. The amplified product was then cloned into a suicide vector pDM4 vector. Following a double recombination step, deletion of the gene of interest was obtained. The previous finding revealed the defined clean mutants did not show the same reduced secretion of EspC. Another study by Dr Mahmoud Ashawesh suggested EspC and AaaA ATs exit bacteria through dynamic spiral secretion(244). This study combines microscopy with AT accessory factor candidates with aim of elucidating interactions and mechanism involved in secretion (Figure 3.1 , 3.2).

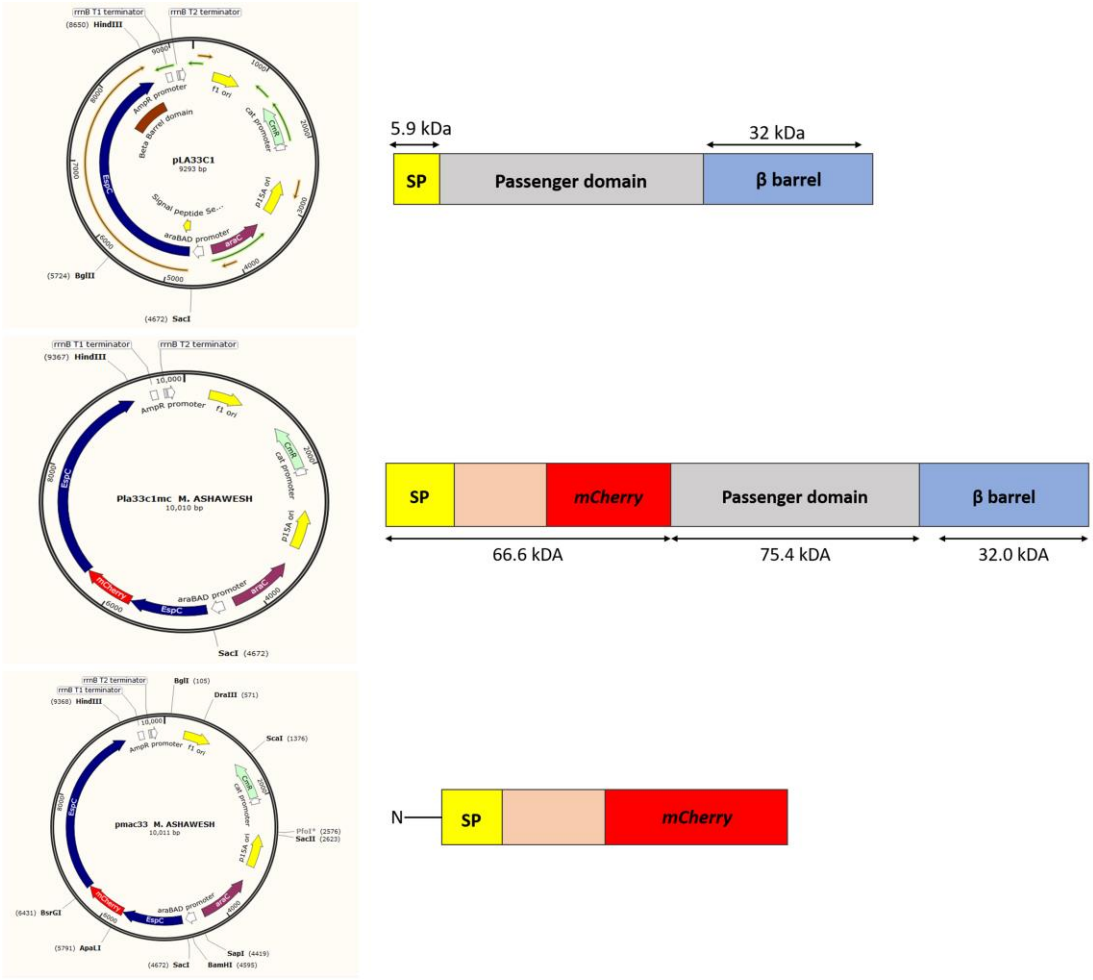

Figure 3.1: Schematic representation of plasmids used in this study with restriction sites and EspC constructs(113).

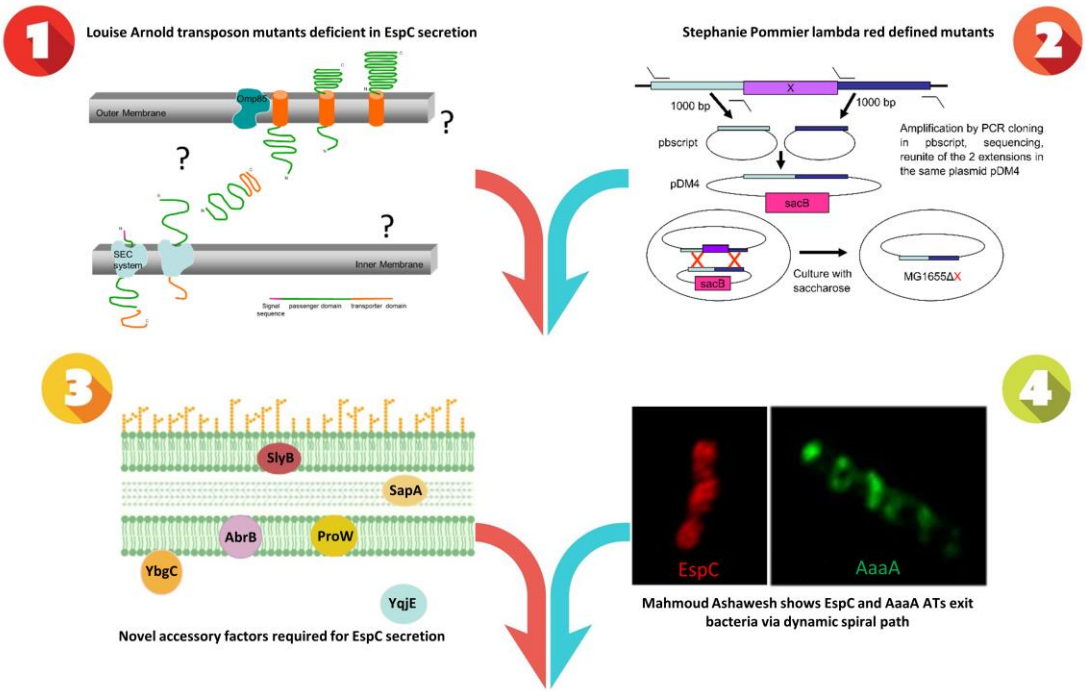

Figure 3.2: Predicted localization of accessory factors implicated in the secretion of EspC. Previously, a transposon mutagenesis screen was undertaken that identified mutants deficient in EspC secretion (310)(Panel 1). Subsequently defined mutations in the identified genes were constructed by Stephanie Pommier (Panel 2). The predicted cellular localisation for each encoded protein is shown in the cartoon (Panel 3). Panel 4 represents the hypothesis that a dynamic spiral localisation pathway is followed by ATs to exit the producing bacterium(244). This study aimed to investigate whether the AFs contributed to this spiral path of AT secretion.

Table 3.1: List of accessory factor secretory mutant and their function (149).

Interrupted Gene	Genbank ID	Gene function	Reference
proW	GI 147374	Inner membrane protein involved in osmoregulation	(149)
slyB	GI 15802055	Outer membrane lipoprotein	(149)
sapA	GI 1787551	Part of ABC transporter uptake system	(149)
ybgC	GI 15800451	homologue in *H. influenzae* identified as a catalyst for acyl-coenzyme A thioester hydrolysis	(149)
yqjE	GI 1789486	putative membrane protein in *Salmonella* Spp	(149)
abrB	EG 13310	Transport protein	(149)

3.2. Results

3.2.1. Previously constructed plasmids encode the expected fluorescently-tagged EspC suitable for monitoring secretion accessory in factor mutants

Three plasmids encoding EspC were selected for insertion into the AT secretion accessory factor mutants (Figure 3.1). One plasmid encoding native EspC (pLA33C1) and two producing EspC fused to the red fluorescent protein mCherry were used to facilitate tracking within the cell. Of the latter, one encoded a product with an intact transporter domain (pLA33C1MC), and the other lacked the C-terminal β-barrel domain (pMAC33). The mCherry fusions remain tethered to the bacterial cell surface rather than being released to the surrounding media, and thus provide a tool to assess whether any of the AT AFs contribute to the dynamic spiral secretion pathway. *E. coli* MG1655 containing these plasmids individually were grown overnight in LB containing chloramphenicol, and

plasmids were extracted and subjected to PCR (Supplementary Figure 1 Panel A) and restriction digestion (Supplementary Figure 1 Panel B & C).

As expected, DNA products of 4028bp, 4753bp and 4753bp were observed with plasmids pLA33C1, pLA33C1MC and pMAC33 by PCR (Supplementary Figure 1 Panel A). Moreover, restriction digestion with HindIII generated DNA fragments of 9293bp for PLA33C1 and 10,010bp for PLA33C1MC and PMAC33 plasmids, (Supplementary Figure 1 Panel B) as expected. In addition, restriction digestion with BglII also produced the expected DNA fragments of 9293bp for pLA33C1; a fragment of 717bp representing mCherry was separated from 9265bp that represents the rest of the vector for pLA33C1MC; and finally for pMAC33 a fragment of 718bp representing mCherry separated from 9294bp that accounted for the rest of the vector (Supplementary Figure 1 Panel C).

After confirming that the plasmids were correct, it was important to assess whether the expected proteins were produced from them. To do this, protein profile analysis and immunoblotting of arabinose induced MG1655(pLA33C1), MG1655 (pLA33C1MC) and MG1655 (pMAC33) was performed using whole cell lysates along with culture supernatants since native EspC is a secreted protein. Immunoblotting was performed with Anti-EspC or anti-Dsred as primary antibody so that both the size of the EspC (native or fusion) and the presence of mCherry could be confirmed respectively (Figure 3.3 Panel B,C).

The SDS-PAGE analysis clearly revealed more proteins in the whole cell lysates than in the culture supernatant as expected (Figure 3.3 Panel A). In addition, it was evident that the samples contained equivalent levels of protein overall. There was also proteins migrating at the size expected for EspC (145kDa) or EspC-mCherry (172kDa).

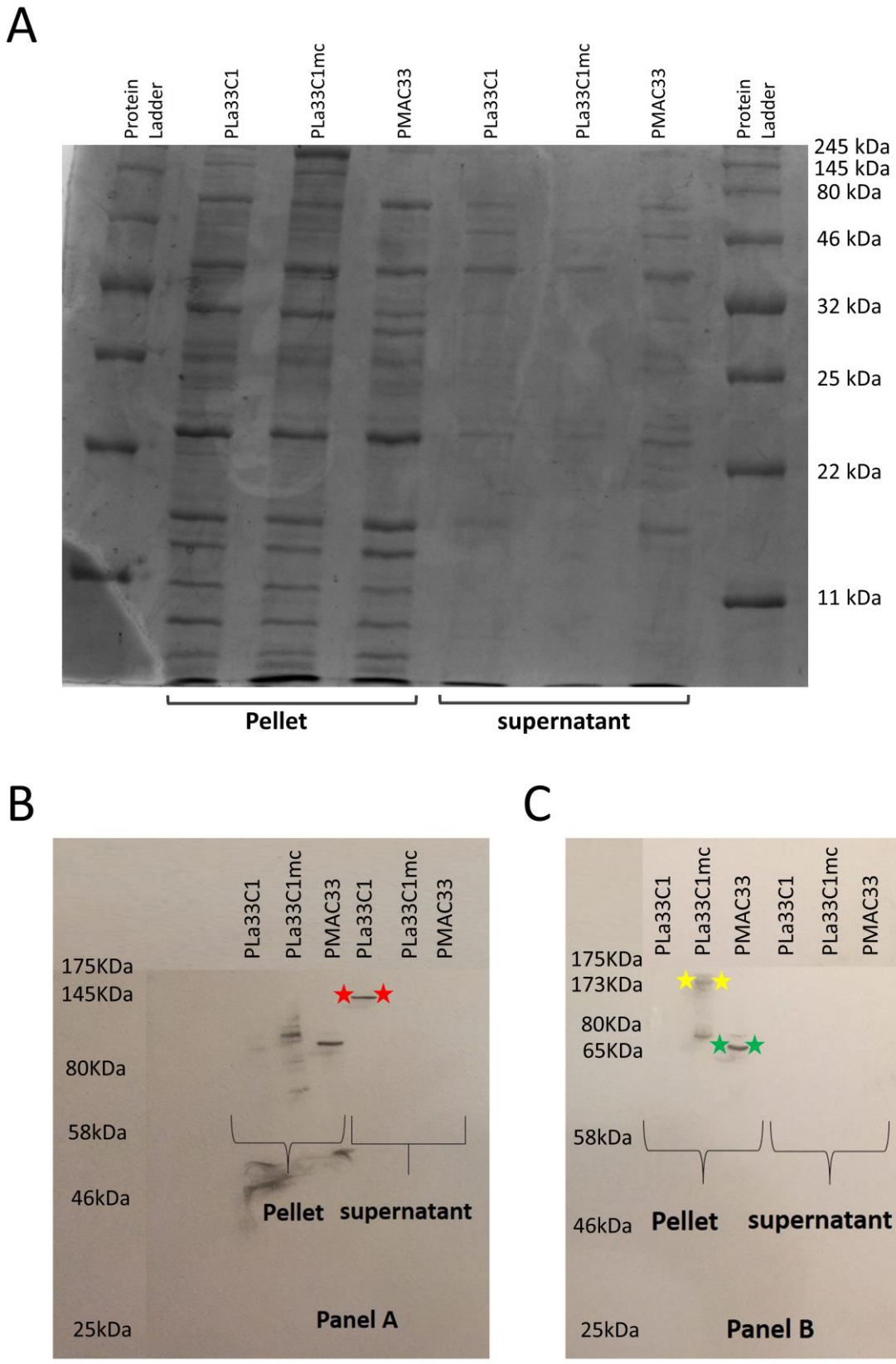

Figure 3.3: *E. coli* MG1655 secretes native EspC from plasmid pLA33C1, or accumulates intracellular full length or truncated

EspC fused to mCherry from plasmids pLA33C1MC or pMAC33 respectively as expected. Protein profile of pLA33C1, pLA33C1MC and pMAC33 pellet and supernatant analyzed by SDS-PAGE, Coomassie stained. EspC (145kDa) migration through the gel (Panel A). Western blotting analysis of arabinose induced MG1655 (pLA33C1), MG1655 (pLA33C1MC) and MG1655 (pMAC33) using whole cell lysates along with culture supernatants. Panel B: Immunoblotting analysis using primary antibody Anti-EspC; 145kDa protein (shown in red) detected for MG1655 (pLA33C1) in the culture supernatant as expected. Panel C: Immunoblotting analysis using primary antibody anti-dsred; 172kDa protein (shown in Yellow) of MG1655 (pLA33C1MC) and 65kDa protein (shown in green) of MG1655 (pMAC33) identified in the whole cell lysate as expected.

Absolute negative controls (empty vectors) had previously been performed during construction of the plasmids used(113). The immunoblot analysis demonstrated that MG1655(pLA33C1) did not produce any proteins that could be detected by anti-dsRed, in line with the absence of mCherry. Moreover, the anti-EspC detected a protein in the culture supernatant of 145kDa as expected. In contrast, anti-dsred recognized a protein of 172kDa in the whole cell lysate of MG1655(pLA33C1MC) and a smaller one (65kDa) in the whole cell lysate of MG1655(pMAC33) which is commiserate with both containing mCherry (27kDa) and the latter lacking the β-barrel. Neither MG1655(pLA33C1MC) nor MG1655(pMAC33) had any proteins in their culture supernatant that could be detected by either of the antibodies used.

3.2.2. Transformation of pLA33C1, pLA33C1MC and pMAC33 into defined AT secretion accessory factor mutants revealed that the EspC secretion defect observed in the transposon mutants was not retained, and that the absence of slyB may affect EspC stability or cell integrity.

Having confirmed the plasmid construction and profile of protein production was correct in parental MG1655; each plasmid (pLA33C1, pLA33C1MC and pMAC33) was transformed into the set of AT secretion accessory factor mutants (*ΔproW, ΔslyB, ΔsapA, ΔybgC, ΔyqjE and ΔabrB*). Subsequently, plasmids were prepared and confirmed by PCR and restriction digestion as previously (Supplementary Figure 2 Panels A-C) shows the expected DNA PCR fragments and (Supplementary Figure 2 Panels D-M) shows the expected Restriction enzyme products for the AT AFs *ΔproW, ΔslyB, ΔsapA, ΔybgC, ΔyqjE* and *ΔabrB*

respectively. After successful transformation of pLA33C1, pLA33C1MC and pMAC33 into the set of AT secretion accessory factor mutants (Δ*proW*, Δ*slyB*, Δ*sapA*, Δy*bgC*, Δ*yqjE* and Δ*abrB*) ATs were induced with arabinose as described in section 2.6. Immunoblotting of whole cell lysates and culture supernatants followed for comparison with wild type and detection of possible defects in the mutant (Figure 3.4 Panels A-F). Primary antibodies Anti-EspC and anti-dsred were used for confirmation of presence of EspC (native or fusion) and mCherry protein.

Non-quantified visual inspection of Immunoblots (Figure 3.4) of AT AF deficient mutants compared to MG1655 revealed that a 175kDa protein was detected for pLA33C1 in all whole cell lysates as expected (Panel A). A 145kDa protein was detected for pLA33C1 in all culture supernatant as expected (Panel B). A 173kDa protein was detected for pLA33C1MC in the whole cell lysate of MG1655 and all the other mutants except Δ*slyB* (Panel C). No protein was detected for pLA33C1MC in the culture supernatant of any of the strains (Panel D). A 65kDa protein was detected for pMAC33 in the whole cell lysate of all strains as expected since it lacks the translocation domain and suggests that the AF mutants did not degrade it (Panel E). A 65kDa protein was detected for pMAC33 in Δ*slyB* and Δ*sapA* mutant backgrounds in the culture supernatant (Panel F). As expected, the MG1655 (pLA33C1MC) whole cell lysates control provided a visible protein at the expected size and no protein was detected for the MG1655 (pMAC33) whole cell lysate control. Since the secretion of the native EspC was not reduced in the mutants, this data contradicts the previous findings by Louise Arnold (310). This may mean that in addition to the transposon insertion that another mutation occurred which is not present in the defined mutants constructed by Stephanie Pommier (Figure 3.2).

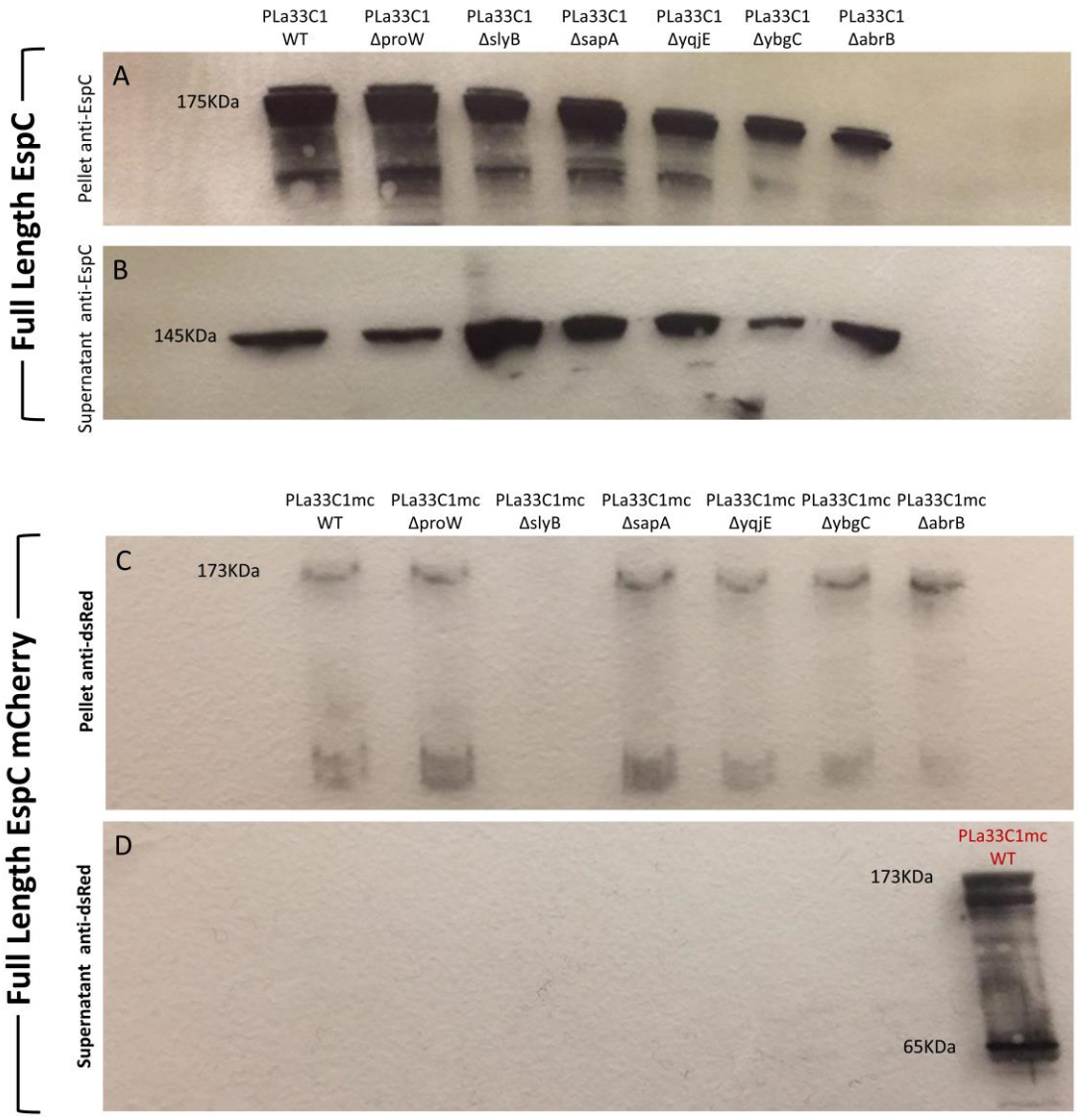
Full Length EspC
PLa33C1 WT
PLa33C1 ΔproW
PLa33C1 ΔslyB
PLa33C1 ΔsapA
PLa33C1 ΔyqjE
PLa33C1 ΔybgC
PLa33C1 ΔabrB
A
175KDa
Pellet anti-EspC
B
145KDa
Supernatant anti-EspC
Full Length EspC mCherry
PLa33C1mc WT
PLa33C1mc ΔproW
PLa33C1mc ΔslyB
PLa33C1mc ΔsapA
PLa33C1mc ΔyqjE
PLa33C1mc ΔybgC
PLa33C1mc ΔabrB
C
173KDa
Pellet anti-dsRed
D
PLa33C1mc WT
173KDa
65KDa
Supernatant anti-dsRed

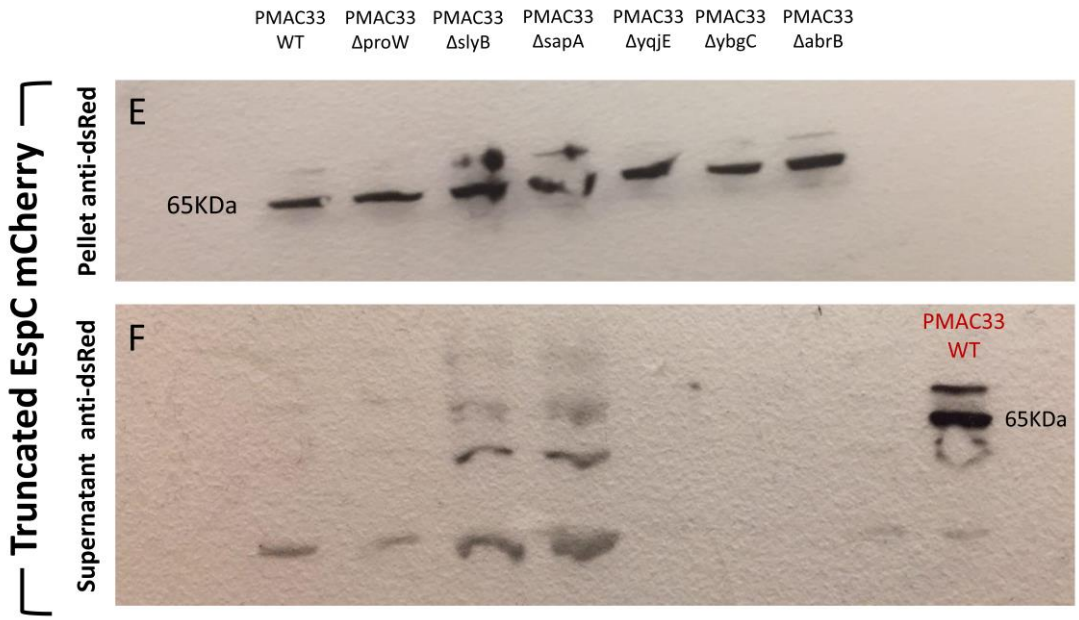

Figure 3.4: ΔslyB does not produce detectable FL EspC-mCherry and releases more tEspC-mCherry than MG1655. Plasmids pLA33C1, pLA33C1MC and pMAC33 were transformed into *ΔproW, ΔslyB, ΔsapA, ΔybgC, ΔyqjE and ΔabrB* autotransporter accessory factors. Immunoblot analysis of AT AF deficient mutants compared to MG1655: EspC wild type whole cell lysate (A), culture supernatant (B) using Anti-EspC and EspC FL mCherry whole cell lysate (C), culture supernatant (D), Truncated EspC mCherry whole cell lysate (E) and culture supernatant (F) using anti-dsred. MG1655 (pLA33C1MC) whole cell lysate were applied as a control. A 65kDa protein was detected for pMAC33 in the whole cell lysate of all strains as expected (E). No protein was detected for the MG1655 (pMAC33) whole cell lysate which was applied as a control.

3.2.3. Localisation of EspC-mCherry is not altered in the AT AF mutants, whilst localisation of tEspC-mCherry mirrors the wild type control in all AT AF mutants except ΔslyB, where it is less polar.

Previous data in our lab revealed that EspC-mCherry localizes in a spiral pattern during secretion. Our Immunoblotting data was suggestive of altered stability of EspC-mCherry or potentially the promotion of cell lysis in *ΔslyB*. One possibility would be that the overproduced protein forms inclusion bodies. To investigate this further, bacterial physiology was evaluated in parallel with localizing the fluorescently tagged AT in each potential AF mutant. Transformed AT accessory factor mutants (Δ*proW*, Δ*slyB*, Δ*sapA*, Δ*ybgC*, Δ*yqjE* and Δ*abrB*) containing

pLA33C1, pLA33C1MC and pMAC33 were cultured and induced for florescent microscopy observation as described in section 2.17. Control cells were also prepared for comparison. As expected in induced bacterial cells, protein localization observed in red during florescent light exposure. Localization of EspC-mCherry in all AT AF mutants mirrors the wild type control (Figure 3.5). Similarly, Localization of tEspC-mCherry mirrors the wild type control in all AT AF mutants except Δ*slyB*, where it is less polar (Figure 3.6).

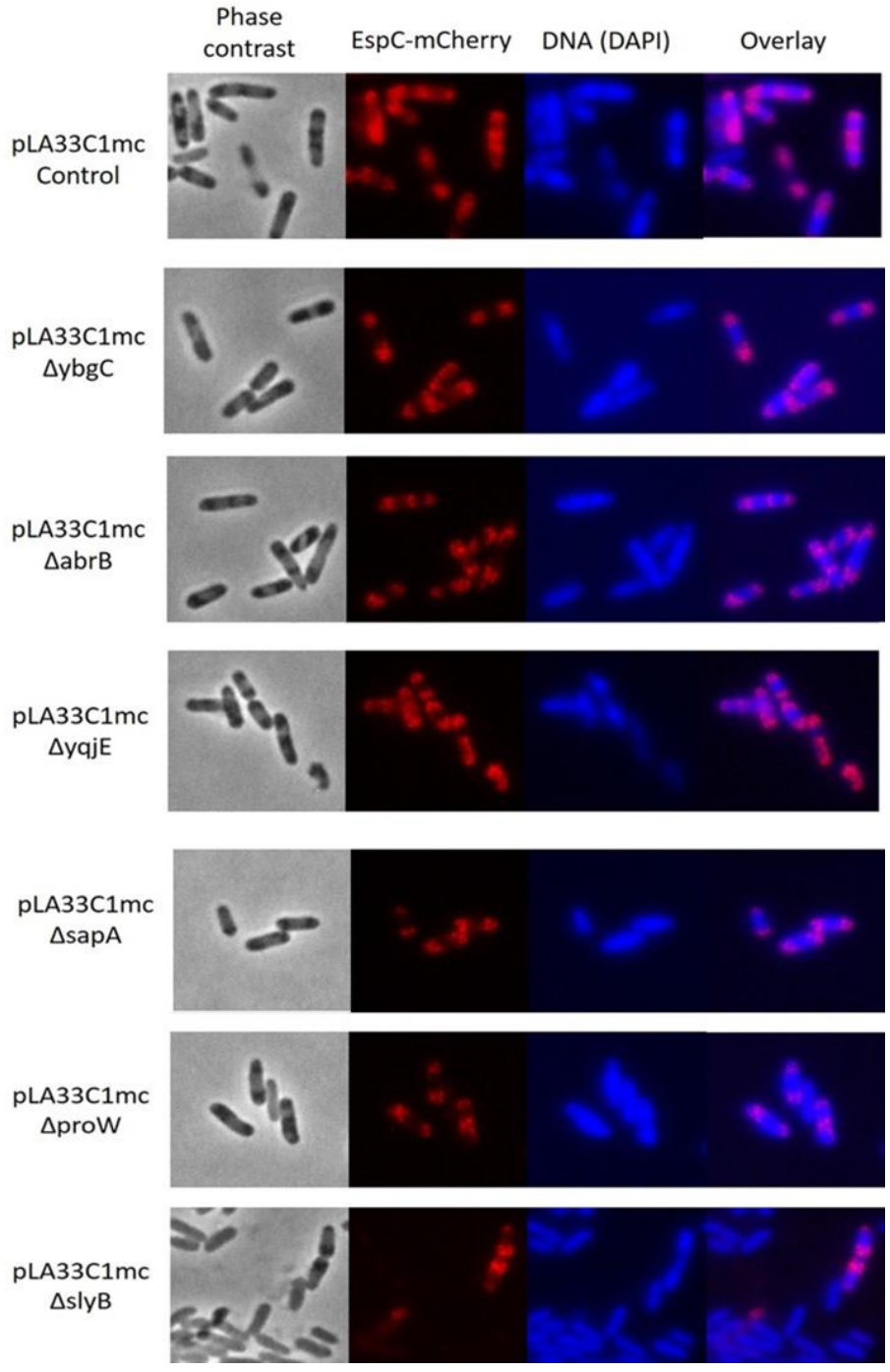

Figure 3.5: Localization of EspC-mCherry in all AT AF mutants mirrors the wild type control. MG1655 (Control) and derived accessory factor mutants producing FL. EspC-mCherry form pLA33C1MC were first grown in LB, induced in 0.2% arabinose of OD_{600nm}=0.5 and subjected to fluorescent microscopy as described in section 2.17. The images were visually inspected, thus conclusions are not based on quantification and should be interpreted with caution as it is a subjective assessment.

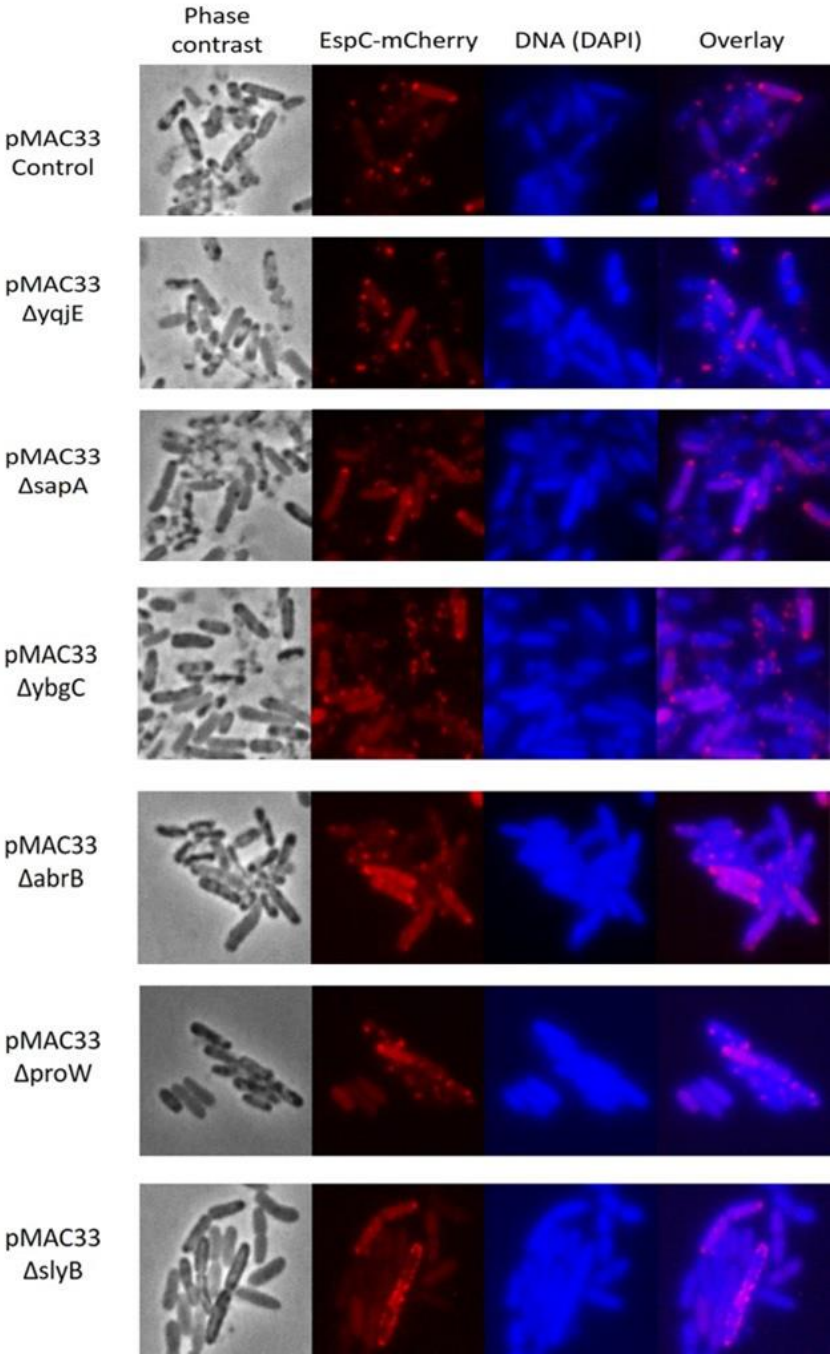

Figure 3.6: Localization of tEspC-mCherry mirrors the wild type control in all AT AF mutants except ΔslyB, where it is less polar. MG1655 (Control) and derived accessory factor mutants producing truncated EspC-mCherry form pMAC33 were first grown in LB, induced in 0.2% arabinose of OD_{600nm}=0.5 and subjected to fluorescent microscopy as described in section 2.17. The images were visually inspected, thus conclusions are not based on quantification and should be interpreted with caution as it is a subjective assessment

3.2.4. Plasmids encoding SlyB with and without His tag did not detectably complement secretion of EspC from the Δ*slyB* mutant

In order to complement Δ*slyB* containing pLA33C1, pLA33C1MC and pMAC33, SlyB overproduction vectors (2 versions of pBAD24: one encoding SlyB fused to a C-terminal His tag and the other with SlyB lacking a -His tag) under arabinose promotor control and with ampicillin resistance were cotransformed into each mutant strains. The two plasmids were first extracted from DH5α and confirmed by restriction digestion and sequencing. Plasmids were digested with ClaI and SphI from the multiple cloning site. A 3191 bp DNA fragment separated from the 1651 bp fragment bearing the arabinose promotor and partial *slyB* gene as expected based on the plasmid map (Supplementary Figure 3 Panel A). Confirmed plasmids were then transformed into Δ*slyB* competent cells by electroporation.

After successful transformation of plasmids into Δ*slyB* containing pLA33C1, pLA33C1MC or pMAC33, these newly made complemented mutants (along with Δ*slyB* and MG1655 WT strains) were cultured in appropriate antibiotic and induced with 0.2% arabinose final concentration at OD_{600nm}= 0.5. Analysis of protein profiles by SDS-PAGE and Immuno blotting of whole cell lysates and culture supernatants followed as described in section 2.16.3. Primary antibodies Anti-EspC, anti-dsred and anti-His tag were used for confirmation of the presence of EspC (native or fusion), mCherry and the 6 histidine tag protein respectively. For EspC, a 175kDa protein was detected for MG1655 WT, Δ*slyB* and the complemented strains in the whole cell lysate as expected. In addition, a 145kDa protein was detected in the culture supernatants as expected, although the levels in the complemented mutants were very low (Figure 3.7 Panel A). For EspC-mCherry, 173kDa and 65KDa proteins were detected for all strain backgrounds in the whole cell lysate and supernatant as expected,

although levels were lower in the supernatants of the Δ*slyB* mutant regardless of whether it was complemented (Figure 3.7 Panel B). Moreover, for tEspC-mCherry, a 65kDa protein was detected for all strains in the whole cell lysate and supernatant as expected, again with levels being lower in the supernatants of the complemented Δ*slyB* mutant (Figure 3.7 Panel C). For confirmation of complementation, the 28kDa SlyB with 6-histidine residues fused to the C-Terminus was observed in the whole cell lysates and not found in the supernatant as expected (Figure 3.7 Panel D). Overall, Figure 3.7 reveals that the ΔslyB mutant containing pLA33C1, pLA33C1MC and pMAC33 produced a similar protein profile as the complemented mutant.

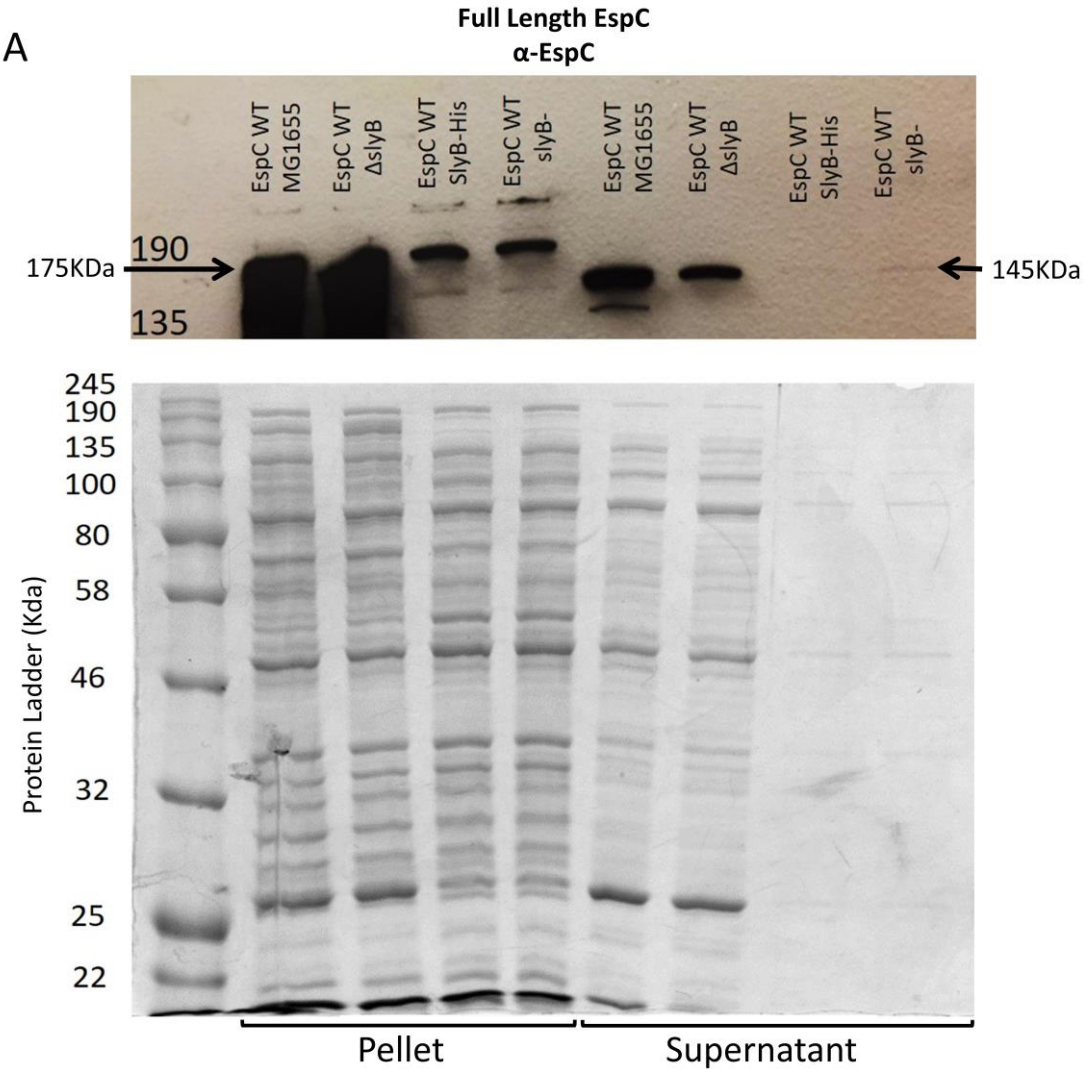

B

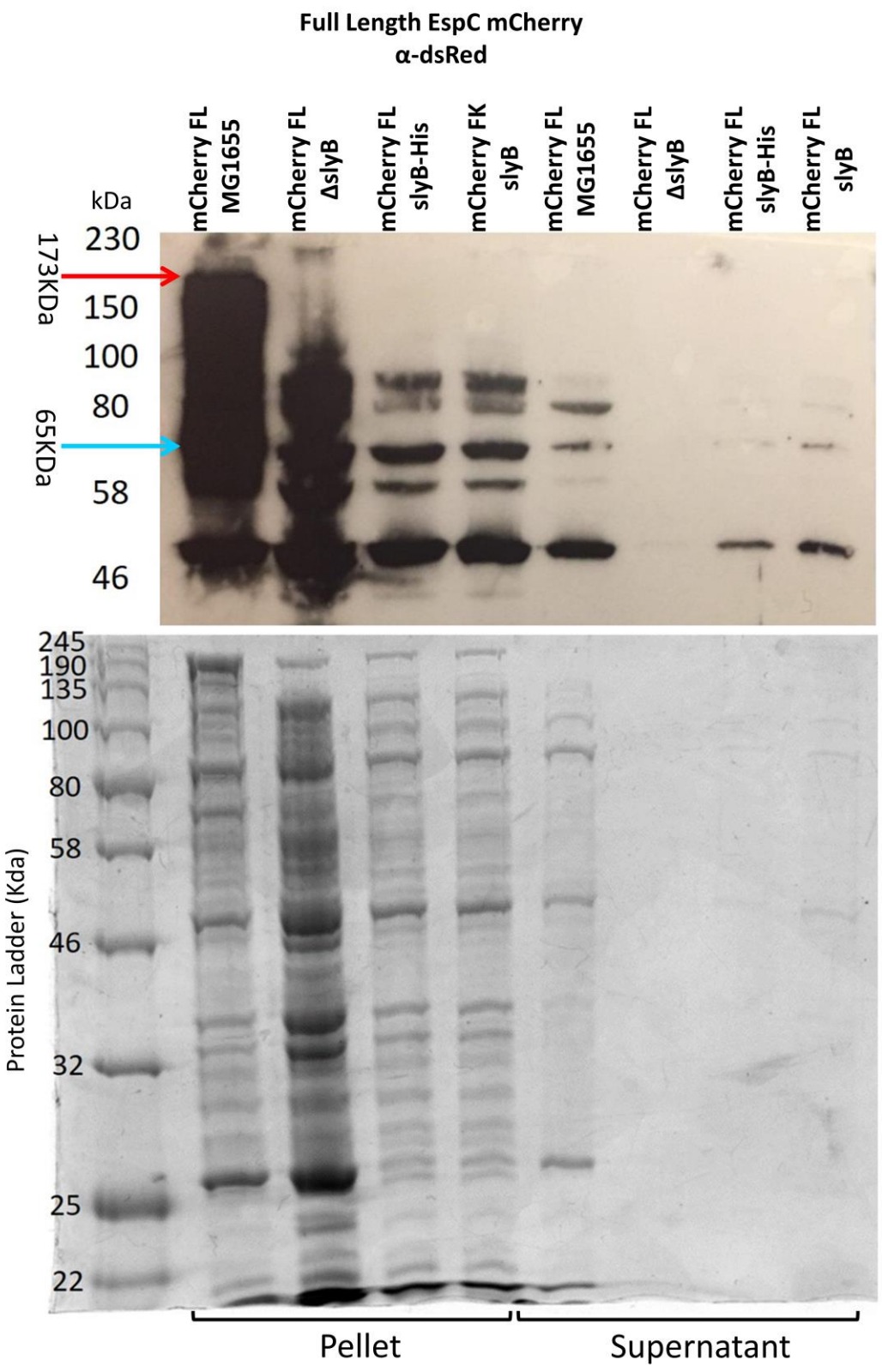
Full Length EspC mCherry
α-dsRed
mCherry FL MG1655
mCherry FL ΔslyB
mCherry FL slyB-His
mCherry FK slyB
mCherry FL MG1655
mCherry FL ΔslyB
mCherry FL slyB-His
mCherry FL slyB
kDa
230
150
100
80
58
46
173KDa
65KDa
Protein Ladder (Kda)
245
190
135
100
80
58
46
32
25
22
Pellet
Supernatant

C

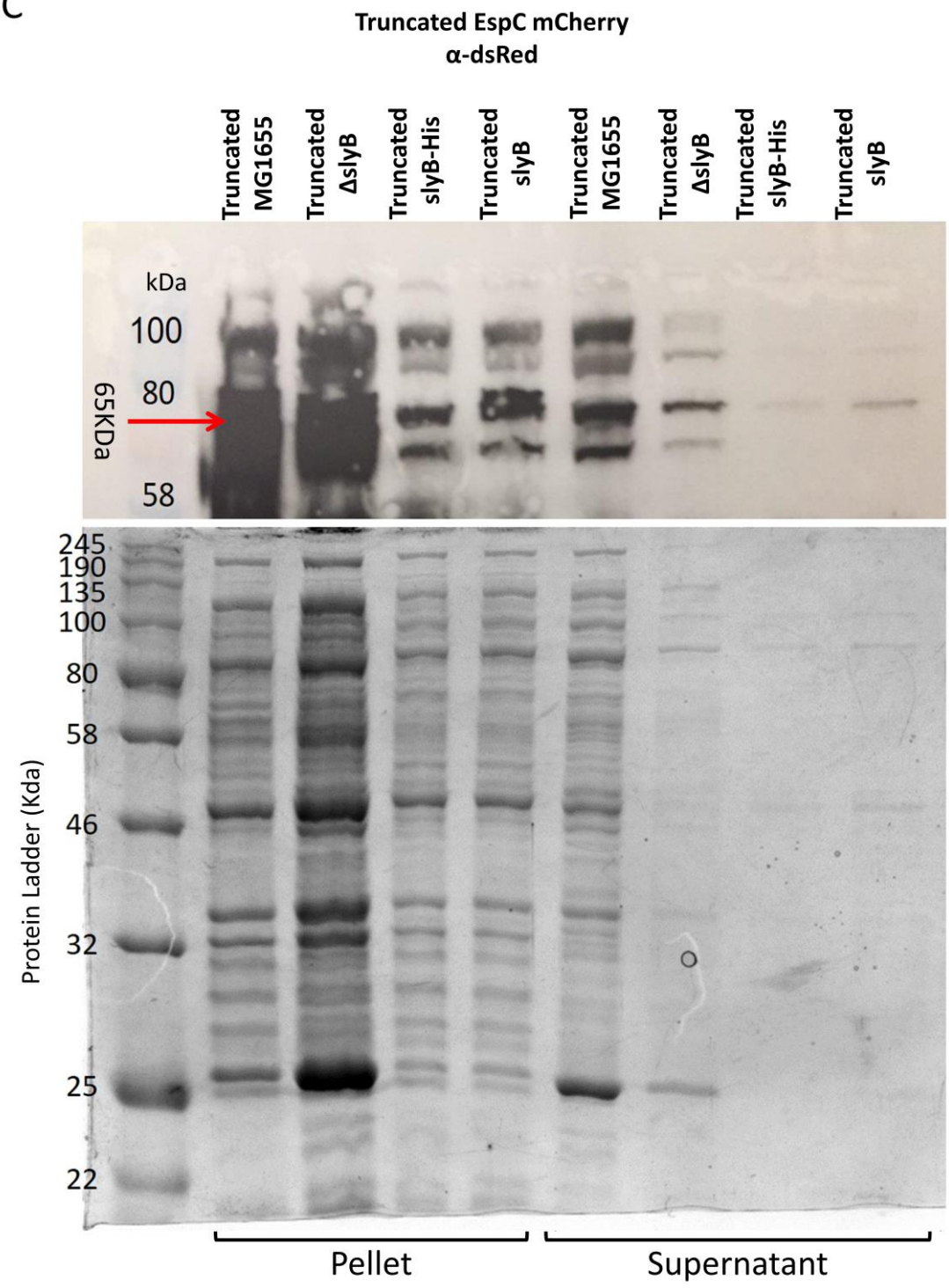
Truncated EspC mCherry
α-dsRed
Truncated MG1655
Truncated ΔslyB
Truncated slyB-His
Truncated slyB
Truncated MG1655
Truncated ΔslyB
Truncated slyB-His
Truncated slyB
kDa
100
80
65KDa
58
245
190
135
100
80
58
46
32
25
22
Protein Ladder (Kda)
Pellet
Supernatant

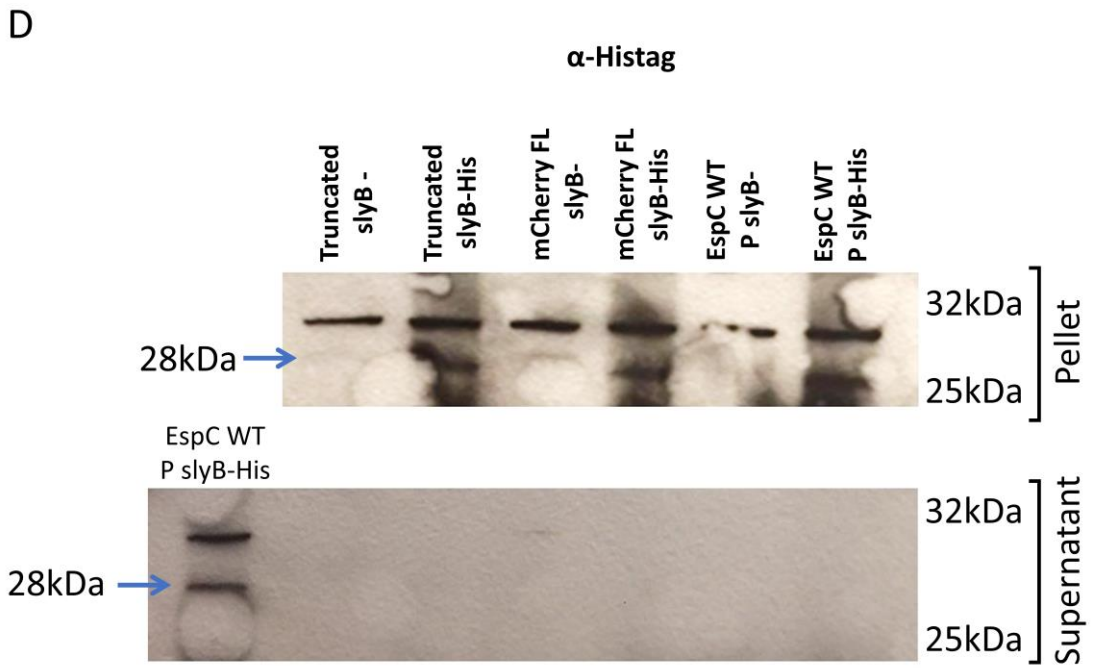

Figure 3.7: The Δ*slyB* mutant containing pLA33C1, pLA33C1MC and pMAC33 produced a similar protein profile as the complemented mutant. Immunoblot analysis of whole cell and supernatants fractionated from MG1655 (pLA33C1) and the Δ*slyB* mutant in the presence and absence of complementation plasmids plus either pLA33C1, pLA33C1MC or pMAC33. Cells were grown, induced in 0.2% final concentration of arabinose. Blots were incubated in primary anti-EspC 1:1000 dilution (Panel A), anti-dsRed 1:1000 dilution (Panels B,C) or anti-HIS tag 1:1000 dilution (Panel D). black arrow indicates 175-kDa and 145kDa EspC wild type (Panel A). Protein profiles of pellet and supernatant stained by Coomassie Brilliant Blue on SDS-gel are also presented with samples applied in the same order (Panels A ,B, C). Red arrow indicates 173-kDa EspC-mCherry and Blue arrow indicates 65kDa mCherry (Panel B). Red arrow indicates 65-kDa tEspC- mCherry (Panel C). Blue arrow indicates 28-kDa SlyB-HIS tag (Panel D). No protein was detected in supernatant (Panel D).

3.2.5. Localisation pattern of EspC-mCherry and tEspC-mCherry in the presence and absence of SlyB is unaltered when analysed by fluorescent microscopy

Genetic complementation of the putative AT secretion accessory factor SlyB was assessed for its impact upon AT localization by fluorescent microscopy. To do this, strains containing pLA33C1MC and pMAC33 were cultured in appropriate antibiotics and induced as described in section 2.17. The Δ*slyB* mutant and MG1655 WT strains were also used for comparison with the complemented Δ*slyB* mutant. Plasmids encoding SlyB and also SlyB-His were analysed. As expected in induced bacterial cells, protein localization was detected in red during florescent light exposure for all samples. In MG1655, EspC-mCherry localises throughout the cells and is most prominent in the poles and center of the bacterium whilst for tEspC-mCherry exhibited a more diffuse pattern (Fig 3.8, 3.9). This was in agreement with the previous analysis (Fig 3.5 and 3.6). In the Δ*slyB* mutant, EspC-mCherry and tEspC-mCherry displayed similar localization patterns. As would be expected, the complemented Δ*slyB* mutants mirrored this distribution. The control mCherry was observed as a diffuse red cloud with no preference for the bacterial poles (Figure 3.8 and 3.9).

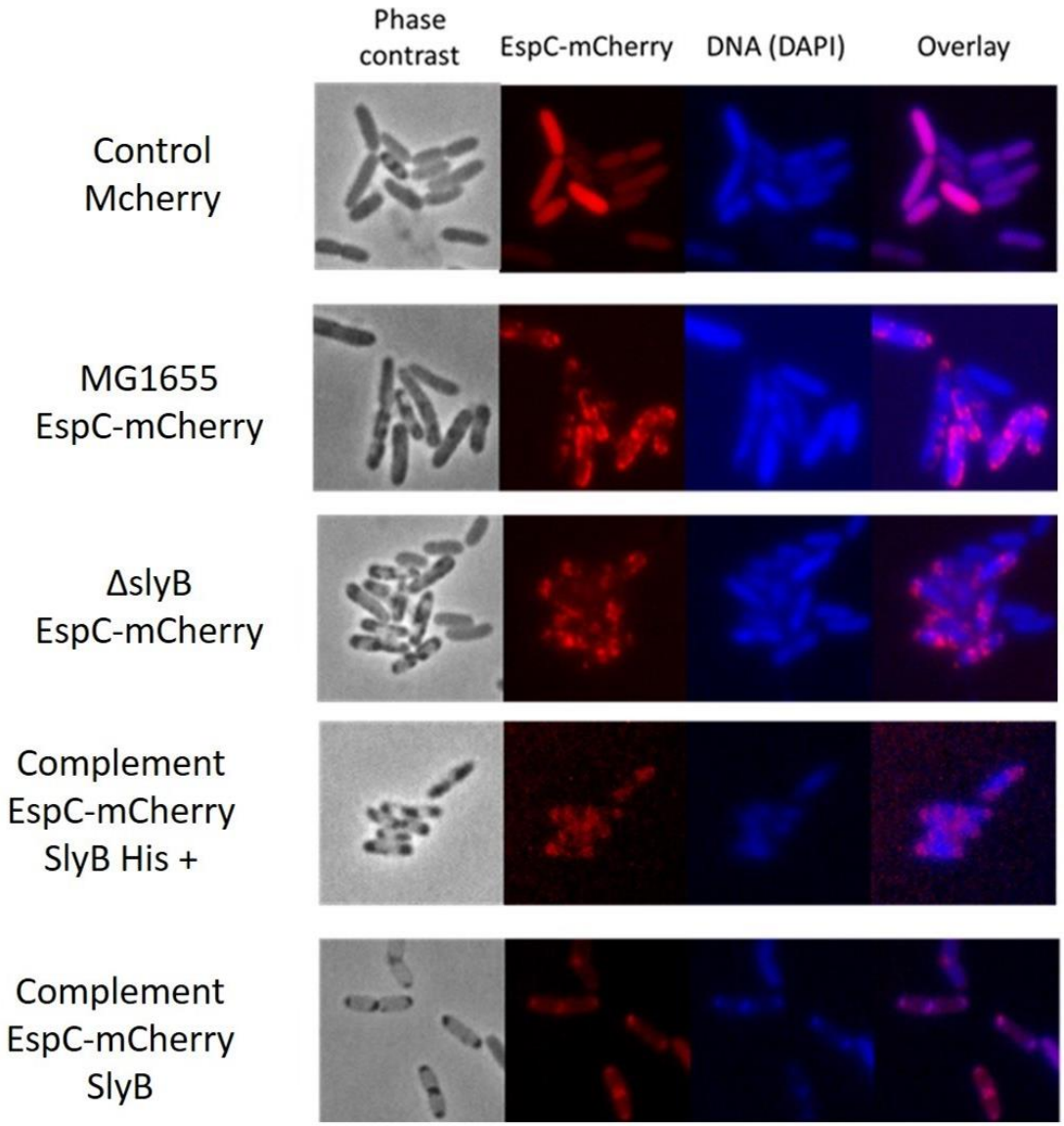

Figure 3.8: Localization of EspC-mCherry in the complemented Δ*slyB* mutant mirrors the Δ*slyB* mutant and parental MG1655 by being located mainly towards the bacterial poles. EspC-mCherry, produced in MG1655 and the Δ*slyB* mutant in the presence and absence of complementation plasmids was grown, induced in 0.2% arabinose and OD_{600nm}=0.5. Cells were then analyzed by fluorescent microscopy as described in section 2.17. Cytoplasmic mCherry cells were prepared in parallel as control.

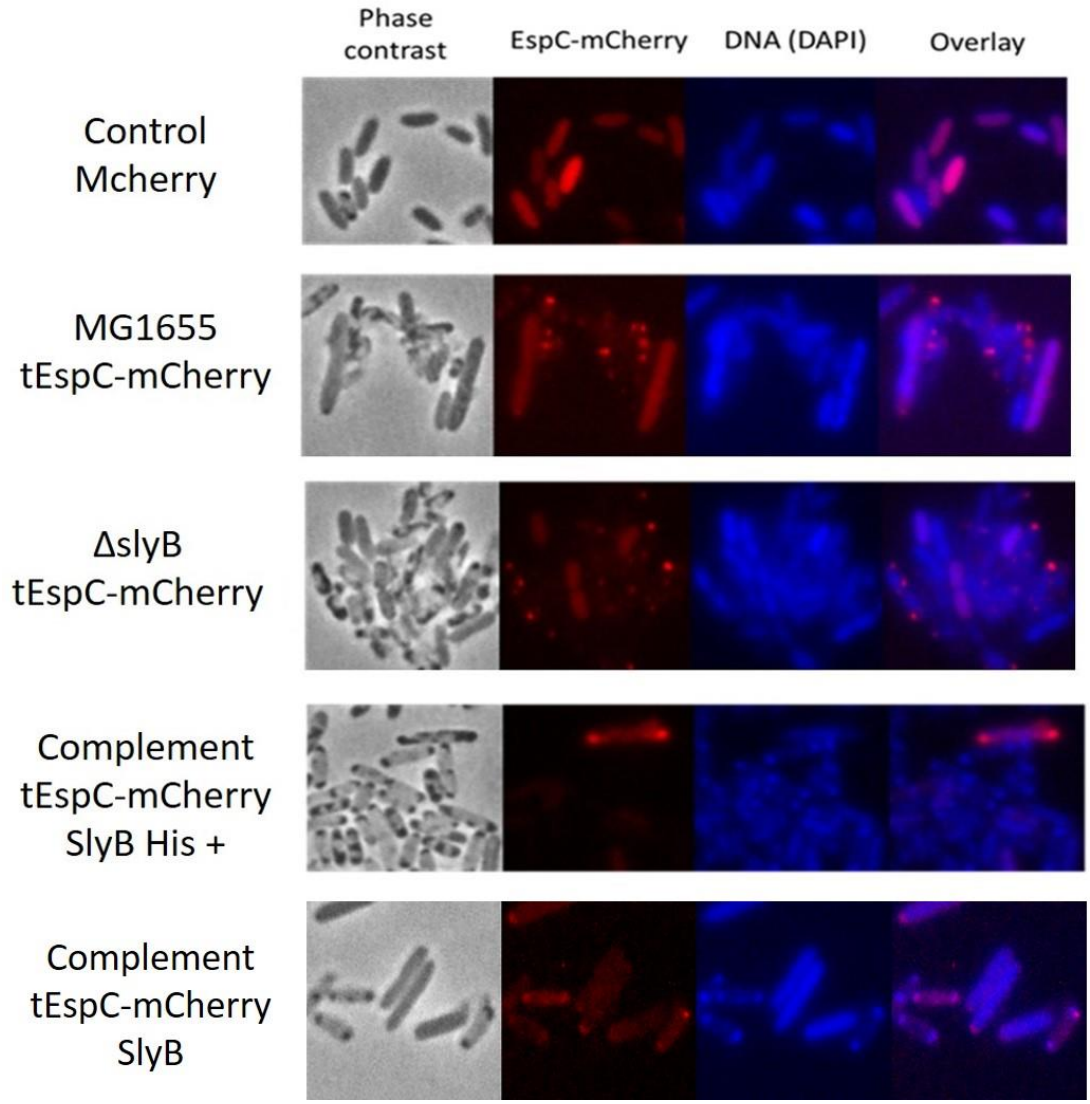

Figure 3.9: Localization of tEspC-mCherry in the complemented Δ*slyB* mutant mirrors the Δ*slyB* mutant and parental MG1655 by being located mainly towards the bacterial poles. tEspC-mCherry, produced in MG1655 and the Δ*slyB* mutant in the presence and absence of complementation plasmids was grown, induced in 0.2% arabinose and OD_{600nm}=0.5. Cells were then analyzed by fluorescent microscopy as described in section 2.17. Cytoplasmic mCherry cells were prepared in parallel as control.

3.2.6. MG1655 and the Δ*slyB* secretion accessory factor mutant produce similar levels of another fluorescently tagged AT, AaaA.

Although fluorescent microscopy could not detect the role of SlyB in EspC localization, it was hypothesized that a different AT may reveal its contribution. AaaA was selected as it is an AT that naturally remains tethered to the bacterial cell surface (unlike EspC), and since a proportion would not be lost to the supernatant, it was reasoned that changes in localization may be more evident. It had previously been demonstrated that like EspC, AaaA follows a spiral path out of the bacteria (113). The monitoring of AaaA secretion had been achieved with the fluorescent FIAsH tag, and this was selected for the experiments here as it is significantly smaller than mCherry, and thus less likely to obstruct the observation of a secretion defect.

In order to compare with EspC AT secretion, plasmids encoding AaaA were selected for insertion into the parental MG1655 WT and Δ*slyB* accessory factor mutant. All plasmids contain the motif for FlAsH tagging (CCPGCC) within the autotransporter gene to facilitate tracking within cells by confocal microscopy. One plasmid encoded native AaaA tagged at position 531aa (pLA33AaaA-TC), one has the FL EspC gene control tagged at position 531aa by SDM (pLA33C1-TC 531aa) while the other produced AaaA tagged at position 292aa and also containing an amber stop codon at position 343aa to generate a truncated version of AaaA lacking the β-barrel (pLA33AaaA-TC-TAG343aa). *E. coli* MG1655 containing these plasmids individually were grown overnight in LB containing chloramphenicol, and plasmids were extracted. After plasmid extraction, DNA was transformed into parental MG1655 and the Δ*slyB* accessory factor mutant. Transformations were then confirmed by double digest with BglII and SalI. As expected, ~1064 bp upstream portion of EspC and 2059bp native AaaA fragments were separated from 5327 bp open pBAD33 vector (Supplementary Figure 4 Panel A-C). After confirming that the plasmids were correct, it was important to assess whether the expected proteins were produced from MG1655 and the accessory factor mutant in whole cell lysates. Towards that end, immunoblotting was performed with Anti-EspC and anti-AaaA as primary antibody so that both the size of the EspC and the presence of AaaA could be confirmed respectively (Figure 3.10). The immunoblot analysis revealed similar patterns between MG1655 and the Δ*slyB* mutant containing AaaA AT variants.

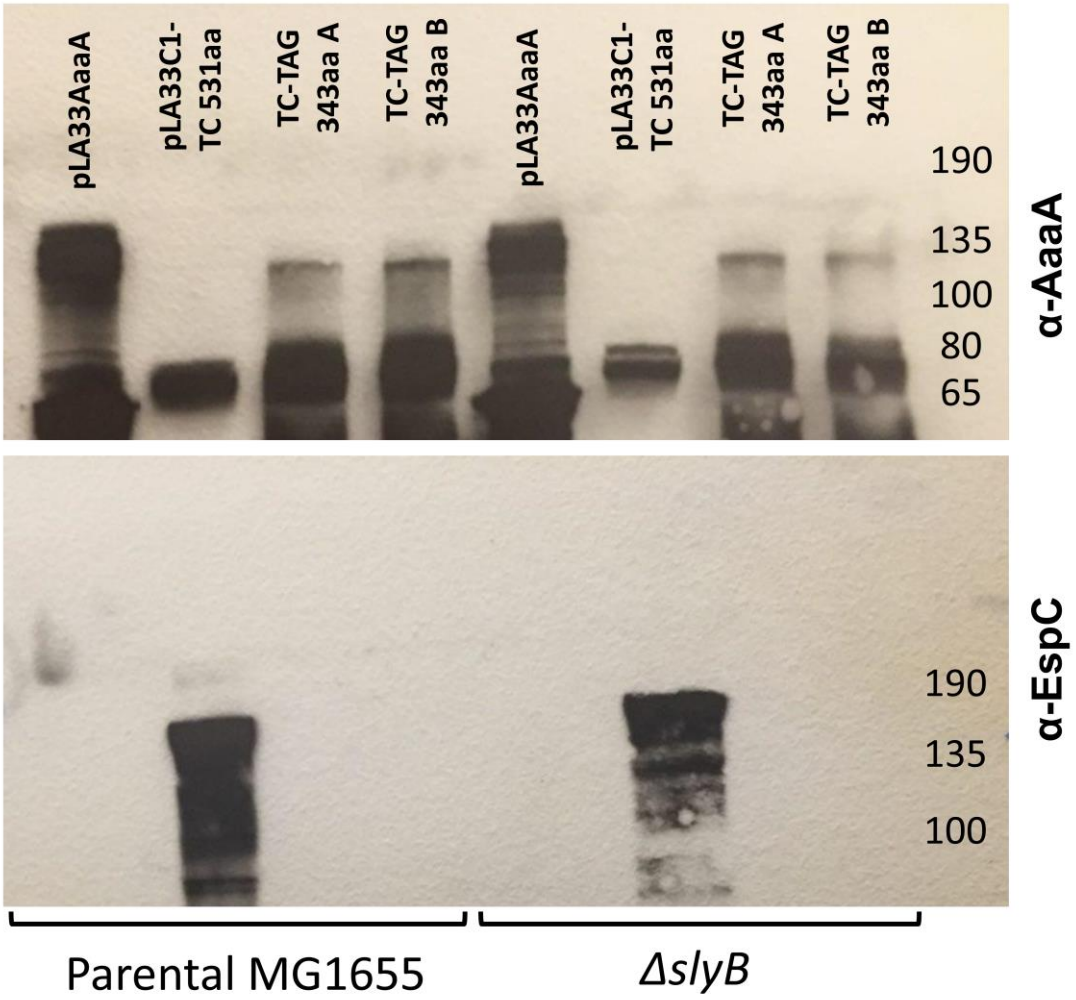

Figure 3.10: Parental MG1655 and the Δ*slyB* mutant containing native AaaA (pLA33AaaA), FL EspC FlAsH tag (pLA33C1-TC 531aa) and AaaA truncated version (pLA33AaaA-TC-TAG343aa) produced similar detectable AaaA and EspC protein in whole cell lysates. Immunoblot analysis of whole cell lysates from MG1655 and the Δ*slyB* mutant bearing these plasmids was undertaken. Cells were grown, induced in 0.2% final concentration of arabinose and incubated in primary α-EspC antibody in 1:1000 dilution and α-AaaA in 1:2000 as described in section 2.16.3. 80-kDa AaaA was detected in both MG1655 and the Δ*slyB* mutant containing native AaaA (pLA33AaaA) and tAaaA (pLA33AaaA-TC-TAG343aa). The larger unprocessed >135kDa AaaA was only detected when pLA33AaaA was present as expected (Top panel). 174kDa EspC was only detected in MG1655 and the Δ*slyB* mutant bearing EspC (pLA33C1-TC 531aa) whole cell lysate as expected (Bottom Panel).

3.2.7. Confocal microscopy of EspC, AaaA and tAaaA in MG1655 WT and the Δ*slyB* mutant verified that the contribution of SlyB to AT secretion is not sufficiently impactful to be interrogated using this approach with the current resolution available.

Previous study suggested that different ATs adopt a helical localization during secretion. To investigate if SlyB has a role in this distribution, localization of surface exposed AaaA and its truncated version *were* compared with EspC in parental MG1655 and the Δ*slyB* mutant. In order to track the secretion of the AaaA, the intracellular FlAsH labelling technology for TC-tagged AaaA was performed according to conditions described in the section 2.18. MG1655 and the Δ*slyB* mutant containing pLA33aaaA (control), pLA33C1-TC 531aa and pLA33AaaA-TC-TAG343aa were diluted 1:100 in LB containing Cm, grown to OD_{600nm} of 0.05 and induced with 0.2% arabinose for 2h. Subsequently, cells were harvested and prepared for FlAsH staining following the protocol described in section 2.18. Confocal fluorescence images revealed that the Δ*slyB* mutant localizes autotransporters in the similar manner compare to MG1655. Full-length proteins (AaaA and EspC) localized in a spirals pattern while truncated AaaA forming discrete foci within the cells (Figure 3.11).

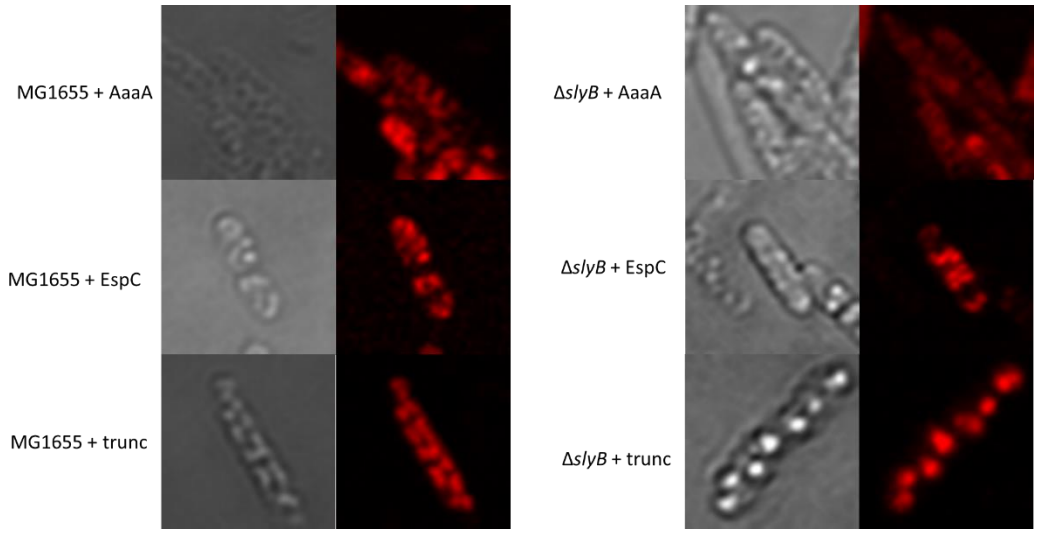

Figure 3.11: Full-length proteins (AaaA and EspC) localized in a spiral pattern while truncated AaaA formed discrete foci within the cells of both MG1655 WT and the ΔslyB mutant. MG1655 and the Δ*slyB* mutant containing pLA33aaaA (control), pLA33C1-TC 531aa and pLA33AaaA-TC-TAG343aa were diluted 1:100 in LB containing Cm, grown to

OD_{600nm} of 0.05 and induced with 0.2% arabinose for 2h. Subsequently, cells were harvested and prepared for FlAsH staining following the protocol described in section 2.18 and visualized by confocal microscopy. I would like to acknowledge the contribution of Dr. James Brown from CBS, Nottingham University for confocal microscopy imaging and processing.

3.3. Discussion and future work

Bacterial proteins are not fixed objects, and they localise to different positions within the cell such as the cytoplasm, membranes, or periplasm. Localisation can occur via diffusion and/or directed movement mediated by mechanical secretion pathways and active intracellular transport systems. Correct location enables virulence protein function, and thus pathogenicity so it is important to characterize the mechanisms involved. Progress has been made in recent years to study protein localization and also the interactive dynamics that proteins participate in, following discovery of fluorescent tracking protocols based on the green fluorescent protein (GFP) from Jellyfish and the red fluorescent protein (DsRed) and higher resolution microscopy. This chapter describes the use of fluorescent protein fusions and labelling with smaller fluorescent tags to compare the localization of autotransporters in putative secretion accessory factors.

The red fluorescent monomer mCherry was chosen for this study due to its unique characteristics. mCherry consists of a GFP-type terminus which facilitates stability of N- or C-terminal fusions. In addition, it provides higher photostability, speeds up maturation and pH resistance. Moreover, it indicates long excitation and emission wavelengths (587/610 nm) and better fluorescence quality along with reducing artefacts(311–313). Being a monomer, it is also conducive to membrane translocation. Moreover, mCherry fluorescence can be detected in an active form in the periplasm.

The autotransporters chosen for this study were EspC and AaaA as the laboratory had access to the tools required for their analysis. All the plasmids used were verified genetically and the production of the expected proteins confirmed by immunoblotting. Likewise, introduction of these plasmids into the AT accessory factor secretory mutants (Δ*proW*, Δ*slyB*, Δ*sapA*, Δ*ybgC*, Δ*yqjE* and Δ*abrB*) was confirmed prior to AT localization. The only putative secretion accessory factor mutant showing potential after the EspC-mCherry screen was

the Δ*slyB* mutant, however using EspC-TC or AaaA-TC tracked proteins, a role in AT secretion could not be reliably observed in this study.

The putative AT secretion accessory proteins had been identified by a screen of transposon mutants for deficient EspC secretion conducted by Louise Arnold(310). Following on from this, the defined mutants used in this study were constructed by Dr Stephanie Pommier using Lambda Red (unpublished). Previous characterization that had given us hope that the putative AT secretion accessory proteins might influence AT localization includes the following. ProW (accessory factor of the osmoregulatory transporter ProU) gathers at the poles of the cells and polar localization was reported to occur in a phospholipid cardiolipin independent manner(279). SapA is a periplasmic protein that is putatively involved in peptide transport. In previous studies SapA was revealed to play a role in resistance to antimicrobial Peptide PR-39 and is considered as a virulence factor of *Actinobacillus pleuropneumoniae*(314). PR-39 is a linear porcine antimicrobial peptide including 39 amino acid residues with a high proline profile. PR-39 enhances expression of the *sapA* gene in *A. pleuropneumoniae* (314). Another study found SapA in the periplasm along with FhuD, and with PstS in the inner membrane. This forms an ABC transporter complex associated with other IM proteins during active transport(315,316). YbgC is part of the Tol-Pal system which is found in diverse groups of Gram-negative bacteria, and its function is mainly described as protection of the cell envelope and periplasmic translocation(317). In *E. coli*, the *tol-pal* gene cluster encodes seven proteins: YbgC is a cytoplasmic protein, whilst TolA, TolQ, and TolR are inner membrane proteins, TolB and YbgF are periplasmic proteins, and Pal is a peptidoglycan-associated lipoprotein(318). The function of the YbgC protein and its pathway is not fully characterized, and its homolog found in *Pseudomonas* sp. is CBS3 4-hydroxybenzoyl-CoA (4-HBA-CoA) thioesterase(303). Another study suggested that deletion of *ybgC* caused *Salmonella enteritidis* to adopt an egg white morphology involving a change to a round shape and cell lysis that could be genetically complemented(300). Recent studies in *S. enteritidis* also revealed that deletion of *ybgC* activates membrane lipid composition-related genes that ultimately reduced resistance to lysozyme(301). YqjE is a putative inner membrane protein found in *E. coli* that is also known as non-TA toxic protein and can increase the persistence and dormant state in bacteria by reducing cell growth(307). AbrB is known as a regulatory protein of antibiotic resistance in *B. subtilis*(319–321). This protein regulates genes involved in biofilm formation and

bacterial response to environmental stress(319,320). SlyB is a tiny lipoprotein that consists of only 158 amino acids. SlyB is located in the outer membrane of different Gram-negative bacteria, and plays an important role in cell envelope integrity(262). In *Burkholderia multivorans*, a mutant in *slyB* produced long filamentous cells which were not identified in our cultures of wild type or *slyB*-complemented cells (262). The *slyB* mutant also revealed high sensitivity to EDTA and SDS and low siderophore activity(262).

In this study, plasmids encoding fluorescently tagged EspC and AaaA were introduced into the defined putative accessory factor mutants, and the construction of these new strains was verified at the genetic and protein level. During the preparation of the data presented in this chapter, a number of optimisation steps were developed, although further changes could also be considered as outlined below. In the first PCR analysis for the plasmids presented here, primer-dimers were observed (Supplementary Figure 1 panel A). The result was optimised by increasing the annealing temperature to 60°C and preparing 1:10 dilution of F-espC and R-ApaI-espC primers. Therefore, non-specific bands disappeared in the PCR confirmation of plasmid transformation (Supplementary Figure 2 Panels A-C). Concerning restriction enzyme digestion, preparation of 50µl reaction mixes and 5µl buffer for 1000ng plasmid DNA along with an increase in the incubation period for up to 1.5 hour generated clearer bands for both primary plasmid verification and plasmid transformation confirmation. In terms of transformation, the primary control for competent cells and original mutant strains was set following optimisation and incorporated using a maximum of 100 ng (1.5µl) of plasmid DNA. Furthermore, utilising 2ml instead of 1ml of the bacterial overnight for plasmid preparation increased the quality of the DNA, and subsequently the efficiency of chemical transformation was significantly increased. In addition, it appeared that using DNAase-free water instead of gene elution buffer (provided by the manufacturer) increased the efficiency and sharpness of bands for following restriction enzyme digestion. As an alternative for competent cell preparation, the less time-consuming, one-step protocol of Transformation storage solution (TSS) could have been used(322).

The defined mutants (created by Dr Stephanie Pommier using lambda red) did not show the same reduced secretion of EspC that the transposon mutants had done, with some unexpectedly secreting higher levels. The distribution of EspC-mCherry between whole cells and culture supernatant was different in the Δ*slyB*

deficient mutant compared to in the parental MG1655 *E. coli*. A difference was observed when EspC was fused to mCherry, irrespective of the presence of the β-barrel. In general, Immunoblotting was suggestive of altered stability of EspC-mCherry, or potentially the promotion of cell lysis, in the Δ*slyB* mutant. One possibility would be that the overproduced protein forms inclusion bodies. The rapid accumulation of the overproduced protein may lead to an increase in the tendency to form inclusion bodies. When it was induced at 25°C, the enzyme production rate was slower compared to when it was induced at 37°C and equally the lower concentration in terms of the proteins could help in the prevention of the formation of the insoluble aggregates(323).Bacterial physiology was evaluated in parallel with localizing the fluorescently tagged AT in each potential AF mutant. Microscopy revealed that EspC fused to mCherry with a functional β-barrel transporter (pLA33C1MC), accumulated in discrete patches in AT AF mutants and the parent (MG1655) in a similar way. When EspC lacking its C-terminal β-barrel transporter domain was fused to mCherry (pMAC33), it was detected diffusely along the length of the bacterial cell but appeared to have distinct foci in the parent (MG1655) and AT AF mutants except for Δ*slyB*. In the Δ*slyB* mutant, the localization of tEspC-mCherry resembled that of full length EspC-mCherry. In general, it appears that lack of β-barrel transporter domain has an effect on the localisation and dispersion of the the EspC secretion pattern.

In general, no significant difference was identified between the complemented Δ*slyB* mutants, the Δ*slyB* mutant and MG1655 parental strains containing EspC, EspC-mCherry and tEspC-mCherry for both protein secretion and microscopy localization patterns, but there was the possibility that the resolution of fluorescent microscopy was not sufficient to detect subtle changes. It is also possible that in the complemented strains that the necessity to include two antibiotics in the culture medium to select for the plasmids may have hampered growth and affected the analysis. This may have been circumvented by altering the induction conditions to increase the number of induced cells.

In order to compare localization patterns at a greater resolution, another labelling technique (small tetracysteine tag technology) was employed, and the study was extended to include two ATs. This Flash tag technology is widely used to investigate protein dynamics (localisation over time and stability) and activity inside eukaryotic cells. Compared to mCherry fusion, this technique is more technically convenient. In addition, the TC-tag is composed of only 6 amino acids

compared to mCherry (~235) that provides better understanding of localization and protein function since it provides the potential for higher resolution. Stability, brightness and color diversity are other advantages of using this technology.

Localization of EspC and AaaA variants in both MG1655 and the Δ*slyB* mutant were analyzed by FLASH tag labelling and confocal Microscopy. The data suggested that the localization patterns were similar between MG1655 and the Δ*slyB* mutant. The tAaaA looked like it was in discrete foci while EspC and AaaA adopted a distribution that resembled the previously observed spiral pattern in some bacteria. The low fluorescence of EspC observed in this experiment may be as the construct used has the non-optimal substrate-binding motif (CCKGCC) instead of the optimal one (CCPGCC). Recent studies have extensively explained diverse applications for small tetracysteine tag technology in protein localization both in eukaryotic and prokaryotic cells to follow up the dynamics, motility and interactions of molecules inside living cells(324–328). Advantages of FlAsH-tag technology include the freedom to insert the TC motif at a specific site in the protein of study(329,330). In addition, the TC-Tag is composed of only a small (6 amino acid) sequence compared to ~235 amino acids (mCherry) which facilitates insertion and study of the activity of the target protein(331). However, a high level of background staining can cause low specificity in this technology(332,333). In addition, non-specific binding to cysteine pairs increases toxicity(332,333).

For future work and microscopy optimization, it would be advisable to compare these constructs in terms of fluorescent intensity and incubate for different time intervals with different arabinose concentrations to determine if there were any side effects of the labelling. Super resolution analysis would also be useful for better detection of the localization pattern. However, as there was no major difference between the strains, it may be more beneficial to understand other aspects of AT production. Novel super resolution imaging technologies, for example electron cryotomography, which can identify molecules in near-native states, enhancing the certainty about localization, might be considered in future studies(311). In general, the use of advanced imaging technologies to detect protein localization provides better understanding about their behaviour than conventional fluorescence microscopy(334).

Since the data shown here suggested that the transposon screen had not identified bone fide AT secretion accessory factors, the decision was made to follow a related direction that would have the potential to optimize the conditions for another screen. As an alternative to pursuing the identification of AT secretion accessory factors immediately, the regulation of AaaA production was interrogated, and is presented in the following chapter. The aim of this was to enable AaaA secretion to be studied with more optimal growth conditions e.g. at endogenous production levels rather than following high level overproduction. In addition, such an analysis would have the potential to inform the characterization of the role of AaaA in pathogenesis of *P. aeruginosa*, which is currently an unexplored field. A number of tools including transcriptional reporters were available in the laboratory to facilitate such an investigation.

Table 3.2: Phenotypic analysis of secretion and localization of AF mutants.

AT AF Interrupted gene	pla33c1	pLA33C1MC	pMAC33	Phenotype Analysis
proW	WT	Absent	Absent	Secretion
	Absent	Polar	Polar	Localisation
slyB	WT>	Absent	WT<	Secretion
	Absent	Polar	Diffuse	Localisation
sapA	WT>	Absent	WT<	Secretion
	Absent	Polar	Polar	Localisation
ybgC	WT<	Absent	Absent	Secretion
	Absent	Polar	Polar	Localisation
yqjE	WT>	Absent	Absent	Secretion
	Absent	Polar	Polar	Localisation
abrB	WT>	Absent	Absent	Secretion
	Absent	Polar	Polar	Localisation

Chapter 4

Investigation of gene expression in response to internal regulators of the *aaaA* promoter by using Mini CTX-lux

4.1. Introduction

The previous chapter revealed that the transposon mutagenesis undertaken previously by Louise Arnold (Figure 3.2) had not reliably identified AT secretion accessory factors(310). Since this may be due to the high level AT production form the overexpression plasmid present in the strain mutated, it was possible that a screen of a bacteria producing endogenous AT levels. To settle on the appropriate conditions for a new transposon mutagenesis, the project focussed on identifying optimal conditions of AT production, using AaaA as the target. Transcriptional activation of *aaaA* is predicted to be complex since motifs potentially recognized by various transcriptional factors have been previously identified in its promotor. Understanding this regulation will enable more in depth functional analysis of AaaA since it would facilitate studying the bacteria under conditions that AaaA is most active. Since AaaA liberates arginine from an unknown proteinaceous substrate, and as arginine can serve as a source of nitrogen for metabolism or as an alternative energy source when oxygen is scarce, it was hypothesized that *aaaA* may be regulated by regulators linked to arginine metabolism, nitrogen and oxygen(258).

4.1.1. Metabolism in *P. aeruginosa*

The large genome in *P. aeruginosa* provides diverse metabolic pathways for this organism. Ideally, this bacterium will aerobically obtain energy but it can also survive in oxygen-limited conditions and is therefore classified as a facultative anaerobic bacterium (335).

4.1.2. Regulation of aerobic respiration

For aerobic respiration, *P. aeruginosa* can use 3 different cytochrome c oxidases and 2 quinol oxidases(253). Bacterial cytochrome cbb3 oxidases are members of the haeme-copper oxidase superfamily that facilitate energy conservation in low

level oxygen environments for a diverse group of proteobacteria(336). In *P. aeruginosa,* two operons are found that each potentially encode a cbb3 oxidase (cbb3-1 or cbb3-2). Previous studies found that each of the two *P. aeruginosa* cbb3 oxidases varied in their respiratory and regulatory functions and that the cbb3-1 enzyme had an important role in oxygen rich cultures as well(336). cbb3 oxidases of *P. aeruginosa* PAO1 in anaerobic conditions can change anaerobic growth, the denitrification process, cell morphology and facilitate biofilm formation through cell elongation induced by NO accumulation(337). Their affinity towards oxygen is different from each other and therefore provides a selection mechanism that can be exploited as a survival advantage in certain environmental conditions (253). Regulation occurs mainly through the transcriptional regulator ANR, the two-component transcriptional regulator RoxSR and RpoS, the stationary phase sigma factor(335,338,339). The main oxidases identified in recent years and their regulation mechanisms are shown in Table 4.1.

P. aeruginosa prefers to utilize carbon from the surrounding environment and represses acquisition of alternative nutritional sources in the process known as carbon catabolite repression (CCR)(340). CCR enables bacteria to manage available nutritional resources to maximise growth(341). Unlike *E. coli, P. aeruginosa* prefers to utilize amino acids and some organic acids instead of glucose as their central energy source. Further evidence supported that the presence of succinate and acetate inhibit gluconate, glycerol, fructose and mannitol related genes(342). It appears that hydrocarbons are the last resort nutritional source used by *P. aeruginosa*(253,343).

Table 4.1: The aerobic oxidases elements and regulation of aerobic respiration in *P. aeruginosa*(253).

Oxidase	Group	Regulation	Oxygen affinity	Role
Cbb_3-1	Cytochrome c oxidase	Upregulated by RoxSR	High	Dominant oxidase expressed
Cbb_3-2	Cytochrome c oxidase	Upregulated by ANR Upregulated by RoxSR	High	Upregulated in low oxygen or stationary phase conditions
aa_3	Cytochrome c oxidase	Downregulated by RoxSR Upregulated by RpoS	Low	Induced under carbon, nitrogen or iron starvation
Bo_3	Quinol oxidase	Upregulated by RoxSR	Low	Induced under iron starvation or presence of s-nitrosoglutathione (NO producer)
CIO	Quinol oxidase	Down regulated by ANR Upregulated by RoxSR Upregulated by RpoS	Low	Important low oxygen concentrations when cyanide concentrations inhibit haem-copper oxidases Expressed under conditions of copper starvation

4.1.3. Aerobic Arginine metabolism and related catabolic pathways

The preferred Arginine succinyltransferase (AST), the arginine decarboxylase (ADC) and the arginine dehydrogenase or transaminase (ADH, or ATA) pathways are the 3 main aerobic arginine catabolic mechanisms identified in *P. aeruginosa.* In addition, conversion of D-arginine to L-arginine via chemical or heat reaction (racemization pathway) was also found in recent studies(253,344–347).

In the AST pathway, before glutamate formation, a group of enzymes encoded by *aruCFGDBE* operon are initially active (253). After glutamate is synthesized, the *gdhB* gene contributes by encoding an enzyme that converts glutamate into

2-ketoglutarate(Figure 4.1)(253). In the presence of environmental arginine, ArgR induces the *aruCFGDBE* operon and *gdhB* gene (346,348,349). In the absence of the AST pathway, the ADH (ATA) mechanism is an alternative option (Figures 4.1, 4.2) (253). The ArgR arginine sensing and utilization regulator is not involved in the induction process of this pathway, but recent studies suggested that an *argR* mutant upregulates ADH (ATA) in the absence of AST and another operon known as *aruHI* (350). This is triggered through the AruRS two-component system (TCS) that helps arginine activation(344,345,348).

ADC pathway is another aerobic catabolic pathway in which arginine is converted to agmatine and putrescine (Figure 4.3)(253). The main goal of this metabolic mechanism is proposed to be for putrescine provision that can be converted to spermidine (351). Instead of ArgR regulation, agmatine, N-carbamoylputrescine and arginine upregulate *aguBA* (agmatine deiminase operon) and N-carbamoylputrescine amidohydrolase, that convert agmatine to putrescine (352,353). Moreover, the ADC pathway is regulated by CCR and nitrogen repression(352,353). Previous studies suggested that succinate or citrate repress this pathway in media including arginine or agmatine; a mixture of succinate and ammonia or glutamine inhibit agmatine deiminase and N-carbamoylputrescine amidohydrolase(253,352).

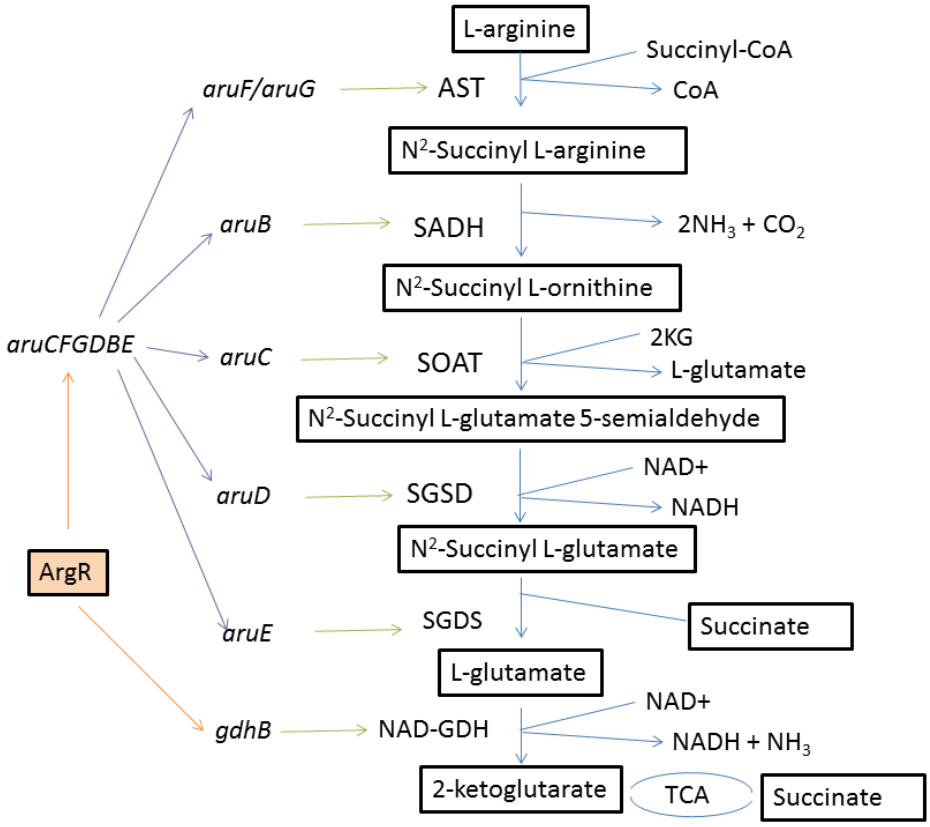

Figure 4.1: The arginine succinyltransferase (AST) pathway(253). L-arginine is converted by the arginine succinyltransferase (AST) enzyme to N2-Succinyl L-arginine releasing CoA. N2-Succinyl L-arginine is then converted to N2-Succinyl L-ornithine by N2-Succinylarginine dihydrolase (SADH), releasing ammonia and carbon dioxide. N2-Succinyl L-ornithine is converted to N2-Succinyl L-glutamate 5-semialdehyde by N2-Succinylornithine 5-aminotransferase (SOAT) with the release of L-glutamate. N2-Succinyl L-glutamate 5-semialdehyde is converted to N2-Succinyl L-glutamate by N-Succinylglutamate 5-semialdehyde dehydrogenase (SGSD) with the conversion of NAD+ to NADH. N2-Succinyl L-glutamate is converted to L-glutamate and succinate by N-Succinylglutamate desuccinylase (SGDS). Succinate enters the TCA cycle while L-glutamate is converted by the NAD+ dependent glutamate dehydrogenase (NAD-GDH) to 2-ketoglutarate with the conversion of NAD+ to NADH and release of ammonia. The 2-ketoglutarate enters the TCA cycle. The operon aruCFGDBE encodes AST, SADH, SOAT, SGSD and SGDS. The gene *gdhB* encodes NAD-GDH. Both *aruCFGDBE* and *gdhB* are upregulated by ArgR (Yang and Lu 2007; Li and Lu 2009; Itoh 1997; Lu and Abdelal 2001; Nakada and Itoh 2003).

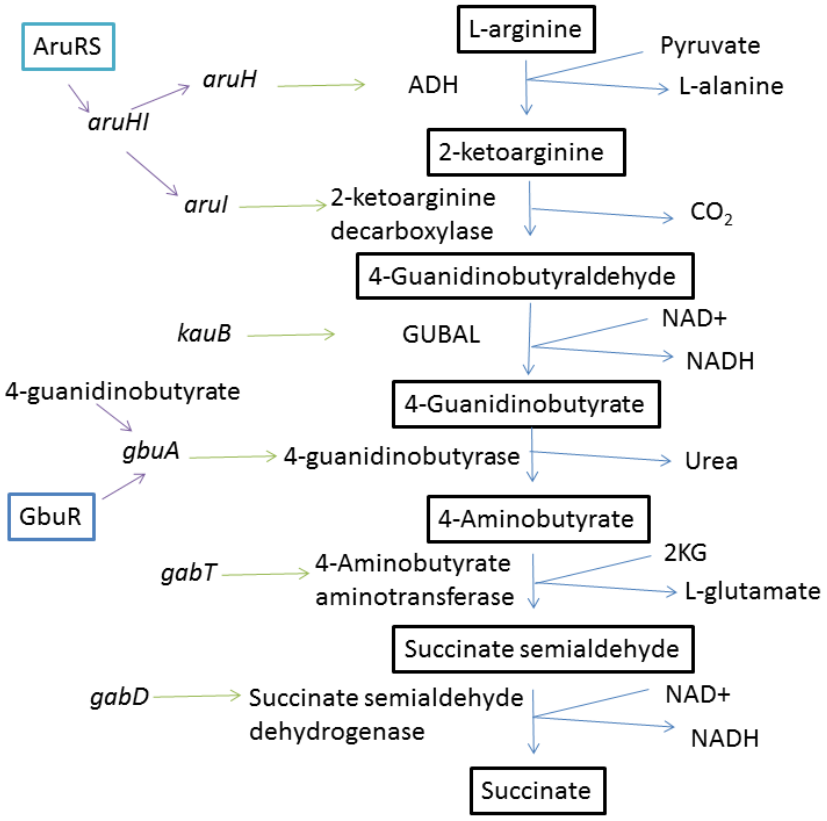

Figure 4.2: The arginine dehydrogenase (ADH, or ATA) pathway(253)**.** L-arginine is converted to 2-ketoarginine with the L-arginine dehydrogenase (ADH) enzyme, with the addition of pyruvate and release of alanine. The 2-ketoarginine decarboxylase enzyme converts 2-ketoarginine to 4-guanidinobutyralehyde with the release of CO_2. The 4-guanidinobutyraldehyde dehydrogenase (GUBAL) enzyme converts 4-guanidinobutyralehyde to 4-guanidinobutyrate with the conversion of NAD+ to NADH. The 4-guanidinobutyrase enzyme converts 4-guanidinobutyrate to 4-aminobutyrate with the release of urea. The 4-aminobutyrate aminotransferase converts 4-aminobutyrate to succinate semialdehyde with the input of 2-ketoglutamate (2KG) and release of glutamate. Finally, succinate semialdehyde dehydrogenase converts succinate semialdehyde to succinate with the conversion of NAD+ to NADH. Succinate enters the TCA cycle (not shown). Regulation of the *aruHI* operon encoding ADH and 2-ketoarginine carboxylase is through AruRS which responds to arginine. The *gbu* gene, which encodes the 4-guanidinobutyrase enzyme, is regulated by Gbu and its substrate 4-guanidinobutyrate (Yang and Lu 2007; Li and Lu 2009; Itoh 1997).

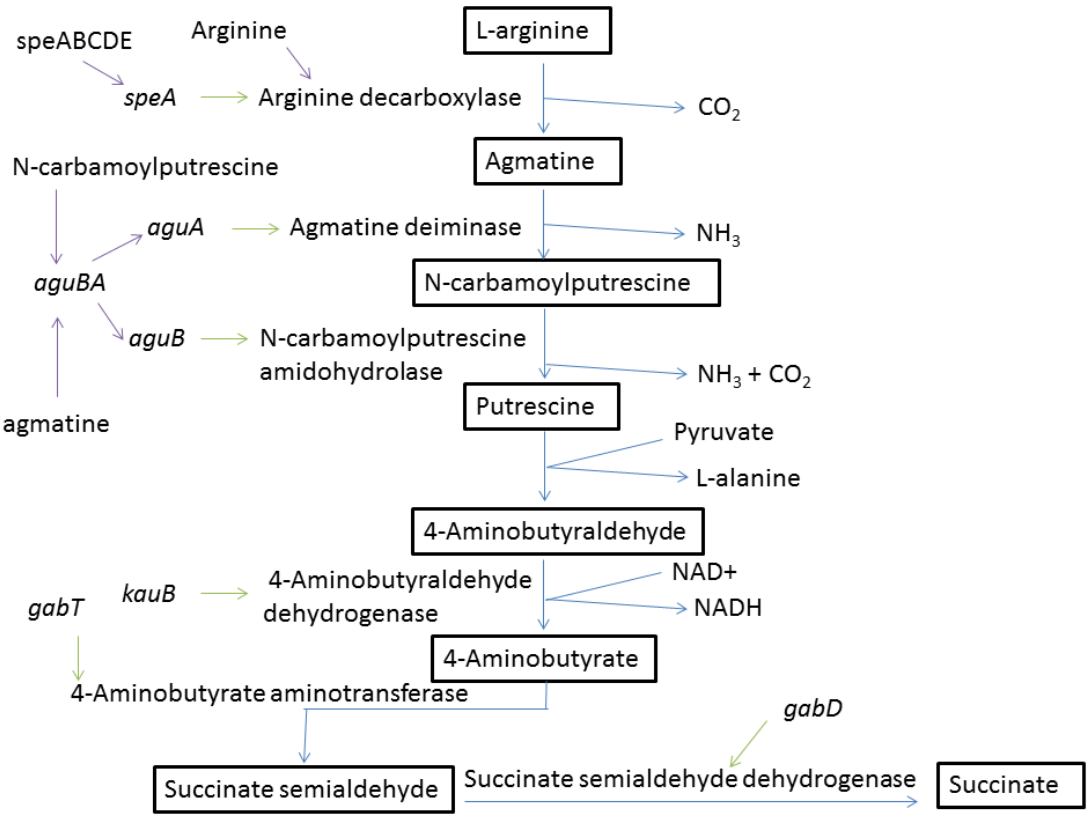

Figure 4.3: The ADC pathway(253)**.** L-arginine is converted to agmatine by arginine decarboxylase (ADC) with the release of ammonia. Agmatine is converted to N-carbamoylputrescine by agmatine deiminase. N-carbamoylputrescine is converted to putrescine by N-carbamoylputrescine amidohydrolase with the release of ammonia and carbon dioxide. Putrescine can then be converted to 4-amminobutyraldehyde with the addition of pyruvate and release of alanine. The enzyme 4-aminobutyrate dehydrogenase then converts 4-amminobutyraldehyde to 4-aminobutyrate with the conversion of NAD+ to NADH. Penultimately, 4-aminobutyrate is converted to succinate semialdehyde with 4-aminobutyrate aminotransferase. Succinate semialdehyde is then converted to succinate by succinate semialdehyde dehydrogenase. When only arginine is available for growth, the arginine decarboxylase is activated. This enzyme is encoded on the operon *speABCDE*. Agmatine deiminase and N-carbamoylputrescine amidohydrolase are encoded on the *aguBA* operon. Both agmatine and N-carbamoylputrescine upregulate activity of these enzymes but not arginine (Mercenier *et al* 1980; Nakada and Itoh 2003).

4.1.4. Regulation of anaerobic respiration

When availability of oxygen is limited in the environment, the denitrification process and its related genes are stimulated and *P. aeruginosa* can utilize nitrate or nitrite as an alternative electron acceptors (253,354). The denitrification pathway is illustrated below (Figure 4.4). Three nitrate reductases are directly involved in *P. aeruginosa* anaerobic respiration: Nar, Nap and Nas(253,355,356). Nap and Nas are also involved in redox regulation and nitrate regulatory function respectively(253,357).

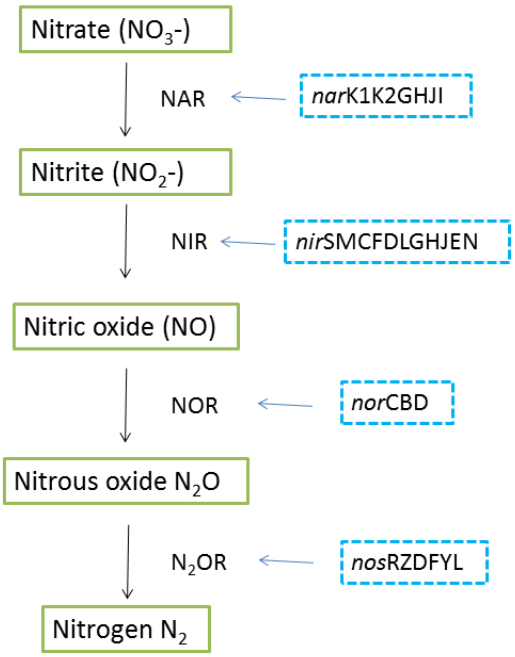

Figure 4.4: The denitrification pathway in *P. aeruginosa*(253)**.** Nitrate (NO_3-) is reduced by the nitrate reductase Nar encoded by the *narK1K2GHJI* operon. Nitrite (NO_2-) is reduced by the nitrite reductase Nir encoded by the *nirSMCFDLGHJEN* operon. Nitric oxide (NO) is converted into nitrous oxide (N_2O) by Nor, a nitric reductase encoded by *norCBD,* and the nitrous reductase N_2OR (*nosRZDFYL* operon) completes the process through conversion of nitrous oxide into nitrogen. (Berks *et al* 1995; Arai 2011; Palmer *et al* 2007).

In anaerobic conditions with high nitrate availability, regulation of the genes for the denitrification pathway is mainly mediated by ANR and DNR that are very similar to the *E. coli* fumarate and nitrate reductase (FNR) activator along with the nitrate sensing TCS NarXL (Figure 4.5) (253,358–361). Nar expression

(*narK1K2GHJI*) causes activation of ANR, DNR and NarXL(253,362–365). In addition, Nir (*nirSMCFDLGHJEN*) is regulated by NirQ(366,367). NirQ provides equilibrium to NO concentration and reduces the cytotoxic effect on cells (Figure 4.6)(368,369). NirQ is regulated by DNR, which is under the control of ANR and NarXL(253). The *norCBD* (Nor) operon, is also controlled by NirQ regulation(370,371). N_2OR (*nosRZDFYL*) is another reductase in denitrification process that is regulated by DNR. *dnr* gene expression is controlled by NarXL and ANR (253,372,373).

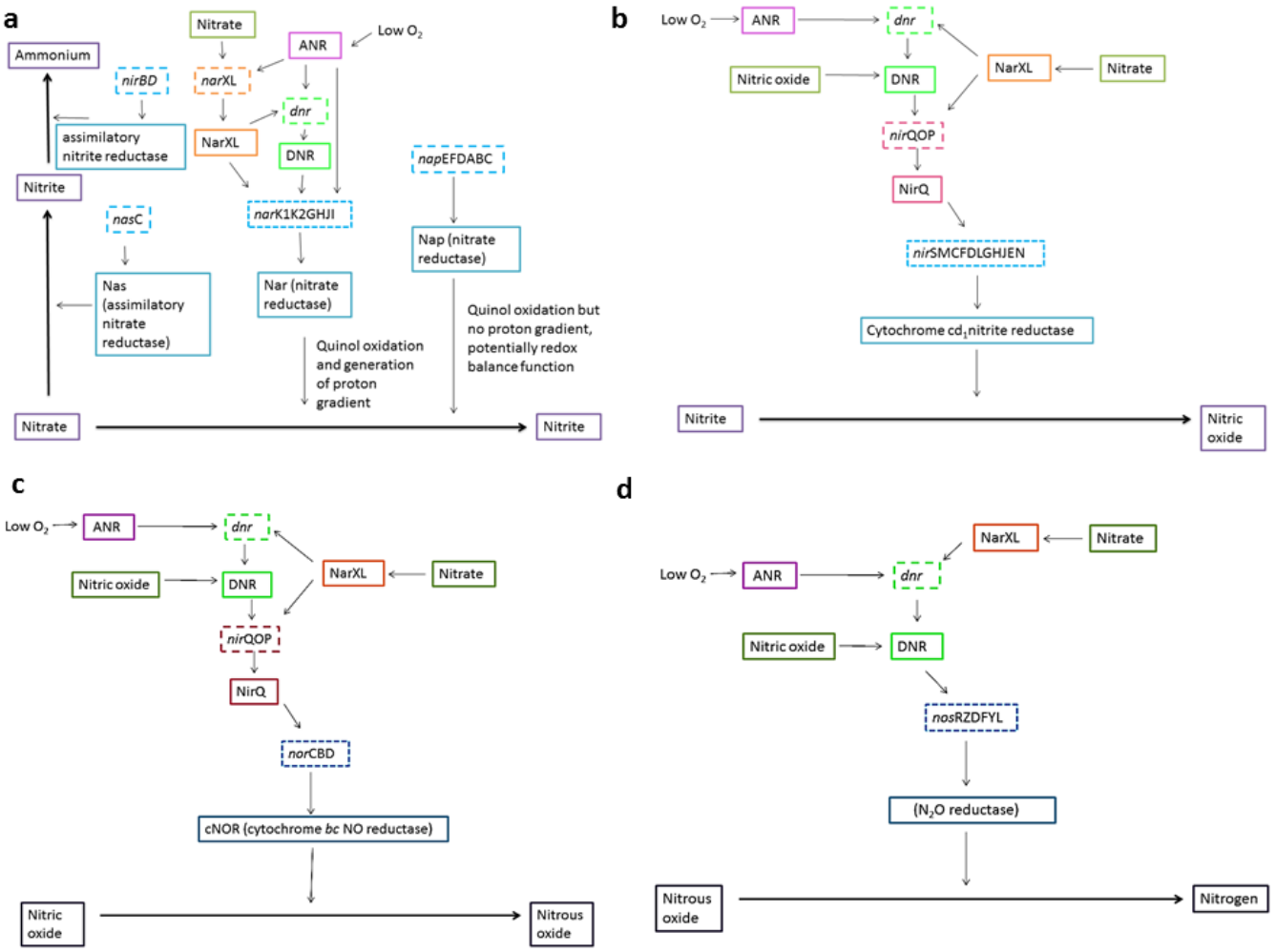

Figure 4.5: Overview of *P. aeruginosa* denitrification mechanism and regulation(253)**.** Reductases are indicated in blue outlined boxes, operons for the reductases depicted in blue dashed outlined boxes. Regulator genes or operons are shown in dashed boxes and regulators in solid outline boxes. In figure 4.5a, there are 3 reductases. While Nas and Nap act as nitrate regulator and possible redox balancing roles accordingly, Nar reduces nitrate to nitrite by quinol oxidation that produce a proton gradient across the membrane. Nar is expressed from the *narK1K2GHJI* operon which responds to ANR, DNR and NarXL regulation (Nadine *et al* 1999; Haas *et al* 1995; Arai *et al* 1991; 1994; 1995). In figure 4.5b nitrite is reduced to nitric oxide by the cytochrome cd1 nitrite reductase. This reductase is encoded by the nirSMCFDLGHJEN operon (Silvestrini *et al* 1989; 1994) which is regulated by NirQ. NirQ is under DNR and NarXL control (Arai *et al* 1998; Jungst and Zumft 1992).

In figure 4.5c NOR reduces nitric oxide to nitrous oxide. NOR is regulated by NirQ (Schreiber *et al* 2007; Arai *et al* 2003). In figure 4.5d nitrous oxide is reduced to nitrogen by N_2O reductase which is regulated by DNR (Arai *et al* 1997; Trunk *et al* 2010).

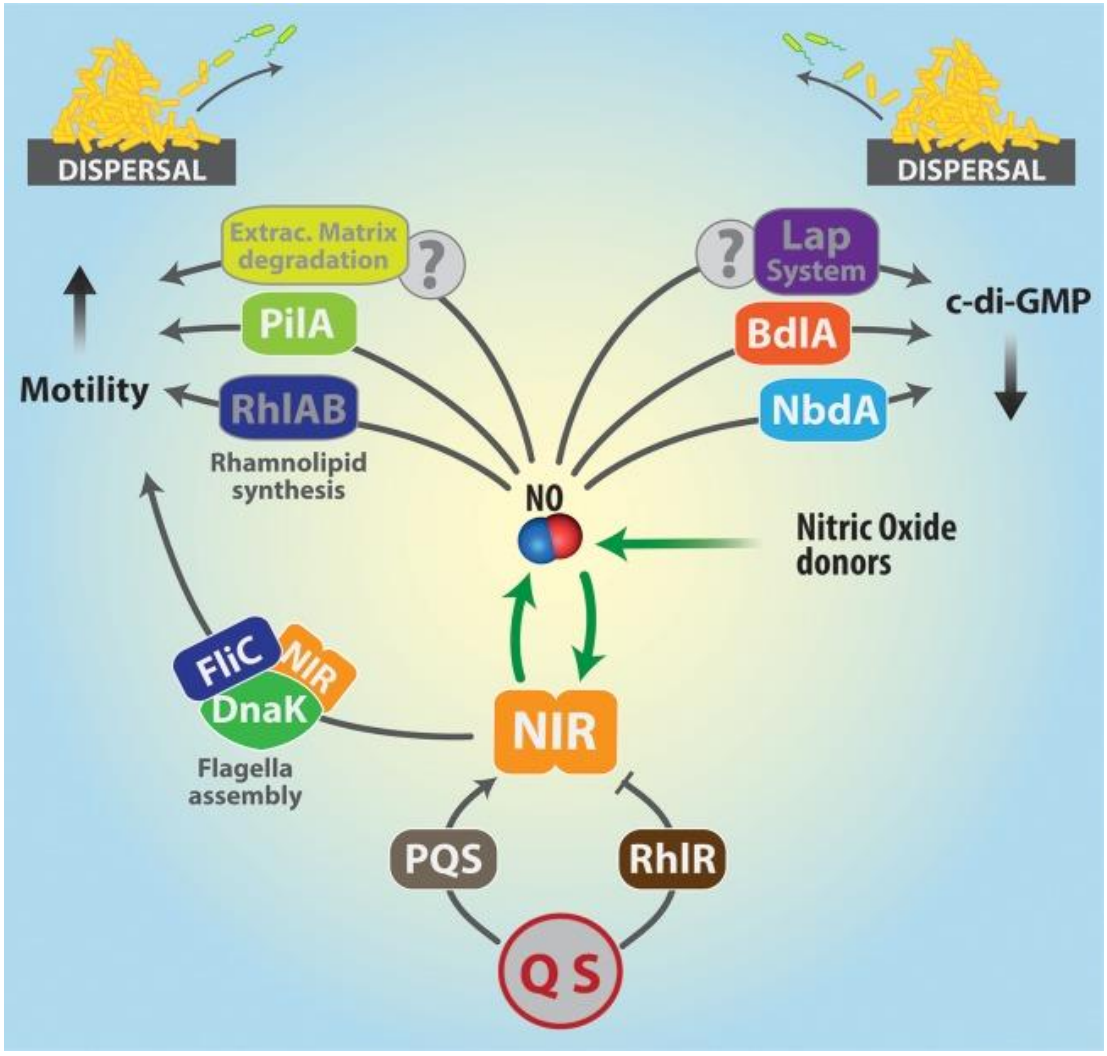

Figure 4.6: An overview of the potential effects of NO on *P. aeruginosa* biofilm dispersal process. In *P. aeruginosa*, NO can be produced directly by the endogenous enzyme nitrite reductase (NIR) or as a by-product of specific metabolic pathways, such as denitrification in limited oxygen conditions. This process is regulated by the arginine nitrate regulation (ANR) and dissimilative nitrate respiration regulator (DNR) transcription factors. In addition, NO may also be produced from external sources such as eukaryotic host cell NO donors such as SNP to target pathogenic bacteria. As NO triggers NIR synthesis, the two internal and external sources may be connected with each other. The NO molecule can enhance motility directly, by acting on flagella, pili, and/or rhamnolipid production, or indirectly trigger NIR expression to generate more NO or to help flagellum aggregation. NIR expression or activity is also regulated by QS (RhlR and PQS), which in turn controls NO levels in response to population density. NO-induced biofilm dispersal also includes the decrease of c-di-GMP

intracellular levels. Two main signalling pathways are identified that lower c-di-GMP concentrations. These pathways are the chemotaxis receptor BdlA and the membrane protein NbdA. Another possible effector of c-di-GMP decrease is the Lap system, whose mechanism of action is not completely clear. NO-sensitive transcriptional regulators and remodelling of the extracellular matrix mechanism require further investigation(374).

4.1.5. The role of pyruvate and arginine in *P. aeruginosa*

In anaerobic conditions, *P. aeruginosa* can adapt and survive by utilizing the energy arginine and pyruvate(253). Pyruvate fermentation is used mainly for bacterial survival in both aerobic and anoxic conditions in the presence of nitrate (Figure 4.7); pyruvate is converted to acetate that is prerequisite for the Krebs cycle(253). In anoxic non-nitrate environmental conditions, pyruvate is metabolised into 3 components: lactate, acetate and succinate(Figure 4.7)(253). The presence of Arginine can enhance this metabolic process due to complementary effect of low pH of acidic pyruvate fermentation components and the high pH generated from ammonia in arginine fermentation(253,375). *ack-pta* operon encodes the phosphotransacetylase (PtA) and the acetate kinase (Ack) regulated by ANR and integration host factor (IHF)(375). Integration host factor (IHF) is a heterodimeric 22 kDa DNA-binding protein, composed of two subunits of IHFα encoded by *himA* and IHFβ encoded by *hip* or *himD* gene(376). In terms of structure and function, IHF is considered a nucleoid-associated architectural protein, binds to a specific sequence of DNA and forms a U-turn structure(376). IHF is involved in many bacterial cellular processes and metabolic activities including site-specific recombination, replication, transcription and biofilm formation (376,377). IHF also facilitates σ54 and RNA polymerase access to promoters and therefore, triggers formation of closed complexes for transcription initiation (376,378).

Propionate can act as a single carbon source for a wide range of bacteria and its metabolism is directly related to malonate and central metabolic pathways such as tricarboxylic acid (TCA)(379). Propionate is converted to pyruvate through the methylcitrate pathway. PrpR is a sigma-54-dependent transcriptional factor (TF) classified in the Fis family. It acts as transcriptional activator of the *prp* gene in *E.coli*(379).

In the presence of arginine, *P. aeruginosa* can survive and even utilize this amino acid to grow gradually in anaerobic conditions devoid of a nitrate nutritional source by the specific arginine deiminase (ADI) catabolic pathway (Figure 4.8)(253). Minimum arginine requirement for specific yeast extract medium is around 30-40 mM(347). Arginine first enters the cells via the arginine/ornithine antiporter and is then transformed into ornithine by a cascade of reactions mediated by arginine deiminase (ADI), catabolic ornithine carbamoyltransferase (cOTC) and carbamate kinase (CK) enzymes(253,380–383). These proteins are encoded on the *arcDABC* operon (253). In oxygen limited conditions, the *arcDABC* operon is activated in response to the ANR regulator while the global arginine regulator, ArgR, can also upregulate the operon. Moreover, different metabolites such as carbon, phosphate and low energy levels can activate the process(253,352,353).

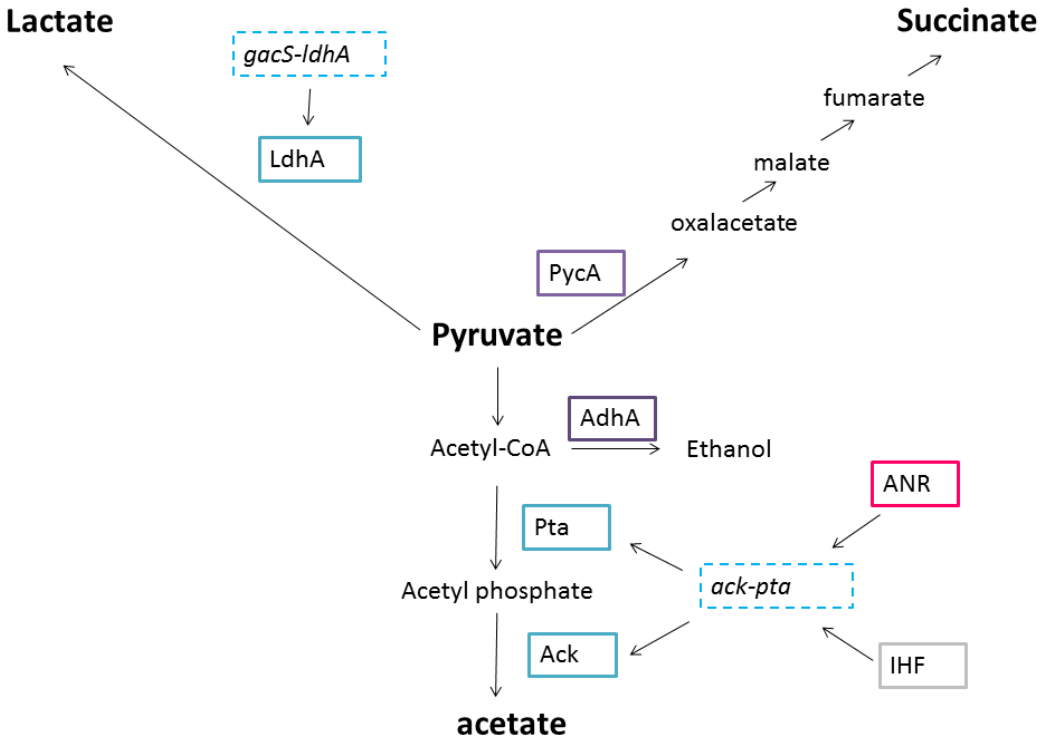

Figure 4.7: Overview of pyruvate fermentation in *P. aeruginosa*(253). Pyruvate is metabolised into acetate, lactase and succinate in anaerobic conditions lacking nitrate. The *gacS-ldh* and *ack-pta* operons are essential to this pathway. The NADH-dependent lactate dehydrogenase LdhA is encoded by *gacS-ldh*. Encoded by *ack-pta* is the acetate kinase Ack and phosphotransacetylase

Pta. AdhA is alcohol dehydrogenase and PycA is pyruvate carboxylase. The *ack-pta* operon is regulated by ANR and IHF. Based on Eschbach *et al* 2004.

Environmental Nitrate can activate NarXL to stimulate preferable and effective denitrification mechanisms that ultimately inhibit ADI catabolic pathway(253). In addition, previous studies suggested that different metabolites such as glucose, fumarate, citrate and pyruvate inhibit ADI pathway as well(352,353).

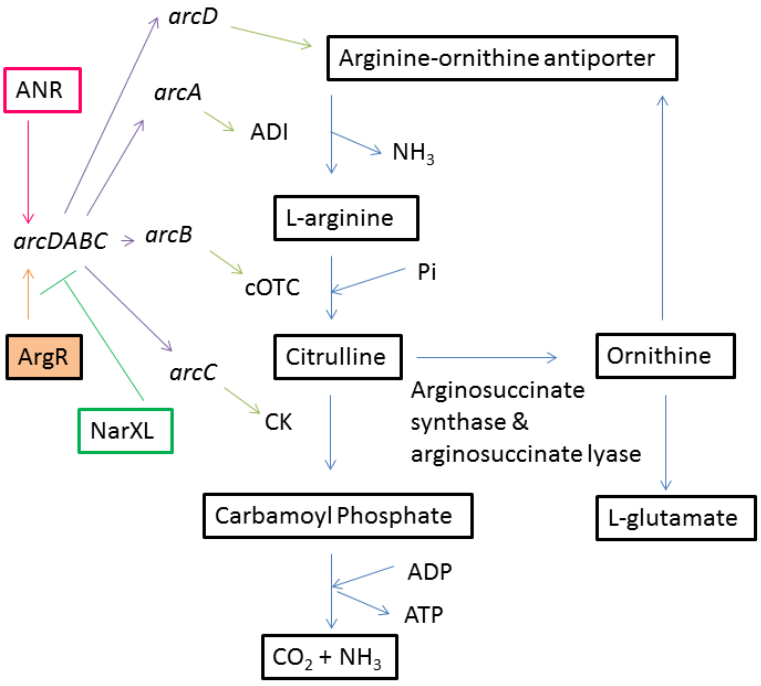

Figure 4.8: The arginine deiminase (ADI) pathway(253)**.** Arginine enters the cell through the arginine-ornithine antiporter and is converted to citrulline by the arginine deiminase (ADI) enzyme. Citrulline is then converted to carbamoyl phosphate by the catabolic ornithine carbamoyltransferase (cOTC) with the addition of phosphate (Pi). Ornithine is released as a by-product and can either be transported outside of the cell through the arginine-ornithine antiporter or converted to L-glutamate by the *aruCFGDBE* operon. Each molecule of carbamoyl phosphate is used to generate 1 molecule of ATP with the assistance of the carbamate kinase enzyme (CK). Carbon dioxide and ammonia is released (Lu *et al* 2001; Maghnouj *et al* 1998).

ANR is involved in direct oxygen sensing and acts as a global regulator for anaerobic gene expression of *P. aeruginosa* (Figure 4.9, 4.10). ANR was found to participate in the transcriptional activation of the *cco2* genes under low oxygen

conditions. ANR also activates the expression of *cbb3-2*, which is a high affinity enzyme and predicted to be dominant under low oxygen conditions(335). ANR also represses the expression of *cio* that is involved in copper starvation and the inhibition of other oxidases(335) .

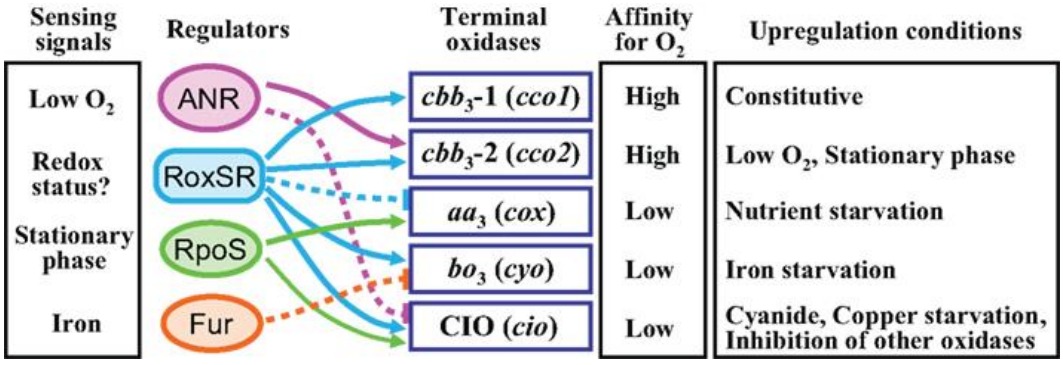

Figure 4.9: Schematic model of the regulatory network controlling the multiple terminal oxidases in P. aeruginosa. The sensing signals for the regulators are shown in the left column(335)**.**

Two transcriptional regulators, ANR and DNR (dissimilatory nitrate respiration regulator), are required for full expression of all denitrification genes (Figure 4.10)(335). Expression of DNR is under the control of ANR(335). Thus, the ANR-mediated anaerobic induction of the denitrification genes is an indirect event that occurs by way of DNR(335). It is not completely clear how ANR and DNR distinguish their target promoters(335).

ANR, the anaerobic regulatory protein is essential for induction of the *arcDABC* operon, which encodes an arginine:ornithine antiporter and enzymes of the ADI pathway, exogenous arginine can further induce its expression level through the interactions of ANR and ArgR(335).

In *P. aeruginosa*, ArgR, the arginine-responsive regulator protein, is autoinduced from the *aot-argR* operon for arginine uptake and regulation(348). The ArgR protein of *P. aeruginosa* belongs to the AraC/XylS family of transcriptional regulators. In the presence of exogenous arginine, the ArgR protein of PAO1 seems to repress the expression of only 3 out of 10 enzymes of the arginine biosynthetic pathway encoded by *argF*, *carAB*, and *argG*(348).

In addition to regulating arginine metabolism, previous studies found that ArgR also regulates genes encoding arginine transporters, that help bacteria to uptake arginine from an extracellular source(384,385). ArgR is a regulatory protein that can function as both a transcriptional repressor and an activator(386). In *E.coli*, ArgR negatively regulates the expression of the arginine biosynthetic genes (the arg regulon) in response to intracellular l-arginine levels(386,387).

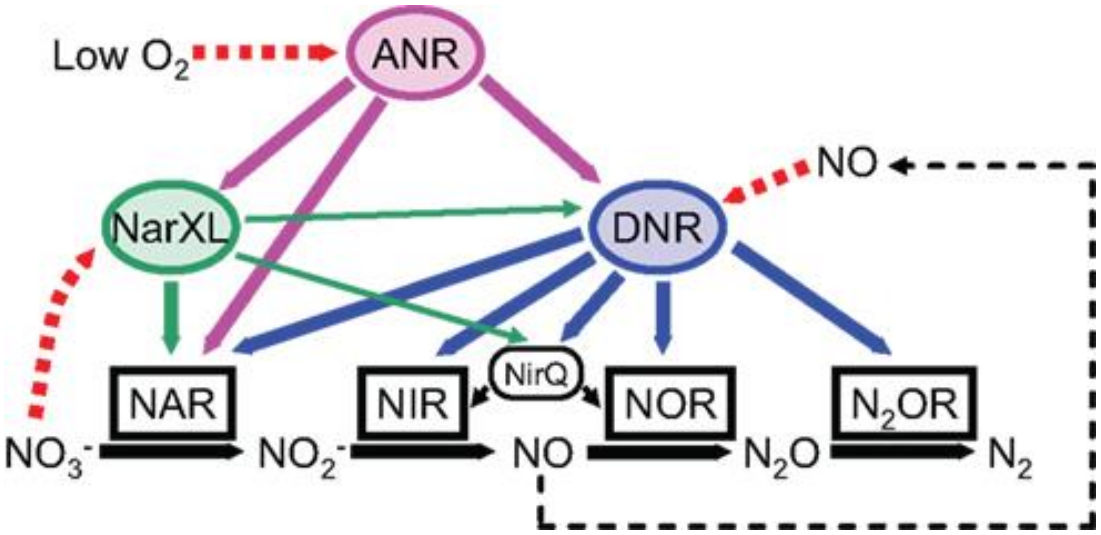

Figure 4.10: Schematic model of the regulatory network controlling the denitrification genes in *P. aeruginosa*. ANR activates the expression of DNR under anaerobic or low oxygen conditions. DNR activates the expression of all denitrification genes in response to nitric oxide. A two-component nitrate sensing regulator, NarXL is required for expression of the *nar* genes encoding nitrate reductase. Both ANR and DNR can activate the *nar* gene expression. NirQ is predicted to be involved in the fine tuning of the activities of nitrite reductase and nitric oxide reductase. NAR, NIR, NOR, and N2OR indicate nitrate reductase, nitrite reductase, nitric oxide reductase, and nitrous oxide reductase, respectively(335)**.**

4.1.6. Regulation and diverse Sigma factors in *P. aeruginosa*

Sigma factors are regulatory proteins that interact with core RNA polymerase, form holoenzyme complex and enhance transcriptional selectivity after binding to their unique target promoters(253,388,389). These accessory elements of the bacterial transcriptional process play an important role in their regulation(390).

In *P. aeruginosa*, nearly 25 different sigma factors have been identified and classified based on their consensus recognition sequence, type of promoter they target plus their adaptation and pathogenic function (Table 4.2). There are alternative sigma factors and extra-cytoplasmic function sigma factors (ECF)(391,392). Transcription initiation is triggered by recognizing specific nucleotide motifs upstream of the desired gene through sigma factors and directing the core polymerase to the transcription initiation point. For instance, sigma 70 factors only recognise -35/-10 of upstream region in promoters(253,391,393).

Table 4.2 : Summary of main function of sigma factors identified in *P. aeruginosa*(253,391).

Sigma factor group	Sigma factor	Description
σ70	RpoD σ70	Binds to a large number of housekeeping gene promoters. Stimulates promoters during exponential phase (Fujita *et al* 1994). Recoginises **T**AtAA**T** at the -10 and **TTG**c**C**c at the -35 sites (Dominguez-Cuevas and Sylvia 2004.
σ32	RpoH σ32	Heat-shock induction response.
σE	AlgU σE	Transcription dependent on AlgU σE. Heat shock and mucoidy.
σ28	FilA (RpoF or σ28)	Flagellin biosynthesis
σS	RpoS (σS or σ38)	Regulates QS (Whiteley *et al* 2000) Activates genes at the beginning of stationary phase (Latifi *et al* 1996).
σ54	RpoN (σ54 or σN or NtrA)	Nitrate assimilation, motility, pili formation and cell-cell communication (Ishimoto and Lory 1989; Totten *et al* 1990). Consensus binding motif of -12GC and -24GG. Transcriptional activator needed.
σECF	Various including PvdS	Regulate genes which provide bacteria with advantages in particular environments. Many linked to OM ferric-siderophore receptors.

4.1.7. RpoN (sigma54), the activator dependent sigma factor

RpoN in *P. aeruginosa*, also known as σ54 and NtrA (253), is an alternative sigma factor that depends on a specialised class of transcription activator, the so called bacterial enhancer-binding proteins (bEBPs) as well as integration host factor (IHF)(253,394,395). It also requires ATP hydrolysis to form an open promoter complex by RNA polymerase (RNAP) holoenzyme during transcription

initiation(253,394). The transcriptional activator often attaches upstream of the RpoN binding site and usually an integration host factor (IHF) binding site mediates close connection between activator-RpoN complex with the rest of the holoenzyme(253,395,396).

EBPs are unique among transcription factors, because they interact exclusively with the sigma factor RpoN to activate transcription of target genes(397). EBPs are the essential machinery of RpoN-mediated transcription(397). They provide spatial and temporal specificity to this process(397). Importantly, signals leading to RpoN-mediated transcription are parlayed through EBPs(397). The signals themselves might be sensed by the EBPs directly or by histidine kinases (HK), which upon receiving the signal, phosphorylate their cognate or partner EBPs(397). The 'active' EBPs interact with RpoN to initiate transcription from target genes(397).

Based on sequence and function, Sigma54 contains two highly conserved domains (Regions I and III) separated by a flexible linker (Region II) (395). The main function of Region I is to keep a closed promoter complex structure and prevent DNA melting along with inhibition of the EBP binding site that ultimately shapes the DNA fork junction near the downstream portion of the promoter in the −12 element(398–400). Region II is a large acidic structure but the role and function is not completely clear(401). Region III is composed of different elements including CBD, helix-turn-helix motif (HTH, residues 365–385) that interrelates with the −12 promoter sequence, and the RpoN domain (residues 386–477) for −24 promoter DNA binding(394,395,402–404). Region III is mainly involved in binding to the promoter DNA at several sites(253). The binding motif for RpoN identified as a -24/-12 format with a highly conserved binding motif region of GG-10bp-GC (Figure 4.11)(253). RpoN can involve and mediate gene repression directly or indirectly through sigma factor binding site competition(253,405).

Recent studies suggested that RpoN regulates a wide range of genes involved in different metabolic pathways including nitrogen fixation and production of glutamine(253,391,406). In addition, RpoN plays an important role in dicarboxylic acid transport, toluene and xylene catabolism, hydrogenase biosynthesis, Quorum sensing via positive regulation of RhlI, and Alginate exopolysaccharide production(253,391,406–408). Moreover, this alternative sigma factor also has roles in structural and pathogenic factors of bacteria such

as pilus production, motility Flagellin biosynthesis and mucin adhesion, internalization into host cells, transport of nutrients, colonization and biofilm formation (253,391,406,409,410). RpoN was also found in *Bacillus subtilis* to have regulatory effects on arginine and ornithine uptake (411). Recognition of arginine and nitrate promoters by RpoN can unlock the relationship between the two metabolic pathways(253).

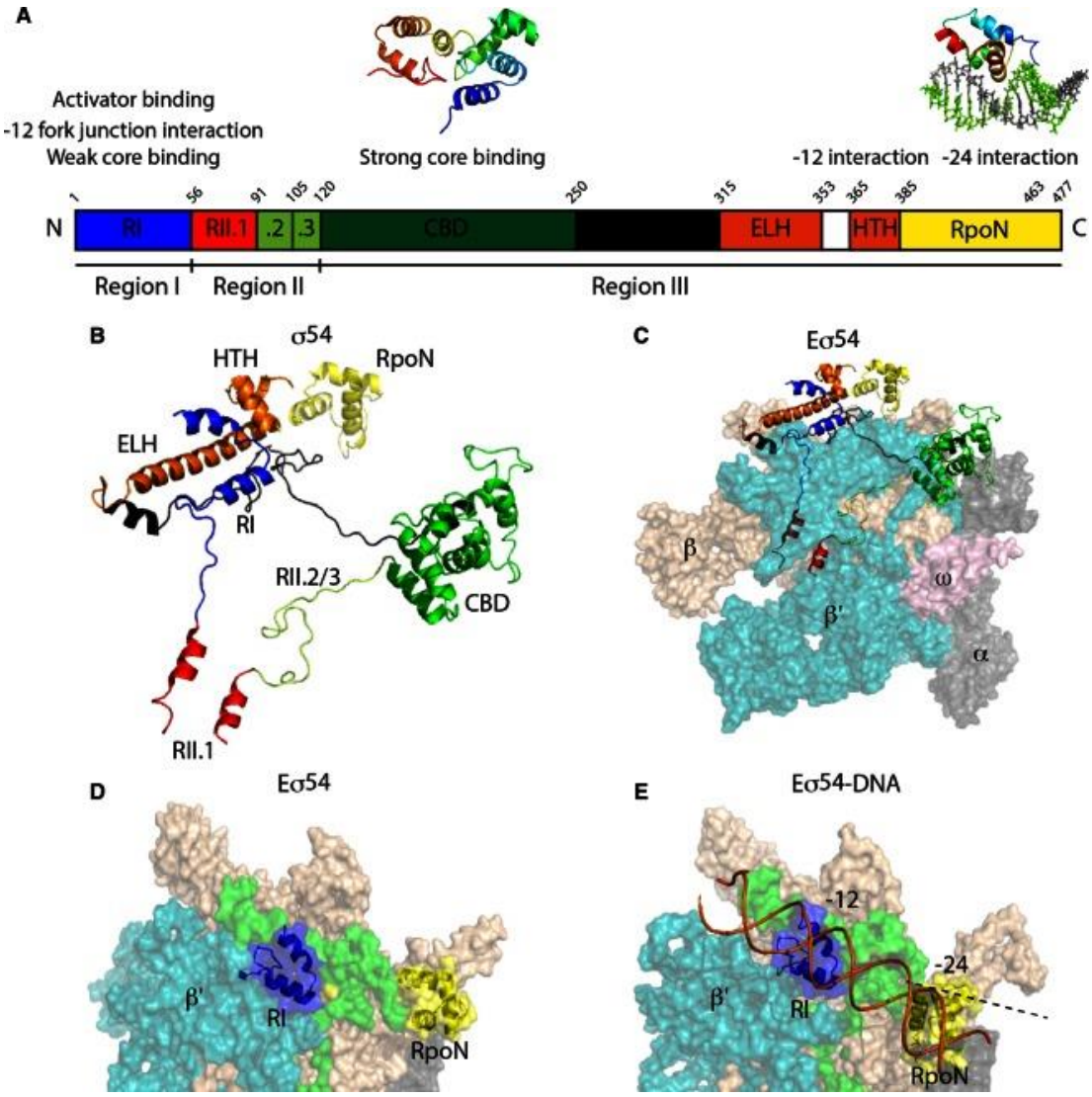

Figure 4.11: Structure of σ^{54}-RNAP and transcription initiation process(395)**.** (**A**) Domain structure of σ^{54}. NMR structures of the CBD and RpoN domains are illustrated (PDB entries 2K9L and 2O8K). (**B**) Crystal structure of σ^{54} (PDB entry 5BYH). Individual domains are coloured as in (**A**). (**C**–**E**) σ^{54}-RNAP holoenzyme in different orientations, coloured by subunits, α — grey; β —

wheat; β′ — teal; ω — light pink. The dotted line in (**E**) depicts the trajectory of the σ^{54} RpoN domain in (**D**) before binding to the promoter.

4.1.8. Quorum sensing, regulator of virulence gene expression in *P. aeruginosa*

Much of the *P. aeruginosa* virulence gene expression occurs in a cell density related manner by utilizing a quorum-sensing (QS) network(412). QS uses small diffusible chemicals (autoinducers) to sense and facilitate communication between adjacent cells within bacterial communities and regulate their behaviour via gene expression changes (Figure 4.12) (413,414). Classical QS systems are composed of an autoinducer synthase along with a specific receptor which detects the cognate signal molecule (253,415,416). As the bacterial population increases, the autoinducers produced and released into the environment rise until they reach a critical concentration. At this quorum threshold, the signal molecule and receptor induce effector gene transcription (253,415,416). Bacteria can possess more than one QS system (417). in *P. aeruginosa*, 4 *QS systems* have been reported (253). *N*-acyl-homoserine lactones (AHL) was the first group of autoinducers found in *P. aeruginosa*(418). The *Pseudomonas* Quinolone Signal (PQS), that is one of a superfamily of alkylquinolones (AQs), was identified as another QS system(419).

The lasR/I and RhlR/I systems are both members of AHL-based QS systems in *P. aeruginosa*. The Las system is composed *lasR(*encodes the transcriptional regulator protein LasR) and *lasI* (AHL synthase) for the production of *N*-(3-oxododecanoyl)-L-homoserinelactone (3-oxo-C12-HSL) (412,420–422). The Rhl system consists of *rhlI* (encoding the AHL synthase RhlI) and *rhlR* genes (transcriptional activator RhlR) for the production of *N*-butanoyl-L-homoserine lactone (C4-HSL)(422–424). The two QS systems are interlinked, with the Rhl system positively regulated by the Las system(423). Rhl can also act independently from Las system as *lasR* mutants are still able to produce pyocyanin(425). Previous study from our lab (Paredes 2014) suggested that RhlR could have a negative effect on *aaaA* transcription(253).

PQS (2-heptyl-3-hydroxy-4-quinolone) is responded to by PqsR(426–428). PQS is induced and activated by the *lasIR* system and inhibited by *rhlIR* system while it activates the *rhlIR* system(253,427,428). 2-(2-hydroxyphenyl)-thiazole-4-carbaldehyde (IQS) autoinducer is a newly identified QS system in *P. aeruginosa*,

activated upon phosphate starvation during infection by a mechanism that depends upon *lasR*(253,429).

QS systems play an important role in pathogenicity and biofilm formation(253). For instance, elastase, LasA protease, alkaline protease and exotoxin A are all regulated by the *las* system(253,430). The *rhl* system is involved in the regulation control of cyanide, pyocyanin and lectin(253,430). The PQS system is involved in iron chelation, redox homeostasis and induces nanoparticle Membrane vesicles (MVs) production which can promote bacterial adaptability(431).

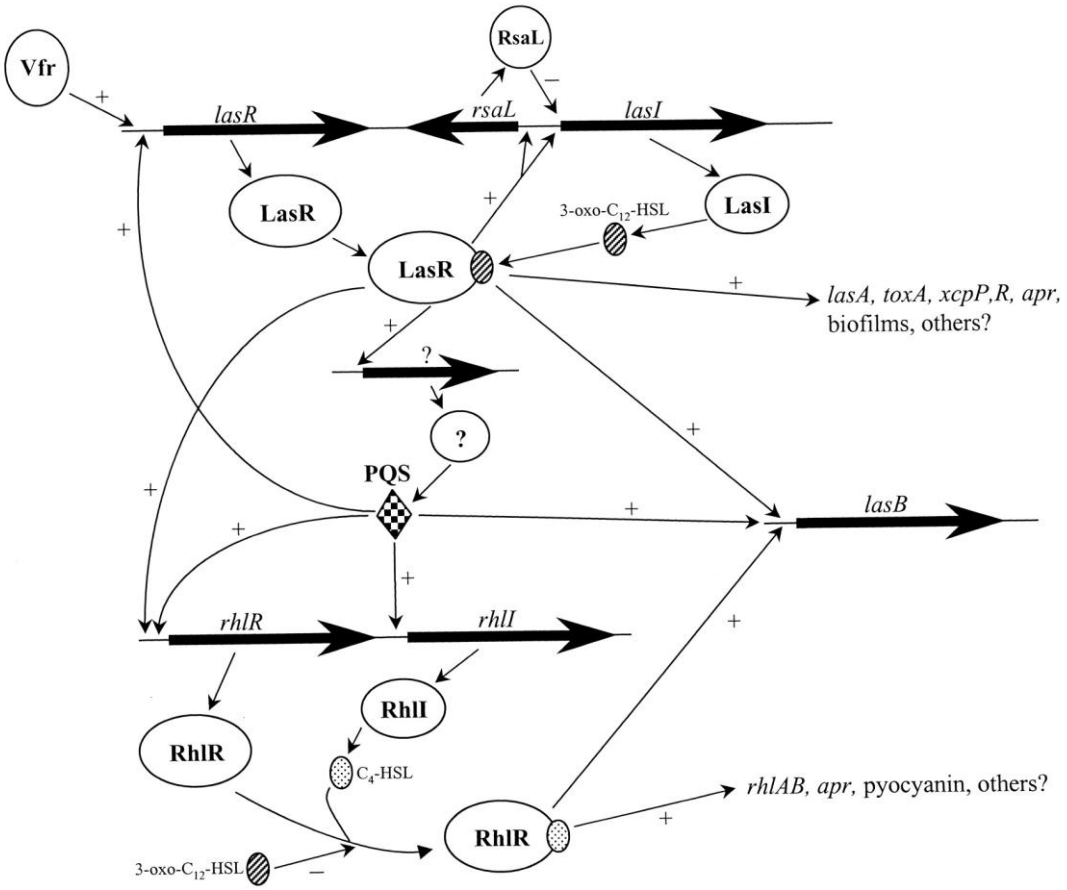

Figure 4.12: Proposed model of the *P. aeruginosa* QS (430). The QS cascade begins with induction when cells reach a threshold density. Vfr induces *lasR*, and the concentration of 3-oxo-C_{12}-HSL increases to the point where it binds to and activates LasR. The LasR–3-oxo-C_{12}-HSL complex induces genes controlled by the *las* quorum-sensing system, including a negative regulator gene (*rsaL*), *rhlR*, and an unidentified gene required for PQS

production. PQS either directly or indirectly induces *rhlI*, which leads to the production of C_4-HSL that binds to and activates RhlR. The RhlR–C_4-HSL complex can then induce genes controlled by the *rhl* quorum-sensing system. At this time, it is not known whether PQS is capable of directly activating RhlR or acts through another regulator. (Two additional unanalyzed LuxR homologs, which may play a role in the activity of PQS, are encoded by *P. aeruginosa* [www.pseudomonas.com].) Genes and proteins are indicated by thick arrows and unfilled circles, respectively. Plus or minus symbols indicate transcriptional activation or repression of the gene(s) at the end of an arrow, respectively. Blocking of the association between RhlR and C_4-HSL by 3-oxo-C_{12}-HSL is indicated by a minus symbol next to the arrow between 3-oxo-C_{12}-HSL and C_4-HSL at the bottom of the figure. Question marks indicate an unknown member(s) of the PQS synthesis pathway that is affected by LasR–3-oxo-C_{12}-HSL.

4.1.9. RsaL, global regulator and QS homeostasis provider of *Pseudomonas aeruginosa*

RsaL is another important and central QS system regulator protein, encoded by the *rsaL* gene. RsaL, along with LasR, can repress expression by binding to P_{lasI} and significantly effects $3OC_{12}$-HSL formation(432,433). RsaL is classified as a QS system inhibitor that directly relies upon LasR-$3O_{C12}$-HSL for its own expression and plays an important role in quorum sensing signal homeostasis(434,435). RsaL is a global regulator that acts as transcriptional activator for more than 130 genes by inhibiting $3OC_{12}$-HSL production or direct interaction with target gene promoters(435). Another study suggested that *rsaL* mutant can enhance pathogenicity, twitching and swarming motility, biofilm formation along with hypersecretion of virulence factors such as pyocyanin, elastase, hemolysins compared to the WT strain(436).

4.1.10. AaaA complex regulatory network

Deciphering the regulatory network controlling *aaaA* is key to unlocking the relationship between this autotransporter and the surrounding environment. It appears that internal and external factors regulate *aaaA* expression in *P. aeruginosa*. Initial investigation of this regulatory network has been undertaken by Esteban Paredes Osses and Daniella Spencer (253,258). This chapter aims to extend this investigation, by examining the role of the proposed RpoN binding

motif identified in the promoter of *aaaA* in mutants that are likely to have altered *aaaA* expression.

The regulatory network of *P. aeruginosa* is considered as the third most complex system among bacteria, and was first proposed and identified in 2011 based on pooled RT-PCR, gel-shift assays, and DNA-foot printing data(253,437). Among the diverse network of regulatory effector elements, a few systems have relevance to *aaaA*. AaaA has a role in biofilm formation because the *aaaA*-deficient mutant did not form bacterial clusters in murine (Luckett et al,2012) or human skin chronic infection models like its parent(258). Work by others with the same chronic skin wound infection model (conducted in collaboration with Dr Kendra Rumbaugh, Luckett et al,2012) has shown that *aaaA* expression is upregulated in this context (Marvin Whitely unpublished), and AaaA is amongst the 20 most produced proteins in PA biofilms(258,438). The global regulatory systems of c-di-GMP (biofilm co-ordination) Ret/Gac/Rsm (acute/chronic switch) and QS (cell density) could all indirectly regulate *aaaA* via their interaction with biofilm formation and pathogenicity (439–443). Moreover, recent studies have shed light on the role of effector regulators in metabolic pathways associated with AaaA, and their effect on *aaaA* promoter (*PaaaA*) activation by miniCTX-*lux* based transcriptional reporter(253,258).

4.1.10.1 The role of arginine in *P. aeruginosa* and its effect on *aaaA* expression

As previously discussed, the AST, ADH (or ATA) and ADC pathways are the main catabolic pathways for L-arginine metabolism in oxygen rich conditions, while the ADI pathway is designed for anaerobic environmental conditions to generate ATP energy for the cell (Figure 4.13) (253). The presence of arginine is a prerequisite for activation of these catabolic pathways(253). For instance, when Arginine is available to the cell, ArgR activates gene expression and controls transcription in both a positive or negative fashion after attaching to its specific motifs (348,384,444). ArgR triggers activation of the AST pathway genes, at the same time as blocking the ADH pathway(253,348,349). Arginine can be used through alternative two-component system (TCS), AruRS, that upregulates *aruH* for activation of ADH pathway(253). Arginine, agmatine and N-carbamoylputrescine can all induce and trigger ADC pathway however, ArgR doesn't play a key role in activation process(253).

In oxygen limited or anaerobic conditions, ArgR increases transcriptional activity of the ADI pathway operon, *arcDABC* and arginine-ornithine transportation operon, *aotJQMOP-argR* that can also effect on ArgR regulator and upregulate it (253,348,384,445). Previous studies found a relationship between AaaA as arginine-releasing enzyme and regulators of Arginine metabolic pathways described above(253,258,348). At first it was thought that *aaaA* expression occurs when *P. aeruginosa* is in an arginine deficit environment (253). However, the data from our lab suggested that ArgR activation triggers *aaaA* expression (253,258,348). Previous study (Paredes Osses thesis 2014) showed that *aaaA* expression was inhibited when arginine is processed during metabolic pathways in aerobic conditions by a negative feedback mechanism. Arginine availability in oxygen limited or anaerobic condition impacts AaaA differently and the complete molecular mechanism is still unknown. Previous study (Paredes Osses thesis 2014) also suggested that elements within ADI pathway contribute in activation and expression of P_{aaaA}. Moreover, ANR positively upregulated *aaaA* expression which could happen indirectly by the ADI pathway after attachment to P_{aaaA} or via other alternative pathways(253,258).

A group of the arginine anabolic pathway components (*argF, argG* and *argJ)* can also activate P_{aaaA}, however, in the presence of arginine, ArgR can inhibit these arginine biosynthetic genes(253,348). As arginine anabolic pathway genes along with ArgR can both activate *aaaA* expression it appears that arginine is a small part of a sophisticated regulatory network of *aaaA*(253).

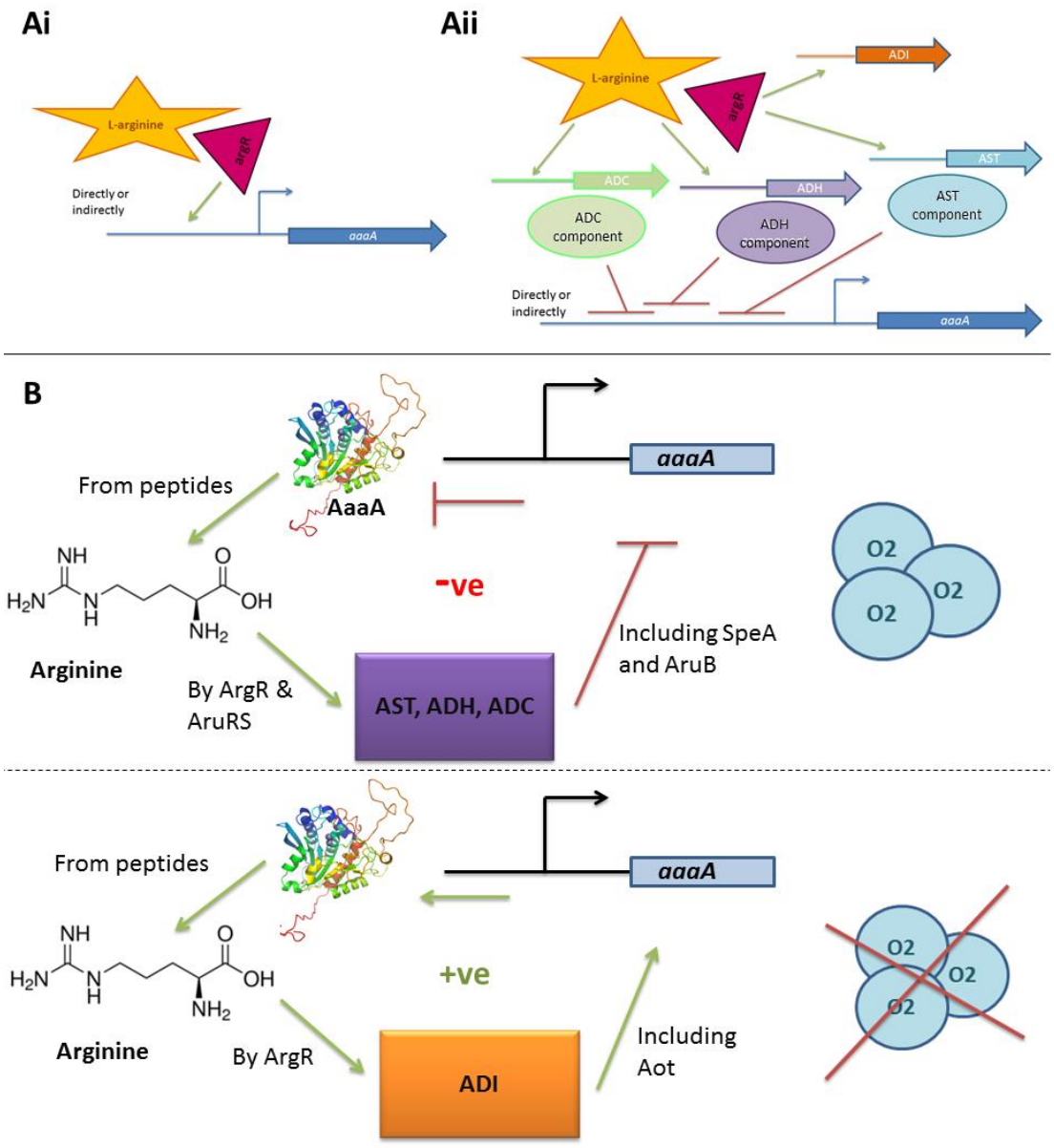

Figure 4.13: Model of relationship between arginine, arginine catabolic pathways, and AaaA (253)**.** The functional significance of AaaA in pathogenicity has been previously reported(258). How this could intercalate with bacterial arginine utilization is represented. Panel A: How AaaA could respond to arginine through the global arginine sensor ArgR. Ai) although counter-intuitive, argR stimulates rather than inhibits *aaaA* expression. B) Arginine stimulates the arginine catalytic pathways in either an ArgR dependent (ADI, AST) or independent manner (ADH, ADC). Components of the AST, ADH and ADC pathway inhibit *aaaA* expression. Green arrows represent a positive influence on expression and red arrows an inhibitory effect. ADI=arginine deiminase pathway, ADC=arginine decarboxylase pathway, ADH (ATA)=arginine

dehydrogenase/transaminase pathway, AST=arginine succinyltransferase pathway. Based on data by: Paredes Osses (2014) and Lu *et al* (2004). Panel B: Hypothesis of how the metabolic feedback loops differ in different oxygen tensions. Data from Paredes Osses (2014) suggests that *aaaA* expression is under a negative feedback loop in aerobic conditions and under a positive feedback loop in anaerobic conditions. ADI=arginine deiminase pathway, ADC=arginine decarboxylase pathway, ADH (ATA)=arginine dehydrogenase/transaminase pathway, AST=arginine succinyltransferase pathway.

4.1.10.2 Sigma factor RpoN, EBPs, and DNA bending proteins: relationship with aaaA expression

Previously (Paredes 2014), our lab reported that RpoN can inhibit *aaaA* expression and play an important role in nitrate-related repression of *aaaA*(253,258). In addition, RpoN can also activate *rhlR* which inhibits *aaaA* expression(258,408). RpoN may exert its inhibitory effect by interacting with P_{aaaA} directly or indirectly(253).

RpoN functions with the transcriptional activators known as EBPs (396,397,446). In previous studies in our lab, Paredes (2014) showed that 2 EBPs known as Sfa2 and Sfa3 are involved in *aaaA* upregulation. In addition, their related binding sites were identified in the T6SS genetic locus and with RpoN found to regulate expression of the gene encoding H2-T6SS(253,447).

Histone-like nucleoid-structuring proteins (H-NS) are another group of proteins that affect transcription(253). MvaT and MvaU are both H-NS like proteins found in *P. aeruginosa*(253). The function of these effector proteins, unlike RpoN sigma factor, is not entirely depending upon recognition of a specific sequence motif. They usually bind to curved areas of DNA with AT rich content(253,448–450). Recent studies revealed that these regulatory proteins are involved in the regulation of the arginine uptake and direct repression of the operon aotJQMOP-argR(349). Our lab (Paredes 2014) has data that suggested MvaT and MvaU can inhibit *aaaA* expression by direct negative regulation of the *aaaA* promoter or may indirectly repress the ArgR and AotJ. Double MvaT/MvaU deletion mutant also had an inhibitory effect on pyocyanin secretion and it appears that these regulatory proteins are involved in anaerobic metabolic pathways including

arginine uptake(253,349). MvaT, MvaU and RpoN are all members of the polyamine modulon, and it appears that they all negatively regulate *aaaA*(253).

4.1.10.3 Complex regulatory network impacting the *aaaA promoter*

Thus it appears that *aaaA* is subjected to a complex regulatory network that requires unravelling (Figure 4.14). Previous studies found conserved putative motifs potentially recognized by different transcription factors or sigma factor binding through Prodoric Virtual Footprint method in the promotor (253,258,451,452). Virtual Footprint is an online framework especially designed to analyse transcription factor binding sites in whole bacterial genomes and their underlying regulatory networks. This included an RpoN binding site and transcriptional initiation site located in the *aaaA* upstream region (258,453) **.**

To evaluate the regulation of *aaaA*, a transcriptional reporter containing the *aaaA* promoter was constructed by Paredes (2014), and conjugated into different mutants that were deficient in regulatory proteins hypothesized to be involved(258). Paredes (2014) showed that the promoter region of *aaaA* was negatively regulated by RpoN, RhlR, MvaT and MvaU, and positively regulated by ArgR using a bioluminescent transcriptional reporter. Although their regulatory effects have been identified, it is not yet clear whether these effects are caused by direct binding of these regulatory proteins to the *aaaA* promoter putative binding regions or not. The aim of this study is to decipher the influence of RpoN upon *aaaA* expression. To see if RpoN regulates *aaaA* expression through direct interaction with the *rpoN* binding motif identified in the *aaaA* promotor, it was mutated and the *aaaA* promoter with the disrupted *rpoN* binding motif was cloned upstream of the *lux* genes to generate a new transcriptional reporter. This novel reporter was then conjugated into different mutants potentially related to *aaaA* expression, and their transcriptional driven light activity monitored alongside the relative activity of AaaA to provide a parallel measure of translation.

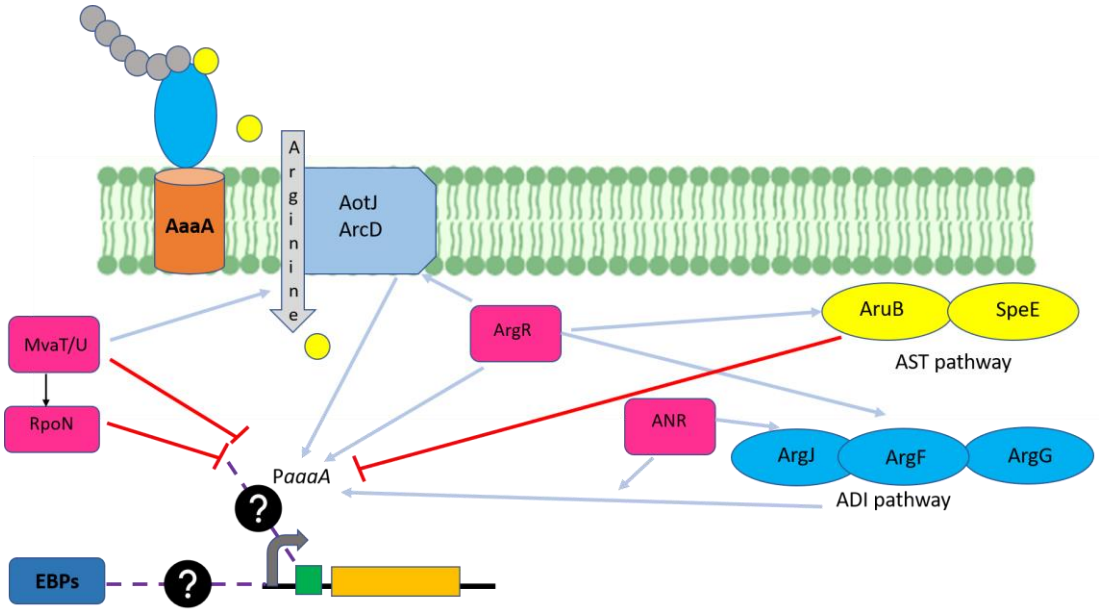

Figure 4.14: Interrogation of the promoter of *aaaA* to identify potential regulators. Paredes (2014) showed that the promoter region of *aaaA* was negatively regulated by RpoN, RhlR, MvaT and MvaU (Red lines), and positively regulated by ArgR (blue arrow) using a bioluminescent transcriptional reporter. Although their regulatory effects have been identified, it is not yet clear whether these effects are caused by direct binding of these regulatory proteins to the *aaaA* promoter putative binding regions or not.The aim of this study is to decipher the influence of RpoN upon *aaaA* expression. To see if RpoN regulates *aaaA* expression through direct interaction with the *rpoN* binding motif identified in the *aaaA* promotor, it was mutated and the *aaaA* promoter with the disrupted *rpoN* binding motif was cloned upstream of the *lux* genes to generate a new transcriptional reporter. This novel reporter was then conjugated into different mutants potentially related to *aaaA* expression, and their transcriptional driven light activity monitored alongside the relative activity of AaaA to provide a parallel measure of translation.

4.2. Results

4.2.1. The putative RpoN binding site in the promoter region of *aaaA* was successfully mutated

To further understand the regulation of *aaaA*, substitution mutations were made in the 500bp upstream promoter region using site directed mutagenesis (Figure 4.15). The 500bp upstream region of *aaaA* had previously been cloned onto a plasmid encoding the *lux* operon, called miniCTX:paaaA:lux by Paredes (2014). Mini CTX-lux was chosen as the reporter for this study because this luciferase reporter provides rapid and quantitative measurements of gene expression. To see if RpoN regulates *aaaA* expression through direct interaction with the putative RpoN binding motif identified in the *aaaA p*romotor, it was mutated. The *aaaA* promoter with the disrupted RpoN binding motif was cloned upstream of the *lux* genes to generate a new transcriptional reporter. To do so, site directed mutagenesis was carried out according to section 2.10.6. First, miniCTX:p*aaaA:lux* vectors were extracted from DH5α cells. Then, PCR amplification was carried out based on KOD Xtreme standard reaction setup and step-down cycling conditions with the mutant primers RpoN SDM Forward II and Reverse II (Table 2.4 and 2.5). The PCR reaction product was then extracted from the gel and digested with KLD mix reaction from NEB to remove methylated template DNA. The product was then transformed into competent cells by chemical transformation. After transformation, plasmids were extracted, and the expected DNA fragment obtained. For further confirmation, plasmids were sequenced and it was confirmed that the predicted RpoN binding site was mutated with SA1 Forward and SA2 reverse sequencing primers.

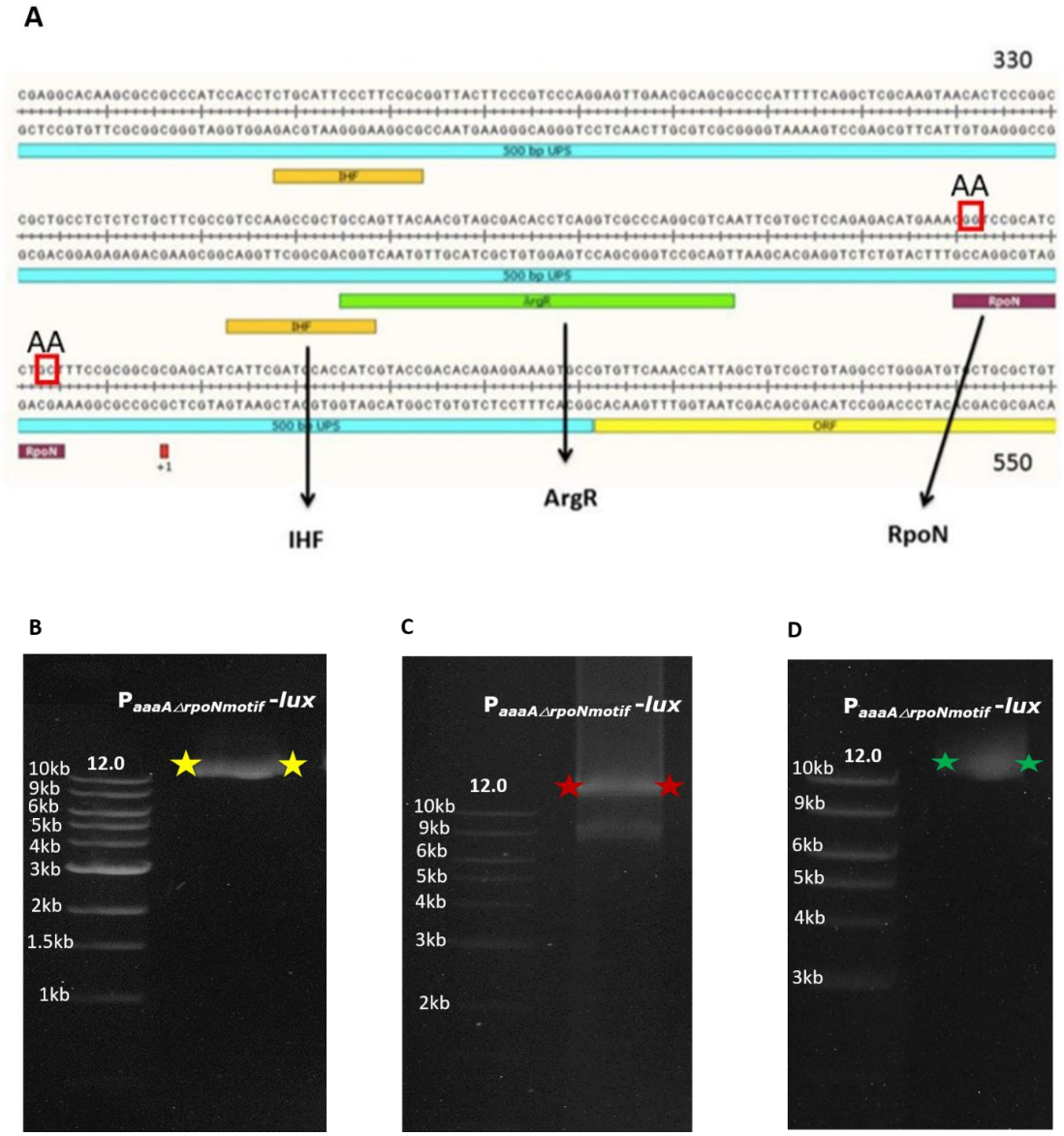

Figure 4.15: The successful strategy designed using the miniCTX:p*aaaA*:*lux* vector for putative *rpoN* binding motif mutation by site directed mutagenesis. The strategy for mutating binding sites in the promoter region of *aaaA* by site directed mutagenesis is shown above the gel images. One IHF site overlaps an ArgR binding site and is in a good location to bring the RpoN binding site into contact with other transcription regulator sites. Orange boxes show IHF, the green box shows ArgR and the mauve box show RpoN putative binding site. The red box shows the putative start of transcription (Panel A). In this study, miniCTX:p*aaaA*:*lux* vectors were extracted from DH5α cells. Then PCR amplification was carried out based on KOD Xtreme standard

reaction setup and step-down cycling condition with the mutant primers RpoN SDM Forward II and Reverse II (Panel B). In Panel (B-D) the asterisks indicate the expected amplification products of 12kb for P_{aaaA} △rpoNmotif –lux transcriptional reporter (yellow). The PCR reaction products were then extracted from the gel (Red) and digested with KLD mix reaction from NEB to remove methylated template DNA (Panel C). The products were then transformed into competent cells by chemical transformation. After transformation, plasmids were extracted and expected DNA fragment (green) obtained (Panel D). For further confirmation, plasmids were sequenced and confirmed with SA1 Forward and SA2 reverse sequencing primers.

4.2.2. AaaA negatively affects its own expression and disruption of the putative RpoN binding motif prevents this negative effect

After successful site directed mutagenesis of the predicted RpoN binding motif in the *aaaA* upstream region and confirmation of nucleotide substitution by sequencing, the $P_{aaaA\triangle rpoNmotif}$–*lux* transcriptional reporter was transformed into the *E. coli* S17-1 strain. The reporter was then conjugated into *P. aeruginosa* PAO1 WT and Δ*aaaA* mutants. As a control the previously constructed constitutive promoter of the kanamycin resistance cassette cloned next to the *lux* operon was used to monitor whether the production of light altered independently of the *aaaA* promoter (Mini CTX-$P_{kan\text{-}lux}$)(258).

It had been previously observed that transcription of the *lux* operon from the P_{aaaA} promoter changed considerably in the absence of active AaaA. Thus, expression from the Mini CTX-P_{aaaA}-*lux* reporter was monitored in the background of the *P. aeruginosa* PAO1 WT and Δ*aaaA* mutant. To do this, the bacterial strains were incubated O/N at 37°C in LB medium containing tetracycline 150 µg/mL. The next day, the cells were normalized to OD_{600nm} 0.05 and placed into a 96 well-plate. The reading of relative luminescence units (RLU) and absorbance (600nm) was analysed in parallel in the TECAN reader System (Infinite® 200 pro) at 37°C for 24 h. The data were plotted (RLU, OD_{600nm} and RLU/OD_{600nm}) and the average under the curve RLU measured for each strain. No significant difference was observed across all conditions with the P_{kan} strains. However, when the *aaaA* gene was absent, light production driven from the intact P_{aaaA} promoter was more than doubled. A paired t-test generated a p-value of <0.0001, revealing that this difference was significant (Figure 4.16).

To see if the putative RpoN binding motif plays a role in this autoregulation, the light production from *P. aeruginosa* PA01 WT or the Δ*aaaA* mutant carrying the $P_{aaaA\triangle rpoNmotif}$-*lux* reporter was similarly analysed. The bioluminescence was monitored over 24 hours since mutants can grow at different speeds, and it is important to identify whether the level of light is low overall, or delayed. This data (Figure 4.16) suggests that disruption of the putative RpoN binding motif in the *aaaA* promotor prevented the negative autoregulation of *aaaA* since no significant difference was observed between WT and the Δ*aaaA* mutant carrying $P_{aaaA\triangle rpoNmotif}$-lux reporter.

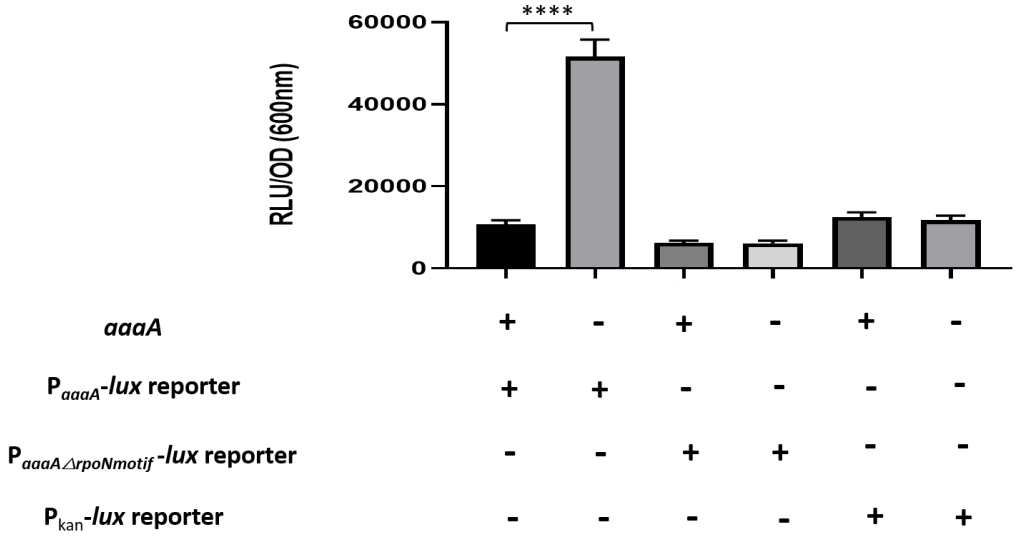

Figure 4.16: AaaA negatively effects its own expression and disruption of the RpoN motif prevents this negative effect.

P. aeruginosa PAO1 WT and *P. aeruginosa* PAO1 Δ*aaaA* carrying the P_{aaaA}-*lux* reporter (either intact or with the disrupted putative RpoN binding motif) or P_{kan} reporter were grown and bioluminescence analysed over time. The bacterial strains were incubated O/N at 37°C in LB medium containing tetracycline 150 µg/mL. The next day, the cells were normalized to OD_{600nm} 0.05 and placed into a 96 well-plate. The reading of relative luminescence unit (RLU) and absorbance (600nm) was analysed in parallel in the TECAN reader System (Infinite® 200 pro) at 37°C for 24 h. The data were plotted (RLU/OD_{600nm}) for each strain. Three biological replicates were used for each sample and the bar represents the average of these. The error bars show the standard deviation from the mean.

General ANOVA summary test analysis performed and P value <0.0001 reported with **** indicating a significant difference.

4.2.3. Exogenous arginine has minimal effect on *aaaA* expression

Based on the rationale that AaaA liberates arginine from its substrates(258), and thus its expression may be regulated by environmental arginine concentrations, different concentrations of exogenous arginine were applied to the reporter strains to investigate whether arginine had an inhibitory feedback effect, particularly with regard to negative regulation in the WT. PAO1 WT and Δ*aaaA* mutants carrying mini CTX-P_{aaaA}-*lux* and mini CTX-P_{kan}-*lux* were incubated in ASM with no exogenous arginine; normal arginine levels (36 μM); and twice the amount of arginine (62 μM). Data plotted is area under the curve: luminescence overgrowth at OD_{600nm} for 24h (Figure 4.17).

Arginine showed no complementation effect. A similar observation was also made previously by Jack Whitmore and Daniella Spencer, indicating it was reproducible that free arginine does not regulate *aaaA* (253). The slight differences in bioluminescence across all strains may suggest that another group of genes is involved in regulation and expression of *aaaA* and suggests that arginine deficiency is not the main controller of *aaaA* upregulation.

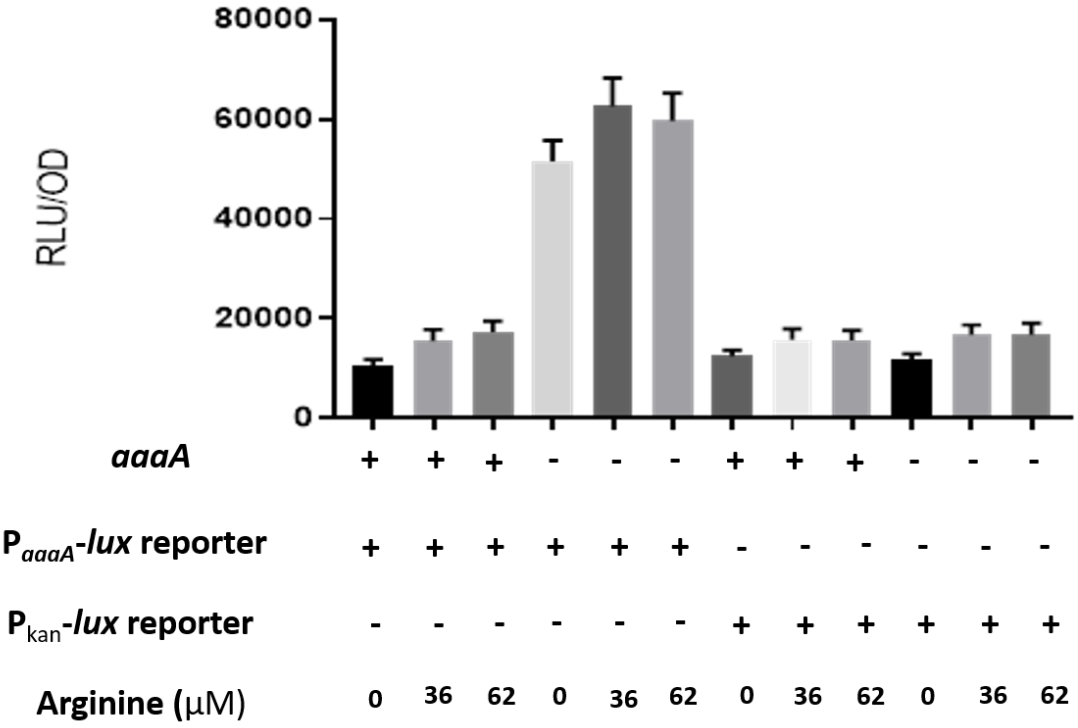

Figure 4.17: Exogenous arginine has minimal impact on *aaaA* expression. PAO1 WT and the Δ*aaaA* mutant carrying either mini CTX-P_{aaaA}-*lux* or mini CTX-P_{kan}-*lux* reporters were incubated in ASM with no exogenous arginine; normal arginine levels (36 μM); and twice the amount of arginine (62 μM). Data plotted is area under the curve: luminescence over growth at OD_{600nm} for 24h. Each experiment was performed in triplicate; error bars indicate the standard deviation. General ANOVA summary test analysis performed and P value <0.0001 reported.

4.2.4. The motif disrupted in the *aaaA* promotor has a negative effect on *aaaA* expression independent of RpoN

Previous study found RpoN negatively regulates the *aaaA* promoter after conjugation of Mini CTX-P_{aaaA}-*lux* and Mini CTX-P_{kan}-*lux* reporters into one *P. aeruginosa* strain, PA14 (258). Luminescence expression in the *ΔrpoN* mutant was five times higher than in the parent strain according to Paredes Osses (2014). In order to further investigate the role of RpoN and its putative binding motif in expression of *aaaA,* in this study *P. aeruginosa* stain PAO1 was used. WT and Δ*rpoN* mutant (plus its complement) were grown carrying the intact P_{aaaA} reporter, or the P_{aaaA} reporter with a disrupted putative RpoN binding motif. Bioluminescence was analysed over time. These strains were grown in LB medium at 37 °C, and luminescence emission followed in the TECAN reader System (Infinite ® 200 pro) as previously. Figure 4.18A shows that mutation of *rpoN* reduces bioluminescence from the intact P_{aaaA} reporter in the PA01 background. In Figure 4.18B, it can be seen that when the putative RpoN binding motif sequence is altered, luminescence expression is five times higher in the *rpoN* deficient mutant compared to WT, and this can be genetically complemented by providing RpoN from a plasmid. General ANOVA summary test p-value of <0.0001, revealing that this difference was significant.

Interestingly, in the *rpoN* mutant background, the reporter driven by the altered promoter generates considerably more bioluminescence than the intact P_{aaaA}-reporter, suggestive of a negative effect of the motif upon *aaaA* expression. It is likely that RpoN binds to the *aaaA* promoter at a site distant to the previously identified binding motif. A double *rpoN*/*aaaA* mutant is required for future studies to see if AaaA negatively regulates itself using this motif.

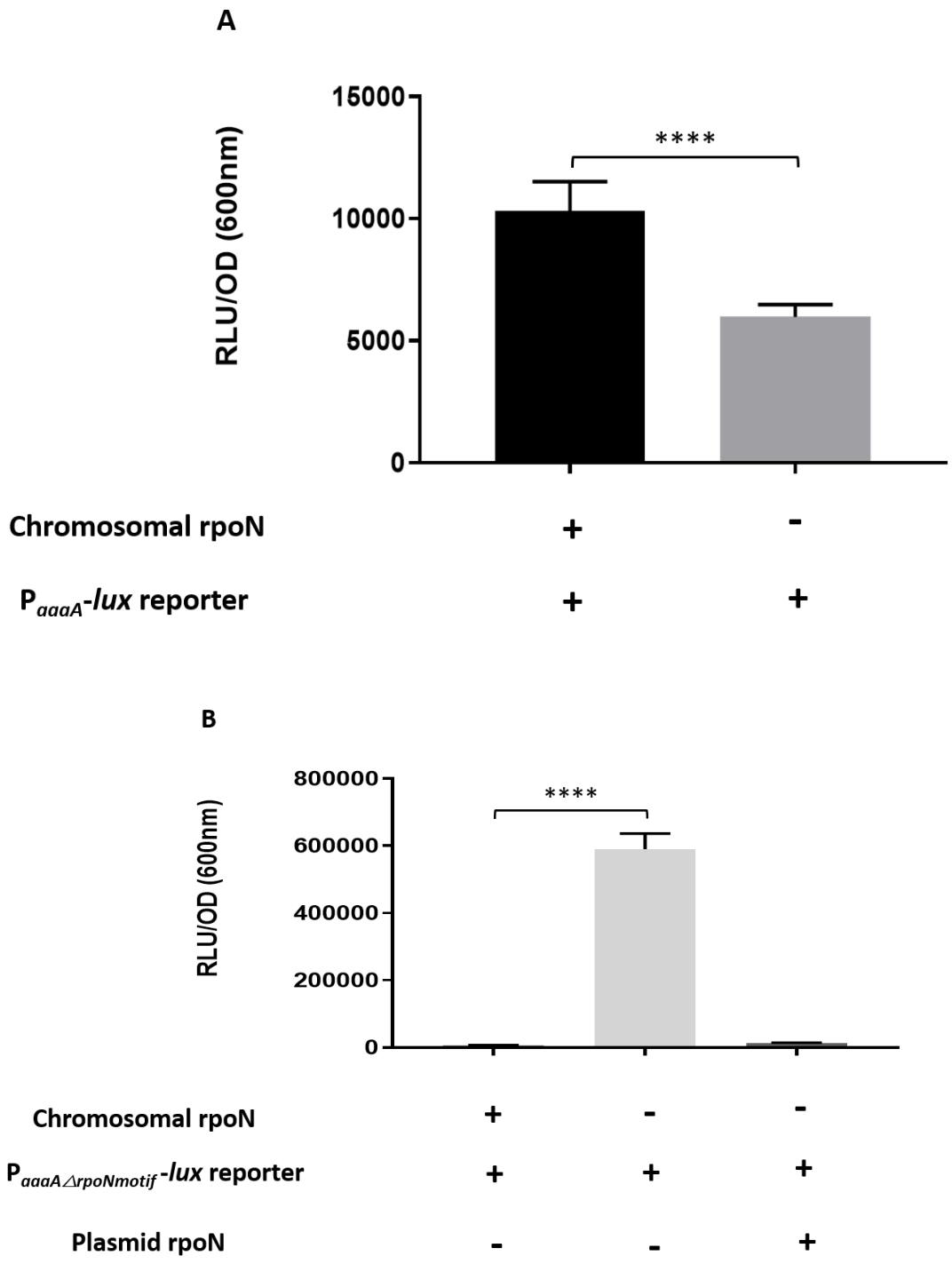

Figure 4.18: The motif disrupted in the *aaaA* promotor has a negative effect on *aaaA* expression independent of RpoN. *P. aeruginosa* PAO1 WT and *P. aeruginosa* PAO1 Δ*rpoN* and its complement carrying the P_{aaaA}-*lux* reporter (either intact or with the disrupted putative RpoN binding motif) were grown and bioluminescence analysed over time as described in Figure 4.12.

Three biological replicates were used for each sample and the bar represents the average of these. The error bars show the standard deviation from the mean. General ANOVA summary test analysis performed and P value <0.0001 reported, with **** indicating a significant difference.

4.2.5. AaaA activity in the Δ*aaaA*, Δ*rpoN* and complemented *rpoN* mutant was reduced in *P. aeruginosa* PAO1

Since *aaaA* is autoregulated, in a Δ*aaaA* mutant there is high level of transcription generated from the *aaaA* promoter reporter, but no AaaA activity is measured. To understand in all constructs whether transcription and translation of *aaaA*/AaaA mirror each other. In order to investigate translational AaaA activity in the Δ*aaaA*, Δ*rpoN* and complemented Δ*rpoN* mutants, the Arginine-*p*-nitroanilide degradation assay was performed. To do this, overnight cultures of each strain were normalized to an OD_{600nm}=0.25. The cells were then washed 2 times in MMP with centrifugation at 3707 Xg for 5 minutes to separate the pellet from supernatant. Following the final centrifugation, the supernatant was discarded and the pellet resuspended in 1 ml of MMP. For each bacterial strain, 3 wells in a sterile clear bottomed 96 well plate (greiger bio1 F bottom) were prepared with 150 µl of the 1 mM working solution of arginine-*p*-nitroanilide and 150 µl of the OD_{600nm} 0.25 bacterial suspensions. The degradation of arginine-*p*-nitroanilide was determined by hourly measurements of OD_{405nm} over 24 h at 37°C in an automated plate reader.

The data showed that AaaA activity in the Δ*aaaA*, Δ*rpoN* and complemented Δ*rpoN* mutants was reduced (Figure 4.19). This suggests that reduction of *aaaA* transcription was reflected directly in lower levels of AaaA activity.

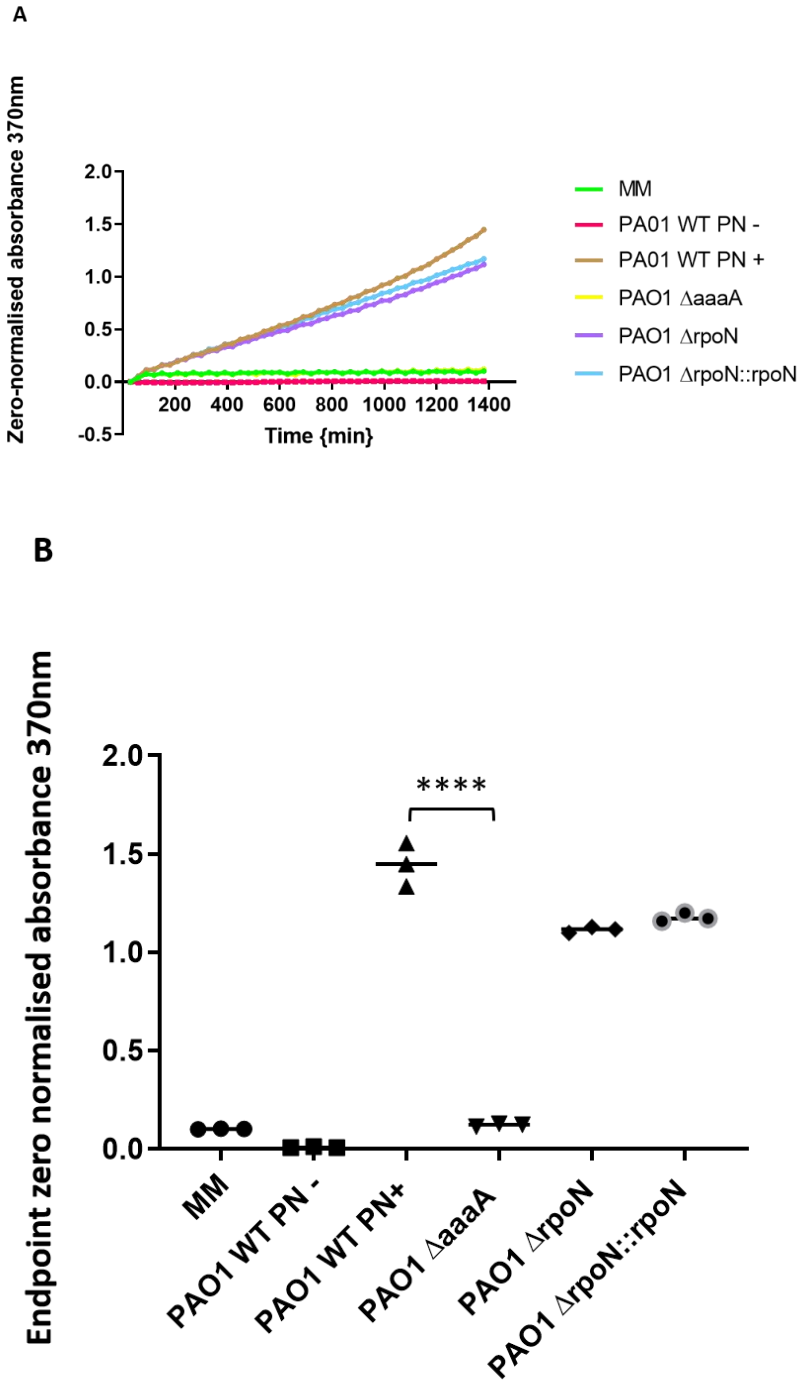

Figure 4.19: The arginine-*p*-nitroanilide degradation assay for AaaA verified that AaaA activity in the Δ*aaaA*, Δ*rpoN* and complemented Δ*rpoN* mutants was reduced in *P. aeruginosa* PAO1. Overnight cultures were normalized to OD_{600nm}=0.25. The cells were then washed 2 times in MMP with centrifugation at 3707 Xg for 5 minutes to separate the pellet from supernatant. Following the final centrifugation, the supernatant was discarded

and the pellet resuspended in 1 ml of MMP. For each bacterial strain, 3 wells in a sterile clear bottomed 96 well plate (Greiner bio1 F bottom) were prepared with 150 µl of the 1 mM working solution of arginine-*p*-nitroanilide and 150µl of the OD_{600nm}=0.25 bacterial suspension. The degradation of arginine-*p*-nitroanilide was determined by hourly measurements at OD_{405nm} for 24 h at 37°C in an automated plate reader. Zero-normalised absorbance 370nm (Panel A) and Endpoint zero normalised absorption 370nm (Panel B) plots were analysed by Graphpad prism software and Friedman test P value reported <0.0001, with **** indicating a significant difference.

4.2.6. In the absence of MvaT or MvaU, *aaaA* expression decreased when the motif in the *aaaA* promotor was altered

Previous data from our lab suggested more light was produced from the *aaaA* promoter-*lux* reporter when it is in a mutant deficient in either of the HN-S proteins MvaT or MvaU whilst the constitutive *kan* promoter was unaffected by either mutation of *mvaT* or *mvaU* (258). It was not known if the suggested negative effect of MvaT and MvaU was mediated through the putative RpoN-binding motif. To find this out the $P_{aaaA\triangle rpoNmotif}$ –*lux* reporter was conjugated into PA01 Δ*mvaU* and Δ*mvaT* mutants.

P. aeruginosa PAO1 WT, Δ*mvaU*, and Δ*mvaT* mutants carrying the mini-CTX-P_{aaaA}-*lux* reporter or the mini-CTX $P_{aaaA\triangle rpoNmotif}$ –*lux* were then compared in terms of light expression level by Tecan assay as described previously. Figure 4.20 shows that in the absence of MvaT or MvaU, light production decreased when the motif in the *aaaA* promotor was altered, indicating that these proteins may interact in this region of the promotor. This suggested that in contrast to the negative effect of MvaT and MvaU on the intact *aaaA* promoter, these HN-S proteins have a positive effect on the genetically altered *aaaA* promoter. Thus, it is possible that either these two proteins may interact with the mutated motif directly or indirectly. Tukey's multiple comparisons test p-value of <0.0001, revealed that this difference between WT and mutants was significant.

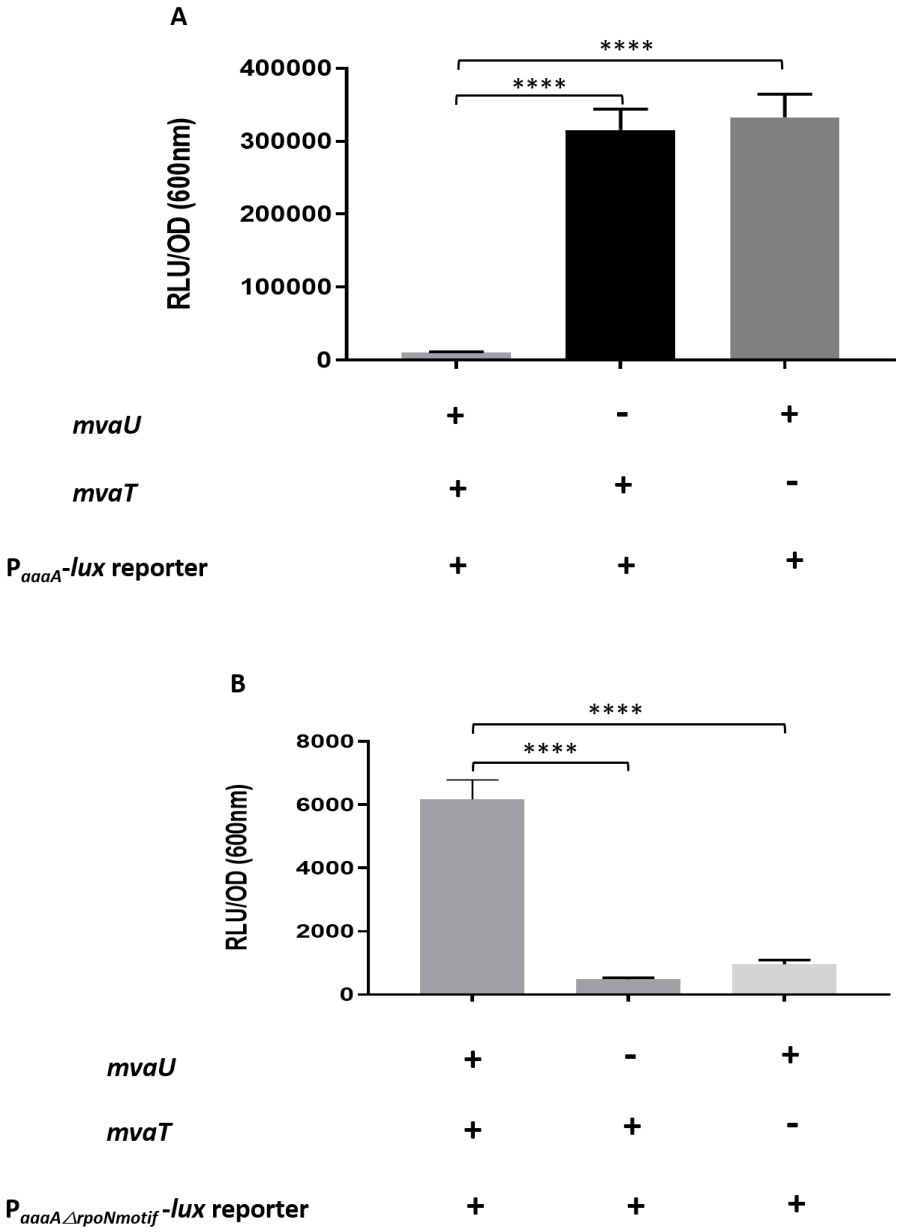

Figure 4.20: In the absence of MvaT or MvaU, *aaaA* expression decreased when the motif in the *aaaA* promotor was altered. *P. aeruginosa* PAO1 WT or *P. aeruginosa* PAO1 Δ*mvaU*, Δ*mvaT* mutants carrying the intact P_{aaaA} reporter either intact (Panel A) or with a disrupted RpoN motif (panel B) were grown and bioluminescence analysed over time as described in Figure 4.16. Each experiment was performed in triplicate; error bars indicate the standard deviation. General ANOVA summary test analysis performed and P value <0.0001 reported, **** indicating a significant difference.

4.2.7. AaaA activity in the Δ*mvaU* or Δ*mvaT* mutants was reduced in *P. aeruginosa* PAO1

To investigate translational AaaA activity in the Δ*mvaU* and Δ*mvaT* mutants and verify if this echoes the transcriptional profile, the arginine-*p*-nitroanilide degradation assay was performed as described previously. Figure 4.21 shows that AaaA activity in Δ*mvaU* and Δ*mvaT* mutants was reduced in line with the transcription of *aaaA*.

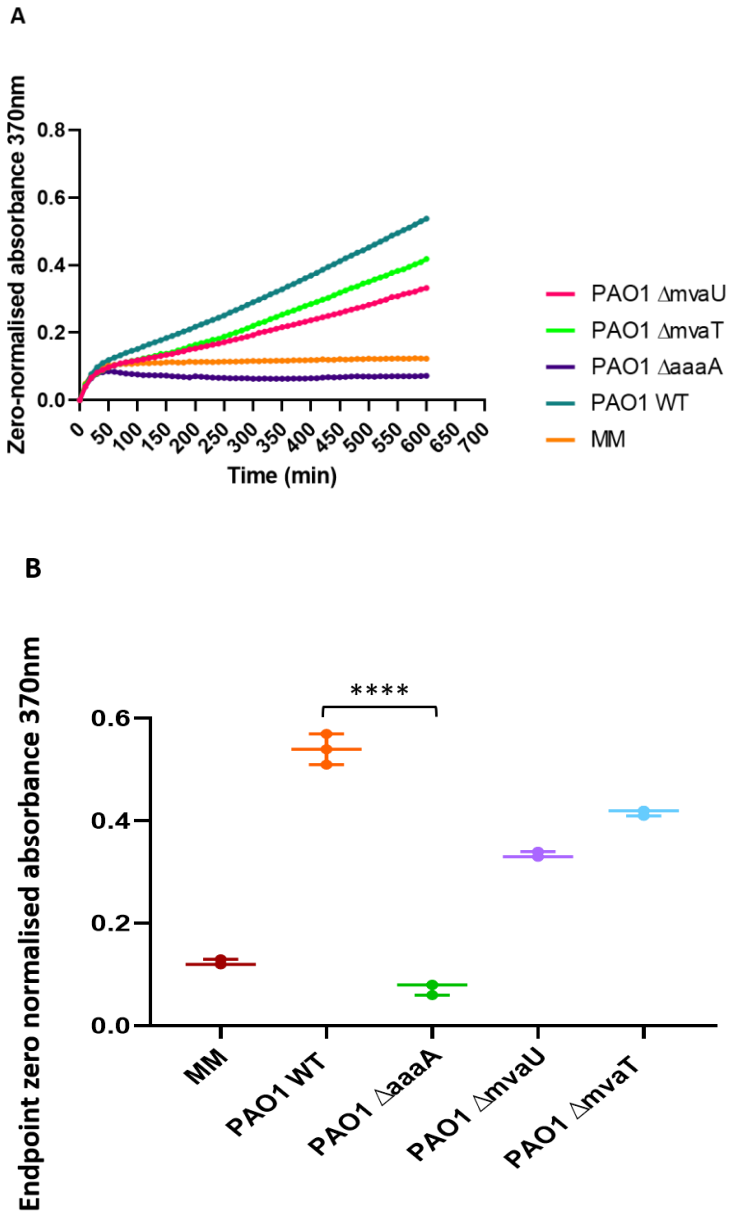

Figure 4.21: Arginine-*p*-nitroanilide degradation assay for AaaA verified that AaaA activity in the Δ*mvaU* or Δ*mvaT* mutant was reduced in *P. aeruginosa* PAO1. Overnight cultures were normalized to 0.25 OD600 nm. The cells were then washed 2 times in MMP with centrifugation at 3707 Xg for 5 minutes (PA01-N) to separate the pellet from supernatant. Following the final centrifugation, the supernatant was discarded and the pellet resuspended in 1 ml of MMP. For each bacterial strain, 3 wells in a sterile clear bottomed 96 well plate (Greiner bio1 F bottom) were prepared with 150 µl of the 1 mM working solution of arginine-*p*-nitroanilide and 150 µl of the OD 600 nm 0.25 bacterial suspensions. The degradation of arginine-*p*-nitroanilide was determined by 1h measurements of OD 405 nm for 24 h at 37°C in an automated plate reader. Zero-normalised absorbance 370nm (Panel A) and Endpoint zero normalised absorption 370nm (Panel B) plots were analysed by Graphpad prism software and general ANOVA summary test analysis performed and P value <0.0001 reported, **** indicating a significant difference.

4.2.8. In the absence of ArgR (arginine sensing and utilization regulator), *aaaA* expression was unaffected when the motif in the *aaaA* promotor was altered

Since AaaA releases arginine from peptides it was not surprising when the arginine responsive regulator ArgR was found to influence *aaaA* transcription (258). In *P. aeruginosa* PA14 WT Δ*argR* did not significantly affect the constitutive CTX-P_{kan}-*lux* reporter. However, the arginine regulatory protein ArgR positively regulated the light production from the intact P_{aaaA} reporter as significantly less light was measured in the Δ*argR* mutant compared to WT (Esteban Paredes 2014).

To investigate whether the influence of ArgR upon *aaaA* expression was mediated through the predicted RpoN-binding motif, the $P_{aaaA\triangle rpoNmotif}$–*lux* reporter was conjugated into PA14 WT and the Δ*argR* mutant, and light production monitored as described previously. Figure 4.22 confirms that in the absence of ArgR, light production from the intact *aaaA* promoter reporter was significantly reduced. However, light production was unaffected when the motif in the *aaaA* promotor was altered and no significant difference found between the Δ*argR* mutant and WT. It appears that this arginine sensing regulator has no major effect on the *aaaA* promoter when the motif is disrupted.

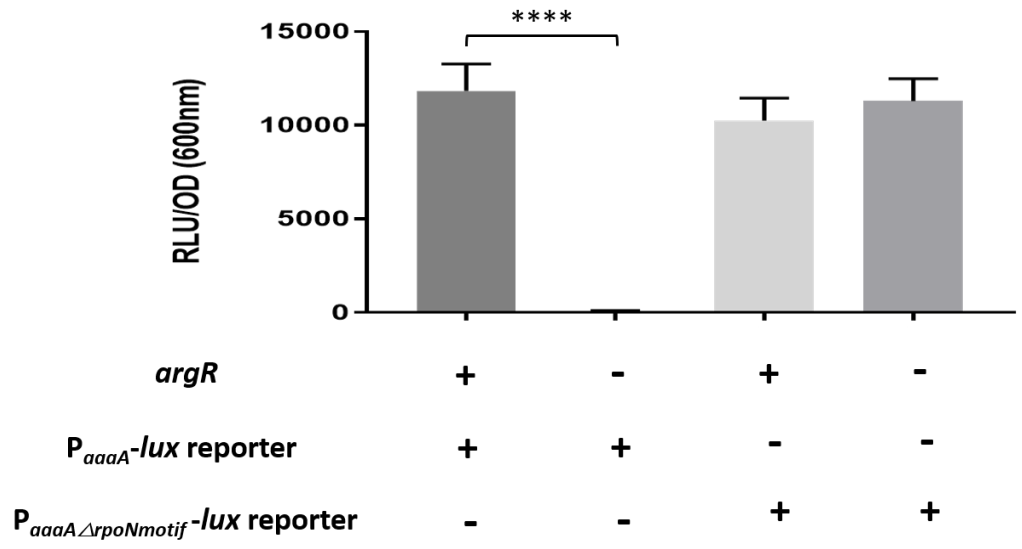

Figure 4.22: In the absence of ArgR, *aaaA* expression was unaffected when the motif in the *aaaA* promotor was altered. *P. aeruginosa* PA14 WT or the Δ*argR* mutant carrying the intact P_{aaaA} reporter or the reporter with the disrupted motif were grown and bioluminescence analysed over time as described in Figure 4.16. Each experiment was performed in triplicate; error bars indicate the standard deviation. Friedman test analysis performed and P value <0.0001 reported, **** indicating a significant difference.

4.2.9. AaaA activity in the Δ*argR* was reduced in *P. aeruginosa* PA14

To investigate translational AaaA activity in the Δ*argR*, the arginine-*p*-nitroanilide degradation assay was performed as described previously. Figure 4.23 shows that AaaA activity in Δ*argR* was reduced, in line with the observed reduction of *aaaA* expression (Figure 4.19).

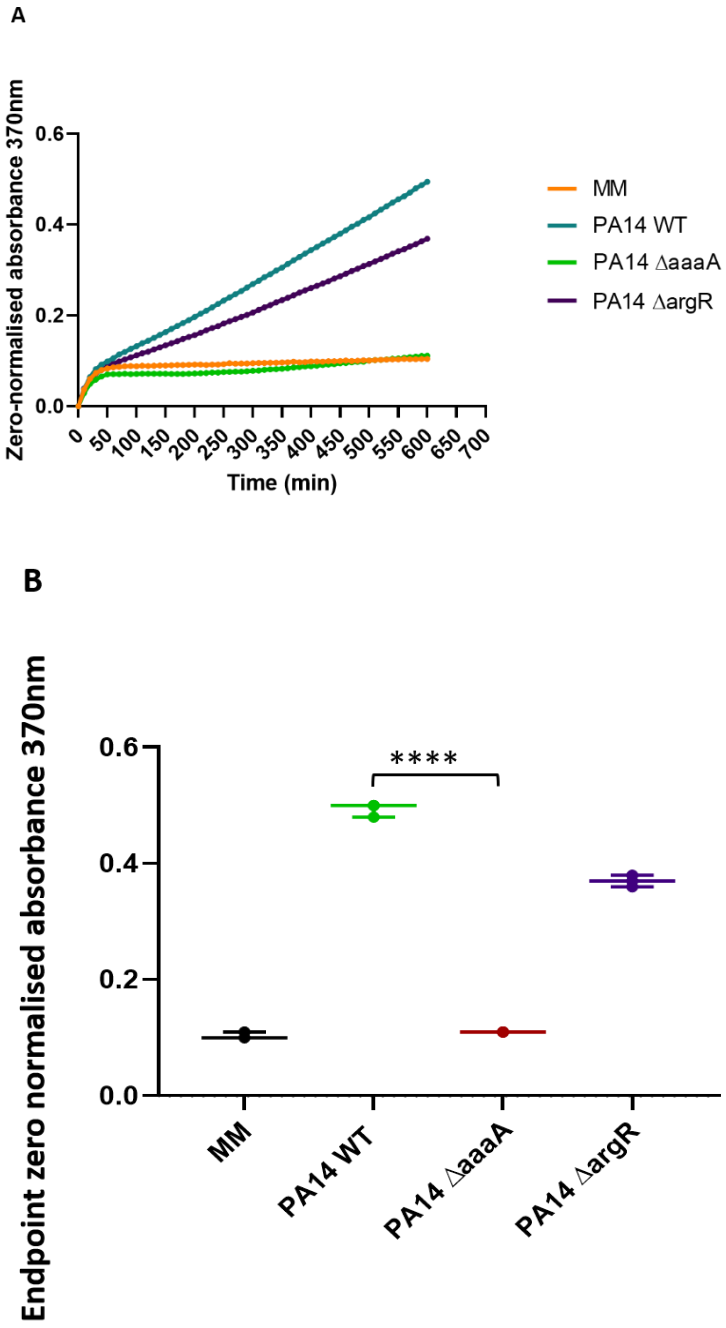

Figure 4.23: Arginine-*p*-nitroanilide degradation assay for AaaA verified that AaaA activity in the Δ*argR* was reduced in *P. aeruginosa* PAO1. Overnight cultures were normalized to 0.25 OD600 nm. The cells were then washed 2 times in MMP with centrifugation at 3707 Xg for 5 minutes (PA01-N) to separate the pellet from supernatant. Following the final centrifugation, the supernatant was discarded and the pellet resuspended in 1 ml of MMP. For each bacterial strain, 3 wells in a sterile clear bottomed 96 well plate (Greiner bio1 F bottom) were prepared with 150µl of the 1 mM working solution of arginine-*p*-

nitroanilide and 150µl of the OD_{600nm} 0.25 bacterial suspensions. The degradation of arginine-*p*-nitroanilide was determined by 1h measurements of OD 405 nm for 24 h at 37°C in an automated plate reader. Zero-normalised absorbance 370nm (Panel A) and Endpoint zero normalised absorption 370nm (Panel B) plots were analysed by Graphpad prism software and General ANOVA summary test analysis performed and P value <0.0001 reported, **** indicating a significant difference.

4.2.10. In the absence of the enhancer binding protein Sfa3 in PA14, *aaaA* expression significantly decreased when the motif in the *aaaA* promotor was altered

The enhancer binding proteins (EBPs) Sfa2 and Sfa3 are RpoN activators (454). They were implicated in the regulation of *aaaA* expression previously by monitoring the CTX-P_{aaaA}-*lux* reporter in *P. aeruginosa* PA01 Δ*sfa2* and Δ*sfa3* mutants(258). The constitutive control reporter indicated that the *kan* promoter was unaffected by both mutants. However, for the CTX-P_{aaaA}-*lux* reporter, light production in Δ*sfa2* and Δ*sfa3* mutants was significantly lowered compared to *P. aeruginosa* WT, suggesting Sfa2 and Sfa3 positively regulate the *aaaA* intact promoter expression.

To verify and investigate the role of Sfa2 and Sfa3 on *aaaA* expression further, the CTX-P_{aaaA}-*lux*, $P_{aaaA\triangle rpoNmotif}$ –*lux* and P_{kan}-*lux* reporters were conjugated into PA01 and PA14 Δ*sfa2* and Δ*sfa3* mutants and bioluminescence monitored as described previously in section 2.14.

In the PA14 background, no significant difference in light production was found between Δ*sfa2* and WT for either reporter. By contrast, lower levels of light production were found in the Δ*sfa3* mutants when the motif in the *aaaA* promotor was altered suggesting this EBP may have a positive effect on the mutated *aaaA* promoter (Figure 4.24). Tukey's multiple comparisons test p-value of 0.0039, revealing that this difference between WT and mutant was significant. However, no significant difference was found between Δ*sfa3* and WT using the intact *aaaA* promoter reporter. Since this differs from the phenotype observed in Δ*rpoN*, it appears that Sfa3 is not an activator of the native p*aaaA*.

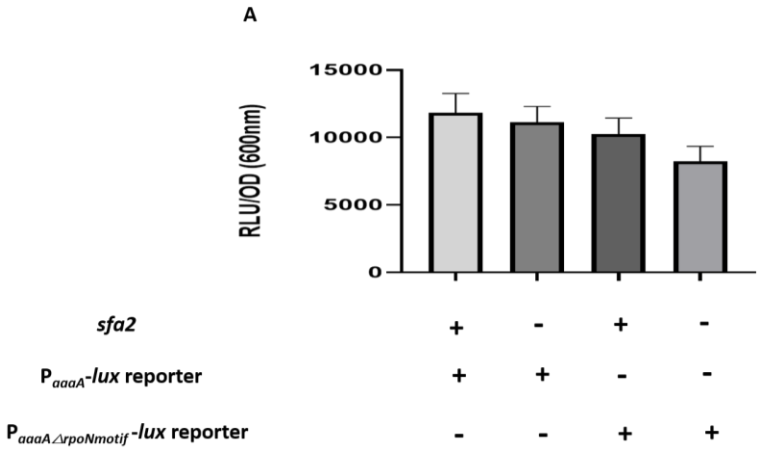
A
RLU/OD (600nm)
15000
10000
5000
0
sfa2
+ - + -
P aaaA-lux reporter
+ + - -
P aaaA△rpoNmotif -lux reporter
- - + +

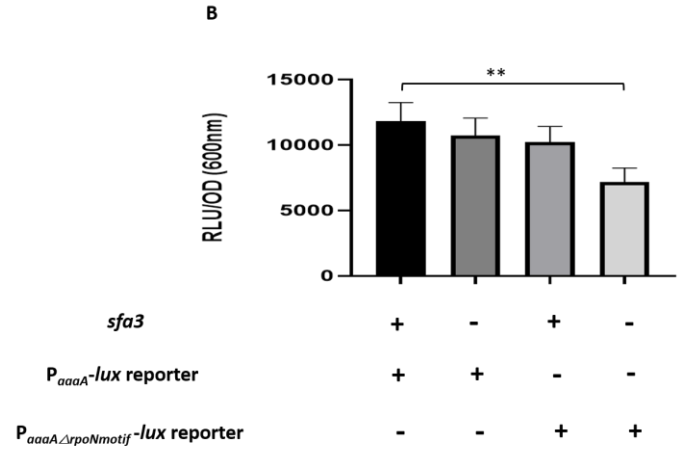
B
RLU/OD (600nm)
15000
10000
5000
0
**
sfa3
+ - + -
P aaaA-lux reporter
+ + - -
P aaaA△rpoNmotif -lux reporter
- - + +

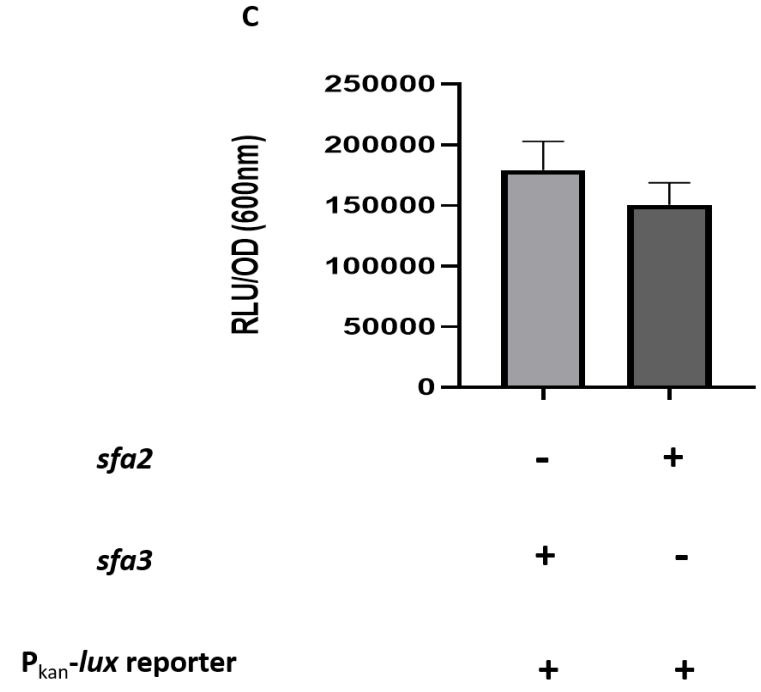
C
RLU/OD (600nm)
250000
200000
150000
100000
50000
0
sfa2
- +
sfa3
+ -
P kan-lux reporter
+ +

Figure 4.24: In the absence of Sfa3 in PA14, *aaaA* driven expression significantly decreased when the motif in the *aaaA* promotor was altered. *P. aeruginosa* PA14 WT and *P. aeruginosa* PA14 Δ*sfa2* and Δ*sfa3* mutants carrying reporters with P_{aaaA} either P_{kan} reporter (Panel C), intact or with a disrupted putative RpoN-binding motif (Panel A and Panel B) were grown and bioluminescence analysed over time as described in Figure 4.16. Each experiment was performed in triplicate; error bars indicate the standard deviation. General ANOVA summary test analysis performed, and no significant difference reported for Sfa2 and P value 0.0039 reported for Sfa3 as showed by ** indicating a significant difference.

4.2.11. In the absence of Sfa2 and Sfa3 in PA01 strain, *aaaA* expression was significantly decreased in Δ*sfa2* and significantly increased in Δ*sfa3* when the motif in the *aaaA* promotor was altered

In contrast to the observations in PA14, when light production from *P. aeruginosa* PA01 Δ*sfa2* and Δ*sfa3* mutants carrying reporters was observed, a different trend was noted. In both mutants, with the intact P_{aaaA} promoter, there was more bioluminescence in the mutant than the WT which contradicted the observation in PA14 (Figures 4.24 , 4.25), although the extent of this increase in bioluminescence was more evident in the *Δsfa2* mutant which produced 4 times more light than the WT and a paired t-test generated a p-value of <0.0001, revealing that this difference was significant and therefore suggests that *sfa2* negatively regulates the *aaaA* intact promoter driven expression in this context.

However, lower levels of light production were found in Δ*sfa2* compared to WT when the motif in the *aaaA* promotor was altered and a paired t-test generated a p-value of <0.0001, revealing that this difference was also significant and this EBP has a positive effect on the *aaaA* Promoter in RpoN motif disruptive state.

For Sfa3 in PA01 background strain, Δ*sfa3* produced higher light expression compared to WT for both intact *aaaA* promoter reporter and when the motif in the *aaaA* promotor was altered. Tukey's multiple comparisons test generated a p-value of 0.0016 for intact promoter and <0.0001 for RpoN motif disruptive state. Since the differences between mutant and WT were significant and Sfa3 has negative effect on both intact and disrupted motif of *aaaA* Promoter expression, it could be a direct or indirect repressor.

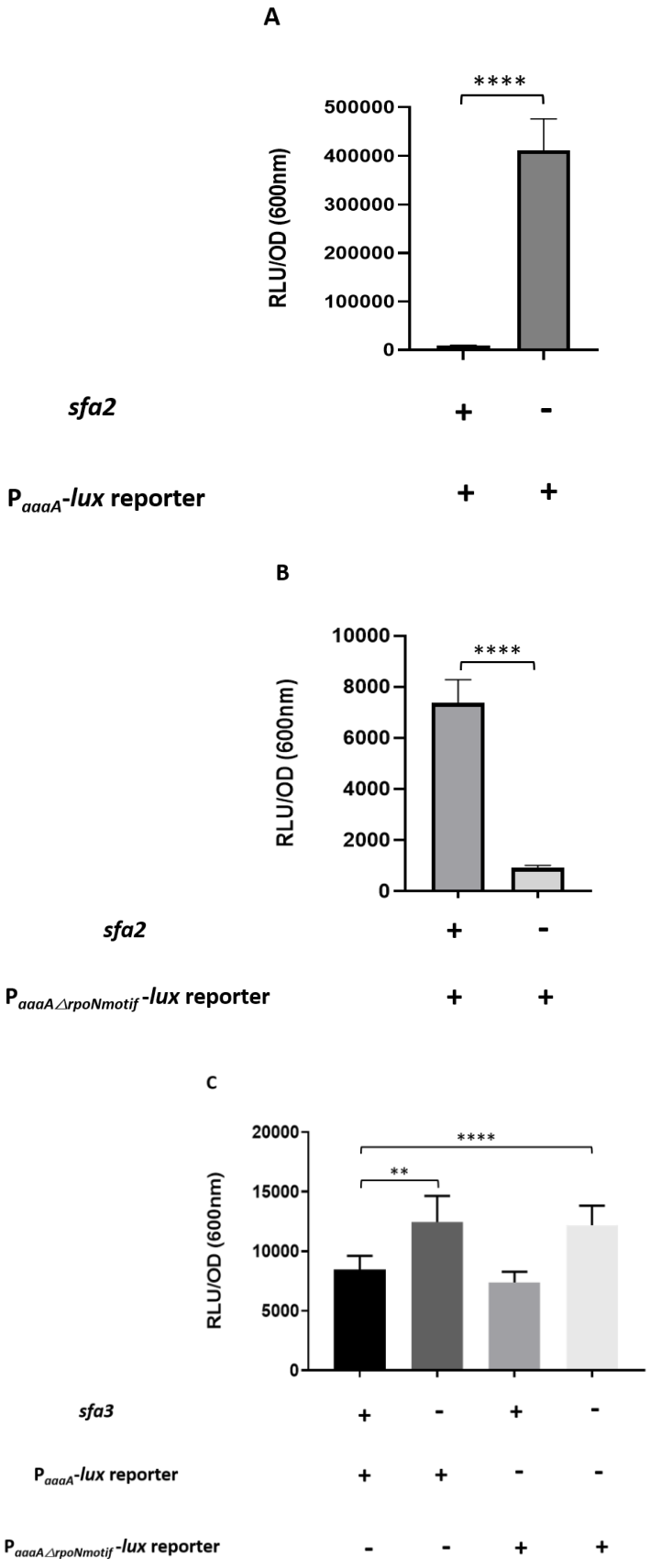
A
****
500000
400000
300000
200000
100000
0
RLU/OD (600nm)
sfa2
+
-
PaaaA-lux reporter
+
+
B
10000
8000
6000
4000
2000
0
****
RLU/OD (600nm)
sfa2
+
-
PaaaA△rpoNmotif -lux reporter
+
+
C
20000
15000
10000
5000
0
**
****
RLU/OD (600nm)
sfa3
+
-
+
-
PaaaA-lux reporter
+
+
-
-
PaaaA△rpoNmotif -lux reporter
-
-
+
+

Figure 4.25: In PA01, *aaaA* expression significantly decreased in Δ*sfa2* and significantly increased in Δ*sfa3* when the motif in the *aaaA* promotor was altered. *P. aeruginosa* PA01 WT and *P. aeruginosa* PA01 Δ*sfa2* or Δ*sfa3* mutants carrying lux reporters with the intact P_{aaaA} (Panels A, C), or $P_{aaaA\triangle rpoNmotif}$ promoters were grown and bioluminescence analysed over time as described in Figure 4.16. Each experiment was performed in triplicate; error bars indicate the standard deviation. General ANOVA summary test analysis performed and P value <0.0001 reported shown by the asterisks and **** indicating a significant difference. P value of 0.0016 also reported for intact promoter, ** indicating a significant difference.

4.2.12. AaaA activity in the Δ*sfa2* and Δ*sfa3* was reduced in *P. aeruginosa* PA14

To investigate if the transcriptional influence of the EBPs Sfa2 and Sfa3 are reflected in changes in AaaA translation, AaaA activity was determined in the Δ*sfa2* and Δ*sfa3* mutants using the arginine-*p*-nitroanilide degradation assay as described previously in section 2.13. In Figures 4.26 and 4.27 it is evident that AaaA activity in Δ*sfa2* and Δ*sfa3* mutants was reduced, with the effect being more obvious in the Δ*sfa2* mutant. This is in contrast with the transcription of the promoter which was increased, but may reflect the autoregulation of *aaaA*.

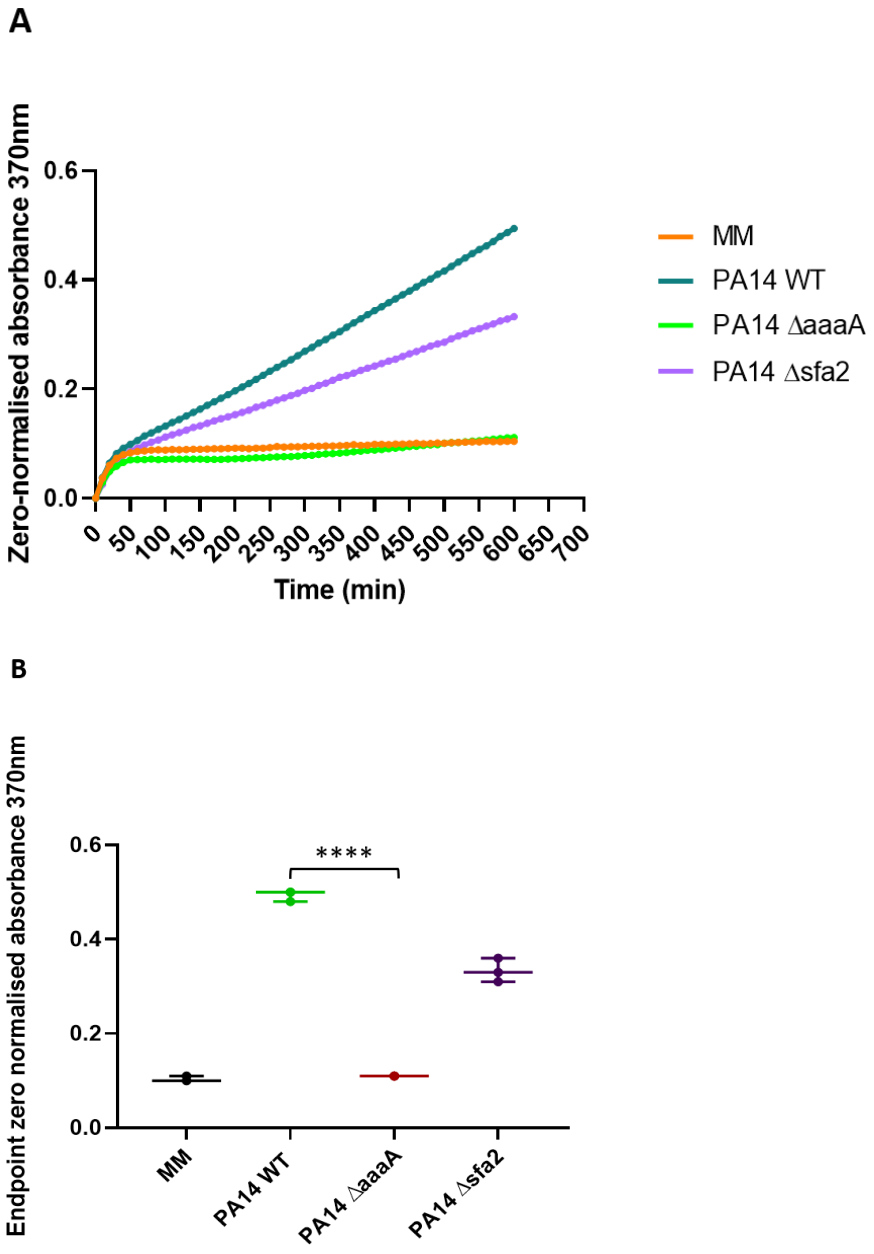

Figure 4.26: Arginine-*p*-nitroanilide degradation assay for AaaA revealed that AaaA activity in the Δ*sfa2* was reduced in *P. aeruginosa* PA14. Overnight cultures were normalized to 0.25 OD600 nm. The cells were then washed 2 times in MMP with centrifugation at 3707 Xg for 5 minutes to separate the pellet from supernatant. Following the final centrifugation, the supernatant was discarded and the pellet resuspended in 1 ml of MMP. For each bacterial strain, 3 wells in a sterile clear bottomed 96 well plate (Greiner bio1 F bottom) were prepared with 150µl of the 1 mM working solution of arginine-*p*-nitroanilide and 150µl of the OD 600nm 0.25 bacterial suspensions. The degradation of

arginine-*p*-nitroanilide was determined by 1h measurements of OD 405nm for 24 h at 37°C in an automated plate reader. Zero-normalised absorbance 370nm (Panel A) and Endpoint zero normalised absorption 370nm (Panel B) plots were analysed by Graphpad prism software and General ANOVA summary test analysis performed and P value <0.0001 reported, **** indicating a significant difference.

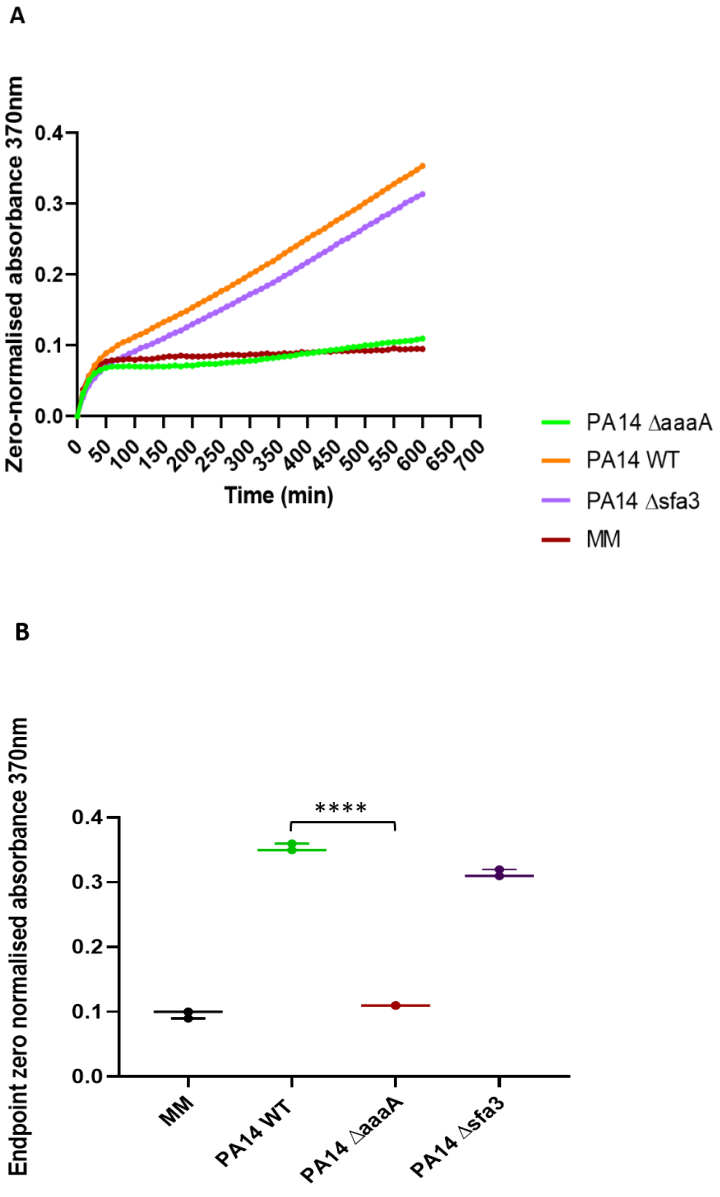

Figure 4.27: Arginine-*p*-nitroanilide degradation assay for AaaA verified that AaaA activity in the Δ*sfa3* was reduced in *P. aeruginosa* PA14. Overnight cultures were normalized to 0.25 OD 600nm. The cells were then washed 2 times in MMP with centrifugation at 3707 Xg for 5 minutes to separate

the pellet from supernatant. Following the final centrifugation, the supernatant was discarded and the pellet resuspended in 1 ml of MMP. For each bacterial strain, 3 wells in a sterile clear bottomed 96 well plate (Greiner bio1 F bottom) were prepared with 150µl of the 1 mM working solution of arginine-*p*-nitroanilide and 150µl of the OD 600 nm 0.25 bacterial suspensions. The degradation of arginine-*p*-nitroanilide was determined by 1h measurements of OD 405 nm for 24 h at 37°C in an automated plate reader. Zero-normalised absorbance 370nm (Panel A) and Endpoint zero normalised absorption 370nm (Panel B) plots were analysed by Graphpad prism software and General ANOVA summary test analysis performed and P value <0.0001 reported, **** indicating a significant difference.

4.2.13. AaaA activity in the Δ*sfa2* and Δ*sfa3* mutants was reduced in *P. aeruginosa* PA01

To determine if PA14 exhibited similar translational regulation of AaaA as PA01 when mutated for *sfa2* and *sfa3*, the arginine-*p*-nitroanilide degradation assay was performed on the mutants as described in section 2.13. As can be seen in Figure 4.28, AaaA activity in Δ*sfa2* and Δ*sfa3* mutants of PA14 was also reduced, but this time the reduction was more extreme with AaaA activities closely mimicking the Δ*aaaA* mutant. This provides supporting evidence that the *aaaA* autoregulation may be occurring to boost transcription from the promoter because the native gene product is not being produced.

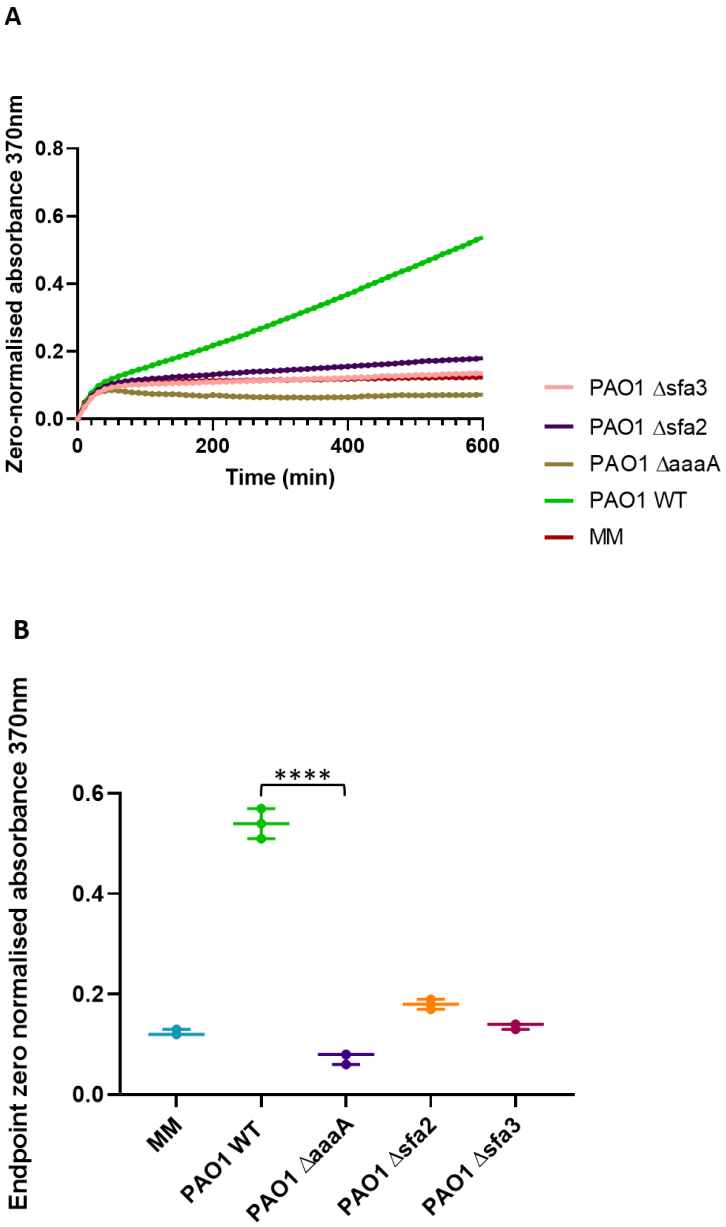

Figure 4.28: Arginine-*p*-nitroanilide degradation assay for AaaA verified that AaaA activity in the Δ*sfa2* and Δ*sfa3* was reduced in *P. aeruginosa* PAO1. Overnight cultures were normalized to 0.25 OD600 nm. The cells were then washed 2 times in MMP with centrifugation at 3707 Xg for 5 minutes (PA01-N) to separate the pellet from supernatant. Following the final centrifugation, the supernatant was discarded and the pellet resuspended in 1 ml of MMP. For each bacterial strain, 3 wells in a sterile clear bottomed 96 well plate (Greiner bio1 F bottom) were prepared with 150µl of the 1 mM working solution of arginine-*p*-nitroanilide and 150µl of the OD 600 nm 0.25 bacterial suspensions. The

degradation of arginine-*p*-nitroanilide was determined by 1h measurements of OD 405 nm for 24 h at 37°C in an automated plate reader. Zero-normalised absorbance 370nm (Panel A) and Endpoint zero normalised absorption 370nm (Panel B) plots were analysed by Graphpad prism software and General ANOVA summary test analysis performed and P value <0.0001 reported, **** indicating a significant difference.

4.2.14. In PA01, in the absence of QS, expression from the intact *aaaA* promoter increased. Similar, but more obvious changes were seen with expression driven by the altered motif in the *aaaA* promoter.

It is hypothesized that AaaA plays a role in biofilm formation, and that this underlies its contribution to chronic infections caused by *P. aeruginosa* in skin and lungs. Thus it was interesting to investigate *aaaA* expression in mutants of regulators of biofilm formation such as QS. Previously, *P. aeruginosa* PA01 Δ*lasR, ΔrhlR,* and *ΔpqsE* carrying CTX-*lux* reporters were monitored (Esteban Paredes 2014). The constitutive control reporter indicated that the *kan* promoter was unaffected by QS. No significant difference in *lux* expression was observed in Δ*lasR* and Δ*pqsE* mutants compared to WT with the intact P_{aaaA}-*lux reporter.* However, more light was measured in the *ΔrhlR mutant*, suggesting RlhR negatively regulates *aaaA* (Esteban Paredes 2014).

In this study, to investigate whether RhlR, or the other QS regulators could influence *aaaA* expression through the disrupted motif in *aaaA* promoter, the reporters CTX-P_{aaaA}-*lux* (Esteban Paredes 2014) and $P_{aaaA\triangle rpoNmotif}$ –lux were conjugated into PA01 WT and QS-regulator mutants (*ΔlasR, ΔrhlR, ΔpqsE*) as described in section 2.11.1.

In Figure 4.29, it can be seen that there was no significant difference in *lux* expression from the intact P_{aaaA} promoter in Δ*lasR* and Δ*pqsE* mutants compared to WT*.* By contrast, a significant difference was found in *ΔrhlR* (Paired t test P value 0.0089), where greater light production was observed*.*

Notably, with the $P_{aaaA\triangle rpoNmotif}$ –lux reporter a significant difference in light production was observed in all the QS related mutants: Δ*lasR* (Paired t test P value <0.0001)*, ΔrhlR*(Paired t test P value 0.0002)*, ΔpqsE* (Paired t test P value <0.0001) compared to WT. In all 3 mutants, light production increased,

suggesting QS negatively regulates the *aaaA* promoter when the motif is altered and it is similar to what was seen previously in PA01 Δ*rpoN*.

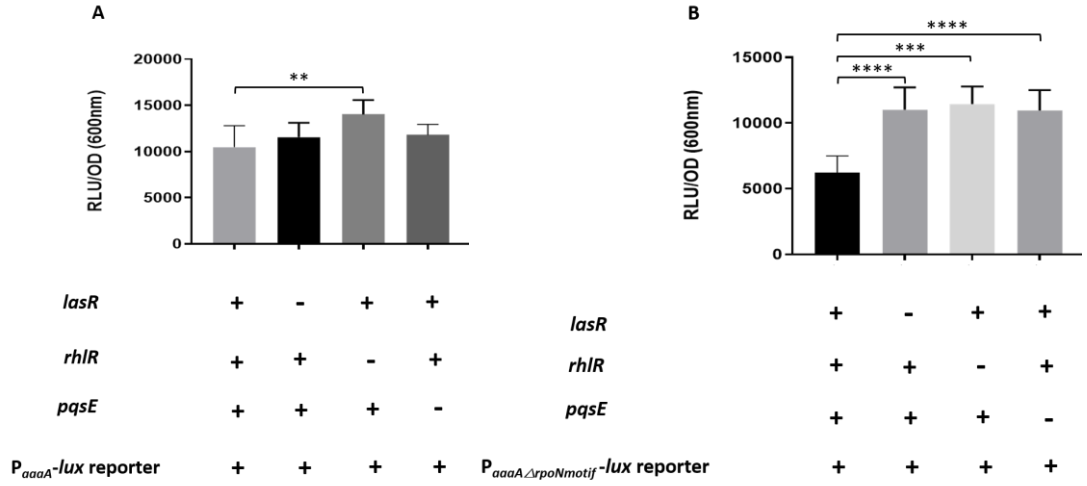

Figure 4.29: In the absence of the QS and biofilm regulator in PA01, *aaaA* expression significantly increased in *ΔlasR, ΔrhlR, ΔpqsE* when the motif in the *aaaA* promotor was altered. *P. aeruginosa* PA01 of WT, *ΔlasR* and *ΔrhlR, ΔpqsE* carrying the intact P*aaaA* reporter, disrupted RpoN motif were grown and bioluminescence analysed over time as described in Figure 4.16. Each experiment was performed in triplicate; error bars indicate the standard deviation. General ANOVA summary test analysis performed and P value <0.0001 reported, **** indicating a significant difference. Paired t test P value 0.0089, ** indicating a significant difference and Paired t test P value 0.0002, *** indicating a significant difference.

4.2.15. AaaA activity in all QS related mutants was increased in *P. aeruginosa* PA01

As described previously, the translation of AaaA was characterized by assessing its activity using the arginine-*p*-nitroanilide activity assay in the *ΔlasR*, *ΔrhlR,* and *ΔpqsE* mutants. Figure 4.30 shows increased AaaA activity in all the QS related mutants, despite no significant differences being observed in transcription from the intact promoter reporter (Figure 4.29).

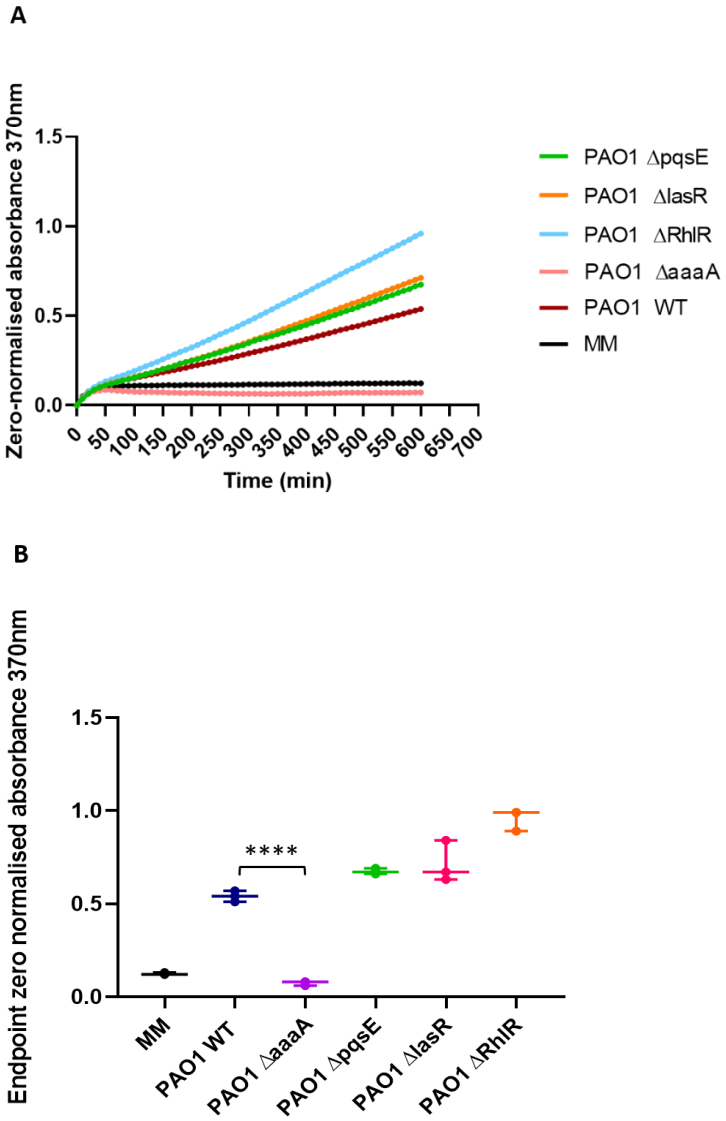

Figure 4.30: Arginine-*p*-nitroanilide degradation assay for AaaA verified that AaaA activity in all QS related mutants and biofilm regulator was increased in *P. aeruginosa* PAO1. Overnight cultures were normalized to 0.25 OD600 nm. The cells were then washed 2 times in MMP with centrifugation at 3707 Xg for 5 minutes (PA01-N) to separate the pellet from supernatant. Following the final centrifugation, the supernatant was discarded and the pellet resuspended in 1 ml of MMP. For each bacterial strain, 3 wells in a sterile clear bottomed 96 well plate (Greiner bio1 F bottom) were prepared with 150µl of the 1 mM working solution of arginine-*p*-nitroanilide and 150µl of the OD 600 nm 0.25 bacterial suspensions. The degradation of arginine-*p*-nitroanilide was determined by 1h measurements of OD 405 nm for 24 h at 37°C in an

automated plate reader. Zero-normalised absorbance 370nm and Endpoint zero normalised absorption 370nm plots were analysed by Graphpad prism software and General ANOVA summary test analysis performed and P value <0.0001 reported, **** indicating a significant difference.

4.2.16. In the absence of the denitrification regulatory protein NirQ in PA01-L, *aaaA* expression significantly increased when the motif in the *aaaA* promotor was altered

P. aeruginosa can survive under anaerobic conditions through denitrification using nitrate as an electron receptor to produce atmospheric N_2(455)(456). The complete denitrification process is composed of four continuous stages to reduce nitrate (NO_3) to dinitrogen (N_2) converted by nitrite (NO_2), nitric oxide (NO), and nitrous oxide (N_2O)(455). This metabolic pathway is catalyzed by (denitrification) enzymes including nitrate reductase (Nar), nitrite reductase (Nir), nitric oxide reductase (Nor), and nitrous oxide reductase (Nos)(455). Transcription of the genes encoding these metabolic effectors is mediated by transcriptional regulators classified into different groups including the FNR-like Crp family transcription factors ANR and DNR, the two-component system NarXL, and the CbbQ family protein NirQ(455)(370).

Since AaaA liberates arginine, a potential source of nitrogen when oxygen is scarce, the role of *ΔnirQ* on *aaaA* expression through the disrupted motif in *aaaA* promoter was investigated. The reporters CTX-P_{kan}-*lux* control (Esteban Paredes 2014), CTX-P_{aaaA}-*lux* reporter (Esteban Paredes 2014) and $P_{aaaA\Delta rpoNmotif}$ –*lux* were conjugated into PA01 L WT, and *ΔnirQ* mutant.

Although Figure 4.31 shows a significant difference between *ΔnirQ* and WT with the P_{kan} constitutive promoter strains (Paired t test P value <0.0001), this was in the opposite direction to that seen with the $P_{aaaA\Delta rpoNmotif}$ –lux reporter (Paired t test P value 0.0003). The increased light production suggests that NirQ negatively regulates the *aaaA* promoter when the motif is disrupted. The effect of NirQ on the p*Kan* control cannot currently be explained, and requires a separate constitutive expression reporter to investigate further. NirQ is likely to interact with RpoN as it is similar to the previous observations in PA01 Δ*rpoN* .

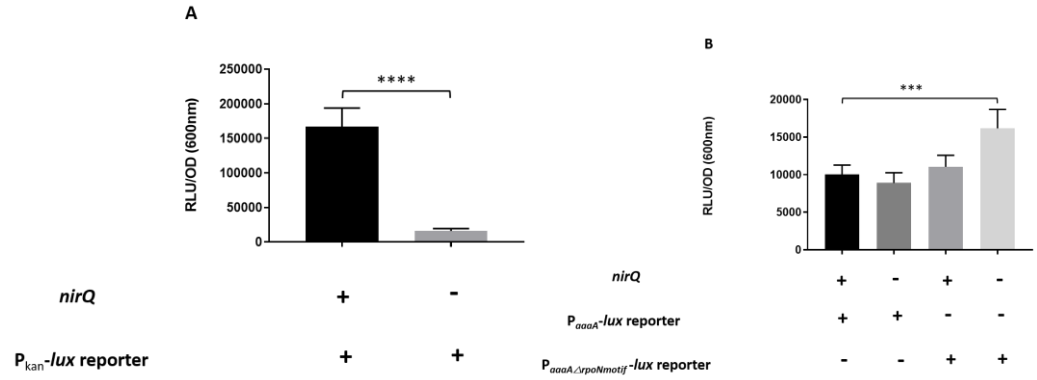

Figure 4.31: In the absence of the denitrification regulatory protein in PA01 L, *aaaA* expression significantly increased in *ΔnirQ* when the motif in the *aaaA* promotor was altered. *P. aeruginosa* PAO1 WT and *P. aeruginosa* PAO1 *ΔnirQ* carrying the intact P*aaaA* reporter, disrupted RpoN motif and P*kan* reporter were grown and bioluminescence analysed over time as described in Figure 4.16. Three biological replicates used for each sample and the bar represents the average of these. The error bars show the standard deviation from the mean. General ANOVA summary test analysis performed and P value <0.0001 reported, **** indicating a significant difference. Paired t test P value 0.0003 also reported, *** indicating a significant difference.

4.2.18. AaaA activity in the denitrification regulator *ΔnirQ* mutant was decreased in *P. aeruginosa* PA01 L

To investigate translational AaaA activity in the denitrification regulator *ΔnirQ* mutant, the arginine-*p*-nitroanilide degradation assay was performed. Figure 4.32 shows that AaaA activity in the *ΔnirQ* mutant was reduced, mirroring what had been observed with the expression from the native promoter (Figure 4.31).

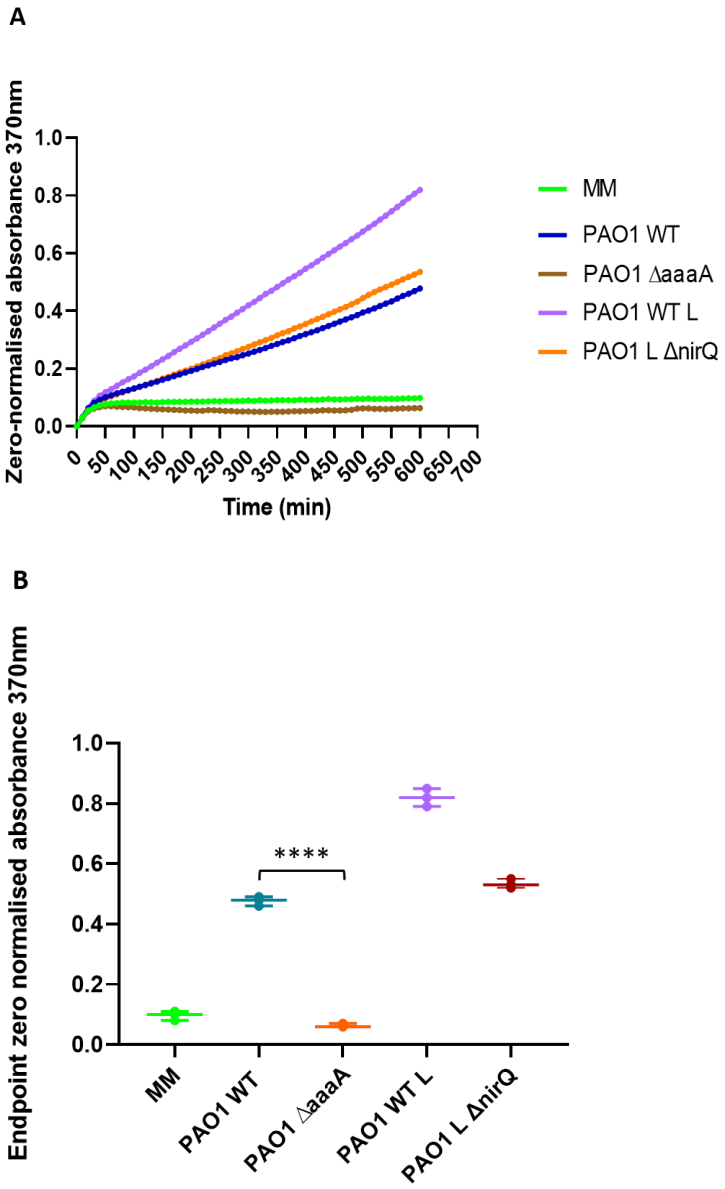

Figure 4.32: *Arginine-p-nitroanilide* degradation assay for AaaA verified that AaaA activity in denitrification regulator *ΔnirQ* was decreased in *P. aeruginosa* PA01. Overnight cultures were normalized to 0.25 OD600 nm. The cells were then washed 2 times in MMP with centrifugation at 3707 Xg for 5 minutes (PA01-N) to separate the pellet from supernatant. Following the final centrifugation, the supernatant was discarded and the pellet resuspended in 1 ml of MMP. For each bacterial strain, 3 wells in a sterile clear bottomed 96 well plate (Greiner bio1 F bottom) were prepared with 150 µl of the 1 mM working solution of arginine-*p*-nitroanilide and 150 µl of the OD 600 nm 0.25 bacterial suspensions. The degradation of arginine-*p*-nitroanilide was determined by 1h

measurements of OD 405 nm for 24 h at 37°C in an automated plate reader. Zero-normalised absorbance 370nm (Panel A) and Endpoint zero normalised absorption 370nm (Panel B) plots were analysed by Graphpad prism software and General ANOVA summary test analysis performed and P value <0.0001 reported, **** indicating a significant difference.

4.2.19. Systematic evaluation of putative EBPs in *aaaA* transcription and activity.

Since RpoN functions with the input from EBPs, and because a potential RpoN-binding motif had been mutated in the *aaaA* promoter, expression of the reporter was monitored in mutants in all the predicted EBPs. The mutants in putative EBPs were kindly provided by Dr Nicholas Tucker (Strathclyde Institute of Pharmacy and Biomedical Sciences, and originated from the Held et al (2012) Washington transposon mutant library created in PA14. In each case the reporters were conjugated into the mutant, and the light production monitored as a measure of transcription as described previously in section 2.11.1 and 2.14. In addition, the activity of AaaA was characterized in each mutant as a reflection of translation using the previously described arginine-p-nitroanilide assay, see section 2.13.

4.2.20. In the absence of *phhR* and *dctD* in PA14 strains, P_{aaaA} driven expression significantly decreased in △*phhR and* △*dctD* when the motif in the *aaaA* promotor was altered

P. aeruginosa PA14 *⧋phhR, ⧋gscR, ⧋algB* and *⧋dctD* mutants exhibited similar light emission compared to WT with the intact P*aaaA*-lux reporter (Figure 4.33). Similarly, no significant difference in light production was observed between the *⧋gscR* and *⧋algB* mutants compared to WT when the motif in the *aaaA* promotor was altered. However, a significant difference in light production by the *⧋phhR* mutant (Tukey's multiple comparisons test P value 0.0012) and *⧋dctD* mutant (Tukey's multiple comparisons test P value 0.0018) was observed. In both cases, the reduced light suggests positive regulation.

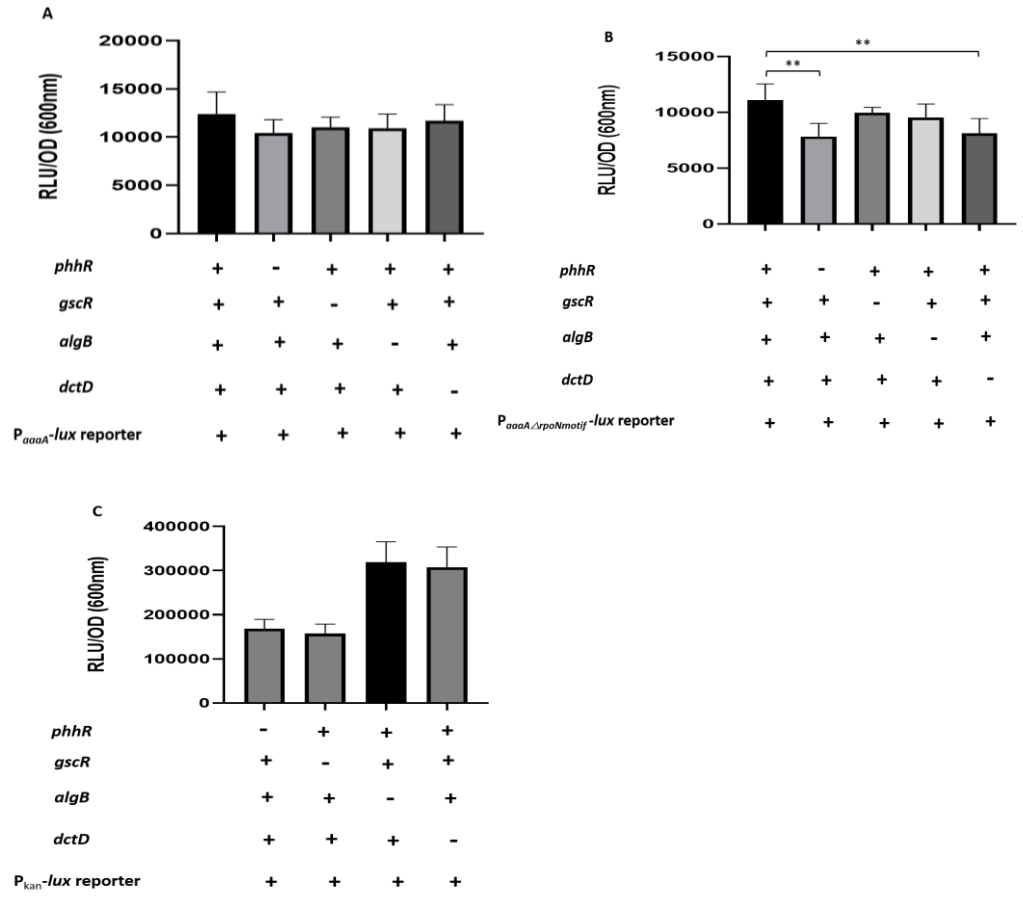

Figure 4.33: In the absence of *phhR* and *dctD* in PA14 strains, P_{aaaA} driven expression significantly decreased in Δ*phhR and* Δ*dctD* when the motif in the *aaaA* promotor was altered. *P.aeruginosa PA14 of WT, ⊿phhR* **,** *⊿gscR, ⊿algB* and *⊿dctD* carrying the intact P*aaaA* reporter (Panel A), disrupted RpoN motif (Panel B) and P_{kan} reporter (Panel C) were grown and bioluminescence analysed over time as described in Figure 4.16. Each experiment was performed in triplicate; error bars indicate the standard deviation. General ANOVA summary test analysis performed and P value 0.0007 reported, ** indicating a significant difference.

4.2.21. AaaA activity in the *⊿phhR* and *⊿algB* mutants were reduced while, AaaA activity in the *⊿dctD was* increased in *P. aeruginosa* PA14. AaaA activity in the *⊿gscR* mutant was similar compare to WT in *P. aeruginosa* PA14

Figure 4.34 shows that AaaA activity in the *⊿phhR* and *⊿algB* mutants were reduced while, AaaA activity in the *⊿dctD was* increased in *P. aeruginosa* PA14.

AaaA activity in the *⊿gscR* mutant was similar compared to WT in *P. aeruginosa* PA14.

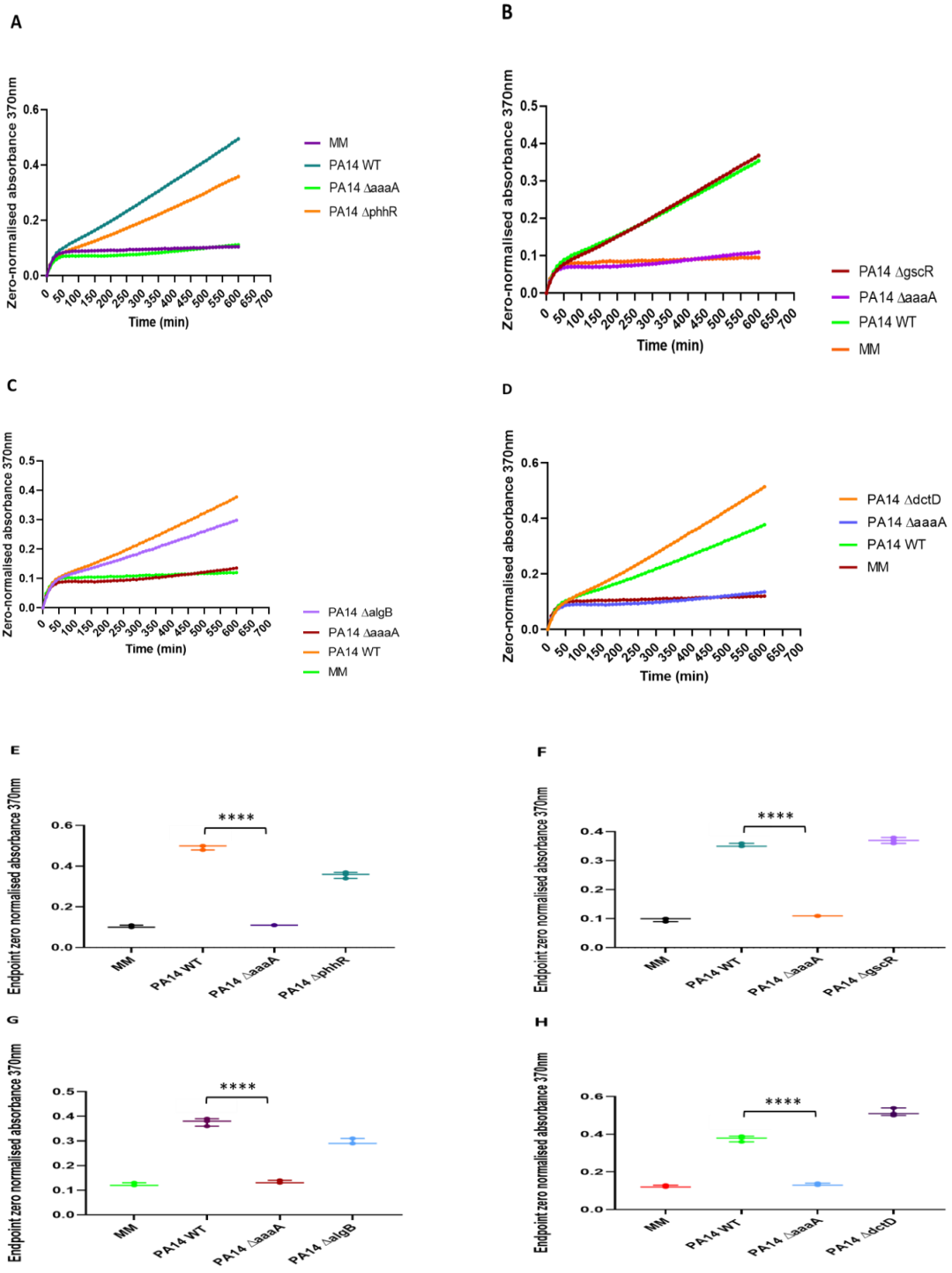

Figure 4.34: *Arginine-p*-nitroanilide degradation assay for AaaA verified that AaaA activity in the *⊿phhR* and *⊿algB* mutants was reduced in *P. aeruginosa* PA14 while, AaaA activity in the *⊿dctD was* increased in *P.*

aeruginosa* PA14. AaaA activity in the ⊿*gscR* mutant was similar compare to WT in *P. aeruginosa* PA14.** Overnight cultures were normalized to 0.25 OD600 nm. The cells were then washed 2 times in MMP with centrifugation at 3707 Xg for 5 minutes to separate the pellet from supernatant. Following the final centrifugation, the supernatant was discarded and the pellet resuspended in 1 ml of MMP. For each bacterial strain, 3 wells in a sterile clear bottomed 96 well plate (Greiner bio1 F bottom) were prepared with 150µl of the 1 mM working solution of arginine-*p*-nitroanilide and 150µl of the OD 600 nm 0.25 bacterial suspensions. The degradation of arginine-*p*-nitroanilide was determined by 1h measurements of OD 405 nm for 24 h at 37°C in an automated plate reader. Zero-normalised absorbance 370nm (Panel A-D) and Endpoint zero normalised absorption 370nm (Panel E-H) plots were analysed by Graphpad prism software and General ANOVA summary test analysis performed and P value <0.0001 reported, * indicating a significant difference.

4.2.22. In PA14 strains, *lux* expression significantly decreased in △*fleQ* , △*ntrC* , △*cbrB* and ⊿*acoR* mutants when the motif in the *aaaA* promotor was altered

P. aeruginosa PA14, △*fleQ*, △*ntrC*, △*cbrB* and ⊿*acoR* mutants showed a trend towards reduced light emission from the reporters, which was most evident with mini-CTX $P_{aaaA\triangle rpoNmotif}$ –*lux* (Figure 4.35), suggesting they could positively regulate *aaaA*.

4.2.23. AaaA activity in the △*fleQ* and △*ntrC* mutants were similar compared to WT in *P. aeruginosa* PA14. AaaA activity in the △*cbrB was* increased while AaaA activity in the ⊿*acoR was* reduced in *P. aeruginosa* PA14

Figure 4.36 shows that AaaA activity in the △*fleQ* and △*ntrC* mutants were similar compared to WT *P. aeruginosa* PA14, indicating that the potential positive regulation did not alter functional activity. AaaA activity in the △*cbrB was* increased in line with the expression. In contrast, AaaA activity in the ⊿*acoR was* reduced, that does not align with the expression and suggests a more complicated regulatory influence.

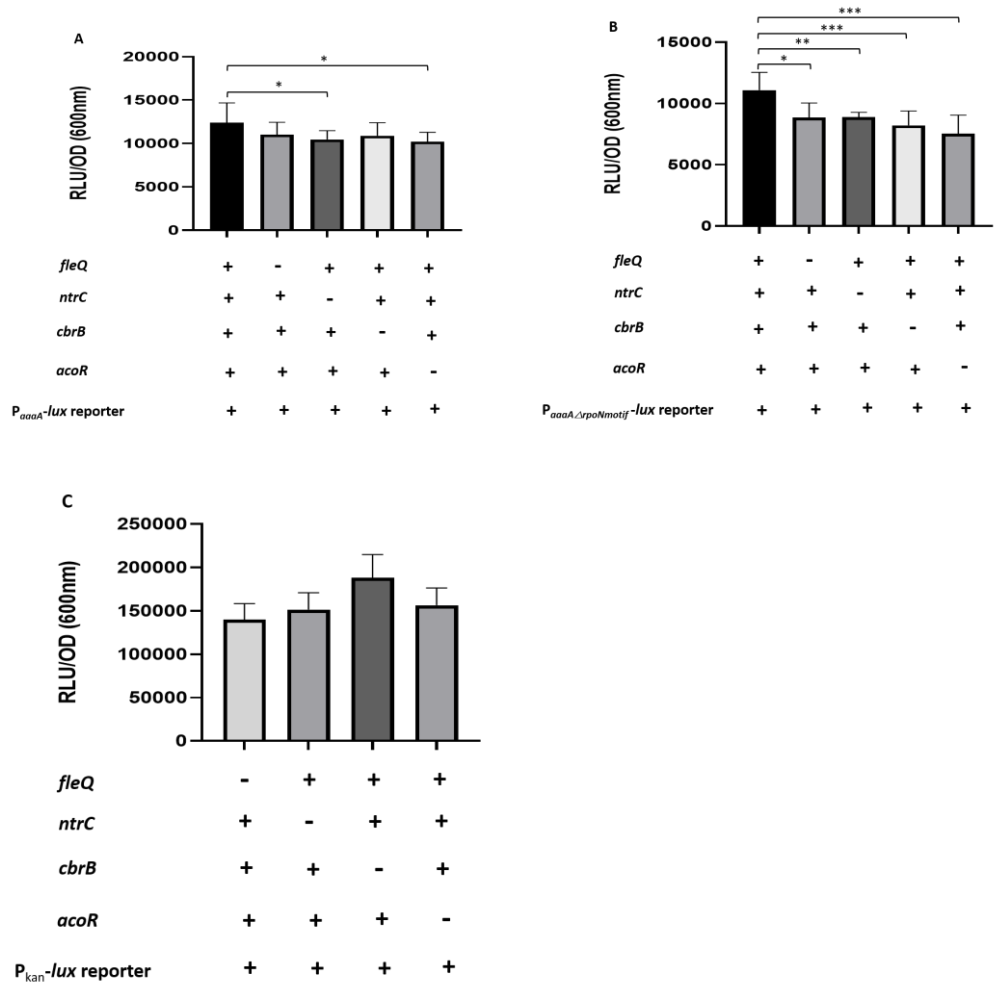

Figure 4.35: In the absence of *fleQ*, *ntrC*, *cbrB* and *acoR* in PA14 strains, P_{aaaA} driven expression significantly decreased in △*fleQ* , △*ntrC* , △*cbrB* and △*acoR* when the motif in the *aaaA* promotor was altered. *P.aeruginosa PA14 of WT, ⊿fleQ , ⊿ntrC , ⊿cbrB and ⊿acoR* carrying the intact P*aaaA* reporter (Pane A), disrupted RpoN motif (Panel B) and P_{kan} reporter (Panel C) were grown and bioluminescence analysed over time as described in Figure 4.16. Each experiment was performed in triplicate; error bars indicate the standard deviation. General ANOVA summary test analysis performed and △*ntrC* (*P* value 0.0498) and *⊿acoR (P* value 0.0363) reported for intact promoter, * indicating a significant difference. △*fleQ* (P value 0.0367), △*ntrC* (P value 0.0058), △*cbrB* (P value 0.0008) and *⊿acoR (P value 0.0004)* reported for RpoN motif disruptive state promoter. *, **,*** indicating a significant difference.

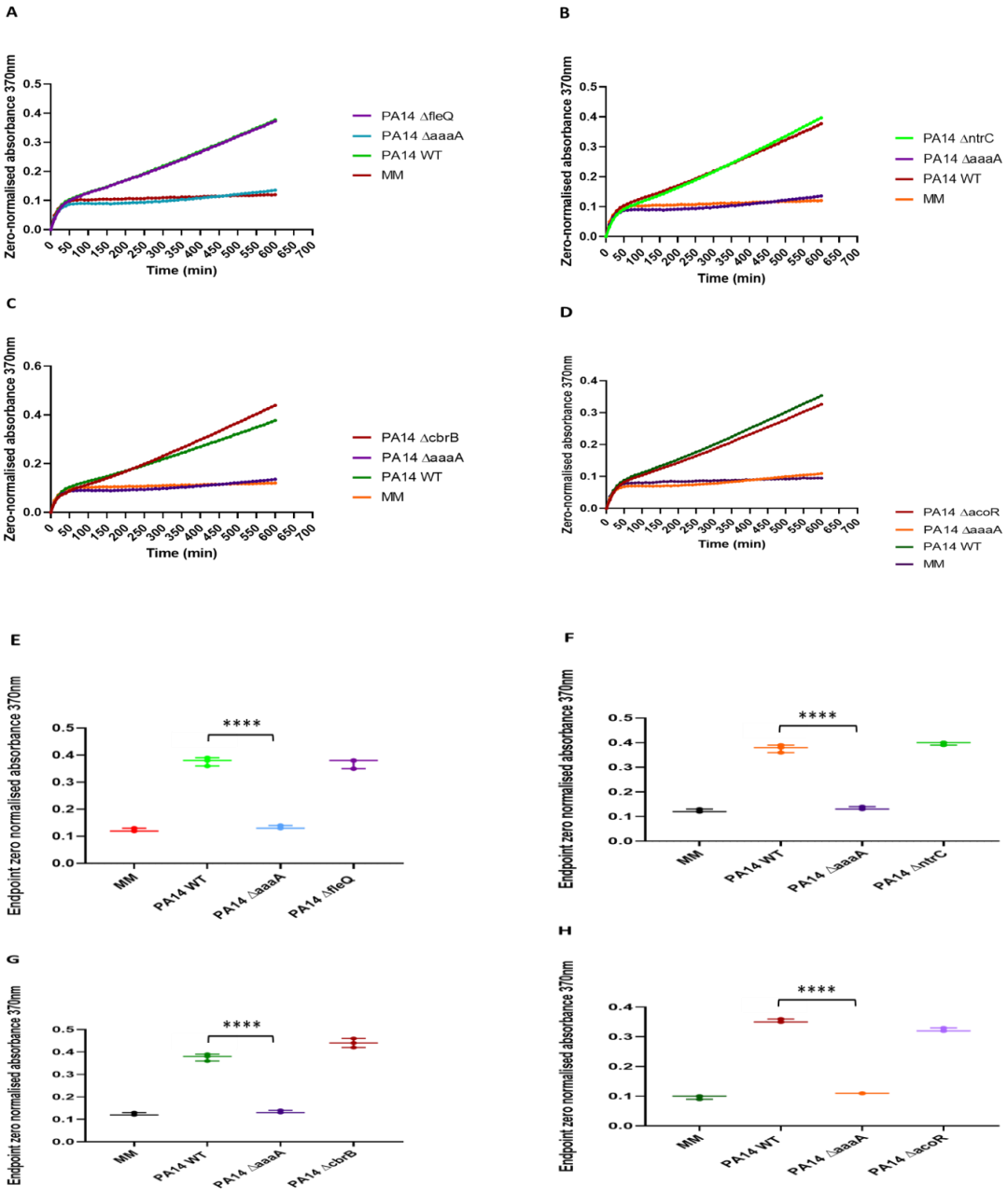

Figure 4.36: Arginine-*p*-nitroanilide degradation assay for AaaA verified that AaaA activity in the △*fleQ* and △*ntrC* mutants were similar compared to WT in *P. aeruginosa* PA14. AaaA activity in the △*cbrB was* increased while AaaA activity in the *⊿acoR was* reduced in *P. aeruginosa* PA14. Overnight cultures were normalized to 0.25 OD600 nm. The cells were then washed 2 times in MMP with centrifugation at 3707 Xg for 5 minutes to separate the pellet from supernatant. Following the final centrifugation, the supernatant was discarded and the pellet resuspended in 1 ml of MMP. For each bacterial strain, 3 wells in a sterile clear bottomed 96 well plate (Greiner bio1 F

bottom) were prepared with 150µl of the 1 mM working solution of arginine-*p*-nitroanilide and 150µl of the OD 600 nm 0.25 bacterial suspensions. The degradation of arginine-*p*-nitroanilide was determined by 1h measurements of OD 405 nm for 24 h at 37°C in an automated plate reader. Zero-normalised absorbance 370nm (Panel A-D) and Endpoint zero normalised absorption 370nm (Panel E-H) plots were analysed by Graphpad prism software and General ANOVA summary test analysis performed and P value <0.0001 reported, **** indicating a significant difference.

4.2.24. In PA14 strains, P_{aaaA} *driven expression* significantly decreased in △*fleR* , ⊿*NorR and* ⊿*mifR* mutants while no significant difference was found in the ⊿*ddaR* mutant when the motif in the *aaaA* promotor was altered

Figure 4.37 shows no significant difference in *lux* expression in ⊿*NorR,* ⊿*ddaR and* ⊿*mifR* mutants compared to WT with the intact P_{aaaA} reporter. However, the △*fleR* mutant showed a significant reduction in light emission (Tukey's multiple comparisons test P value 0.0020) compared to WT. With the mini-CTX $P_{aaaA\triangle rpoNmotif}$ –lux reporter, all except the ⊿*ddaR* mutant showed a significantly reduced light emission suggesting a potential to be involved in positive regulation for all except DdaR.

4.2.25. AaaA activity in the △*fleR*, ⊿*NorR* and ⊿*ddaR* mutants were reduced while AaaA activity in the ⊿*mifR* mutant was similar compare to WT in *P. aeruginosa* PA14

Figure 4.38 shows that AaaA activity in the △*fleR*, ⊿*NorR* and ⊿*ddaR* mutants were reduced in line with observed expression. In contrast, AaaA activity in the ⊿*mifR* mutant was similar to WT in *P. aeruginosa* PA14 suggesting no functional impact of the potential positive regulation of MifR indicated by the transcriptional reporter assay.

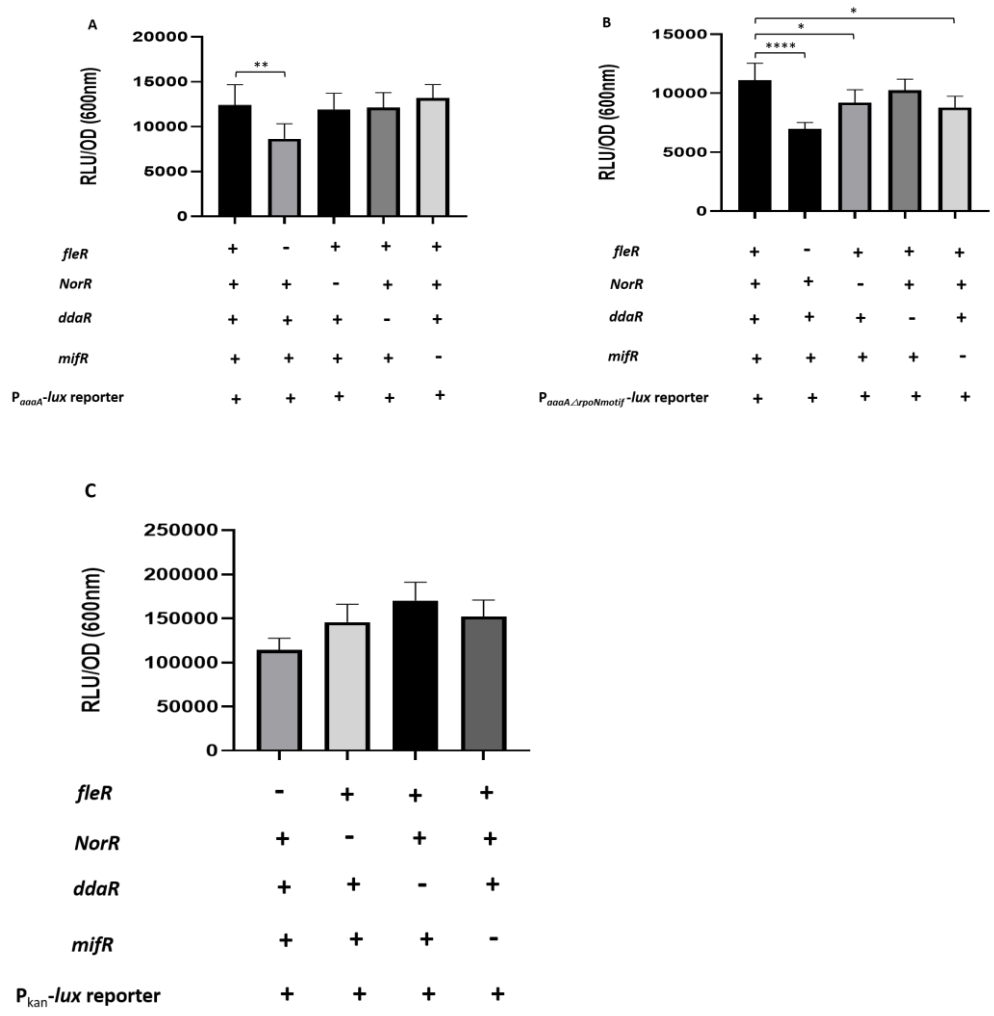

Figure 4.37: In the absence of *fleR*, *NorR*, *ddaR* and *mifR* in PA14 strains, P_{aaaA} driven expression significantly decreased in *△fleR, △NorR and △mifR* while no significant difference found in *△ddaR* compared to WT when the motif in the *aaaA* promotor was altered. *P.aeruginosa PA14 of WT, △fleR , △NorR , △ddaR and △mifR* carrying the intact P*aaaA* reporter (Panel A), disrupted RpoN motif (Panel B) and P_{kan} reporter (Panel C) were grown and bioluminescence analysed over time as described in Figure 4.16. Each experiment was performed in triplicate; error bars indicate the standard deviation. General ANOVA summary test analysis performed and P value 0.0020 reported for intact promoter, ** indicating a significant difference. while *△fleR* P value <0.0001, *△NorR* P value 0.0298 and *△mifR* P value 0.0254 reported for RpoN motif disruptive state promoter, **** and * indicating a significant difference.

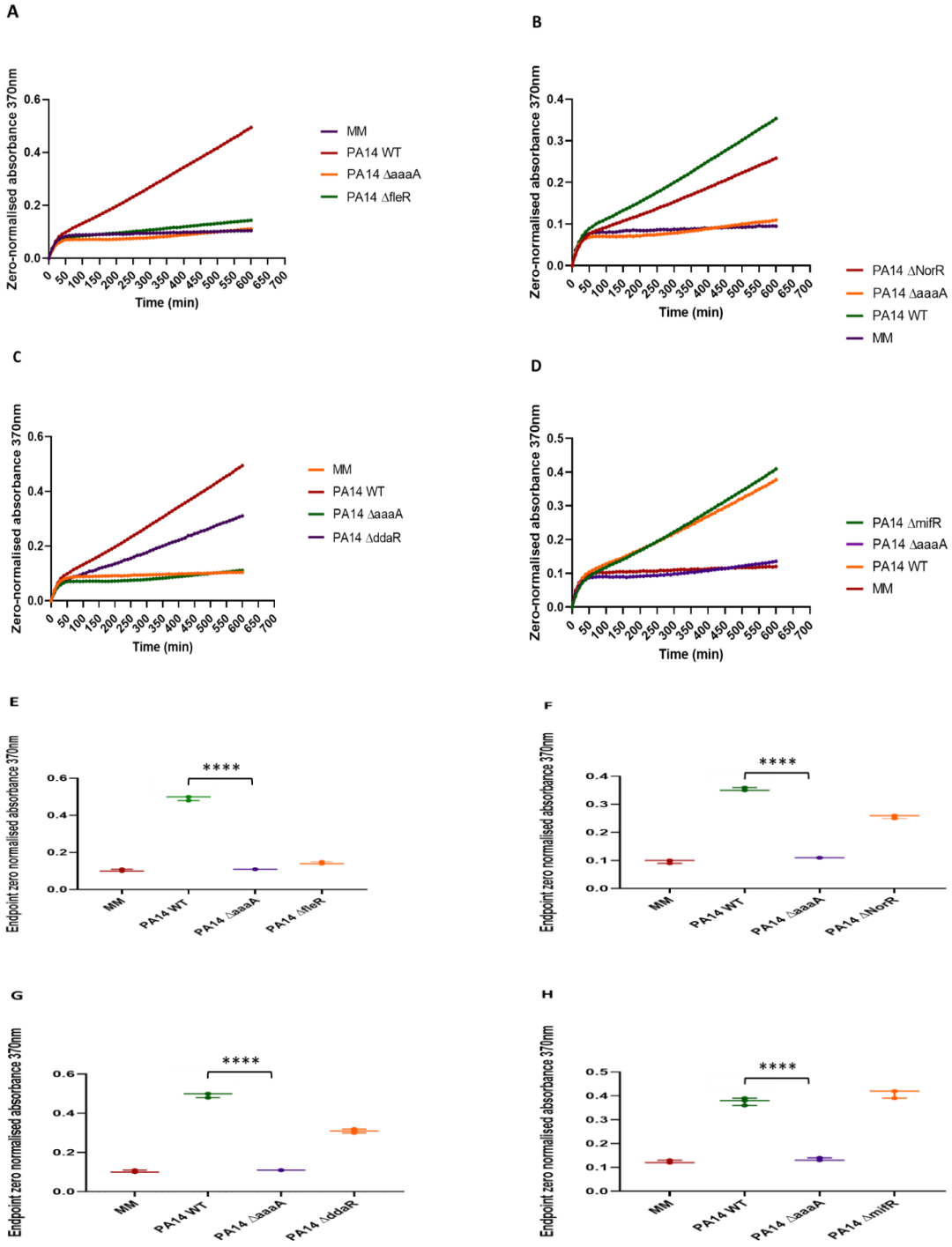

Figure 4.38: Arginine-*p*-nitroanilide degradation assay for AaaA verified that AaaA activity in *ΔfleR*, *ΔNorR* and *ΔddaR* mutants were reduced while AaaA activity in the *ΔmifR* mutant was similar to WT in *P. aeruginosa* PA14. Overnight cultures were normalized to 0.25 OD600 nm. The cells were then washed 2 times in MMP with centrifugation at 3707 Xg for 5

minutes to separate the pellet from supernatant. Following the final centrifugation, the supernatant was discarded and the pellet resuspended in 1 ml of MMP. For each bacterial strain, 3 wells in a sterile clear bottomed 96 well plate (Greiner bio1 F bottom) were prepared with 150 µl of the 1 mM working solution of arginine-*p*-nitroanilide and 150 µl of the OD 600 nm 0.25 bacterial suspensions. The degradation of arginine-*p*-nitroanilide was determined by 1h measurements of OD 405 nm for 24 h at 37°C in an automated plate reader. Zero-normalised absorbance 370nm (Panel A-D) and Endpoint zero normalised absorption 370nm (Panel E-H) plots were analysed by Graphpad prism software and General ANOVA summary test analysis performed and P value <0.0001 reported, **** indicating a significant difference.

4.2.26. In PA14 strains, P_{aaaA} *driven expression* is significantly decreased in △*eatR and ⊿13000* mutants*,* while no significant difference is found in △*hbcR* compared to WT when the motif in the *aaaA* promotor was altered

Figure 4.39 shows that in the *P. aeruginosa* PA14 background, *lux* expression in *⊿eatR, ⊿13000* and *⊿hbcR* mutants is similar to WT with the intact $P_{aaaA.}$ However, with the mini-CTX $P_{aaaA\triangle rpoNmotif}$ –*lux* reporter, whilst the *⊿hbcR* mutant remained similar to the WT, the other two mutants produced significantly less light: *⊿eatR* (Tukey's multiple comparisons test P value <0.0001), *⊿13000* (Tukey's multiple comparisons test P value 0.0370) suggesting positive regulation.

4.2.27. AaaA activity in the △*eatR*, *⊿13000* and △*hbcR* mutants was reduced in *P. aeruginosa* PA14

Figure 4.40 shows that AaaA activity in the △*eatR*, *⊿13000* and △*hbcR* mutants were reduced in *P. aeruginosa* PA14 in line with the expression detected from the reporter.

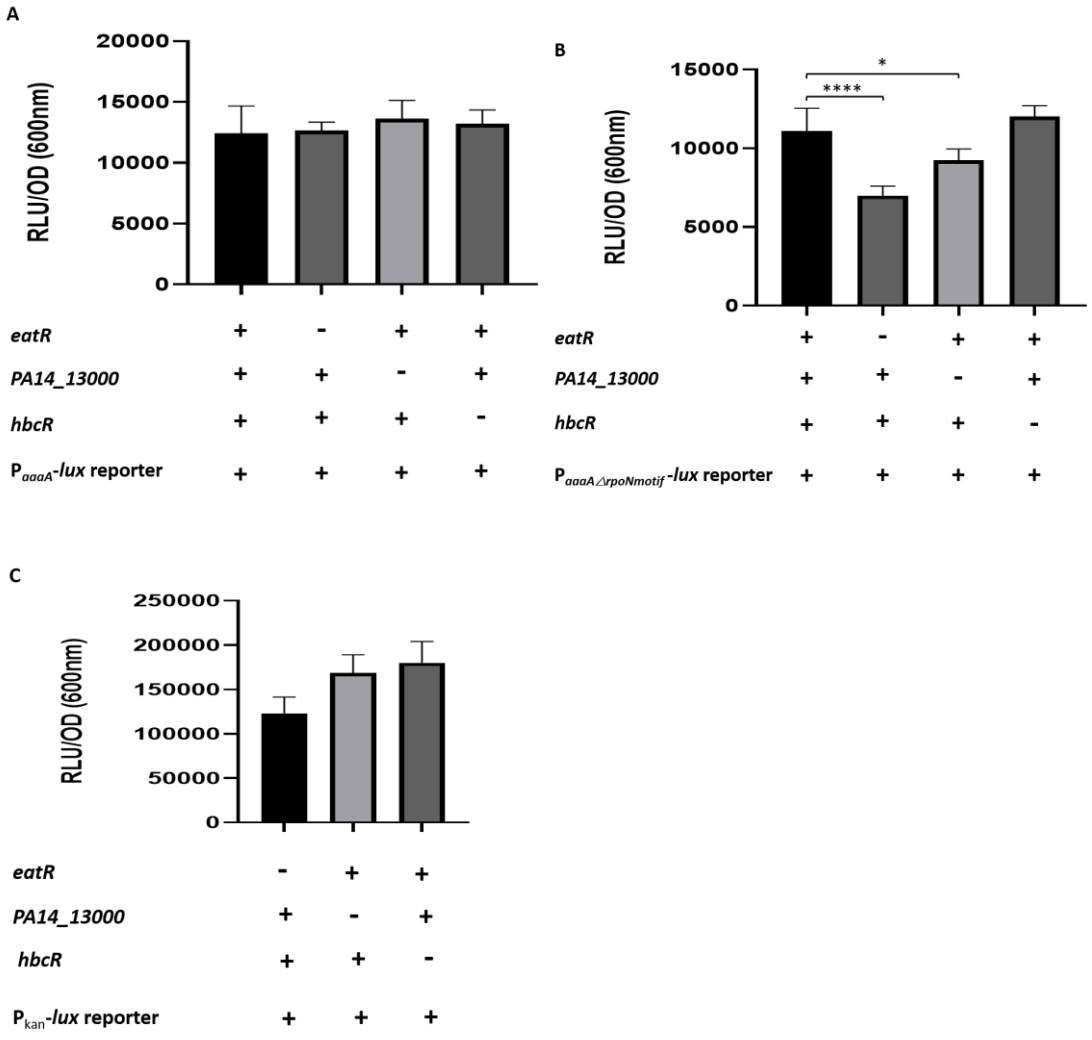

Figure 4.39: In the absence of *eatR, 13000* and *hbcR in* PA14 strains, P_{aaaA} driven expression significantly decreased in *△eatR and △13000* while no significant difference was found in *△hbcR* compared to WT when the motif in the *aaaA* promotor was altered. *P. aeruginosa PA14* of *WT, △eatR, △13000* and *△hbcR* carrying the intact P*aaaA* reporter (Panel A), disrupted RpoN motif (Panel B) and P_{kan} reporter (Panel C) were grown and bioluminescence analysed over time as described in Figure 4.16. Each experiment was performed in triplicate; error bars indicate the standard deviation. General ANOVA summary test analysis performed and P value <0.0001 reported for RpoN motif disruptive state promoter, **** indicating a significant difference. *△13000* (P value 0.0370) also reported, * indicating a significant difference.

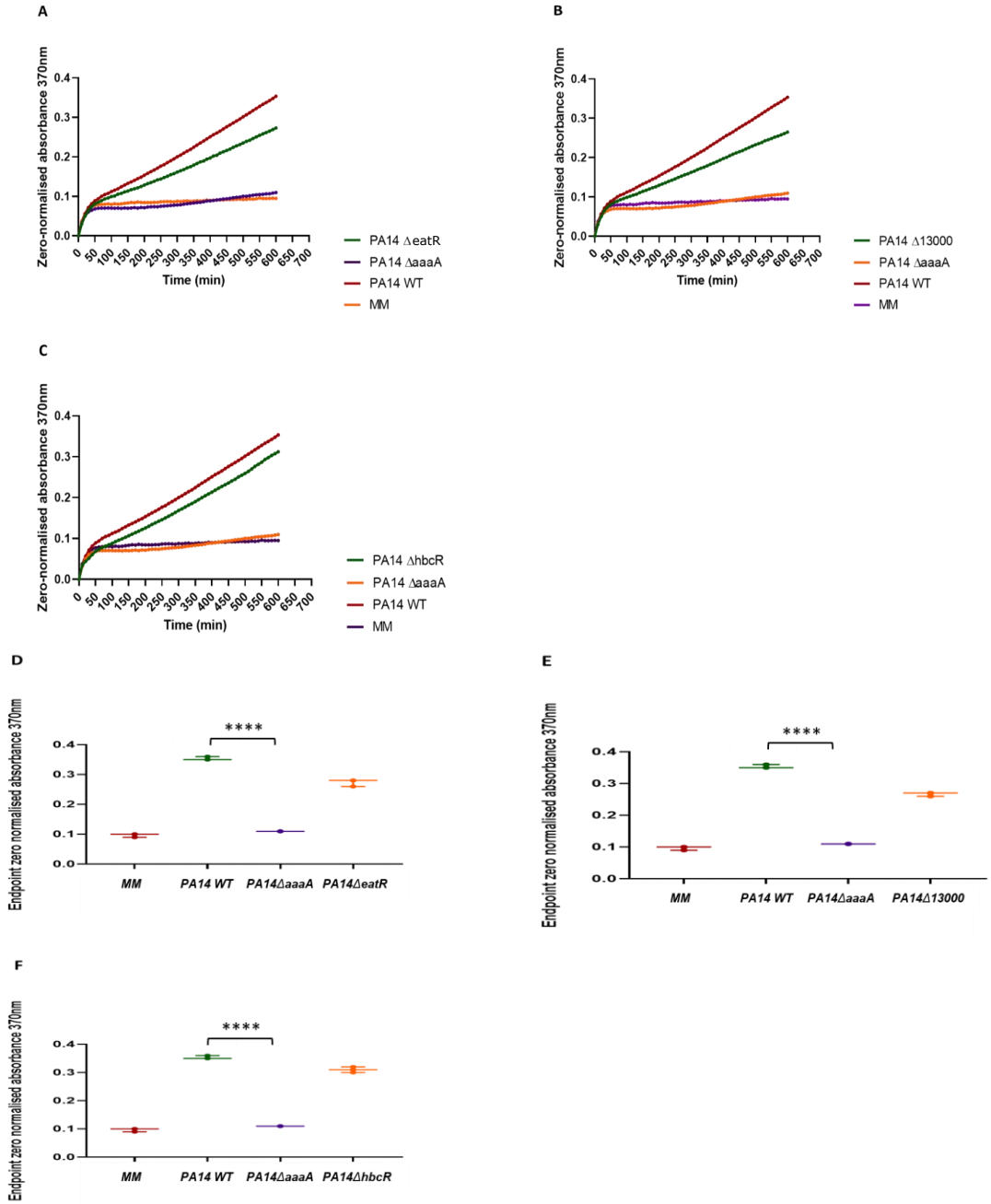

Figure 4.40: Arginine-*p*-nitroanilide degradation assay for AaaA verified that AaaA activity in the Δ*eatR*, Δ*13000* and Δ*hbcR* mutants was reduced in *P. aeruginosa* PA14. Overnight cultures were normalized to 0.25 OD600 nm. The cells were then washed 2 times in MMP with centrifugation at 3707 Xg for 5 minutes to separate the pellet from supernatant. Following the final centrifugation, the supernatant was discarded and the pellet resuspended in 1 ml of MMP. For each bacterial strain, 3 wells in a sterile clear bottomed 96 well plate (Greiner bio1 F bottom) were prepared with 150µl of the 1 mM working solution of arginine-*p*-nitroanilide and 150µl of the OD 600 nm 0.25 bacterial

suspensions. The degradation of arginine-*p*-nitroanilide was determined by 1h measurements of OD 405 nm for 24 h at 37°C in an automated plate reader. Zero-normalised absorbance 370nm (Panel A-C) and Endpoint zero normalised absorption 370nm (Panel D-F) plots were analysed by Graphpad prism software and General ANOVA summary test analysis performed and P value <0.0001 reported, **** indicating a significant difference.

4.2.28. In PA14, with the reporter bearing the altered motif in the *aaaA* promoter, *lux* expression was significantly decreased in the △*pilR* mutant while no significant difference was found in △*rtcR* and △*39360* mutants

Figure 4.41 shows that in the *P. aeruginosa* PA14 background, no significant difference is observed in *lux* expression in △*pilR, ⊿rtcR,* and *⊿39360* mutants compared to WT with the intact P_{aaaA} reporter. With the mini-CTX $P_{aaaA\triangle rpoNmotif}$ – *lux* reporter, light production in the *⊿rtcR* and *⊿39360* mutants was also similar to WT but was significantly reduced in the △*pilR* mutant (Tukey's multiple comparisons test P value 0.0476) suggesting positive regulation.

4.2.29. AaaA activity in the △*pilR* mutant was increased while in the *⊿rtcR* mutant it was similar to WT in *P. aeruginosa* PA14. AaaA activity in the *⊿39360* mutant was reduced in *P. aeruginosa* PA14

Figure 4.42 shows that AaaA activity in the △*pilR* mutant was increased while in the *⊿rtcR* mutant was similar compare to WT in *P. aeruginosa* PA14, reflecting the expression measured from the intact promotor reporter. AaaA activity in the *⊿39360* mutant was reduced in *P. aeruginosa* PA14, which did not match the expression from the intact reporter, suggesting a potential indirect regulation.

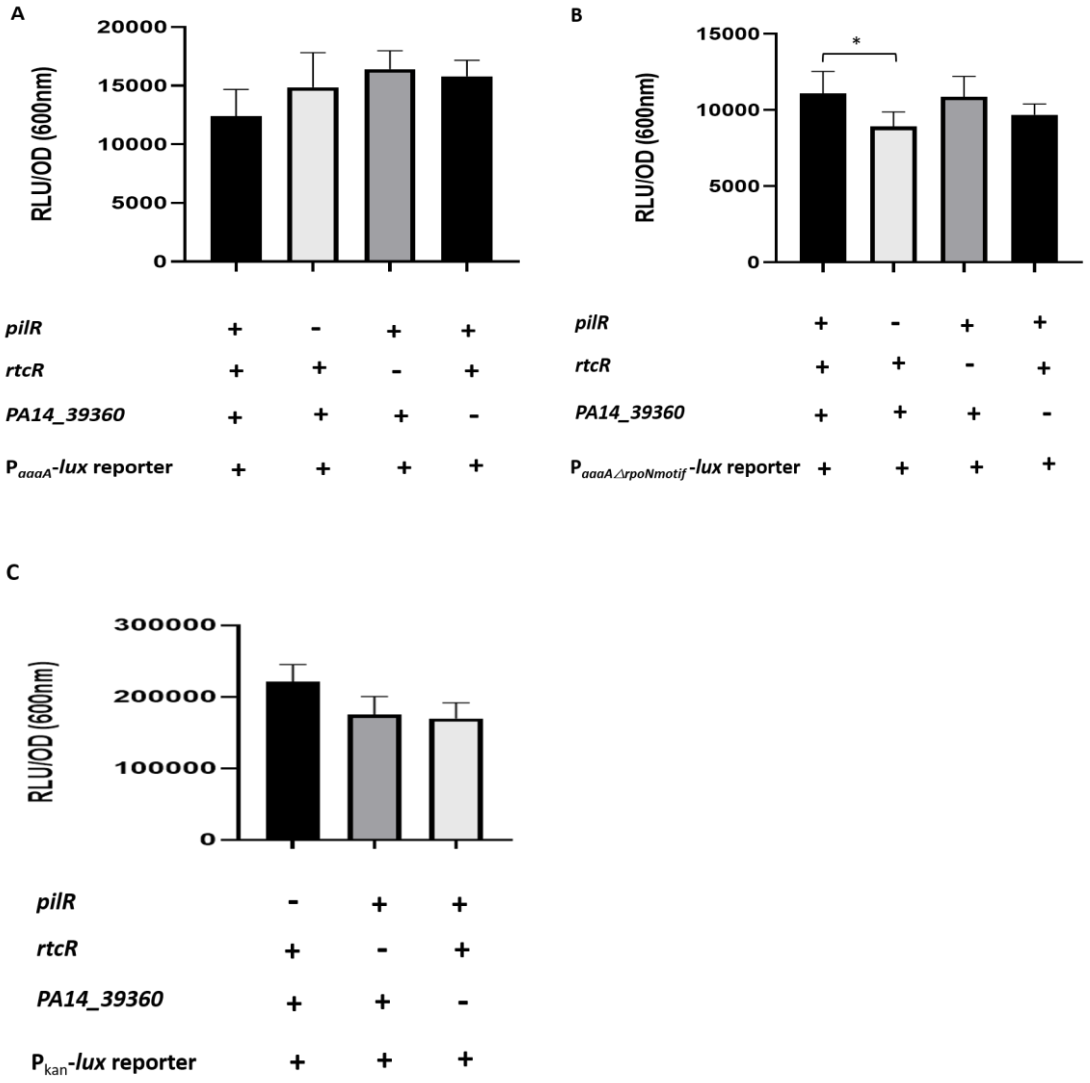

Figure 4.41: In the absence of *pilR*, *rtcR* and *39360* in PA14 strains, P_{aaaA} driven expression significantly decreased in △*pilR while* no significant difference found in △*rtcR* and △*39360* compared to WT when the motif in the *aaaA* promotor was altered. *P. aeruginosa PA14 of WT, ⊿pilR, ⊿rtcR, ⊿39360* carrying the intact P*aaaA* reporter (Panel A), disrupted RpoN motif (Panel B) and P_{kan} reporter (Panel C) were grown and bioluminescence analysed over time as described in Figure 4.16. Each experiment was performed in triplicate; error bars indicate the standard deviation. General ANOVA summary test analysis performed and P value 0.0471 reported for RpoN motif disruptive state promoter, * indicating a significant difference.

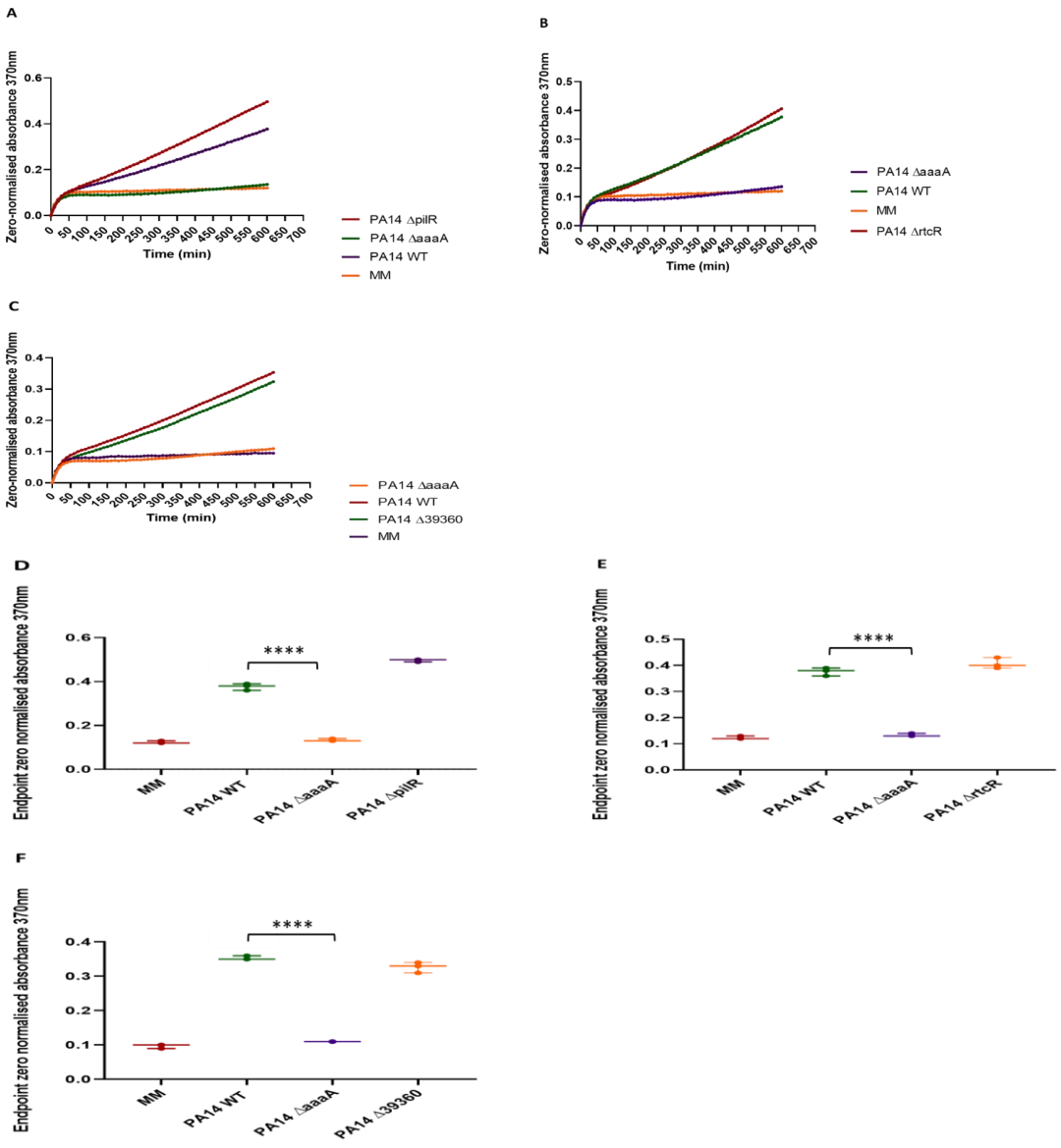

Figure 4.42: Arginine-*p*-nitroanilide degradation assay for AaaA verified that AaaA activity in the Δ*pilR* was increased in *P. aeruginosa* PA14. Overnight cultures were normalized to 0.25 OD600 nm. The cells were then washed 2 times in MMP with centrifugation at 3707 Xg for 5 minutes to separate the pellet from supernatant. Following the final centrifugation, the supernatant was discarded and the pellet resuspended in 1 ml of MMP. For each bacterial strain, 3 wells in a sterile clear bottomed 96 well plate (Greiner bio1 F bottom) were prepared with 150µl of the 1 mM working solution of arginine-*p*-nitroanilide and 150µl of the OD 600 nm 0.25 bacterial suspensions. The degradation of arginine-*p*-nitroanilide was determined by 1h measurements of OD 405 nm for 24 h at 37°C in an automated plate reader. Zero-normalised absorbance 370nm

(Panel A-C) and Endpoint zero normalised absorption 370nm (Panel D-F) plots were analysed by Graphpad prism software and General ANOVA summary test analysis performed and P value <0.0001 reported, **** indicating a significant difference.

4.3. Discussion and future work

The large genome of *P. aerugunosa* with its wide variety of regulators, enables the bacterium to be successful in a range of environmental conditions. The selective advantage that this brings enables *P. aeruginosa* to optimally control its virulence and be such a successful opportunistic pathogen. In this study, To further understand the regulation of *aaaA* and to see if RpoN regulates *aaaA* expression through direct interaction with the putative RpoN binding motif previously identified in the *aaaA* promotor, a substitution mutation strategy was successfully performed.

The data presented in this chapter shows that AaaA, like many other *P. aeruginosa* virulence factors, is subject to dynamic multifactorial regulatory system. Previous studies found AaaA could give *P. aeruginosa* an advantage in chronic lung and skin infections, and therefore it is essential to unlock the factors involved in its regulation. Dr Esteban Paredes Osses (2014) found a group of putative regulators of *aaaA* by using a miniCTX-*lux* based reporter system to measure the expression of *aaaA* in different transposon mutants. Further analysis of the promoter of *aaaA* was carried out *in silico* by Daniella Spencer (2018). Different putative regulator binding sites were found in previous studies and it was hypothesized that these regions could interact with each other to control *aaaA* expression in different conditions.

In this study, data suggests that AaaA negatively effects its own expression and disruption in the putative RpoN binding motif prevents this negative effect. This confirms previous findings in which transcription of the *lux* operon from the P_{aaaA} promoter can change considerably in the absence of active AaaA.

The discovery that *aaaA* is involved in a negative feedback loop was surprising and posed the question of whether it was a direct or indirect influence. Direct regulation is unlikely, as AaaA is not predicted to have any domains for DNA binding. Moreover, AaaA is bound to the external surface of the outer membrane, making it difficult to understand how it will come in contact with the

chromosome. Two unbiased ways to screen for intermediates in this auto-regulation would be: (i) comparative transcriptomics of an *aaaA* deficient mutant and its parental counterpart, or (ii) scanning a random transposon library generated in the *aaaA* deficient mutant bearing the CTX-P_{aaaA}-lux reporter for a loss of bioluminescence. Both of these approaches would benefit from understanding the optimal conditions for AaaA production. To determine this, evaluation of AaaA levels in a variety of environmental niches would be useful, and might also indicate how such factors favour *aaaA* autoregulation. Previous work has already highlighted a wide range of relevant conditions such an availability of arginine, nitrogen and oxygen. This chapter took a step towards narrowing down the variables by targeting some specific factors already implicated in *aaaA* regulation for more in depth analysis, with the hope that there might be a link to *aaaA*'s self-regulation. Some of the strongest evidence for regulation of *aaaA* derives from a logical link with arginine availability and metabolism. For example, expression of a reporter driven by the native P_{aaaA} was shown previously to be controlled by enzymes and regulators involved with arginine assimilation and degradation.

As AaaA releases arginine from its substrates, its expression may be regulated by external source of arginine, thus different concentrations of exogenous arginine were applied to the reporter strains and it was found that exogenous arginine has minimal effect on *aaaA* expression, further confirming previous findings that Arginine showed no complementation effect. The data suggested that arginine deficiency is not the main controller of *aaaA* upregulation.

One of the overriding controls in this arginine-influenced network is the sigma factor RpoN, and in the promoter of *aaaA* there is a putative RpoN-binding motif which in this study was successfully mutated to create the reporter $P_{aaaA\triangle rpoNmotif}$ – *lux*. The engineered CTX-P_{aaaA}-*lux* transcriptional reporters allowed the discovery that *aaaA* negatively regulates its expression, and that superimposed on this is the negative regulation of the alternative sigma factor RpoN. Previous study found RpoN negatively regulates the *aaaA* promoter after conjugation of Mini CTX-P_{aaaA}-*lux* and Mini CTX-P_{kan}-*lux* reporters into *P. aeruginosa* PA14 WT. in this study, the role of RpoN and its putative binding motif in expression of *aaaA* was investigated, and the data suggested that the motif disrupted in the *aaaA* promotor has a negative effect on *aaaA* expression independent of RpoN. In addition, the arginine-*p*-nitroanilide degradation assay for AaaA verified that

AaaA activity in the Δ*aaaA*, Δ*rpoN* and complemented *rpoN* mutant was reduced in *P. aeruginosa* PAO1. It is more likely that RpoN binds to the *aaaA* promoter at a remote site to the previously identified binding motif. A double *rpoN*/*aaaA* mutant is required for future studies to see if AaaA negatively regulates itself using this motif.

Several attempts have been made to conjugate pDM4:Δ*aaaA* into PAO1 Δ*rpoN* to construct the double *rpoN*/*aaaA* mutant. First pDM4 plasmid carrying Δ*aaaA* was extracted and transformed into *E. coli* S17-1. The transformant was then conjugated with PAO1 Δ*rpoN*. Different optimizations including changing O/N temperature between 42°C and 37°C, volumes of cultures combined, incubation time and antibiotic (chloramphenicol) concentration above 375mg/ml. Only in 42°C scenario with 100ml culture mixture obtained *Pseudomonas* following growth on 400mg/ml chloramphenicol O/N. The candidate double mutant was cultured and crossing over was successful to make a presumed clean double mutant. To further test the double mutant, the genomic DNA was extracted, but PCR did not confirm the presence of *rpoN* and *aaaA* mutations as no DNA fragments were amplified for either gene. One possibility would be PAO1 Δ*rpoN* is intrinsically resistance to CM. To test this hypothesis, PAO1 Nottingham strain was cultured in LB+CM and no colonies grew discounting this. Transformation of pDM4 containing Δ*aaaA* into PAO1 Δ*rpoN* also did not work. A new gene transfer strategy such as phage transduction or use of a different compatible suicide plasmid may be useful to construct the double *rpoN*/*aaaA* mutant in the future.

Confirmation that the RpoN putative binding site is necessary for expression is required to find out how it regulates *aaaA* expression. Previous studies suggested that RpoN is the only sigma factor to interact directly with *PaaaA* and that this involves the EBP, NtrC, interacting with a closed RpoN complex in low level nitrate conditions to initiate transcription(253). FleQ can also interact with RpoN in a similar manner when c-di-GMP (Baraquet *et al* 2012) is available during biofilm formation. Another study (Schaefer *et al* 2015) suggested that RpoN could compete with another sigma factor such as RpoS. However, for further confirmation, comparing P*aaaA* activation in *Δrpos*, *ΔrpoN*, and *ΔrpoSΔrpoN* mutants using the miniCTX-*lux* reporter can be investigated. In addition, two transcript feedback mechanisms proposed by Zafar *et al* (2013) found that RpoN could also work with another sigma factor.

In this study it is shown that in the absence of MvaT or MvaU, *aaaA* expression decreased when the motif in the *aaaA* promotor was altered and our data suggested that in contrast to the negative effect of MvaT and MvaU on the intact *aaaA* promoter, these HN-S proteins have a positive effect on the genetically altered *aaaA* promoter. Moreover, we found that AaaA activity in the Δ*mvaU* or Δ*mvaT* mutants was reduced in *P. aeruginosa* PAO1.

According to previous studies, activators of *aaaA* seem to be arginine, limited-oxygen and limited-nitrate. In nitrate-low level conditions, NtrC would activate P_{aaaA}. Previous study found *aaaA* is positively controlled by the arginine-responsive regulator ArgR, the anaerobic adaptation regulator ANR, genes encoding arginine-absorbing transporters, and the ADI pathway. Our data suggested that in the absence of ArgR (arginine sensing and utilization regulator), *aaaA* expression was unaffected when the motif in the *aaaA* promotor was altered. It seems like the arginine sensing regulator has no major effect on the *aaaA* promoter when the motif is disrupted. However, AaaA activity in the Δ*argR* was reduced in *P. aeruginosa* PA14.

The enhancer binding proteins (EBPs) Sfa2 and Sfa3 are RpoN activators. Previous study found that Sfa2 and Sfa3 positively regulate the *aaaA* intact promoter expression in *P. aeruginosa* PA01. In this study our data suggested that in the absence of the enhancer binding protein Sfa3 in PA14, *aaaA* expression significantly decreased when the motif in the *aaaA* promotor was altered and no significant difference in light production was found between Δ*sfa2* and WT for either reporter. By contrast, in the absence of Sfa2 and Sfa3 in PA01 strain, *aaaA* expression was significantly decreased in Δ*sfa2* and significantly increased in Δ*sfa3* when the motif in the *aaaA* promotor was altered. Our data also showed that AaaA activity in the Δ*sfa2* and Δ*sfa3* was reduced in both *P. aeruginosa* PA14 and PA01. Strain to strain variation and genetic differences in *P. aeruginosa* has been previously documented and could be influencing the variation of sfa response (457).

Regulation of *aaaA* expression by QS was studied because QS influences the expression of several *P. aeruginosa* virulence genes affecting biofilm development. This is relevant because AaaA is produced at later growth stages and an *aaaA* deficient mutant is impeded in its ability to form biofilms *in vitro* and *in vivo* (unpublished results, personal correspondence Owen Darch and Daniella Spencer). Previous study showed that AaaA plays a role in biofilm

formation and chronic infection. Of the three QS regulators assessed here (LasR, RhlR, PqsE), only RhlR impaired the transcription from the native P_{aaaA}, which was revealed by increased expression of the reporter in the *rhlR*-deficient mutant. Presumably, because the altered expression was moderate, it was not sufficient to trigger AaaA-autoregulation since in the Δ*rhlR* mutant the AaaA-activity was also raised. The RhIR transcriptional regulator binds to unique sequences called Rhl-boxes in *P. aeruginosa.* In the presence and absence of C4-HSL, RhlR dimerizes and attaches to certain DNA areas. The mild repression of *aaaA* expression reported for RhlR is supported by the prediction in Virtual Footprint v3.0 (http:/www.prodoric.de/vfp/vfp promoter.php) showing two regions in the 500bp upstream sequence of *aaaA* where motifs with the capacity for RhlR binding occur.

In previous study, *aaaA* expression in mutants of regulators of biofilm formation such as *P. aeruginosa* PA01 Δ*lasR, ΔrhlR,* and *ΔpqsE* carrying CTX-*lux* reporters were monitored. No significant difference in *lux* expression was observed in Δ*lasR* and Δ*pqsE* mutants compared to WT with the intact P_{aaaA}-*lux* reporter. However, more light was measured in the *ΔrhlR mutant*, suggesting RlhR negatively regulates *aaaA* (Esteban Paredes 2014). In this study it was shown that in PA01, in the absence of QS, expression from the intact *aaaA* promoter increased supporting previous findings. Similar, but more obvious changes were seen with expression driven by the altered motif in the *aaaA* promoter. In addition, AaaA activity in all QS related mutants was increased in *P. aeruginosa* PA01.

Since AaaA liberates arginine, a potential source of nitrogen when oxygen is scarce, the role of *ΔnirQ* on *aaaA* expression through the disrupted motif in *aaaA* promoter was investigated. Our data suggested that in the absence of the denitrification regulatory protein NirQ in PA01-L, *aaaA* expression significantly increased when the motif in the *aaaA* promotor was altered. Significant difference between *ΔnirQ* and WT with the P_{kan} control constitutive promoter strains was also found in this study, so testing another WT P_{kan} control constitutive promoter for further confirmation of our finding is recommended. The data here also suggested that AaaA activity in the denitrification regulator *ΔnirQ* mutant was decreased in *P*. *aeruginosa* PA01-L.

In this study, systematic evaluation of putative EBPs in *aaaA* transcription and activity was successfully conducted through conjugation of reporters in each

mutant. The data suggested that in the absence of *phhR* and *dctD* in PA14 strains, P_{aaaA} driven expression significantly decreased in △*phhR and* △*dctD* when the motif in the *aaaA* promotor was altered. In addition, In PA14 strains, *lux* expression significantly decreased in △*fleQ*, △*ntrC*, △*cbrB* and ⊿*acoR* mutants when the motif in the *aaaA* promotor was altered. Moreover, In PA14 strains, *lux* expression significantly decreased in △*fleR, ⊿NorR and ⊿mifR* mutants while no significant difference was found in the ⊿*ddaR* mutant when the motif in the *aaaA* promotor was altered. In another series of putative EBPs it was found that *aaaA* expression is significantly decreased in △*eatR and ⊿13000* mutants*,* while no significant difference was found in △*hbcR* compared to WT in PA14 strains when the motif in the *aaaA* promotor was altered. In the last EBP series of PA14, with the reporter bearing the altered motif in the *aaaA* promoter, *lux* expression was significantly decreased in the △*pilR* mutant while no significant difference was found in △*rtcR* and △*39360* mutants. The data also revealed that AaaA activity in the △*fleQ*, △*ntrC*, ⊿*mifR*, ⊿*rtcR* and ⊿*gscR* mutants was similar to WT in *P. aeruginosa* PA14 while AaaA activity in the △*cbrB*, △*pilR* and ⊿*dctD* mutants was increased. By contrast, AaaA activity in the ⊿*phhR*, ⊿*algB, ⊿acoR, ⊿fleR, ⊿NorR, ⊿ddaR, ⊿eatR, ⊿13000, ⊿hbcR and the ⊿39360 mutants was* reduced in *P. aeruginosa* PA14. For better comparison between putative EBPs, conjugation of the P_{kan}-*lux* reporter into appropriate WT PA14 mutants is needed.

To undertake this study, a number of tools available in the laboratory were utilized. It is possible that since they were designed and created, that more data has become available that should be incorporated into the analysis. For example, transcriptomics is now available that maps the real transcriptional start sites of *Pseudomonas* genes (458). This should be mined to identify the true +1 site that has been experimentally determined and compared to the theoretically predicted ones incorporated in the reporters. If there is a difference, a systematic comparison could be undertaken to determine whether this influences the regulation of *aaaA*.

Future studies using qRT-PCR and site-directed mutagenesis can now be designed to clearly identify the putative regulator binding sites and provide better understanding regarding *aaaA* function within its regulatory network. Further mutagenesis of the other predicted regulator binding sites in the *aaaA* promoter could be designed to determine if they are targeted by the expected regulators, or whether regulatory mutant factors examined in this study can

control the expression of *aaaA* by binding in any of these regions. There is a need to construct double/triple mutations and complementation strains as well as defined (ie non transposon) mutants to remove the potential for downstream genes influencing the data. Exploring the direct regulation networks of *aaaA* expression will provide better understanding of its function *in vivo* and its contribution to the *P. aeruginosa* pathogenic life cycle in chronic infections.

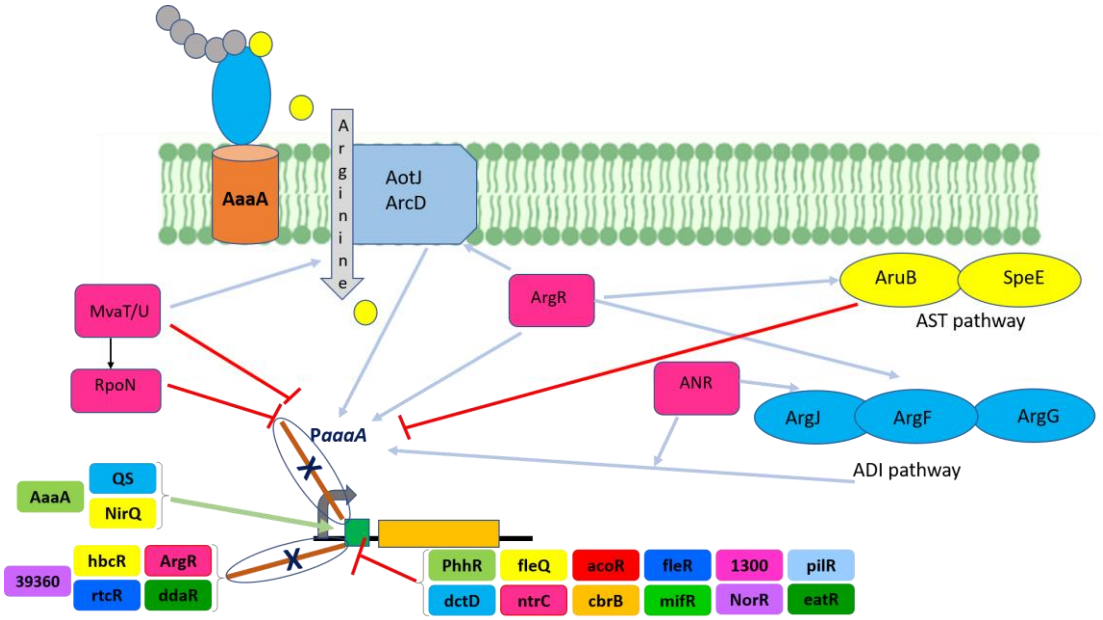

Figure 4.43: An overview of different AF mutants potentially related to aaaA expression used in this study. AaaA negatively affects its own expression and disruption of the putative RpoN binding motif prevents this negative effect. In the absence of the QS and biofilm regulator in PA01, aaaA expression significantly increased in ΔlasR, ΔrhlR, ΔpqsE when the motif in the aaaA promotor was altered. In the absence of the denitrification regulatory protein in PA01 L, aaaA expression also significantly increased in ΔnirQ when the motif in the aaaA promotor was altered. However, In the absence of ArgR, aaaA expression was unaffected when the motif in the aaaA promotor was altered. Systematic evaluation of putative EBPs in *aaaA* transcription and activity was successfully conducted through conjugation of reporters in each. In addition, No significant difference found in △rtcR , △hbcR , △ddaR and △39360 compared to WT when the motif in the aaaA promotor was altered. By contrast, PaaaA driven expression significantly decreased in △phhR , △fleQ, △acoR, △fleR, △13000, △pilR, △dctD, △ntrC, △cbrB, △mifR, △NorR and △eatR when the motif in the aaaA promotor was altered.

Chapter 5

Final conclusions and future directions

In this study, individual localization of potential accessory factors and their possible role in facilitating secretion of the EspC and AaaA autotransporters was compared. Entropathogenic *E. coli* (EPEC) has evolved with conserved bacterial secretion systems for the transport of substrates across the cell membrane. These secretion systems play an important role in pathogenic nutritional uptake, cell-to-cell communication and exploitation of host cells. In addition, through these multi- protein complexes, diverse virulence factors such as adhesions, proteases, toxins, and effector proteins are secreted during colonization of host cells by pathogens. Autotransporters are important virulence factor proteins and utilize the simplest secretion system discovered so far in Gram-negative bacteria. Autotransporters have a characteristic extracellular passenger (α-domain) translocated by a β-barrel transmembrane domain (Transport domain that is inserted in the Outer membrane (OM). Different periplasmic and OM factors like the BAM complex and TAM have been proposed to facilitate translocation. Moreover, the EPEC autotransporter, EspC may utilize T3SS to enter host cells. However, the complete mechanism of EspC secretion, role in pathogenesis, interaction with T3SS system and Bam Complex along with energy source for translocation is not yet completely clear. In previous studies, a transposon screen suggested 6 *E. coli* proteins have a potential role as accessory factors (AF) in EspC secretion(149). In this study, we explored the role of each of the 6 potential AT AFs in EspC secretion and undertook parallel investigations with the autotransporter produced by the opportunistic pathogen *Pseudomonas aeruginosa*, AaaA. Since the production of AaaA is influenced by a potentially complex network of regulatory factors, investigations using a transcriptional reporter were also undertaken to identify whether there was a predominate regulator governing AaaA production.

This study utilized previously constructed plasmids encoding native EspC (pLA33C1), and two versions of EspC fused to the red fluorescent protein mCherry to facilitate tracking within the cell. Of the latter, one encoded a product with an intact transporter domain (pLA33C1MC), and the other lacked the C-terminal β-barrel domain (pMAC33). These plasmids were successfully transformed into the AT accessory factor secretory mutants (Δ*proW*, Δ*slyB*,

Δ*sapA*, Δ*ybgC*, Δ*yqjE* and Δ*abrB*). The only putative secretion accessory factor mutant showing potential after the EspC-mCherry screen was the Δ*slyB* mutant, however using EspC-TC or AaaA-TC tracked proteins, a role in AT secretion could not be reliably observed in this study.

Screening of transposon mutants for deficient EspC secretion would further investigate and find other groups of potential accessory factor mutants to provide a better understanding of the role of the C-terminal β-barrel domain. Previous study in our group suggested that localization of both EspC and AaaA not only requires the AT β-barrel domain but also involves the bacterial cytoskeleton actin homologue MreB along with the Sec translocon, and occurs through discrete patches in a helical pattern surrounding bacterial cytoskeleton. The use of high-resolution imaging technologies for AT localization studies will provide better understanding into the molecular interactions and associated accessory factors in the localization of EspC(113). For instance, co-localization studies of EspC with MreB or other accessory factors investigated in this study like SlyB would be useful to learn whether the previously observed patchy arrangements will be found or not(113). Such observation would enable the proposition of a descriptive model for the AT secretion pathway. Two-hybrid screening could also be used to study AT interaction with accessory proteins(459).

Characterizing the exact secretion pathway and localization along with molecular accessory factors involved in the spiral secretion of EspC would offer the potential to discover inhibitors that might serve as a novel antimicrobials. New antimicrobial agents are urgently needed due to the increasing number of AMR cases in hospital and communities(460). Inhibition of secretion by targeting different segments of the AT structure and other areas of the pathway including Sec machineries, signal peptidase, periplasmic chaperones and OM BAM complex and their associated factors could lead to development of new antibiotics or vaccine candidates in the future(461).

Future studies should also investigate alternative means of fluorescent labelling for the ATs. Smaller tags e.g FlAsH would have the advantage of providing proteins closer to the native form to follow during secretion(244). In addition, this study could be extended to incorporate different types of AT e.g. adhesins. Through these comprehensive studies we would be able to understand more about the function of AT accessory factors(462).

According to previous data in our lab, AaaA is an aminopeptidase specific for arginine tethered to the surface in *P. aeruginosa*. The work presented here has provided evidence of *aaaA* regulatory controls by successful creation of new reporter through site directed mutagenesis. One of the main regulators in this arginine-influenced network is the sigma factor RpoN, and in the promoter of *aaaA* there is a putative RpoN-binding motif which was successfully mutated to create the reporter $P_{aaaA\triangle rpoNmotif}$ –*lux* and compared with constitutive and intact *aaaA* promoter driven reporters in different mutant backgrounds. For future studies, an appropriate WT control in the PA14 background is required since the P_{kan}-*lux* reporter could not be introduced. Moreover, it is necessary to repeat the analysis presented to assess reproducibility. The data presented here confirmed the previous finding that AaaA exerts a negative feed-back over its own expression(258). It would be interesting to perform this experiment in different oxygen concentrations and bacterial growth phases. It would also be an interesting idea to test the effect of diverse periplasmic chaperones (i.e. SurA, Skp and DegP) on *aaaA* expression, and their possible role in autoregulation when the motif disrupted in the *aaaA* promotor and compare them with intact and constitutive promoters for each mutant(461).

In this study, different QS regulators were evaluated to see if they control the *aaaA* promoter. For future study the impact of the arginine binding protein AotJ, the inner membrane protein ArcD, global regulator ANR, three components of the urea cycle (ArgF, ArgG and ArgJ) and one component of the arginine descarboxylase (ADC) pathway, SpeA along with one component of the arginine succinyltransferase (AST) pathway, AruB could be investigated in the same manner using transcription and activity assays for each mutant in the PA14 Washington strain background using the transposon mutants available(258).

Future studies could alternatively be targeted to *in vivo* studies, e.g. tissue culture-based infection models (e.g. skin, lungs)(463,464). AaaA is an ideal target for inhibition as it is crucial for chronic infections and surface exposed. The interaction between autotransporters and their role in bacterial metabolic regulation and infection process is a complex journey and requires novel microscopic analysis tools. New technological platforms will help us to analyse the metabolome and virulence factors at the same time in single bacterial cells in the near future through secondary ion mass spectrometry (SIMS) imaging such as cryo-O rbi SIMS and Nano-SIMS, and Raman coupled to confocal microscopy

or fluorescence *in situ* hybridisation (FISH) which will provide new prospect in this area(465–467).

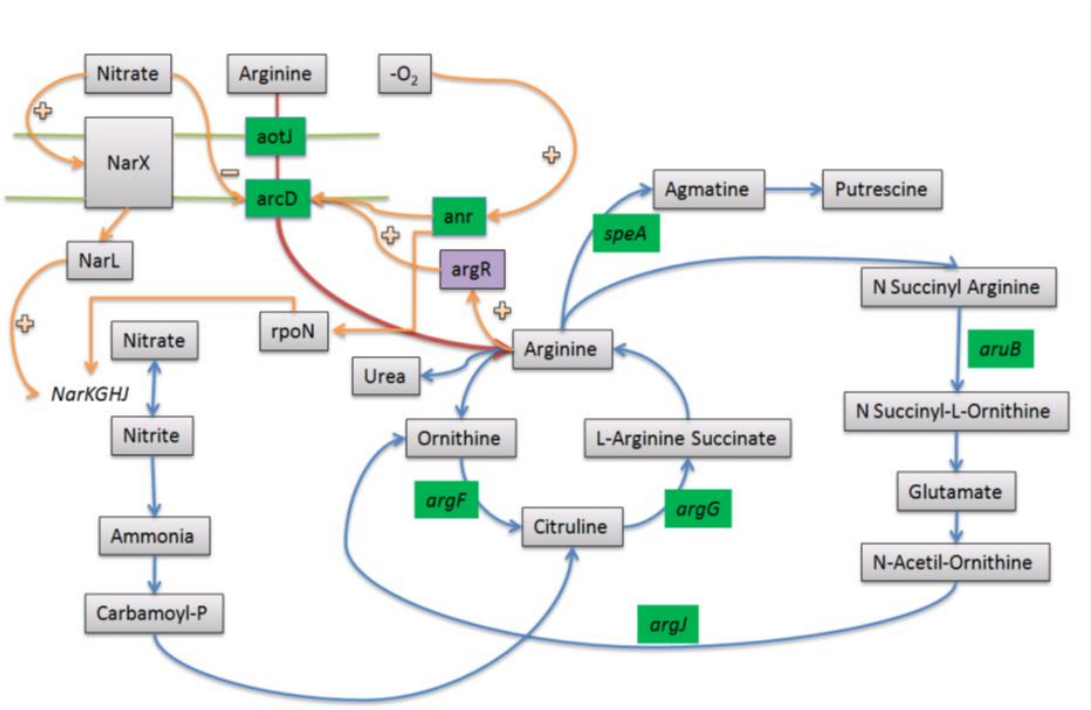

Figure 5.1: Simplified representation of the pathways and effectors involved with arginine metabolism in *P. aeruginosa*. Mutants lacking the enzymes and proteins highlighted in green were selected for this study. Only relevant intermediates and genes are indicated.

Previous study found that oxygen availability, pH and NaCl play an important role in AaaA activity and biofilm formation(253). For future studies, these conditions should also be tested with the mutants investigated in this study. Recent study also found environmental conditions such as arginine, nitrate, glutamine, cell density and biofilm growth could influence AaaA via the identified putative regulator binding sites in the promoter of *aaaA*(253). For future study, all these environmental conditions should also be tested in parallel for all reporters used in this study with appropriate controls. It seems like AaaA is required in low nitrate, low oxygen, and mid to high cell densities, while arginine induces a positive feedback loop(253). The relationship between RpoN, NtrC, FleQ and MvaU/T could be further studied through site-directed mutagenesis and qRT-PCR, or the creation of double and triple mutants into which the reporters are introduced. In addition, microarrays, RNA-Seq, high-throughput sequencing technologies and Quantitative reverse transcription PCR (RT-qPCR) can be used to investigate transcriptional study(468).

References

1. Costa TRD, Felisberto-Rodrigues C, Meir A, Prevost MS, Redzej A, Trokter M, et al. Secretion systems in Gram-negative bacteria: structural and mechanistic insights. Nat Rev Microbiol. 2015;13(6):343–59.

2. Green ER, Mecsas J. Bacterial Secretion Systems–An overview. Microbiol Spectr. 2016;4(1).

3. Wooldridge K. Bacterial secreted proteins: secretory mechanisms and role in pathogenesis. Horizon Scientific Press; 2009.

4. Gerlach RG, Hensel M. Protein secretion systems and adhesins: the molecular armory of Gram-negative pathogens. Int J Med Microbiol. 2007;297(6):401–15.

5. Natale P, Brüser T, Driessen AJM. Sec-and Tat-mediated protein secretion across the bacterial cytoplasmic membrane—distinct translocases and mechanisms. Biochim Biophys Acta (BBA)-Biomembranes. 2008;1778(9):1735–56.

6. Papanikou E, Karamanou S, Economou A. Bacterial protein secretion through the translocase nanomachine. Nat Rev Microbiol. 2007;5(11):839.

7. Robinson C, Bolhuis A. Tat-dependent protein targeting in prokaryotes and chloroplasts. Biochim Biophys Acta (BBA)-Molecular Cell Res. 2004;1694(1–3):135–47.

8. Muheim C. Antibiotic uptake in Gram-negative bacteria. Department of Biochemistry and Biophysics, Stockholm University; 2017.

9. Randall LL, Hardy SJS. SecB, one small chaperone in the complex milieu of the cell. Cell Mol Life Sci C. 2002;59(10):1617–23.

10. Hartl F-U, Lecker S, Schiebel E, Hendrick JP, Wickner W. The binding cascade of SecB to SecA to SecYE mediates preprotein targeting to the E. coli plasma membrane. Cell. 1990;63(2):269–79.

11. Mogensen JE, Otzen DE. Interactions between folding factors and bacterial outer membrane proteins. Mol Microbiol. 2005;57(2):326–46.

12. Luirink J, Sinning I. SRP-mediated protein targeting: structure and function revisited. Biochim Biophys Acta (BBA)-Molecular Cell Res. 2004;1694(1–3):17–35.

13. Sijbrandi R, Urbanus ML, Corinne M, Bernstein HD, Oudega B, Otto BR, et al. Signal recognition particle (SRP)-mediated targeting and Sec-dependent translocation of an extracellular Escherichia coli protein. J Biol Chem. 2003;278(7):4654–9.

14. Paetzel M, Karla A, Strynadka NCJ, Dalbey RE. Signal peptidases. Chem Rev. 2002;102(12):4549–80.

15. Berks BC, Palmer T, Sargent F. Protein targeting by the bacterial twin-arginine translocation (Tat) pathway. Curr Opin Microbiol. 2005;8(2):174–81.

16. Sargent F, Stanley NR, Berks BC, Palmer T. Sec-independent protein translocation in Escherichia coli A distinct and pivotal role for the TatB protein. J Biol Chem. 1999;274(51):36073–82.

17. Pop O, Martin U, Abel C, Müller JP. The twin-arginine signal peptide of PhoD and the TatAd/Cd proteins of Bacillus subtilis form an autonomous Tat translocation system. J Biol Chem. 2002;277(5):3268–73.

18. Müller M. Twin-arginine-specific protein export in Escherichia coli. Res Microbiol. 2005;156(2):131–6.

19. Ochsner UA, Snyder A, Vasil AI, Vasil ML. Effects of the twin-arginine translocase on secretion of virulence factors, stress response, and pathogenesis. Proc Natl Acad Sci. 2002;99(12):8312–7.

20. Lavander M, Ericsson SK, Bröms JE, Forsberg Å. The twin arginine translocation system is essential for virulence of Yersinia pseudotuberculosis. Infect Immun. 2006;74(3):1768–76.

21. Pradel N, Ye C, Livrelli V, Xu J, Joly B, Wu L-F. Contribution of the twin arginine translocation system to the virulence of enterohemorrhagic Escherichia coli O157: H7. Infect Immun. 2003;71(9):4908–16.

22. Rossier O, Cianciotto NP. The Legionella pneumophila tatB gene facilitates

secretion of phospholipase C, growth under iron-limiting conditions, and intracellular infection. Infect Immun. 2005;73(4):2020–32.

23. McDonough JA, McCann JR, Tekippe EM, Silverman JS, Rigel NW, Braunstein M. Identification of functional Tat signal sequences in Mycobacterium tuberculosis proteins. J Bacteriol. 2008;190(19):6428–38.

24. Songer JG. Bacterial phospholipases and their role in virulence. Trends Microbiol. 1997;5(4):156–61.

25. Buchanan G, Maillard J, Nabuurs SB, Richardson DJ, Palmer T, Sargent F. Features of a twin-arginine signal peptide required for recognition by a Tat proofreading chaperone. FEBS Lett. 2008;582(29):3979–84.

26. Abby SS, Cury J, Guglielmini J, Néron B, Touchon M, Rocha EPC. Identification of protein secretion systems in bacterial genomes. Sci Rep. 2016;6.

27. Chagnot C, ZORGANI MA, Astruc T, Desvaux M. Proteinaceous determinants of surface colonization in bacteria: bacterial adhesion and biofilm formation from a protein secretion perspective. Front Microbiol. 2013;4:303.

28. Leyton DL, Rossiter AE, Henderson IR. From self sufficiency to dependence: mechanisms and factors important for autotransporter biogenesis. Nat Rev Microbiol. 2012;10(3):213–25.

29. Gawarzewski I, Smits SHJ, Schmitt L, Jose J. Structural comparison of the transport units of type V secretion systems. Biol Chem. 2013;394(11):1385–98.

30. Leo JC, Grin I, Linke D. Type V secretion: mechanism (s) of autotransport through the bacterial outer membrane. Phil Trans R Soc B. 2012;367(1592):1088–101.

31. McBride MJ, Zhu Y. Gliding motility and Por secretion system genes are widespread among members of the phylum Bacteroidetes. J Bacteriol. 2013;195(2):270–8.

32. Gibson DL, White AP, Rajotte CM, Kay WW. AgfC and AgfE facilitate

extracellular thin aggregative fimbriae synthesis in Salmonella enteritidis. Microbiology. 2007;153(4):1131–40.

33. Lasica AM, Ksiazek M, Madej M, Potempa J. The type IX secretion system (T9SS): highlights and recent insights into its structure and function. Front Cell Infect Microbiol. 2017;7:215.

34. Thomas S, Holland IB, Schmitt L. The type 1 secretion pathway—the hemolysin system and beyond. Biochim Biophys Acta (BBA)-Molecular Cell Res. 2014;1843(8):1629–41.

35. Symmons MF, Bokma E, Koronakis E, Hughes C, Koronakis V. The assembled structure of a complete tripartite bacterial multidrug efflux pump. Proc Natl Acad Sci. 2009;106(17):7173–8.

36. Delepelaire P. Type I secretion in gram-negative bacteria. Biochim Biophys Acta (BBA)-Molecular Cell Res. 2004;1694(1–3):149–61.

37. Kanonenberg K, Schwarz CKW, Schmitt L. Type I secretion systems–a story of appendices. Res Microbiol. 2013;164(6):596–604.

38. Pimenta AL, Young J, Holland IB, Blight MA. Antibody analysis of the localisation, expression and stability of HlyD, the MFP component of the E. coli haemolysin translocator. Mol Gen Genet MGG. 1999;261(1):122–32.

39. Balakrishnan L, Hughes C, Koronakis V. Substrate-triggered recruitment of the TolC channel-tunnel during type I export of hemolysin by Escherichia coli. J Mol Biol. 2001;313(3):501–10.

40. Korotkov K V, Sandkvist M, Hol WGJ. The type II secretion system: biogenesis, molecular architecture and mechanism. Nat Rev Microbiol. 2012;10(5):336.

41. Voulhoux R, Ball G, Ize B, Vasil ML, Lazdunski A, Wu L, et al. Involvement of the twin-arginine translocation system in protein secretion via the type II pathway. EMBO J. 2001;20(23):6735–41.

42. Cianciotto NP. Type II secretion: a protein secretion system for all seasons. Trends Microbiol. 2005;13(12):581–8.

43. Korotkov K V, Gonen T, Hol WGJ. Secretins: dynamic channels for protein transport across membranes. Trends Biochem Sci. 2011;36(8):433–43.

44. Sauvonnet N, Vignon G, Pugsley AP, Gounon P. Pilus formation and protein secretion by the same machinery in Escherichia coli. EMBO J. 2000;19(10):2221–8.

45. Hobbs M, Mattick JS. Common components in the assembly of type 4 fimbriae, DNA transfer systems, filamentous phage and protein-secretion apparatus: a general system for the formation of surface-associated protein complexes. Mol Microbiol. 1993;10(2):233–43.

46. Shevchik VE, Robert-Baudouy J, Condemine G. Specific interaction between OutD, an Erwinia chrysanthemi outer membrane protein of the general secretory pathway, and secreted proteins. EMBO J. 1997;16(11):3007–16.

47. Sandkvist M, Michel LO, Hough LP, Morales VM, Bagdasarian M, Koomey M, et al. General secretion pathway (eps) genes required for toxin secretion and outer membrane biogenesis in Vibrio cholerae. J Bacteriol. 1997;179(22):6994–7003.

48. Lu H-M, Lory S. A specific targeting domain in mature exotoxin A is required for its extracellular secretion from Pseudomonas aeruginosa. EMBO J. 1996;15(2):429–36.

49. Tauschek M, Gorrell RJ, Strugnell RA, Robins-Browne RM. Identification of a protein secretory pathway for the secretion of heat-labile enterotoxin by an enterotoxigenic strain of Escherichia coli. Proc Natl Acad Sci. 2002;99(10):7066–71.

50. Cianciotto NP. Type II secretion and Legionella virulence. In: Molecular Mechanisms in Legionella Pathogenesis. Springer; 2013. p. 81–102.

51. Kulkarni R, Dhakal BK, Slechta ES, Kurtz Z, Mulvey MA, Thanassi DG. Roles of putative type II secretion and type IV pilus systems in the virulence of uropathogenic Escherichia coli. PLoS One. 2009;4(3).

52. Lathem WW, Grys TE, Witowski SE, Torres AG, Kaper JB, Tarr PI, et al. StcE, a metalloprotease secreted by Escherichia coli O157: H7, specifically

cleaves C1 esterase inhibitor. Mol Microbiol. 2002;45(2):277–88.

53. Pugsley AP, Chapon C, Schwartz M. Extracellular pullulanase of Klebsiella pneumoniae is a lipoprotein. J Bacteriol. 1986;166(3):1083–8.

54. Jiang B, Howard SP. The Aeromonas hydrophila exeE gene, required both for protein secretion and normal outer membrane biogenesis, is a member of a general secretion pathway. Mol Microbiol. 1992;6(10):1351–61.

55. He SY, Lindeberg M, Chatterjee AK, Collmer A. Cloned Erwinia chrysanthemi out genes enable Escherichia coli to selectively secrete a diverse family of heterologous proteins to its milieu. Proc Natl Acad Sci. 1991;88(3):1079–83.

56. Abby SS, Rocha EPC. The non-flagellar type III secretion system evolved from the bacterial flagellum and diversified into host-cell adapted systems. PLoS Genet. 2012;8(9):e1002983.

57. Abrusci P, McDowell MA, Lea SM, Johnson S. Building a secreting nanomachine: a structural overview of the T3SS. Curr Opin Struct Biol. 2014;25:111–7.

58. Burkinshaw BJ, Strynadka NCJ. Assembly and structure of the T3SS. Biochim Biophys Acta (BBA)-Molecular Cell Res. 2014;1843(8):1649–63.

59. Troisfontaines P, Cornelis GR. Type III secretion: more systems than you think. Physiology. 2005;20(5):326–39.

60. Deane JE, Cordes FS, Roversi P, Johnson S, Kenjale R, Picking WD, et al. Expression, purification, crystallization and preliminary crystallographic analysis of MxiH, a subunit of the Shigella flexneri type III secretion system needle. Acta Crystallogr Sect F Struct Biol Cryst Commun. 2006;62(3):302–5.

61. Dohlich K, Zumsteg AB, Goosmann C, Kolbe M. A substrate-fusion protein is trapped inside the type III secretion system channel in Shigella flexneri. PLoS Pathog. 2014;10(1).

62. Radics J, Königsmaier L, Marlovits TC. Structure of a pathogenic type 3 secretion system in action. Nat Struct Mol Biol. 2014;21(1):82–7.

63. Kubori T, Matsushima Y, Nakamura D, Uralil J, Lara-Tejero M, Sukhan A, et al. Supramolecular structure of the Salmonella typhimurium type III protein secretion system. Science (80-). 1998;280(5363):602–5.

64. Price SB, Cowan C, Perry RD, Straley SC. The Yersinia pestis V antigen is a regulatory protein necessary for Ca2 (+)-dependent growth and maximal expression of low-Ca2+ response virulence genes. J Bacteriol. 1991;173(8):2649–57.

65. Picking WL, Nishioka H, Hearn PD, Baxter MA, Harrington AT, Blocker A, et al. IpaD of Shigella flexneri is independently required for regulation of Ipa protein secretion and efficient insertion of IpaB and IpaC into host membranes. Infect Immun. 2005;73(3):1432–40.

66. Holmström A, Olsson J, Cherepanov P, Maier E, Nordfelth R, Pettersson J, et al. LcrV is a channel size-determining component of the Yop effector translocon of Yersinia. Mol Microbiol. 2001;39(3):620–32.

67. Håkansson S, Bergman T, Vanooteghem J-C, Cornelis G, Wolf-Watz H. YopB and YopD constitute a novel class of Yersinia Yop proteins. Infect Immun. 1993;61(1):71–80.

68. Håkansson S, Schesser K, Persson C, Galyov EE, Rosqvist R, Homblé F, et al. The YopB protein of Yersinia pseudotuberculosis is essential for the translocation of Yop effector proteins across the target cell plasma membrane and displays a contact-dependent membrane disrupting activity. EMBO J. 1996;15(21):5812–23.

69. Akopyan K, Edgren T, Wang-Edgren H, Rosqvist R, Fahlgren A, Wolf-Watz H, et al. Translocation of surface-localized effectors in type III secretion. Proc Natl Acad Sci. 2011;108(4):1639–44.

70. Edgren T, Forsberg Å, Rosqvist R, Wolf-Watz H. Type III secretion in Yersinia: injectisome or not? PLoS Pathog. 2012;8(5).

71. Pinaud L, Sansonetti PJ, Phalipon A. Host cell targeting by enteropathogenic bacteria T3SS effectors. Trends Microbiol. 2018;26(4):266–83.

72. Cascales E, Christie PJ. The versatile bacterial type IV secretion systems.

Nat Rev Microbiol. 2003;1(2):137–49.

73. Lessl M, Lanka E. Common mechanisms in bacterial conjugation and Ti-mediated T-DNA transfer to plant cells. Cell. 1994;77(3):321–4.

74. Fronzes R, Christie PJ, Waksman G. The structural biology of type IV secretion systems. Nat Rev Microbiol. 2009;7(10):703–14.

75. Atmakuri K, Cascales E, Christie PJ. Energetic components VirD4, VirB11 and VirB4 mediate early DNA transfer reactions required for bacterial type IV secretion. Mol Microbiol. 2004;54(5):1199–211.

76. Babić A, Lindner AB, Vulić M, Stewart EJ, Radman M. Direct visualization of horizontal gene transfer. Science (80-). 2008;319(5869):1533–6.

77. Mougous JD, Cuff ME, Raunser S, Shen A, Zhou M, Gifford CA, et al. A virulence locus of Pseudomonas aeruginosa encodes a protein secretion apparatus. Science (80-). 2006;312(5779):1526–30.

78. Russell AB, Peterson SB, Mougous JD. Type VI secretion system effectors: poisons with a purpose. Nat Rev Microbiol. 2014;12(2):137–48.

79. Russell AB, Hood RD, Bui NK, LeRoux M, Vollmer W, Mougous JD. Type VI secretion delivers bacteriolytic effectors to target cells. Nature. 2011;475(7356):343–7.

80. English G, Trunk K, Rao VA, Srikannathasan V, Hunter WN, Coulthurst SJ. New secreted toxins and immunity proteins encoded within the T ype VI secretion system gene cluster of S erratia marcescens. Mol Microbiol. 2012;86(4):921–36.

81. Pukatzki S, Ma AT, Revel AT, Sturtevant D, Mekalanos JJ. Type VI secretion system translocates a phage tail spike-like protein into target cells where it cross-links actin. Proc Natl Acad Sci. 2007;104(39):15508–13.

82. Jana B, Salomon D. Type VI secretion system: a modular toolkit for bacterial dominance. Future Microbiol. 2019;14(16):1451–63.

83. Pohlner J, Halter R, Beyreuther K, Meyer TF. Gene structure and

extracellular secretion of Neisseria gonorrhoeae IgA protease. Nature. 1986;325(6103):458–62.

84. van Ulsen P, ur Rahman S, Jong WSP, Daleke-Schermerhorn MH, Luirink J. Type V secretion: from biogenesis to biotechnology. Biochim Biophys Acta (BBA)-Molecular Cell Res. 2014;1843(8):1592–611.

85. Klauser T, Pohlner J, Meyer TF. The secretion pathway of IgA protease-type proteins in gram-negative bacteria. Bioessays. 1993;15(12):799–805.

86. Ruiz N, Kahne D, Silhavy TJ. Advances in understanding bacterial outer-membrane biogenesis. Nat Rev Microbiol. 2006;4(1):57–66.

87. Meuskens I, Saragliadis A, Leo JC, Linke D. Type V secretion systems: an overview of passenger domain functions. Front Microbiol. 2019;10.

88. Grijpstra J, Arenas J, Rutten L, Tommassen J. Autotransporter secretion: varying on a theme. Res Microbiol. 2013;164(6):562–82.

89. Wells TJ, Tree JJ, Ulett GC, Schembri MA. Autotransporter proteins: novel targets at the bacterial cell surface. FEMS Microbiol Lett. 2007;274(2):163–72.

90. Ruiz-Perez F, Nataro JP. Bacterial serine proteases secreted by the autotransporter pathway: classification, specificity, and role in virulence. Cell Mol life Sci. 2014;71(5):745–70.

91. Yen M-R, Peabody CR, Partovi SM, Zhai Y, Tseng Y-H, Saier Jr MH. Protein-translocating outer membrane porins of Gram-negative bacteria. Biochim Biophys Acta (BBA)-Biomembranes. 2002;1562(1–2):6–31.

92. van den Berg B. Crystal structure of a full-length autotransporter. J Mol Biol. 2010;396(3):627–33.

93. Henderson IR, Nataro JP. Virulence functions of autotransporter proteins. Infect Immun. 2001;69(3):1231–43.

94. Henderson IR, Navarro-Garcia F, Desvaux M, Fernandez RC, Ala'Aldeen D. Type V protein secretion pathway: the autotransporter story. Microbiol Mol

Biol Rev. 2004;68(4):692–744.

95. Jose J, Jähnig F, Meyer TF. Common structural features of IgA1 protease-like outer membrane protein autotransporters. Mol Microbiol. 1995;18(02):378–80.

96. Tsirigotaki A, De Geyter J, Šoštaric N, Economou A, Karamanou S. Protein export through the bacterial Sec pathway. Nat Rev Microbiol. 2017;15(1):21.

97. Herskovits AA, Bochkareva ES, Bibi E. New prospects in studying the bacterial signal recognition particle pathway. Mol Microbiol. 2000;38(5):927–39.

98. Henderson IR, Navarro-Garcia F, Nataro JP. The great escape: structure and function of the autotransporter proteins. Trends Microbiol. 1998;6(9):370–8.

99. Baclayon M, van Ulsen P, Mouhib H, Shabestari MH, Verzijden T, Abeln S, et al. Mechanical Unfolding of an Autotransporter Passenger Protein Reveals the Secretion Starting Point and Processive Transport Intermediates. ACS Nano. 2016;

100. Heinz E, Stubenrauch CJ, Grinter R, Croft NP, Purcell AW, Strugnell RA, et al. Conserved features in the structure, mechanism and biogenesis of the inverse autotransporter protein family. Genome Biol Evol. 2016;evw112.

101. Yen YT, Kostakioti M, Henderson IR, Stathopoulos C. Common themes and variations in serine protease autotransporters. Trends Microbiol. 2008;16(8):370–9.

102. Koiwai K, Hartmann MD, Linke D, Lupas AN, Hori K. Structural Basis for Toughness and Flexibility in the C-terminal Passenger Domain of an Acinetobacter Trimeric Autotransporter Adhesin. J Biol Chem. 2016;291(8):3705–24.

103. Fan E, Chauhan N, Udatha DG, Leo JC, Linke D. Type V Secretion Systems in Bacteria. Microbiol Spectr. 2016;4(1).

104. Killackey SA, Sorbara MT, Girardin SE. Cellular aspects of Shigella

pathogenesis: Focus on the manipulation of host cell processes. Front Cell Infect Microbiol. 2016;6.

105. Charbonneau M-È, Berthiaume F, Mourez M. Proteolytic processing is not essential for multiple functions of the Escherichia coli autotransporter adhesin involved in diffuse adherence (AIDA-I). J Bacteriol. 2006;188(24):8504–12.

106. Barnard TJ, Dautin N, Lukacik P, Bernstein HD, Buchanan SK. Autotransporter structure reveals intra-barrel cleavage followed by conformational changes. Nat Struct Mol Biol. 2007;14(12):1214–20.

107. Dautin N, Bernstein HD. Protein secretion in gram-negative bacteria via the autotransporter pathway. Annu Rev Microbiol. 2007;61:89–112.

108. Hendrixson DR, De La Morena ML, Stathopoulos C, St Geme III JW. Structural determinants of processing and secretion of the Haemophilus influenzae Hap protein. Mol Microbiol. 1997;26(3):505–18.

109. Coutte L, Antoine R, Drobecq H, Locht C, Jacob-Dubuisson F. Subtilisin-like autotransporter serves as maturation protease in a bacterial secretion pathway. EMBO J. 2001;20(18):5040–8.

110. Egile C, d'Hauteville H, Parsot C, Sansonetti PJ. SopA, the outer membrane protease responsible for polar localization of IcsA in Shigella flexneri. Mol Microbiol. 1997;23(5):1063–73.

111. Shere KD, Sallustio S, Manessis A, D'Aversa TG, Goldberg MB. Disruption of IcsP, the major Shigella protease that cleaves IcsA, accelerates actin-based motility. Mol Microbiol. 1997;25(3):451–62.

112. Bernstein HD. Type V secretion: the autotransporter and two-partner secretion pathways. EcoSal Plus. 2010;4(1).

113. Ashawesh M. Investigation of the spiral secretion pattern of the serine protease autotransporter, EspC using innovative fluorescent labelling approaches. University of Nottingham; 2016.

114. Baud C, Hodak H, Willery E, Drobecq H, Locht C, Jamin M, et al. Role of DegP for two-partner secretion in Bordetella. Mol Microbiol.

2009;74(2):315–29.

115. Ieva R, Bernstein HD. Interaction of an autotransporter passenger domain with BamA during its translocation across the bacterial outer membrane. Proc Natl Acad Sci. 2009;106(45):19120–5.

116. Oberhettinger P, Schütz M, Leo JC, Heinz N, Berger J, Autenrieth IB, et al. Intimin and invasin export their C-terminus to the bacterial cell surface using an inverse mechanism compared to classical autotransport. PLoS One. 2012;7(10).

117. Pavlova O, Peterson JH, Ieva R, Bernstein HD. Mechanistic link between β barrel assembly and the initiation of autotransporter secretion. Proc Natl Acad Sci. 2013;110(10):E938–47.

118. Weirich J, Bräutigam C, Mühlenkamp M, Franz-Wachtel M, Macek B, Meuskens I, et al. Identifying components required for OMP biogenesis as novel targets for antiinfective drugs. Virulence. 2017;8(7):1170–88.

119. Jain S, Goldberg MB. Requirement for YaeT in the outer membrane assembly of autotransporter proteins. J Bacteriol. 2007;189(14):5393–8.

120. Knowles TJ, Scott-Tucker A, Overduin M, Henderson IR. Membrane protein architects: the role of the BAM complex in outer membrane protein assembly. Nat Rev Microbiol. 2009;7(3):206–14.

121. Leo JC, Linke D. A unified model for BAM function that takes into account type Vc secretion and species differences in BAM composition. AIMS Microbiol. 2018;4(3):455.

122. Oliver DC, Huang G, Nodel E, Pleasance S, Fernandez RC. A conserved region within the Bordetella pertussis autotransporter BrkA is necessary for folding of its passenger domain. Mol Microbiol. 2003;47(5):1367–83.

123. Desvaux M, Parham NJ, Henderson IR. Type V protein secretion: simplicity gone awry? Curr Issues Mol Biol. 2004;6:111–24.

124. Choi PS, Bernstein HD. Sequential translocation of an Escherchia coli two-partner secretion pathway exoprotein across the inner and outer membranes. Mol Microbiol. 2010;75(2):440–51.

125. Kang'ethe W, Bernstein HD. Charge-dependent secretion of an intrinsically disordered protein via the autotransporter pathway. Proc Natl Acad Sci. 2013;110(45):E4246–55.

126. Junker M, Schuster CC, McDonnell A V, Sorg KA, Finn MC, Berger B, et al. Pertactin β-helix folding mechanism suggests common themes for the secretion and folding of autotransporter proteins. Proc Natl Acad Sci. 2006;103(13):4918–23.

127. Junker M, Besingi RN, Clark PL. Vectorial transport and folding of an autotransporter virulence protein during outer membrane secretion. Mol Microbiol. 2009;71(5):1323–32.

128. Peterson JH, Tian P, Ieva R, Dautin N, Bernstein HD. Secretion of a bacterial virulence factor is driven by the folding of a C-terminal segment. Proc Natl Acad Sci. 2010;107(41):17739–44.

129. Soprova Z, Sauri A, van Ulsen P, Tame JRH, den Blaauwen T, Jong WSP, et al. A conserved aromatic residue in the autochaperone domain of the autotransporter Hbp is critical for initiation of outer membrane translocation. J Biol Chem. 2010;285(49):38224–33.

130. Chevalier N, Moser M, Koch H-G, Schimz K-L, Willery E, Locht C, et al. Membrane targeting of a bacterial virulence factor harbouring an extended signal peptide. J Mol Microbiol Biotechnol. 2004;8(1):7–18.

131. Jacob-Dubuisson F, Guérin J, Baelen S, Clantin B. Two-partner secretion: as simple as it sounds? Res Microbiol. 2013;164(6):583–95.

132. Kajava A V, Cheng N, Cleaver R, Kessel M, Simon MN, Willery E, et al. Beta-helix model for the filamentous haemagglutinin adhesin of Bordetella pertussis and related bacterial secretory proteins. Mol Microbiol. 2001;42(2):279–92.

133. Delattre A, Clantin B, Saint N, Locht C, Villeret V, Jacob-Dubuisson F. Functional importance of a conserved sequence motif in FhaC, a prototypic member of the TpsB/Omp85 superfamily. FEBS J. 2010;277(22):4755–65.

134. Guérin J, Bigot S, Schneider R, Buchanan SK, Jacob-Dubuisson F. Two-partner secretion: combining efficiency and simplicity in the secretion of

large proteins for bacteria-host and bacteria-bacteria interactions. Front Cell Infect Microbiol. 2017;7:148.

135. Garnett JA, Muhl D, Douse CH, Hui K, Busch A, Omisore A, et al. Structure–function analysis reveals that the Pseudomonas aeruginosa Tps4 two-partner secretion system is involved in CupB5 translocation. Protein Sci. 2015;24(5):670–87.

136. Baud C, Guérin J, Petit E, Lesne E, Dupré E, Locht C, et al. Translocation path of a substrate protein through its Omp85 transporter. Nat Commun. 2014;5(1):1–9.

137. Norell D, Heuck A, Tran-Thi T-A, Götzke H, Jacob-Dubuisson F, Clausen T, et al. Versatile in vitro system to study translocation and functional integration of bacterial outer membrane proteins. Nat Commun. 2014;5(1):1–9.

138. Hodak H, Jacob-Dubuisson F. Current challenges in autotransport and two-partner protein secretion pathways. Res Microbiol. 2007;158(8–9):631–7.

139. Clantin B, Hodak H, Willery E, Locht C, Jacob-Dubuisson F, Villeret V. The crystal structure of filamentous hemagglutinin secretion domain and its implications for the two-partner secretion pathway. Proc Natl Acad Sci. 2004;101(16):6194–9.

140. Clantin B, Delattre A-S, Rucktooa P, Saint N, Méli AC, Locht C, et al. Structure of the membrane protein FhaC: a member of the Omp85-TpsB transporter superfamily. Science (80-). 2007;317(5840):957–61.

141. Mühlenkamp M, Oberhettinger P, Leo JC, Linke D, Schütz MS. Yersinia adhesin A (YadA)–beauty & beast. Int J Med Microbiol. 2015;305(2):252–8.

142. Hoiczyk E, Roggenkamp A, Reichenbecher M, Lupas A, Heesemann J. Structure and sequence analysis of Yersinia YadA and Moraxella UspAs reveal a novel class of adhesins. EMBO J. 2000;19(22):5989–99.

143. Linke D, Riess T, Autenrieth IB, Lupas A, Kempf VAJ. Trimeric autotransporter adhesins: variable structure, common function. Trends Microbiol. 2006;14(6):264–70.

144. Wollmann P, Zeth K, Lupas AN, Linke D. Purification of the YadA membrane anchor for secondary structure analysis and crystallization. Int J Biol Macromol. 2006;39(1–3):3–9.

145. Szczesny P, Lupas A. Domain annotation of trimeric autotransporter adhesins—daTAA. Bioinformatics. 2008;24(10):1251–6.

146. Mikula KM, Leo JC, Łyskowski A, Kedracka-Krok S, Pirog A, Goldman A. The translocation domain in trimeric autotransporter adhesins is necessary and sufficient for trimerization and autotransportation. J Bacteriol. 2012;194(4):827–38.

147. Chauhan N, Hatlem D, Orwick-Rydmark M, Schneider K, Floetenmeyer M, van Rossum B, et al. Insights into the autotransport process of a trimeric autotransporter, Yersinia Adhesin A (YadA). Mol Microbiol. 2019;111(3):844–62.

148. Waksman G, Hultgren SJ. Structural biology of the chaperone–usher pathway of pilus biogenesis. Nat Rev Microbiol. 2009;7(11):765–74.

149. Bishop K. Dissecting protein-protein interactions facilitating secretion of the virulence factor EspC by enteropathogenic Escherichia coli. University of Nottingham; 2009.

150. Surana NK, Cutter D, Barenkamp SJ, Geme JWS. The Haemophilus influenzae Hia autotransporter contains an unusually short trimeric translocator domain. J Biol Chem. 2004;279(15):14679–85.

151. Salacha R, Kovačić F, Brochier-Armanet C, Wilhelm S, Tommassen J, Filloux A, et al. The Pseudomonas aeruginosa patatin-like protein PlpD is the archetype of a novel Type V secretion system. Environ Microbiol. 2010;12(6):1498–512.

152. Casasanta MA, Yoo CC, Smith HB, Duncan AJ, Cochrane K, Varano AC, et al. A chemical and biological toolbox for Type Vd secretion: Characterization of the phospholipase A1 autotransporter FplA from Fusobacterium nucleatum. J Biol Chem. 2017;292(49):20240–54.

153. Emsley P, Charles IG, Fairweather NF, Isaacs NW. Structure of Bordetella pertussis virulence factor P. 69 pertactin. Nature. 1996;381(6577):90–2.

154. da Mata Madeira PV, Zouhir S, Basso P, Neves D, Laubier A, Salacha R, et al. Structural basis of lipid targeting and destruction by the type V secretion system of Pseudomonas aeruginosa. J Mol Biol. 2016;428(9):1790–803.

155. Leo JC, Oberhettinger P, Schütz M, Linke D. The inverse autotransporter family: intimin, invasin and related proteins. Int J Med Microbiol. 2015;305(2):276–82.

156. Oberhettinger P, Leo JC, Linke D, Autenrieth IB, Schütz MS. The inverse autotransporter intimin exports its passenger domain via a hairpin intermediate. J Biol Chem. 2015;290(3):1837–49.

157. Leo JC, Oberhettinger P, Yoshimoto S, Udatha DG, Morth JP, Schütz M, et al. Secretion of the intimin passenger domain is driven by protein folding. J Biol Chem. 2016;291(38):20096–112.

158. Leo JC, Oberhettinger P, Chaubey M, Schütz M, Kühner D, Bertsche U, et al. The I ntimin periplasmic domain mediates dimerisation and binding to peptidoglycan. Mol Microbiol. 2015;95(1):80–100.

159. Coppens F, Castaldo G, Debraekeleer A, Subedi S, Moonens K, Lo A, et al. Hop-family Helicobacter outer membrane adhesins form a novel class of Type 5-like secretion proteins with an interrupted β-barrel domain. Mol Microbiol. 2018;110(1):33–46.

160. Lai Y, Rosenshine I, Leong JM, Frankel G. Intimate host attachment: enteropathogenic and enterohaemorrhagic Escherichia coli. Cell Microbiol. 2013/08/10. 2013;15(11):1796–808.

161. Conway PL. Microbial ecology of the human large intestine. Hum Colon Bact role Nutr Physiol Pathol. 1995;1–24.

162. Kaper JB, Nataro JP, Mobley HLT. Pathogenic escherichia coli. Nat Rev Microbiol. 2004;2(2):123–40.

163. Croxen MA, Law RJ, Scholz R, Keeney KM, Wlodarska M, Finlay BB. Recent advances in understanding enteric pathogenic Escherichia coli. Clin Microbiol Rev. 2013/10/05. 2013;26(4):822–80.

164. Robins-Browne RM. Traditional enteropathogenic Escherichia coli of infantile diarrhea. Rev Infect Dis. 1987;9(1):28–53.

165. Bray J. Isolation of antigenically homogeneous strains of Bact. coli neapolitanum from summer diarrhoea of infants. J Pathol Bacteriol. 1945;57(2):239–47.

166. Low N. Infectious Disease Epidemiology: Theory and Practice: KE Nelson, CM Williams, NMH Graham (eds) MD, USA: Aspen Publishers Inc. 2001, pp. 748, US $79.00, ISBN: 0-8342-1766-X. Int J Epidemiol. 2001;30(1):186-a-186-a.

167. Donnenberg MS, Kaper JB. Enteropathogenic Escherichia coli. Infect Immun. 1992;60(10):3953.

168. Chen Z, Cheng H, Pan W, Zheng J, Li D, Lin F, et al. Comparative genome and evolution analysis of the locus of enterocyte effacement from enteropathogenic Escherichia coli Deng and its transcriptional response to ciprofloxacin. J Med Microbiol. 2018;67(9):1368–82.

169. Croxen MA, Finlay BB. Molecular mechanisms of Escherichia coli pathogenicity. Nat Rev Microbiol. 2009/12/08. 2010;8(1):26–38.

170. Bäumler AJ. The record of horizontal gene transfer in Salmonella. Trends Microbiol. 1997;5(8):318–22.

171. Frost LS, Leplae R, Summers AO, Toussaint A. Mobile genetic elements: the agents of open source evolution. Nat Rev Microbiol. 2005/09/03. 2005;3(9):722–32.

172. Levine MM, Kotloff KL, Nataro JP, Muhsen K. The Global Enteric Multicenter Study (GEMS): impetus, rationale, and genesis. Clin Infect Dis. 2012;55(suppl 4):S215–24.

173. Leimbach A, Hacker J, Dobrindt U. E. coli as an all-rounder: the thin line between commensalism and pathogenicity. Curr Top Microbiol Immunol. 2013/01/24. 2013;358:3–32.

174. Touchon M, Hoede C, Tenaillon O, Barbe V, Baeriswyl S, Bidet P, et al. Organised genome dynamics in the Escherichia coli species results in

highly diverse adaptive paths. PLoS Genet. 2009;5(1):e1000344.

175. Qadri F, Svennerholm A-M, Faruque ASG, Sack RB. Enterotoxigenic Escherichia coli in developing countries: epidemiology, microbiology, clinical features, treatment, and prevention. Clin Microbiol Rev. 2005;18(3):465–83.

176. Tenaillon O, Skurnik D, Picard B, Denamur E. The population genetics of commensal Escherichia coli. Nat Rev Microbiol. 2010;8(3):207–17.

177. Escobar-Páramo P, Clermont O, Blanc-Potard A-B, Bui H, Le Bouguénec C, Denamur E. A specific genetic background is required for acquisition and expression of virulence factors in Escherichia coli. Mol Biol Evol. 2004;21(6):1085–94.

178. Robins-Browne RM. Traditional enteropathogenic Escherichia coli of infantile diarrhea. Rev Infect Dis. 1987/01/01. 1987;9(1):28–53.

179. Kaper JB, Nataro JP, Mobley HL. Pathogenic Escherichia coli. Nat Rev Microbiol. 2004/03/26. 2004;2(2):123–40.

180. Lai Y, Rosenshine I, Leong JM, Frankel G. Intimate host attachment: enteropathogenic and enterohaemorrhagic Escherichia coli. Cell Microbiol. 2013;15(11):1796–808.

181. Nataro JP, Kaper JB. Diarrheagenic escherichia coli. Clin Microbiol Rev. 1998;11(1):142–201.

182. Russo TA, Johnson JR. Proposal for a new inclusive designation for extraintestinal pathogenic isolates of Escherichia coli: ExPEC. J Infect Dis. 2000;181(5):1753–4.

183. Servin AL. Pathogenesis of human diffusely adhering Escherichia coli expressing Afa/Dr adhesins (Afa/Dr DAEC): current insights and future challenges. Clin Microbiol Rev. 2014/10/04. 2014;27(4):823–69.

184. Iguchi A, Thomson NR, Ogura Y, Saunders D, Ooka T, Henderson IR, et al. Complete genome sequence and comparative genome analysis of enteropathogenic Escherichia coli O127:H6 strain E2348/69. J Bacteriol. 2008/10/28. 2009;191(1):347–54.

185. Clarke SC, Haigh RD, Freestone PP, Williams PH. Virulence of enteropathogenic Escherichia coli, a global pathogen. Clin Microbiol Rev. 2003/07/15. 2003;16(3):365–78.

186. Ochoa TJ, Barletta F, Contreras C, Mercado E. New insights into the epidemiology of enteropathogenic Escherichia coli infection. Trans R Soc Trop Med Hyg. 2008;102(9):852–6.

187. Levine M, Nalin D, Hornick R, Bergquist E, Waterman D, Young C, et al. Escherichia coli strains that cause diarrhoea but do not produce heat-labile or heat-stable enterotoxins and are non-invasive. Lancet. 1978;311(8074):1119–22.

188. Lee D-W, Gwack J, Youn S-K. Enteropathogenic Escherichia coli Outbreak and its Incubation Period: Is it Short or Long? Osong Public Heal Res Perspect. 2012;3(1):43–7.

189. Baldwin TJ. Pathogenicity of enteropathogenic Escherichia coli. J Med Microbiol. 1998;47(4):283–93.

190. Shulman ST. The history of pediatric infectious diseases. Pediatr Res. 2004;55(1):163–76.

191. Nataro JP, Kaper JB. Diarrheagenic Escherichia coli. Clin Microbiol Rev. 1998/02/11. 1998;11(1):142–201.

192. Maranhão HS, Medeiros MCC, Scaletsky ICA, Fagundes-Neto U, Morais MB. The epidemiological and clinical characteristics and nutritional development of infants with acute diarrhoea, in north–eastern Brazil. Ann Trop Med Parasitol. 2008;102(4):357–65.

193. Donnenberg MS, Donohue-Rolfe A, Keusch GT. Epithelial cell invasion: an overlooked property of enteropathogenic Escherichia coli (EPEC) associated with the EPEC adherence factor. J Infect Dis. 1989/09/01. 1989;160(3):452–9.

194. Francis CL, Jerse AE, Kaper JB, Falkow S. Characterization of interactions of enteropathogenic Escherichia coli O127:H6 with mammalian cells in vitro. J Infect Dis. 1991/10/01. 1991;164(4):693–703.

195. Trabulsi LR, Keller R, Gomes TAT. Typical and atypical Enteropathogenic Escherichia coli.(Synopsis). Emerg Infect Dis. 2002;8(5):508–14.

196. Blanco M, Blanco JE, Dahbi G, Mora A, Alonso MP, Varela G, et al. Typing of intimin (eae) genes from enteropathogenic Escherichia coli (EPEC) isolated from children with diarrhoea in Montevideo, Uruguay: identification of two novel intimin variants (μB and ξR/β2B). J Med Microbiol. 2006;55(9):1165–74.

197. Moon HW, Whipp SC, Argenzio RA, Levine MM, Giannella RA. Attaching and effacing activities of rabbit and human enteropathogenic Escherichia coli in pig and rabbit intestines. Infect Immun. 1983;41(3):1340–51.

198. Nataro JP, Scaletsky ICA, Kaper JB, Levine MM, Trabulsi LR. Plasmid-mediated factors conferring diffuse and localized adherence of enteropathogenic Escherichia coli. Infect Immun. 1985;48(2):378–83.

199. Sanger JM, Chang R, Ashton F, Kaper JB, Sanger JW. Novel form of actin-based motility transports bacteria on the surfaces of infected cells. Cell Motil Cytoskeleton. 1996;34(4):279–87.

200. McDaniel TK, Kaper JB. A cloned pathogenicity island from enteropathogenic Escherichia coli confers the attaching and effacing phenotype on E. coli K-12. Mol Microbiol. 1997;23(2):399–407.

201. Blanco M, Blanco JE, Dahbi G, Alonso MP, Gutierrez AM, Coira MA, et al. Identification of two new intimin types in atypical enteropathogenic" Escherichia coli". Int Microbiol Off J Spanish Soc Microbiol. 2006;9(2):103–10.

202. Elliott SJ, Sperandio V, Girón JA, Shin S, Mellies JL, Wainwright L, et al. The locus of enterocyte effacement (LEE)-encoded regulator controls expression of both LEE-and Non-LEE-encoded virulence factors in enteropathogenic and enterohemorrhagicEscherichia coli. Infect Immun. 2000;68(11):6115–26.

203. Cabrera-Sosa L, Ochoa TJ. Escherichia coli Diarrhea. In: Hunter's Tropical Medicine and Emerging Infectious Diseases. Elsevier; 2020. p. 481–5.

204. Bugarel M, Martin A, Fach P, Beutin L. Virulence gene profiling of

enterohemorrhagic (EHEC) and enteropathogenic (EPEC) Escherichia coli strains: a basis for molecular risk assessment of typical and atypical EPEC strains. BMC Microbiol. 2011;11(1):142.

205. Ochoa TJ, Contreras CA. Enteropathogenic E. coli (EPEC) infection in children. Curr Opin Infect Dis. 2011;24(5):478.

206. Goosney DL, de Grado M, Finlay BB. Putting E. coli on a pedestal: a unique system to study signal transduction and the actin cytoskeleton. Trends Cell Biol. 1999;9(1):11–4.

207. Goosney DL, Gruenheid S, Finlay BB. Gut feelings: enteropathogenic E. coli (EPEC) interactions with the host. Annu Rev Cell Dev Biol. 2000;16(1):173–89.

208. Dean P, Kenny B. The effector repertoire of enteropathogenic E. coli: ganging up on the host cell. Curr Opin Microbiol. 2009;12(1):101–9.

209. Klapproth J-MA, Sasaki M, Sherman M, Babbin B, Donnenberg MS, Fernandes PJ, et al. Citrobacter rodentium lifA/efa1 is essential for colonic colonization and crypt cell hyperplasia in vivo. Infect Immun. 2005;73(3):1441–51.

210. Deng W, de Hoog CL, Hong BY, Li Y, Croxen MA, Thomas NA, et al. A comprehensive proteomic analysis of the type III secretome of Citrobacter rodentium. J Biol Chem. 2010;285(9):6790–800.

211. Dean P, Maresca M, Kenny B. EPEC's weapons of mass subversion. Curr Opin Microbiol. 2005;8(1):28–34.

212. Girón JA, Donnenberg MS, Martin WC, Jarvis KG, Kaper JB. Distribution of the bundle-forming pilus structural gene (bfpA) among enteropathogenic Escherichia coli. J Infect Dis. 1993;168(4):1037–41.

213. Cleary J, Lai L-C, Shaw RK, Straatman-Iwanowska A, Donnenberg MS, Frankel G, et al. Enteropathogenic Escherichia coli (EPEC) adhesion to intestinal epithelial cells: role of bundle-forming pili (BFP), EspA filaments and intimin. Microbiology. 2004;150(3):527–38.

214. Schmidt H, Hensel M. Pathogenicity islands in bacterial pathogenesis. Clin

Microbiol Rev. 2006;19(1):257.

215. Elliott SJ, Wainwright LA, McDaniel TK, Jarvis KG, Deng Y, Lai L, et al. The complete sequence of the locus of enterocyte effacement (LEE) from enteropathogenic Escherichia coli E2348/69. Mol Microbiol. 1998;28(1):1–4.

216. Ruano-Gallego D, Álvarez B, Fernández LA. Engineering the controlled assembly of filamentous injectisomes in E. coli K-12 for protein translocation into mammalian cells. ACS Synth Biol. 2015;4(9):1030–41.

217. Müller D, Benz I, Liebchen A, Gallitz I, Karch H, Schmidt MA. Comparative analysis of the locus of enterocyte effacement and its flanking regions. Infect Immun. 2009;77(8):3501–13.

218. Deborah Chen H, Frankel G. Enteropathogenic Escherichia coli: unravelling pathogenesis. FEMS Microbiol Rev. 2005;29(1):83–98.

219. Torres AG, Zhou X, Kaper JB. Adherence of diarrheagenic Escherichia coli strains to epithelial cells. Infect Immun. 2005;73(1):18–29.

220. Jerse AE, Yu J, Tall BD, Kaper JB. A genetic locus of enteropathogenic Escherichia coli necessary for the production of attaching and effacing lesions on tissue culture cells. Proc Natl Acad Sci. 1990;87(20):7839–43.

221. Vallance BA, Finlay BB. Exploitation of host cells by enteropathogenic Escherichia coli. Proc Natl Acad Sci. 2000;97(16):8799–806.

222. Frankel G, Candy DC, Everest P, Dougan G. Characterization of the C-terminal domains of intimin-like proteins of enteropathogenic and enterohemorrhagic Escherichia coli, Citrobacter freundii, and Hafnia alvei. Infect Immun. 1994;62(5):1835–42.

223. Jores J, Rumer L, Kießling S, Kaper JB, Wieler LH. A novel locus of enterocyte effacement (LEE) pathogenicity island inserted at pheV in bovine Shiga toxin-producing Escherichia coli strain O103: H2. FEMS Microbiol Lett. 2001;204(1):75–9.

224. Adu-Bobie J, Frankel G, Bain C, Goncalves AG, Trabulsi LR, Douce G, et al. Detection of intimins α, β, γ, and δ, four intimin derivatives expressed by

attaching and effacing microbial pathogens. J Clin Microbiol. 1998;36(3):662–8.

225. Tarr CL, Whittam TS. Molecular evolution of the intimin gene in O111 clones of pathogenic Escherichia coli. J Bacteriol. 2002;184(2):479–87.

226. Yamamoto D, Hernandes RT, Blanco M, Greune L, Schmidt MA, Carneiro SM, et al. Invasiveness as a putative additional virulence mechanism of some atypical Enteropathogenic Escherichia coli strains with different uncommon intimin types. BMC Microbiol. 2009;9(1):146.

227. Zhang WL, Köhler B, Oswald E, Beutin L, Karch H, Morabito S, et al. Genetic diversity of intimin genes of attaching and effacing Escherichia coli strains. J Clin Microbiol. 2002;40(12):4486–92.

228. Kenny B, DeVinney R, Stein M, Reinscheid DJ, Frey EA, Finlay BB. Enteropathogenic E. coli (EPEC) transfers its receptor for intimate adherence into mammalian cells. Cell. 1997;91(4):511–20.

229. Frankel G, Phillips AD. Attaching effacing Escherichia coli and paradigms of Tir-triggered actin polymerization: getting off the pedestal. Cell Microbiol. 2008;10(3):549–56.

230. Phillips AD, Frankel G. Intimin-mediated tissue specificity in enteropathogenic Escherichia coli interaction with human intestinal organ cultures. J Infect Dis. 2000;181(4):1496–500.

231. Xu Y, Bai X, Zhao A, Zhang W, Ba P, Liu K, et al. Genetic Diversity of Intimin Gene of Atypical Enteropathogenic Escherichia coli Isolated from Human, Animals and Raw Meats in China. PLoS One. 2016;11(3):e0152571.

232. Chen W, Zhang B, Mahony T, Gu W, Rolfe B, Xu ZP. Efficient and Durable Vaccine against Intimin β of Diarrheagenic E. Coli Induced by Clay Nanoparticles. Small. 2016;

233. Abreu AG, Bueris V, Porangaba TM, Sircili MP, Navarro-Garcia F, Elias WP. Autotransporter protein-encoding genes of diarrheagenic Escherichia coli are found in both typical and atypical enteropathogenic E. coli strains. Appl Environ Microbiol. 2013;79(1):411–4.

234. Stein M, Kenny B, Stein MA, Finlay BB. Characterization of EspC, a 110-kilodalton protein secreted by enteropathogenic Escherichia coli which is homologous to members of the immunoglobulin A protease-like family of secreted proteins. J Bacteriol. 1996;178(22):6546–54.

235. Soltani S, Emamie AD, Dastranj M, Farahani A, Davoodabadi A, Mohajeri P. Role of Toxins of Uropathogenic Escherichia coli in Development of Urinary Tract Infection. Br J Pharm Res. 2018;21(1).

236. Drago-Serrano ME, Parra SG, Manjarrez-Hernández HA. EspC, an autotransporter protein secreted by enteropathogenic Escherichia coli (EPEC), displays protease activity on human hemoglobin. FEMS Microbiol Lett. 2006;265(1):35–40.

237. Mellies JL, Navarro-Garcia F, Okeke I, Frederickson J, Nataro JP, Kaper JB. espC pathogenicity island of enteropathogenic Escherichia coli encodes an enterotoxin. Infect Immun. 2001;69(1):315–24.

238. Navarro-Garcia F, Serapio-Palacios A, Vidal JE, Salazar MI, Tapia-Pastrana G. EspC promotes epithelial cell detachment by enteropathogenic Escherichia coli via sequential cleavages of a cytoskeletal protein and then focal adhesion proteins. Infect Immun. 2014;82(6):2255–65.

239. Guignot J, Segura A, Van Nhieu GT. The serine protease EspC from enteropathogenic Escherichia coli regulates pore formation and cytotoxicity mediated by the type III secretion system. PLoS Pathog. 2015;11(7):e1005013.

240. Vidal JE, Navarro-García F. EspC translocation into epithelial cells by enteropathogenic Escherichia coli requires a concerted participation of type V and III secretion systems. Cell Microbiol. 2008;10(10):1975–86.

241. Navarro-Garcia F, Sonnested M, Teter K. Host-toxin interactions involving EspC and Pet, two serine protease autotransporters of the Enterobacteriaceae. Toxins (Basel). 2010;2(5):1134–47.

242. Navarro-García F, Canizalez-Roman A, Sui BQ, Nataro JP, Azamar Y. The serine protease motif of EspC from enteropathogenic Escherichia coli produces epithelial damage by a mechanism different from that of Pet

toxin from enteroaggregative E. coli. Infect Immun. 2004;72(6):3609–21.

243. Wandersman C, Delepelaire P. Bacterial iron sources: from siderophores to hemophores. Annu Rev Microbiol. 2004;58:611–47.

244. Ashawesh M, Markus R, Penfold C, Hardie K. Autotransporter secretion exploits the bacterial actin-homologue. bioRxiv. 2018;305441.

245. Ranava D, Caumont-Sarcos A, Albenne C, Ieva R. Bacterial machineries for the assembly of membrane-embedded β-barrel proteins. FEMS Microbiol Lett. 2018;365(10):fny087.

246. Babu M, Bundalovic-Torma C, Calmettes C, Phanse S, Zhang Q, Jiang Y, et al. Global landscape of cell envelope protein complexes in Escherichia coli. Nat Biotechnol. 2018;36(1):103.

247. Crone S, Vives-Flórez M, Kvich L, Saunders AM, Malone M, Nicolaisen MH, et al. The environmental occurrence of Pseudomonas aeruginosa. APMIS. 2019;

248. Moradali MF, Ghods S, Rehm BHA. Pseudomonas aeruginosa lifestyle: a paradigm for adaptation, survival, and persistence. Front Cell Infect Microbiol. 2017;7:39.

249. Balasubramanian D, Schneper L, Kumari H, Mathee K. A dynamic and intricate regulatory network determines Pseudomonas aeruginosa virulence. Nucleic Acids Res. 2013;41(1):1–20.

250. Jarvis WR, Martone WJ. Predominant pathogens in hospital infections. J Antimicrob Chemother. 1992;29(suppl_A):19–24.

251. Kerr KG, Snelling AM. Pseudomonas aeruginosa: a formidable and ever-present adversary. J Hosp Infect. 2009;73(4):338–44.

252. Mohanty S, Baliyarsingh B, Nayak SK. Antimicrobial Resistance in Pseudomonas aeruginosa: A Concise Review. In: Antimicrobial Resistance. IntechOpen; 2020.

253. Spencer DL. Surviving and thriving in the cystic fibrosis lung: contribution of an arginine specific aminopeptidase to sustained infection by

Pseudomonas aeruginosa. University of Nottingham; 2019.

254. Gellatly SL, Hancock REW. Pseudomonas aeruginosa: new insights into pathogenesis and host defenses. Pathog Dis. 2013;67(3):159–73.

255. Stover CK, Pham XQ, Erwin AL, Mizoguchi SD, Warrener P, Hickey MJ, et al. Complete genome sequence of Pseudomonas aeruginosa PAO1, an opportunistic pathogen. Nature. 2000;406(6799):959.

256. Pang Z, Raudonis R, Glick BR, Lin T-J, Cheng Z. Antibiotic resistance in Pseudomonas aeruginosa: mechanisms and alternative therapeutic strategies. Biotechnol Adv. 2019;37(1):177–92.

257. Freschi L, Jeukens J, Kukavica-Ibrulj I, Boyle B, Dupont M-J, Laroche J, et al. Clinical utilization of genomics data produced by the international Pseudomonas aeruginosa consortium. Front Microbiol. 2015;6:1036.

258. Luckett JCA, Darch O, Watters C, AbuOun M, Wright V, Paredes-Osses E, et al. A novel virulence strategy for Pseudomonas aeruginosa mediated by an autotransporter with arginine-specific aminopeptidase activity. PLoS Pathog. 2012;8(8):e1002854.

259. Whitmore JK. Exploring Regulation and Function of the Arginine-Specific Aminopeptidase Autotransporter of Pseudomonas aeruginosa AaaA. 2017;

260. Gamper M, Zimmermann A, Haas D. Anaerobic regulation of transcription initiation in the arcDABC operon of Pseudomonas aeruginosa. J Bacteriol. 1991;173(15):4742–50.

261. Sambrook J, Fritsch EF, Maniatis T. Molecular cloning: a laboratory manual. Cold spring harbor laboratory press; 1989.

262. Plesa M, Hernalsteens J-P, Vandenbussche G, Ruysschaert J-M, Cornelis P. The SlyB outer membrane lipoprotein of Burkholderia multivorans contributes to membrane integrity. Res Microbiol. 2006;157(6):582–92.

263. SAMBROOK HC. Molecular cloning: a laboratory manual. Cold Spring Harbor, NY. 1989;

264. Grünberg S, Coxam B, Chen T-H, Dai N, Saleh L, Corrêa IR, et al. E. coli

RNase I exhibits a strong Ca2+-dependent inherent double-stranded RNase activity. Nucleic Acids Res. 2021;

265. Saiki RK, Gelfand DH, Stoffel S, Scharf SJ, Higuchi R. Primer-directed enzymatic amplification of DNA with a thermostable DNA polymerase. Science (80-). 1988;239(4839):487.

266. Cooksley C, Jenks PJ, Green A, Cockayne A, Logan RPH, Hardie KR. NapA protects Helicobacter pylori from oxidative stress damage, and its production is influenced by the ferric uptake regulator. J Med Microbiol. 2003;52(6):461–9.

267. Jain S, van Ulsen P, Benz I, Schmidt MA, Fernandez R, Tommassen J, et al. Polar localization of the autotransporter family of large bacterial virulence proteins. J Bacteriol. 2006;188(13):4841–50.

268. Charles M, Pérez M, Kobil JH, Goldberg MB. Polar targeting of Shigella virulence factor IcsA in Enterobacteriacae and Vibrio. Proc Natl Acad Sci. 2001;98(17):9871–6.

269. Brandon LD, Goehring N, Janakiraman A, Yan AW, Wu T, Beckwith J, et al. IcsA, a polarly localized autotransporter with an atypical signal peptide, uses the Sec apparatus for secretion, although the Sec apparatus is circumferentially distributed. Mol Microbiol. 2003;50(1):45–60.

270. Janakiraman A, Fixen KR, Gray AN, Niki H, Goldberg MB. A genome-scale proteomic screen identifies a role for DnaK in chaperoning of polar autotransporters in Shigella. J Bacteriol. 2009;191(20):6300–11.

271. Fixen KR, Janakiraman A, Garrity S, Slade DJ, Gray AN, Karahan N, et al. Genetic reporter system for positioning of proteins at the bacterial pole. MBio. 2012;3(2):e00251-11.

272. Greenfield D, McEvoy AL, Shroff H, Crooks GE, Wingreen NS, Betzig E, et al. Self-organization of the Escherichia coli chemotaxis network imaged with super-resolution light microscopy. PLoS Biol. 2009;7(6).

273. Davis BM, Waldor MK. Establishing polar identity in gram-negative rods. Curr Opin Microbiol. 2013;16(6):752–9.

274. Cowles KN, Gitai Z. Surface association and the MreB cytoskeleton regulate pilus production, localization and function in Pseudomonas aeruginosa. Mol Microbiol. 2010;76(6):1411–26.

275. Nilsen T, Yan AW, Gale G, Goldberg MB. Presence of multiple sites containing polar material in spherical Escherichia coli cells that lack MreB. J Bacteriol. 2005;187(17):6187–96.

276. Gitai Z, Dye N, Shapiro L. An actin-like gene can determine cell polarity in bacteria. Proc Natl Acad Sci. 2004;101(23):8643–8.

277. Shih Y, Kawagishi I, Rothfield L. The MreB and Min cytoskeletal-like systems play independent roles in prokaryotic polar differentiation. Mol Microbiol. 2005;58(4):917–28.

278. Wagner JK, Galvani CD, Brun Y V. Caulobacter crescentus requires RodA and MreB for stalk synthesis and prevention of ectopic pole formation. J Bacteriol. 2005;187(2):544–53.

279. Romantsov T, Battle AR, Hendel JL, Martinac B, Wood JM. Protein localization in Escherichia coli cells: comparison of the cytoplasmic membrane proteins ProP, LacY, ProW, AqpZ, MscS, and MscL. J Bacteriol. 2010;192(4):912–24.

280. Faria RSCA, Cia MC, Monteiro-Vitorello CB, Azevedo RA, Camargo LEA. Characterization of genes responsive to osmotic and oxidative stresses of the sugarcane bacterial pathogen Leifsonia xyli subsp. xyli. Brazilian J Microbiol. 2019;1–10.

281. Janakiraman A, Lesser CF. How to manage stress: Lessons from an intracellular pathogen. Virulence. 2017;8(4):359–61.

282. Lucchini S, Liu H, Jin Q, Hinton JCD, Yu J. Transcriptional adaptation of Shigella flexneri during infection of macrophages and epithelial cells: insights into the strategies of a cytosolic bacterial pathogen. Infect Immun. 2005;73(1):88–102.

283. Lo M, Boyce JD, Wilkie IW, Adler B. Characterization of two lipoproteins in Pasteurella multocida. Microbes Infect. 2004;6(1):58–67.

284. Lejona S, Aguirre A, Cabeza ML, Véscovi EG, Soncini FC. Molecular characterization of the Mg2+-responsive PhoP-PhoQ regulon in Salmonella enterica. J Bacteriol. 2003;185(21):6287–94.

285. Minagawa S, Ogasawara H, Kato A, Yamamoto K, Eguchi Y, Oshima T, et al. Identification and molecular characterization of the Mg2+ stimulon of Escherichia coli. J Bacteriol. 2003;185(13):3696–702.

286. Brokx SJ, Ellison M, Locke T, Bottorff D, Frost L, Weiner JH. Genome-wide analysis of lipoprotein expression in Escherichia coli MG1655. J Bacteriol. 2004;186(10):3254–8.

287. Thomson NR, Cox A, Bycroft BW, Stewart G, Williams P, Salmond GPC. The rap and hor proteins of Erwinia, Serratia and Yersinia: a novel subgroup in a growing superfamily of proteins regulating diverse physiological processes in bacterial pathogens. Mol Microbiol. 1997;26(3):531–44.

288. Firoved AM, Boucher JC, Deretic V. Global genomic analysis of AlgU (σE)-dependent promoters (sigmulon) in Pseudomonas aeruginosa and implications for inflammatory processes in cystic fibrosis. J Bacteriol. 2002;184(4):1057–64.

289. Firoved AM, Deretic V. Microarray analysis of global gene expression in mucoid Pseudomonas aeruginosa. J Bacteriol. 2003;185(3):1071–81.

290. Brogden KA. Antimicrobial peptides: pore formers or metabolic inhibitors in bacteria? Nat Rev Microbiol. 2005;3(3):238–50.

291. Sitaram N, Nagaraj R. Host-defense antimicrobial peptides: importance of structure for activity. Curr Pharm Des. 2002;8(9):727–42.

292. Mount KLB, Townsend CA, Rinker SD, Gu X, Fortney KR, Zwickl BW, et al. Haemophilus ducreyi SapA contributes to cathelicidin resistance and virulence in humans. Infect Immun. 2010;78(3):1176–84.

293. Mason KM, Bruggeman ME, Munson RS, Bakaletz LO. The non-typeable Haemophilus influenzae Sap transporter provides a mechanism of antimicrobial peptide resistance and SapD-dependent potassium acquisition. Mol Microbiol. 2006;62(5):1357–72.

294. Mason KM, Munson RS, Bakaletz LO. A mutation in the sap operon attenuates survival of nontypeable Haemophilus influenzae in a chinchilla model of otitis media. Infect Immun. 2005;73(1):599–608.

295. Shelton CL, Raffel FK, Beatty WL, Johnson SM, Mason KM. Sap transporter mediated import and subsequent degradation of antimicrobial peptides in Haemophilus. PLoS Pathog. 2011;7(11):e1002360.

296. Mason KM, Raffel FK, Ray WC, Bakaletz LO. Heme utilization by nontypeable Haemophilus influenzae is essential and dependent on Sap transporter function. J Bacteriol. 2011;193(10):2527–35.

297. Gao T, Meng Q, Gao H. Thioesterase YbgC affects motility by modulating c-di-GMP levels in Shewanella oneidensis. Sci Rep. 2017;7(1):1–12.

298. Swarbrick C, Nanson JD, Patterson EI, Forwood JK. Structure, function, and regulation of thioesterases. Prog Lipid Res. 2020;101036.

299. Egan AJF. Bacterial outer membrane constriction. Mol Microbiol. 2018;107(6):676–87.

300. Qin X, He S, Zhou X, Cheng X, Huang X, Wang Y, et al. Quantitative proteomics reveals the crucial role of YbgC for Salmonella enterica serovar Enteritidis survival in egg white. Int J Food Microbiol. 2019;289:115–26.

301. Qin X, Dong R, He S, Zhou X, Zhang Z, Cui Y, et al. Characterization of the role of ybgC in lysozyme resistance of Salmonella Enteritidis. Food Control. 2020;109:106732.

302. Angelini A, Cendron L, Goncalves S, Zanotti G, Terradot L. Structural and enzymatic characterization of HP0496, a YbgC thioesterase from Helicobacter pylori. Proteins Struct Funct Bioinforma. 2008;72(4):1212–21.

303. Zhuang Z, Song F, Martin BM, Dunaway-Mariano D. The YbgC protein encoded by the ybgC gene of the tol-pal gene cluster of Haemophilus influenzae catalyzes acyl-coenzyme A thioester hydrolysis. FEBS Lett. 2002;516(1–3):161–3.

304. Gully D, Bouveret E. A protein network for phospholipid synthesis

uncovered by a variant of the tandem affinity purification method in Escherichia coli. Proteomics. 2006;6(1):282–93.

305. Starosta AL, Lassak J, Jung K, Wilson DN. The bacterial translation stress response. FEMS Microbiol Rev. 2014;38(6):1172–201.

306. Sanchuki HBS, Gravina F, Rodrigues TE, Gerhardt ECM, Pedrosa FO, Souza EM, et al. Dynamics of the Escherichia coli proteome in response to nitrogen starvation and entry into the stationary phase. Biochim Biophys Acta (BBA)-Proteins Proteomics. 2017;1865(3):344–52.

307. Chowdhury N, Kwan BW, Wood TK. Persistence increases in the absence of the alarmone guanosine tetraphosphate by reducing cell growth. Sci Rep. 2016;6:20519.

308. Pontes MH, Groisman EA. Slow growth determines nonheritable antibiotic resistance in Salmonella enterica. Sci Signal. 2019;12(592):eaax3938.

309. Volkert MR, Hajec LI, Matijasevic Z, Fang FC, Prince R. Induction of the Escherichia coli aidB gene under oxygen-limiting conditions requires a functional rpoS (katF) gene. J Bacteriol. 1994;176(24):7638–45.

310. Arnold L. Characterisation of factors involved in the secretion of EspC in enteropathogenic Escherichia coli. University of Nottingham; 2003.

311. Margolin W. The price of tags in protein localization studies. J Bacteriol. 2012;194(23):6369–71.

312. Shemiakina II, Ermakova G V, Cranfill PJ, Baird MA, Evans RA, Souslova EA, et al. A monomeric red fluorescent protein with low cytotoxicity. Nat Commun. 2012;3(1):1–7.

313. Shaner NC, Campbell RE, Steinbach PA, Giepmans BNG, Palmer AE, Tsien RY. Improved monomeric red, orange and yellow fluorescent proteins derived from Discosoma sp. red fluorescent protein. Nat Biotechnol. 2004;22(12):1567–72.

314. Xie F, Wang Y, Li G, Liu S, Cui N, Liu S, et al. The SapA protein is involved in resistance to antimicrobial peptide PR-39 and virulence of Actinobacillus pleuropneumoniae. Front Microbiol. 2017;8:811.

315. Moussatova A, Kandt C, O'Mara ML, Tieleman DP. ATP-binding cassette transporters in Escherichia coli. Biochim Biophys Acta (BBA)-Biomembranes. 2008;1778(9):1757–71.

316. Sueki A, Stein F, Savitski M, Selkrig J, Typas A. Systematic localization of Gram-negative bacterial membrane proteins. BioRxiv. 2019;855171.

317. Lazzaroni JC, Germon P, Ray M-C, Vianney A. The Tol proteins of Escherichia coli and their involvement in the uptake of biomolecules and outer membrane stability. FEMS Microbiol Lett. 1999;177(2):191–7.

318. Sturgis JN. Organisation and evolution of the tol-pal gene cluster. J Mol Microbiol Biotechnol. 2001;3(1):113–22.

319. Wang H, Chou C, Hsu K, Lee C, Wang AH. New paradigm of functional regulation by DNA mimic proteins: recent updates. IUBMB Life. 2019;71(5):539–48.

320. Hamon MA, Stanley NR, Britton RA, Grossman AD, Lazazzera BA. Identification of AbrB-regulated genes involved in biofilm formation by Bacillus subtilis. Mol Microbiol. 2004;52(3):847–60.

321. Sullivan DM, Bobay BG, Kojetin DJ, Thompson RJ, Rance M, Strauch MA, et al. Insights into the nature of DNA binding of AbrB-like transcription factors. Structure. 2008;16(11):1702–13.

322. Chung CT, Niemela SL, Miller RH. One-step preparation of competent Escherichia coli: transformation and storage of bacterial cells in the same solution. Proc Natl Acad Sci. 1989;86(7):2172–5.

323. García-Fruitós E. Inclusion bodies: a new concept. Microb Cell Fact. 2010;9(1):80.

324. Gold VAM, Robson A, Bao H, Romantsov T, Duong F, Collinson I. The action of cardiolipin on the bacterial translocon. Proc Natl Acad Sci. 2010;107(22):10044–9.

325. Crivat G, Tokumasu F, Sa JM, Hwang J, Wellems TE. Tetracysteine-based fluorescent tags to study protein localization and trafficking in Plasmodium falciparum-infected erythrocytes. PLoS One. 2011;6(8).

326. Estévez JM, Somerville C. FlAsH-based live-cell fluorescent imaging of synthetic peptides expressed in Arabidopsis and tobacco. Biotechniques. 2006;41(5):569–74.

327. Cabeen MT, Charbon G, Vollmer W, Born P, Ausmees N, Weibel DB, et al. Bacterial cell curvature through mechanical control of cell growth. EMBO J. 2009;28(9):1208–19.

328. Cabeen MT, Murolo MA, Briegel A, Bui NK, Vollmer W, Ausmees N, et al. Mutations in the lipopolysaccharide biosynthesis pathway interfere with crescentin-mediated cell curvature in Caulobacter crescentus. J Bacteriol. 2010;192(13):3368–78.

329. Adams SR, Campbell RE, Gross LA, Martin BR, Walkup GK, Yao Y, et al. New biarsenical ligands and tetracysteine motifs for protein labeling in vitro and in vivo: synthesis and biological applications. J Am Chem Soc. 2002;124(21):6063–76.

330. Ignatova Z, Gierasch LM. Monitoring protein stability and aggregation in vivo by real-time fluorescent labeling. Proc Natl Acad Sci. 2004;101(2):523–8.

331. Griffin BA, Adams SR, Jones J, Tsien RY. Fluorescent labeling of recombinant proteins in living cells with FlAsH. In: Methods in enzymology. Elsevier; 2000. p. 565–78.

332. Stroffekova K, Proenza C, Beam KG. The protein-labeling reagent FLASH-EDT 2 binds not only to CCXXCC motifs but also non-specifically to endogenous cysteine-rich proteins. Pflügers Arch. 2001;442(6):859–66.

333. Crivat G, Taraska JW. Imaging proteins inside cells with fluorescent tags. Trends Biotechnol. 2012;30(1):8–16.

334. Errington J. Bacterial morphogenesis and the enigmatic MreB helix. Nat Rev Microbiol. 2015;13(4):241–8.

335. Arai H. Regulation and function of versatile aerobic and anaerobic respiratory metabolism in Pseudomonas aeruginosa. Front Microbiol. 2011;2:103.

336. Comolli JC, Donohue TJ. Differences in two Pseudomonas aeruginosa cbb3 cytochrome oxidases. Mol Microbiol. 2004;51(4):1193–203.

337. Hamada M, Toyofuku M, Miyano T, Nomura N. cbb3-type cytochrome c oxidases, aerobic respiratory enzymes, impact the anaerobic life of Pseudomonas aeruginosa PAO1. J Bacteriol. 2014;196(22):3881–9.

338. Arai H, Kawakami T, Osamura T, Hirai T, Sakai Y, Ishii M. Enzymatic characterization and in vivo function of five terminal oxidases in Pseudomonas aeruginosa. J Bacteriol. 2014;196(24):4206–15.

339. Fujita M, Tanaka K, Takahashi H, Amemural A. Transcription of the principal sigma-factor genes, rpoD and rpoS, in Pseudomonas aeruginosa is controlled according to the growth phase. Mol Microbiol. 1994;13(6):1071–7.

340. Rojo F. Carbon catabolite repression in Pseudomonas: optimizing metabolic versatility and interactions with the environment. FEMS Microbiol Rev. 2010;34(5):658–84.

341. Görke B, Stülke J. Carbon catabolite repression in bacteria: many ways to make the most out of nutrients. Nat Rev Microbiol. 2008;6(8):613–24.

342. Collier DN, Hager PW, Phibbs Jr P V. Catabolite repression control in the Pseudomonads. Res Microbiol. 1996;147(6–7):551–61.

343. Moreno R, Fonseca P, Rojo F. The Crc global regulator inhibits the Pseudomonas putida pWW0 toluene/xylene assimilation pathway by repressing the translation of regulatory and structural genes. J Biol Chem. 2010;285(32):24412–9.

344. Yang Z, Lu C-D. Functional genomics enables identification of genes of the arginine transaminase pathway in Pseudomonas aeruginosa. J Bacteriol. 2007;189(11):3945–53.

345. Li C, Lu C-D. Arginine racemization by coupled catabolic and anabolic dehydrogenases. Proc Natl Acad Sci. 2009;106(3):906–11.

346. Itoh Y. Cloning and characterization of the aru genes encoding enzymes of the catabolic arginine succinyltransferase pathway in Pseudomonas

aeruginosa. J Bacteriol. 1997;179(23):7280–90.

347. Vander Wauven C, Pierard A, Kley-Raymann M, Haas D. Pseudomonas aeruginosa mutants affected in anaerobic growth on arginine: evidence for a four-gene cluster encoding the arginine deiminase pathway. J Bacteriol. 1984;160(3):928–34.

348. Lu C-D, Yang Z, Li W. Transcriptome analysis of the ArgR regulon in Pseudomonas aeruginosa. J Bacteriol. 2004;186(12):3855–61.

349. Li C, Wally H, Miller SJ, Lu C-D. The multifaceted proteins MvaT and MvaU, members of the H-NS family, control arginine metabolism, pyocyanin synthesis, and prophage activation in Pseudomonas aeruginosa PAO1. J Bacteriol. 2009;191(20):6211–8.

350. Cunin R, Eckhardt T, Piette J, Boyen A, Pièrard A, Glansdorff N. Molecular basis for modulated regulation of gene expression in the arginine regulon of Escherichia coli K-12. Nucleic Acids Res. 1983;11(15):5007–19.

351. Nakada Y, Itoh Y. Identification of the putrescine biosynthetic genes in Pseudomonas aeruginosa and characterization of agmatine deiminase and N-carbamoylputrescine amidohydrolase of the arginine decarboxylase pathway. Microbiology. 2003;149(3):707–14.

352. Mercenier A, Simon J-P, Haas D, Stalon V. Catabolism of L-arginine by Pseudomonas aeruginosa. Microbiology. 1980;116(2):381–9.

353. Mercenier A, Simon J-P, Vander Wauven C, Haas D, Stalon V. Regulation of enzyme synthesis in the arginine deiminase pathway of Pseudomonas aeruginosa. J Bacteriol. 1980;144(1):159–63.

354. Palmer KL, Brown SA, Whiteley M. Membrane-bound nitrate reductase is required for anaerobic growth in cystic fibrosis sputum. J Bacteriol. 2007;189(12):4449–55.

355. Gavira M, Roldán MD, Castillo F, Moreno-Vivián C. Regulation of nap gene expression and periplasmic nitrate reductase activity in the phototrophic bacterium Rhodobacter sphaeroides DSM158. J Bacteriol. 2002;184(6):1693–702.

356. Flanagan DA, Gregory LG, Carter JP, Karakas-Sen A, Richardson DJ, Spiro S. Detection of genes for periplasmic nitrate reductase in nitrate respiring bacteria and in community DNA. FEMS Microbiol Lett. 1999;177(2):263–70.

357. Berks BC, Ferguson SJ, Moir JWB, Richardson DJ. Enzymes and associated electron transport systems that catalyse the respiratory reduction of nitrogen oxides and oxyanions. Biochim Biophys Acta (BBA)-Bioenergetics. 1995;1232(3):97–173.

358. Hasegawa N, Arai H, Igarashi Y. Activation of a consensus FNR-dependent promoter by DNR of Pseudomonas aeruginosa in response to nitrite. FEMS Microbiol Lett. 1998;166(2):213–7.

359. Rabin RS, Stewart V. Dual response regulators (NarL and NarP) interact with dual sensors (NarX and NarQ) to control nitrate-and nitrite-regulated gene expression in Escherichia coli K-12. J Bacteriol. 1993;175(11):3259–68.

360. Stewart PS. Diffusion in biofilms. J Bacteriol. 2003;185(5):1485–91.

361. Härtig E, Schiek U, Vollack K-U, Zumft WG. Nitrate and Nitrite Control of Respiratory Nitrate Reduction in Denitrifying Pseudomonas stutzeri by a Two-Component Regulatory System Homologous to NarXL ofEscherichia coli. J Bacteriol. 1999;181(12):3658–65.

362. Haas D, Matsumoto H, Moretti P, Stalon V, Mercenier A. Arginine degradation in Pseudomonas aeruginosa mutants blocked in two arginine catabolic pathways. Mol Gen Genet MGG. 1984;193(3):437–44.

363. Arai H, Igarashi Y, Kodama T. Nitrite activates the transcription of the Pseudomonas aeruginosa nitrite reductase and cytochrome c-551 operon under anaerobic conditions. FEBS Lett. 1991;288(1–2):227–8.

364. Arai H, Igarashi Y, Kodama T. Expression of the nir and nor genes for denitrification of Pseudomonas aeruginosa requires a novel CRP/FNR-related transcriptional regulator, DNR, in addition to ANR. FEBS Lett. 1995;371(1):73–6.

365. Arai H, Igarashi Y, Kodama T. Structure and ANR-dependent transcription

of the nir genes for denitrification from Pseudomonas aeruginosa. Biosci Biotechnol Biochem. 1994;58(7):1286–91.

366. Silvestrini MC, Galeotti CL, Gervais M, Schininà E, Barra D, Bossa F, et al. Nitrite reductase from Pseudomonas aeruginosa: sequence of the gene and the protein. FEBS Lett. 1989;254(1–2):33–8.

367. Silvestrini MC, Falcinelli S, Ciabatti I, Cutruzzola F, Brunori M. Pseudomonas aeruginosa nitrite reductase (or cytochrome oxidase): an overview. Biochimie. 1994;76(7):641–54.

368. Arai H, Kodama T, Igarashi Y. The role of the nirQOP genes in energy conservation during anaerobic growth of Pseudomonas aeruginosa. Biosci Biotechnol Biochem. 1998;62(10):1995–9.

369. Jüngst A, Zumft WG. Interdependence of respiratory NO reduction and nitrite reduction revealed by mutagenesis of nirQ, a novel gene in the denitrification gene cluster of Pseudomonas stutzeri. FEBS Lett. 1992;314(3):308–14.

370. Schreiber K, Krieger R, Benkert B, Eschbach M, Arai H, Schobert M, et al. The anaerobic regulatory network required for Pseudomonas aeruginosa nitrate respiration. J Bacteriol. 2007;189(11):4310–4.

371. Arai H, Mizutani M, Igarashi Y. Transcriptional regulation of the nos genes for nitrous oxide reductase in Pseudomonas aeruginosa. Microbiology. 2003;149(1):29–36.

372. Arai H, Kodama T, Igarashi Y. Cascade regulation of the two CRP/FNR-related transcriptional regulators (ANR and DNR) and the denitrification enzymes in Pseudomonas aeruginosa. Mol Microbiol. 1997;25(6):1141–8.

373. Trunk K, Benkert B, Quäck N, Münch R, Scheer M, Garbe J, et al. Anaerobic adaptation in Pseudomonas aeruginosa: definition of the Anr and Dnr regulons. Environ Microbiol. 2010;12(6):1719–33.

374. Cutruzzola F, Frankenberg-Dinkel N. Origin and impact of nitric oxide in Pseudomonas aeruginosa biofilms. J Bacteriol. 2016;198(1):55–65.

375. Eschbach M, Schreiber K, Trunk K, Buer J, Jahn D, Schobert M. Long-term anaerobic survival of the opportunistic pathogen Pseudomonas aeruginosa via pyruvate fermentation. J Bacteriol. 2004;186(14):4596–604.

376. Huang T, Yuan H, Fan L, Morigen M. H-NS, IHF, and DnaA lead to changes in nucleoid organizations, replication initiation, and cell division. J Basic Microbiol. 2020;60(2):136–48.

377. Leite B, Werle CH, Carmo CP do, Nóbrega DB, Milanez GP, Culler HF, et al. Integration host factor is important for biofilm formation by Salmonella enterica Enteritidis. Pathog Dis. 2017;75(6):ftx074.

378. Macchi R, Montesissa L, Murakami K, Ishihama A, De Lorenzo V, Bertoni G. Recruitment of σ54-RNA polymerase to the Pu promoter of Pseudomonas putida through integration host factor-mediated positioning switch of α subunit carboxyl-terminal domain on an UP-like element. J Biol Chem. 2003;278(30):27695–702.

379. Suvorova IA, Ravcheev DA, Gelfand MS. Regulation and evolution of malonate and propionate catabolism in proteobacteria. J Bacteriol. 2012;194(12):3234–40.

380. Verhoogt HJ, Smit H, Abee T, Gamper M, Driessen AJ, Haas D, et al. arcD, the first gene of the arc operon for anaerobic arginine catabolism in Pseudomonas aeruginosa, encodes an arginine-ornithine exchanger. J Bacteriol. 1992;174(5):1568–73.

381. Stalon V, Ramos F, Pierard A, Wiame J-M. The occurrence of a catabolic and an anabolic ornithine carbamoyltransferase in Pseudomonas. Biochim Biophys Acta (BBA)-Enzymology. 1967;139(1):91–7.

382. Thauer RK, Jungermann K, Decker K. Energy conservation in chemotrophic anaerobic bacteria. Bacteriol Rev. 1977;41(1):100.

383. Lu C-D, Winteler H, Abdelal A, Haas D. The ArgR Regulatory Protein, a Helper to the Anaerobic Regulator ANR during Transcriptional Activation of thearcD Promoter in Pseudomonas aeruginosa. J Bacteriol. 1999;181(8):2459–64.

384. Nishijyo T, Park S-M, Lu C-D, Itoh Y, Abdelal AT. Molecular

characterization and regulation of an operon encoding a system for transport of arginine and ornithine and the ArgR regulatory protein in Pseudomonas aeruginosa. J Bacteriol. 1998;180(21):5559–66.

385. Makarova KS, Mironov AA, Gelfand MS. Conservation of the binding site for the arginine repressor in all bacterial lineages. Genome Biol. 2001;2(4):1–9.

386. Schaumburg CS, Tan M. Arginine-dependent gene regulation via the ArgR repressor is species specific in Chlamydia. J Bacteriol. 2006;188(3):919–27.

387. Maas WK. The arginine repressor of Escherichia coli. Microbiol Rev. 1994;58(4):631–40.

388. Campbell EA, Muzzin O, Chlenov M, Sun JL, Olson CA, Weinman O, et al. Structure of the bacterial RNA polymerase promoter specificity σ subunit. Mol Cell. 2002;9(3):527–39.

389. Murakami KS, Masuda S, Darst SA. Structural basis of transcription initiation: RNA polymerase holoenzyme at 4 Å resolution. Science (80-). 2002;296(5571):1280–4.

390. Paget MS. Bacterial sigma factors and anti-sigma factors: structure, function and distribution. Biomolecules. 2015;5(3):1245–65.

391. Potvin E, Sanschagrin F, Levesque RC. Sigma factors in Pseudomonas aeruginosa. FEMS Microbiol Rev. 2008;32(1):38–55.

392. Dötsch A, Schniederjans M, Khaledi A, Hornischer K, Schulz S, Bielecka A, et al. The Pseudomonas aeruginosa transcriptional landscape is shaped by environmental heterogeneity and genetic variation. MBio. 2015;6(4):e00749-15.

393. Gruber TM, Gross CA. Multiple sigma subunits and the partitioning of bacterial transcription space. Annu Rev Microbiol. 2003;57(1):441–66.

394. Buck M, Gallegos M-T, Studholme DJ, Guo Y, Gralla JD. The bacterial enhancer-dependent ς54 (ςN) transcription factor. J Bacteriol. 2000;182(15):4129–36.

395. Zhang N, Darbari VC, Glyde R, Zhang X, Buck M. The bacterial enhancer-dependent RNA polymerase. Biochem J. 2016;473(21):3741–53.

396. Bertoni G, Fujita N, Ishihama A, de Lorenzo V. Active recruitment of σ54-RNA polymerase to the Pu promoter of Pseudomonas putida: role of IHF and αCTD. EMBO J. 1998;17(17):5120–8.

397. Bush M, Dixon R. The role of bacterial enhancer binding proteins as specialized activators of σ54-dependent transcription. Microbiol Mol Biol Rev. 2012;76(3):497–529.

398. Zhang N, Joly N, Buck M. A common feature from different subunits of a homomeric AAA+ protein contacts three spatially distinct transcription elements. Nucleic Acids Res. 2012;40(18):9139–52.

399. Zhang N, Joly N, Burrows PC, Jovanovic M, Wigneshweraraj SR, Buck M. The role of the conserved phenylalanine in the σ54-interacting GAFTGA motif of bacterial enhancer binding proteins. Nucleic Acids Res. 2009;37(18):5981–92.

400. Cannon W, Gallegos M-T, Casaz P, Buck M. Amino-terminal sequences of ςN (ς54) inhibit RNA polymerase isomerization. Genes Dev. 1999;13(3):357–70.

401. Cannon W, Chaney M, Buck M. Characterisation of holoenzyme lacking σ N regions I and II. Nucleic Acids Res. 1999;27(12):2478–86.

402. Zhang N, Buck M. A perspective on the enhancer dependent bacterial RNA polymerase. Biomolecules. 2015;5(2):1012–9.

403. Doucleff M, Malak LT, Pelton JG, Wemmer DE. The C-terminal RpoN domain of σ54 forms an unpredicted helix-turn-helix motif similar to domains of σ70. J Biol Chem. 2005;280(50):41530–6.

404. Doucleff M, Pelton JG, Lee PS, Nixon BT, Wemmer DE. Structural basis of DNA recognition by the alternative sigma-factor, σ54. J Mol Biol. 2007;369(4):1070–8.

405. Schaefer J, Engl C, Zhang N, Lawton E, Buck M. Genome wide interactions of wild-type and activator bypass forms of σ54. Nucleic Acids Res.

2015;43(15):7280–91.

406. Kazmierczak MJ, Wiedmann M, Boor KJ. Alternative sigma factors and their roles in bacterial virulence. Microbiol Mol Biol Rev. 2005;69(4):527–43.

407. Heurlier K, Dénervaud V, Pessi G, Reimmann C, Haas D. Negative control of quorum sensing by RpoN (σ54) in Pseudomonas aeruginosa PAO1. J Bacteriol. 2003;185(7):2227–35.

408. Thompson LS, Webb JS, Rice SA, Kjelleberg S. The alternative sigma factor RpoN regulates the quorum sensing gene rhlI in Pseudomonas aeruginosa. FEMS Microbiol Lett. 2003;220(2):187–95.

409. Dasgupta N, Wolfgang MC, Goodman AL, Arora SK, Jyot J, Lory S, et al. A four-tiered transcriptional regulatory circuit controls flagellar biogenesis in Pseudomonas aeruginosa. Mol Microbiol. 2003;50(3):809–24.

410. Boucher JC, Schurr MJ, Deretic V. Dual regulation of mucoidy in Pseudomonas aeruginosa and sigma factor antagonism. Mol Microbiol. 2000;36(2):341–51.

411. Gardan R, Rapoport G, Débarbouillé M. Role of the transcriptional activator RocR in the arginine-degradation pathway of Bacillus subtilis. Mol Microbiol. 1997;24(4):825–37.

412. Kostylev M, Kim DY, Smalley NE, Salukhe I, Greenberg EP, Dandekar AA. Evolution of the Pseudomonas aeruginosa quorum-sensing hierarchy. Proc Natl Acad Sci. 2019;116(14):7027–32.

413. Miller Melissa B, Bassler Bonnie L. Quorum sensing in bacteria. Annu Rev Microbiol. 2001;55(1):165–99.

414. Raffa RB, Iannuzzo JR, Levine DR, Saeid KK, Schwartz RC, Sucic NT, et al. Bacterial communication ("quorum sensing") via ligands and receptors: a novel pharmacologic target for the design of antibiotic drugs. J Pharmacol Exp Ther. 2005;312(2):417–23.

415. Waters CM, Bassler BL. Quorum sensing: cell-to-cell communication in bacteria. Annu Rev Cell Dev Biol. 2005;21:319–46.

416. Hibbing ME, Fuqua C, Parsek MR, Peterson SB. Bacterial competition: surviving and thriving in the microbial jungle. Nat Rev Microbiol. 2010;8(1):15–25.

417. Schauder S, Shokat K, Surette MG, Bassler BL. The LuxS family of bacterial autoinducers: biosynthesis of a novel quorum-sensing signal molecule. Mol Microbiol. 2001;41(2):463–76.

418. Salmond GPC, Bycroft BW, Stewart GSAB, Williams P. The bacterial 'enigma': cracking the code of cell–cell communication. Mol Microbiol. 1995;16(4):615–24.

419. Heeb S, Fletcher MP, Chhabra SR, Diggle SP, Williams P, Cámara M. Quinolones: from antibiotics to autoinducers. FEMS Microbiol Rev. 2011;35(2):247–74.

420. Passador L, Cook JM, Gambello MJ, Rust L, Iglewski BH. Expression of Pseudomonas aeruginosa virulence genes requires cell-to-cell communication. Science (80-). 1993;260(5111):1127–30.

421. Gambello MJ, Iglewski BH. Cloning and characterization of the Pseudomonas aeruginosa lasR gene, a transcriptional activator of elastase expression. J Bacteriol. 1991;173(9):3000–9.

422. Papenfort K, Bassler BL. Quorum sensing signal-response systems in Gram-negative bacteria. Nat Rev Microbiol. 2016;14(9):576–88.

423. Latifi A, Foglino M, Tanaka K, Williams P, Lazdunski A. A hierarchical quorum-sensing cascade in Pseudomonas aeruginosa links the transcriptional activators LasR and RhIR (VsmR) to expression of the stationary-phase sigma factor RpoS. Mol Microbiol. 1996;21(6):1137–46.

424. Lee J, Zhang L. The hierarchy quorum sensing network in Pseudomonas aeruginosa. Protein Cell. 2015;6(1):26–41.

425. Dekimpe V, Deziel E. Revisiting the quorum-sensing hierarchy in Pseudomonas aeruginosa: the transcriptional regulator RhlR regulates LasR-specific factors. Microbiology. 2009;155(3):712–23.

426. Pesci EC, Milbank JBJ, Pearson JP, McKnight S, Kende AS, Greenberg EP,

et al. Quinolone signaling in the cell-to-cell communication system of Pseudomonas aeruginosa. Proc Natl Acad Sci. 1999;96(20):11229–34.

427. Gallagher LA, McKnight SL, Kuznetsova MS, Pesci EC, Manoil C. Functions required for extracellular quinolone signaling by Pseudomonas aeruginosa. J Bacteriol. 2002;184(23):6472–80.

428. Juhas M, Eberl L, Tümmler B. Quorum sensing: the power of cooperation in the world of Pseudomonas. Environ Microbiol. 2005;7(4):459–71.

429. Azam MW, Khan AU. Updates on the pathogenicity status of Pseudomonas aeruginosa. Drug Discov Today. 2019;24(1):350–9.

430. McKnight SL, Iglewski BH, Pesci EC. The Pseudomonas quinolone signal regulates rhl quorum sensing in Pseudomonas aeruginosa. J Bacteriol. 2000;182(10):2702–8.

431. Tashiro Y, Yawata Y, Toyofuku M, Uchiyama H, Nomura N. Interspecies interaction between Pseudomonas aeruginosa and other microorganisms. Microbes Environ. 2013;28(1):13–24.

432. Rampioni G, Bertani I, Zennaro E, Polticelli F, Venturi V, Leoni L. The quorum-sensing negative regulator RsaL of Pseudomonas aeruginosa binds to the lasI promoter. J Bacteriol. 2006;188(2):815–9.

433. Schuster M, Urbanowski ML, Greenberg EP. Promoter specificity in Pseudomonas aeruginosa quorum sensing revealed by DNA binding of purified LasR. Proc Natl Acad Sci. 2004;101(45):15833–9.

434. De Kievit T, Seed PC, Nezezon J, Passador L, Iglewski BH. RsaL, a novel repressor of virulence gene expression in Pseudomonas aeruginosa. J Bacteriol. 1999;181(7):2175–84.

435. Rampioni G, Schuster M, Greenberg EP, Bertani I, Grasso M, Venturi V, et al. RsaL provides quorum sensing homeostasis and functions as a global regulator of gene expression in Pseudomonas aeruginosa. Mol Microbiol. 2007;66(6):1557–65.

436. Rampioni G, Schuster M, Greenberg EP, Zennaro E, Leoni L. Contribution of the RsaL global regulator to Pseudomonas aeruginosa virulence and

biofilm formation. FEMS Microbiol Lett. 2009;301(2):210–7.

437. Galán-Vásquez E, Luna B, Martínez-Antonio A. The regulatory network of Pseudomonas aeruginosa. Microb Inform Exp. 2011;1(1):3.

438. Toyofuku M, Roschitzki B, Riedel K, Eberl L. Identification of proteins associated with the Pseudomonas aeruginosa biofilm extracellular matrix. J Proteome Res. 2012;11(10):4906–15.

439. Hengge R. Principles of c-di-GMP signalling in bacteria. Nat Rev Microbiol. 2009;7(4):263–73.

440. Römling U, Gomelsky M, Galperin MY. C-di-GMP: the dawning of a novel bacterial signalling system. Mol Microbiol. 2005;57(3):629–39.

441. Jimenez PN, Koch G, Thompson JA, Xavier KB, Cool RH, Quax WJ. The multiple signaling systems regulating virulence in Pseudomonas aeruginosa. Microbiol Mol Biol Rev. 2012;76(1):46–65.

442. Rasamiravaka T, Labtani Q, Duez P, El Jaziri M. The formation of biofilms by Pseudomonas aeruginosa: a review of the natural and synthetic compounds interfering with control mechanisms. Biomed Res Int. 2015;2015.

443. Pearson JP, Feldman M, Iglewski BH, Prince A. Pseudomonas aeruginosa cell-to-cell signaling is required for virulence in a model of acute pulmonary infection. Infect Immun. 2000;68(7):4331–4.

444. Park S-M, Lu C-D, Abdelal AT. Purification and characterization of an arginine regulatory protein, ArgR, from Pseudomonas aeruginosa and its interactions with the control regions for the car, argF, and aru operons. J Bacteriol. 1997;179(17):5309–17.

445. Maghnouj A, de Sousa Cabral TF, Stalon V, Vander Wauven C. The arcABDC gene cluster, encoding the arginine deiminase pathway of Bacillus licheniformis, and its activation by the arginine repressor argR. J Bacteriol. 1998;180(24):6468–75.

446. Rappas M, Bose D, Zhang X. Bacterial enhancer-binding proteins: unlocking σ54-dependent gene transcription. Curr Opin Struct Biol.

2007;17(1):110–6.

447. Sana TG, Soscia C, Tonglet CM, Garvis S, Bleves S. Divergent control of two type VI secretion systems by RpoN in Pseudomonas aeruginosa. PLoS One. 2013;8(10).

448. Winardhi RS, Castang S, Dove SL, Yan J. Single-molecule study on histone-like nucleoid-structuring protein (H-NS) paralogue in Pseudomonas aeruginosa: MvaU bears DNA organization mode similarities to MvaT. PLoS One. 2014;9(11).

449. Castang S, McManus HR, Turner KH, Dove SL. H-NS family members function coordinately in an opportunistic pathogen. Proc Natl Acad Sci. 2008;105(48):18947–52.

450. Falconl M, Gualtierl MT, La Teana A, Losso MA, Pon CL. Proteins from the prokaryotic nucleoid: primary and quaternary structure of the 15-kD Escherichia coli DNA binding protein H-NS. Mol Microbiol. 1988;2(3):323–9.

451. Hernandez-Garcia CM, Finer JJ. Identification and validation of promoters and cis-acting regulatory elements. Plant Sci. 2014;217:109–19.

452. Münch R, Hiller K, Grote A, Scheer M, Klein J, Schobert M, et al. Virtual Footprint and PRODORIC: an integrative framework for regulon prediction in prokaryotes. Bioinformatics. 2005;21(22):4187–9.

453. Petersen TN, Brunak S, Von Heijne G, Nielsen H. SignalP 4.0: discriminating signal peptides from transmembrane regions. Nat Methods. 2011;8(10):785.

454. Casabona M-G, Elsen S, Cogoni V, Attrée I. P. aeruginosa Type VI Secretion Machinery: Another Deadly Syringe. In: Pseudomonas. Springer; 2015. p. 75–97.

455. Arat S, Bullerjahn GS, Laubenbacher R. A network biology approach to denitrification in Pseudomonas aeruginosa. PLoS One. 2015;10(2).

456. Groffman PM, Davidson EA, Seitzinger S. New approaches to modeling denitrification. Biogeochemistry. 2009;93(1–2):1–5.

457. Klockgether J, Munder A, Neugebauer J, Davenport CF, Stanke F, Larbig KD, et al. Genome diversity of Pseudomonas aeruginosa PAO1 laboratory strains. J Bacteriol. 2010;192(4):1113–21.

458. Wurtzel O, Yoder-Himes DR, Han K, Dandekar AA, Edelheit S, Greenberg EP, et al. The single-nucleotide resolution transcriptome of Pseudomonas aeruginosa grown in body temperature. Plos pathog. 2012;8(9):e1002945.

459. Chioccioli S, Bogani P, Del Duca S, Castronovo LM, Vassallo A, Puglia AM, et al. In vivo evaluation of the interaction between the Escherichia coli IGP synthase subunits using the Bacterial Two-Hybrid system. FEMS Microbiol Lett. 2020;367(14):fnaa112.

460. Sartelli M, C Hardcastle T, Catena F, Chichom-Mefire A, Coccolini F, Dhingra S, et al. Antibiotic Use in Low and Middle-Income Countries and the Challenges of Antimicrobial Resistance in Surgery. Antibiotics. 2020;9(8):497.

461. Yang C, Peng S, Chen C, Zhao XS. Molecular mechanism of networking among DegP, Skp and SurA in periplasm for biogenesis of outer membrane proteins. Biochem J. 2020;477(16):2949–65.

462. Ryoo D, Rydmark MO, Pang YT, Lundquist KP, Linke D, Gumbart JC. BamA is required for autotransporter secretion. Biochim Biophys Acta (BBA)-General Subj. 2020;129581.

463. Jordana-Lluch E, Garcia V, Kingdon ADH, Singh N, Alexander C, Williams P, et al. A simple polymicrobial biofilm keratinocyte colonization model for exploring interactions between commensals, pathogens and antimicrobials. Front Microbiol. 2020;11:291.

464. Singh N, Romero M, Travanut A, Monteiro PF, Jordana-Lluch E, Hardie KR, et al. Dual bioresponsive antibiotic and quorum sensing inhibitor combination nanoparticles for treatment of Pseudomonas aeruginosa biofilms in vitro and ex vivo. Biomater Sci. 2019;7(10):4099–111.

465. Zhang J, Brown J, Scurr DJ, Bullen A, MacLellan-Gibson K, Williams P, et al. Cryo-OrbiSIMS for 3D molecular imaging of a bacterial biofilm in its

native state. Anal Chem. 2020;92(13):9008–15.

466. Barzan G, Sacco A, Mandrile L, Giovannozzi AM, Brown J, Portesi C, et al. New frontiers against antibiotic resistance: A Raman-based approach for rapid detection of bacterial susceptibility and biocide-induced antibiotic cross-tolerance. Sensors Actuators B Chem. 2020;309:127774.

467. Harrington NE, Sweeney E, Harrison F. Building a better biofilm-formation of in vivo-like biofilm structures by Pseudomonas aeruginosa in a porcine model of cystic fibrosis lung infection. Biofilm. 2020;100024.

468. Morozova O, Hirst M, Marra MA. Applications of new sequencing technologies for transcriptome analysis. Annu Rev Genomics Hum Genet. 2009;10:135–51.

Supplementary Figures

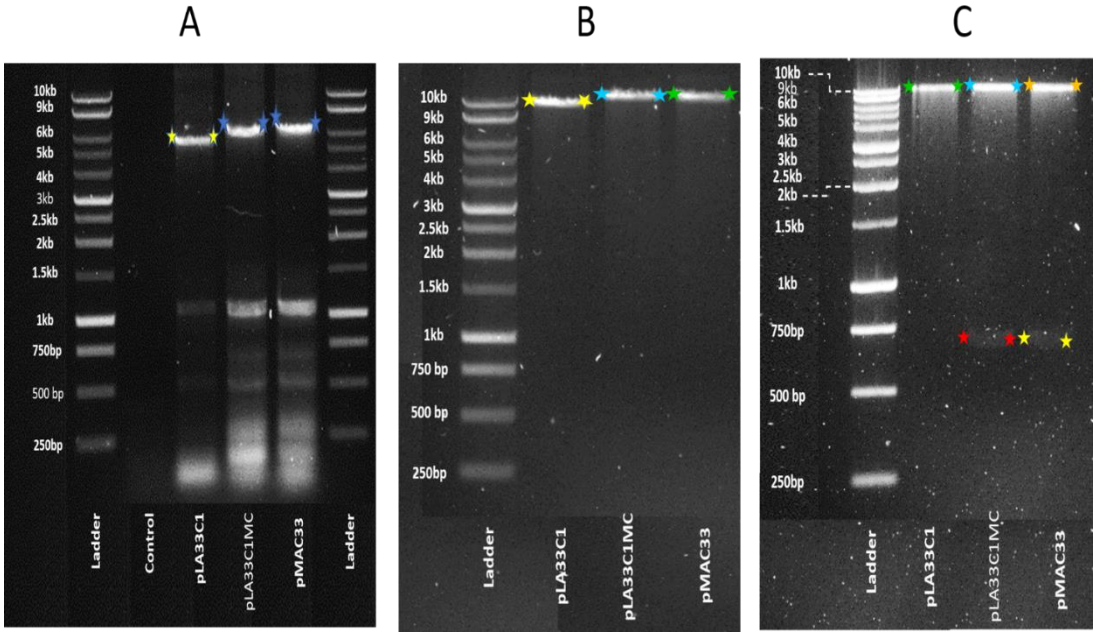

Supplementary Figure 1: *E. coli* MG1655 secretes native EspC from plasmid pLA33C1, or accumulates intracellular full length or truncated EspC fused to mCherry from plasmids pLA33C1MC or pMAC33 respectively as expected. Plasmids pLA33C1, pLA33C1MC and pMAC33 were amplified by PCR using primers F-espC and R-ApaI-espC and the products separated on a 0.8% agarose gel alongside the 1kb molecular weight marker. A control PCR lacking template DNA was also prepared in parallel. The asterisks indicate the expected products of 4028bp (yellow) for pLA33C1 and 4753bp (blue) for pLA33C1MC and pMAC33 plasmids (Panel A). Plasmids pLA33C1, pLA33C1MC and pMAC33 were digested with HindIII (panel B) and BglII (Panel C) as described in the methods. Digestion products were applied to a 0.8% gel alongside the 1kb molecular weight marker. In Panel B the asterisks indicate the expected products of 9293bp for pLA33C1 (Yellow) and 10,010bp for pLA33C1MC and pMAC33 plasmids (Blue and green). In Panel C the asterisks indicate the expected products of 9293bp for pLA33C1 (Green), 717bp mCherry (Red) separated from 9265bp (Blue) that represents the rest of the vector for pLA33C1MC and 718bp (Yellow) mCherry separated from 9294bp rest of the vector for pMAC33 (Orange).

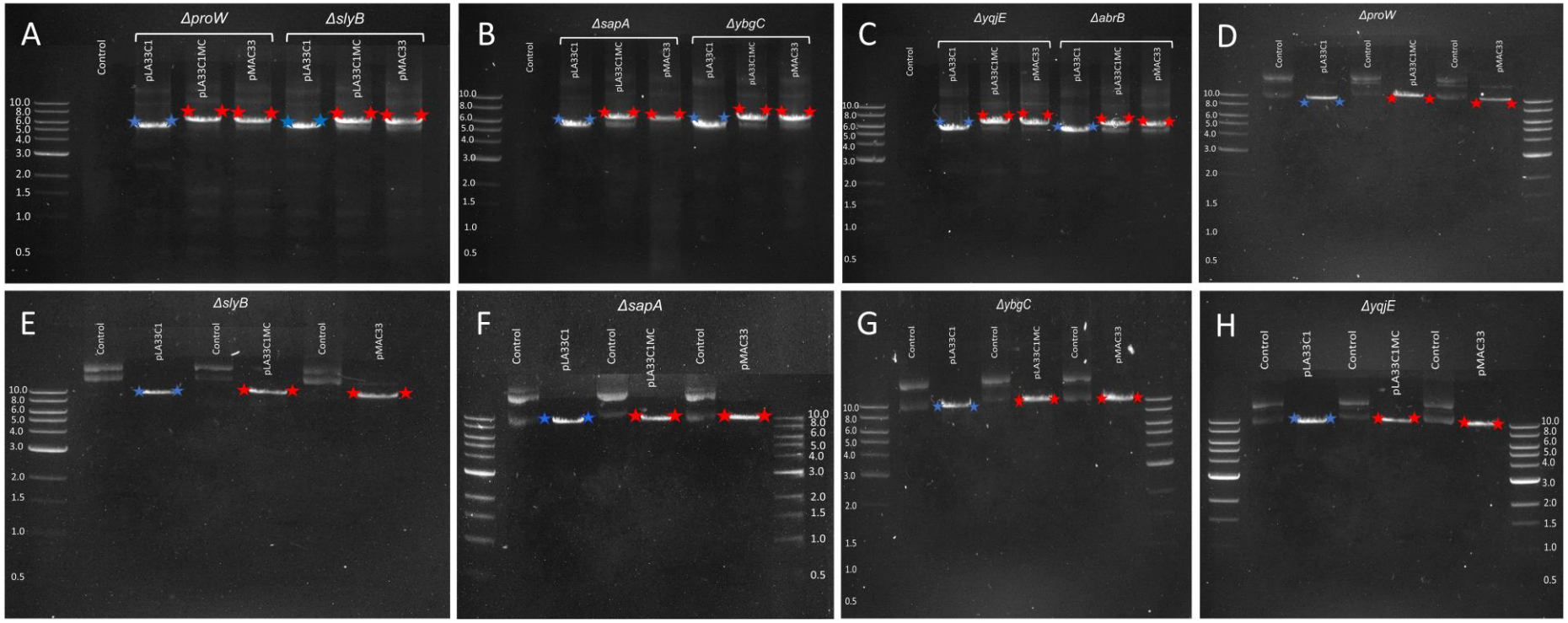
A
ΔproW
ΔslyB
Control
pLA33C1
pLA33C1MC
pMAC33
B
ΔsapA
ΔybgC
C
ΔyqjE
ΔabrB
D
ΔproW
E
ΔslyB
F
ΔsapA
G
ΔybgC
H
ΔyqjE
10.0
8.0
6.0
5.0
4.0
3.0
2.0
1.5
1.0
0.5

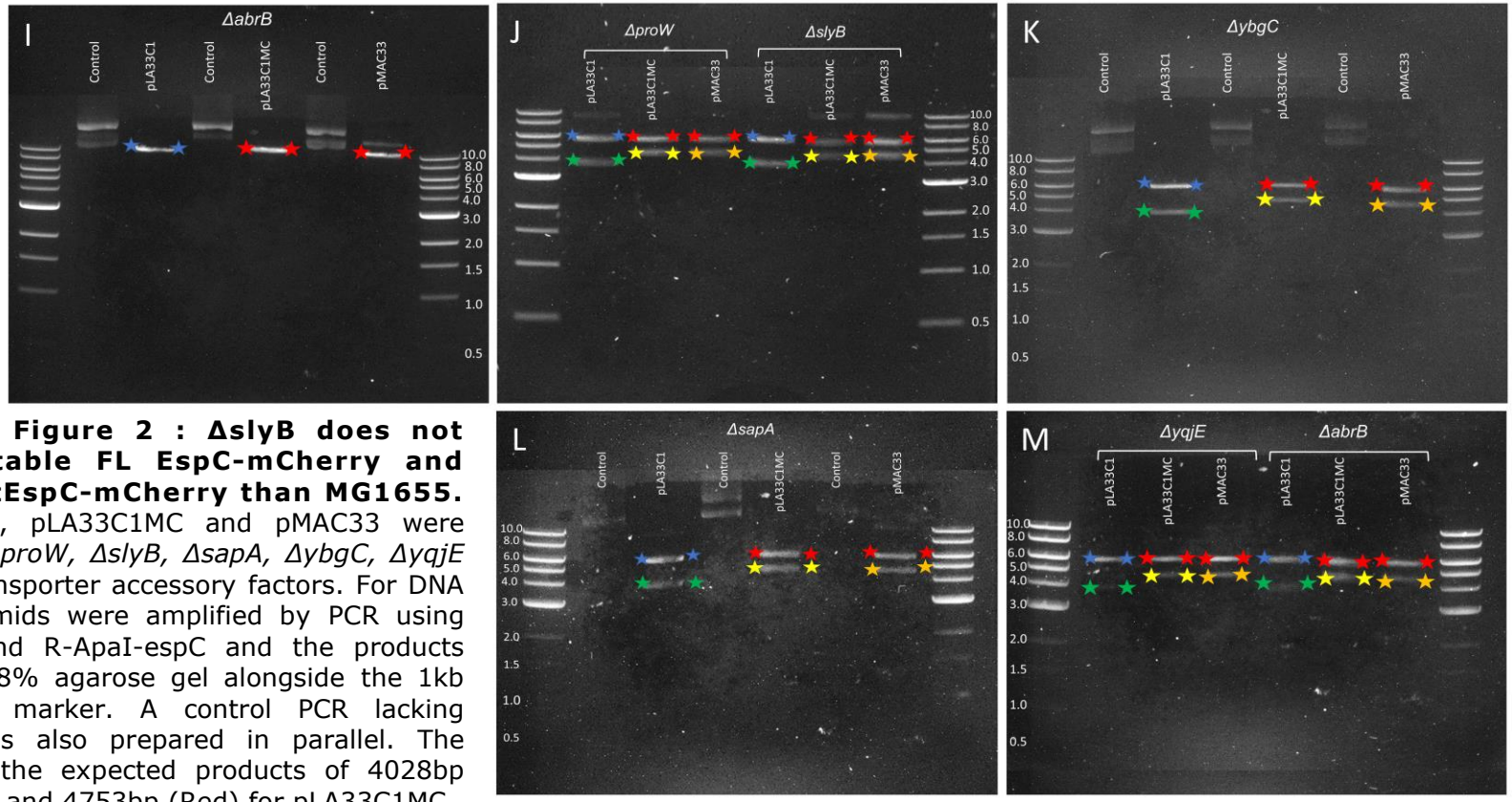

Supplementary Figure 2 : ΔslyB does not produce detectable FL EspC-mCherry and releases more tEspC-mCherry than MG1655. Plasmids pLA33C1, pLA33C1MC and pMAC33 were transformed into *ΔproW, ΔslyB, ΔsapA, ΔybgC, ΔyqjE and ΔabrB* autotransporter accessory factors. For DNA confirmation, plasmids were amplified by PCR using primers F-espC and R-ApaI-espC and the products separated on a 0.8% agarose gel alongside the 1kb molecular weight marker. A control PCR lacking template DNA was also prepared in parallel. The asterisks indicate the expected products of 4028bp (Blue) for pLA33C1 and 4753bp (Red) for pLA33C1MC and pMAC33 plasmids (Panel A-C). For confirmation, plasmids were digested with BamHI as described in the section 2.10.2 (Panel D-I). Digestion products were applied to a 0.8% gel alongside the 1kb molecular weight marker. The asterisks indicate the expected products of 9293bp for PLA33C1 (Blue) and 10,010bp for pLA33C1MC and pMAC33 plasmids (Red). Further confirmation, plasmids were digested with SacI and HindIII as described in the methods (Panel J-M). Digestion products were applied to a 0.8% gel alongside the 1kb molecular weight marker. The asterisks indicate the expected products of 3985bp (Green) and 5308bp (Blue) that indicated the rest of the vector for pLA33C1, 4695bp EspC- mCherry (Yellow) separated from 5315bp (Red) that represents the rest of the vector for pLA33C1MC and 4696bp (Orange) EspC- mCherry separated from 5315bp rest of the vector for pMAC33 (Red).

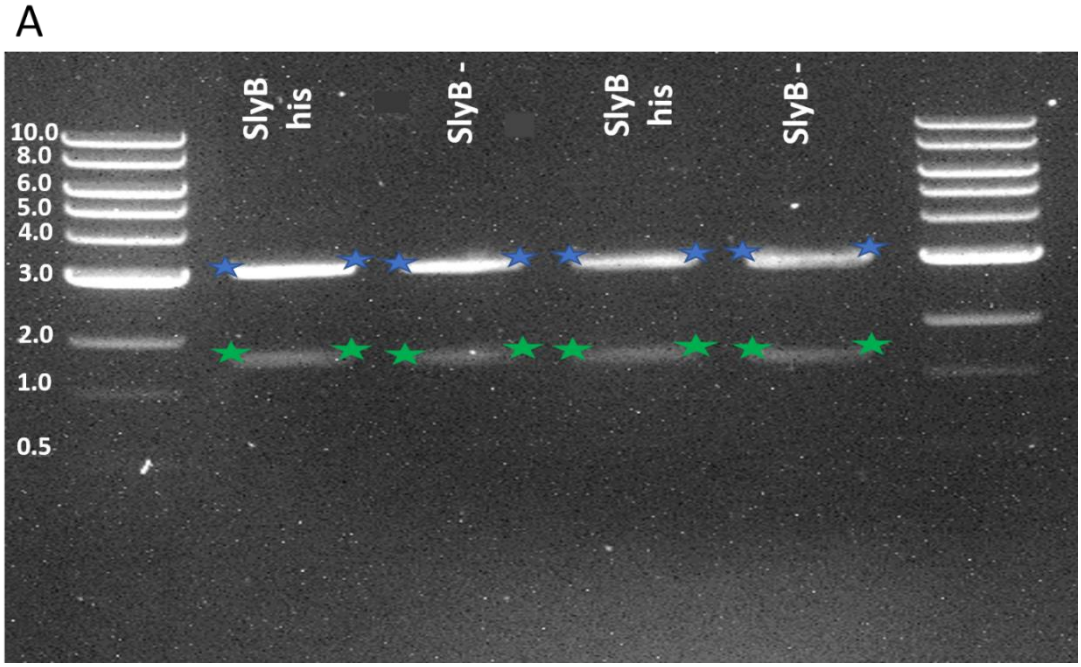

Supplementary Figure 3 : The ΔslyB mutant containing pLA33C1, pLA33C1MC and pMAC33 produced a similar protein profile as the complemented mutant. Confirmation of the *slyB* expression vectors transformed into DH5α cells by restriction digestion with ClaI and SphI. The 3191 bp DNA fragment indicated by blue stars was separated from the 1651 bp arabinose promotor and partial *slyB* indicated with green stars as expected (Panel A).

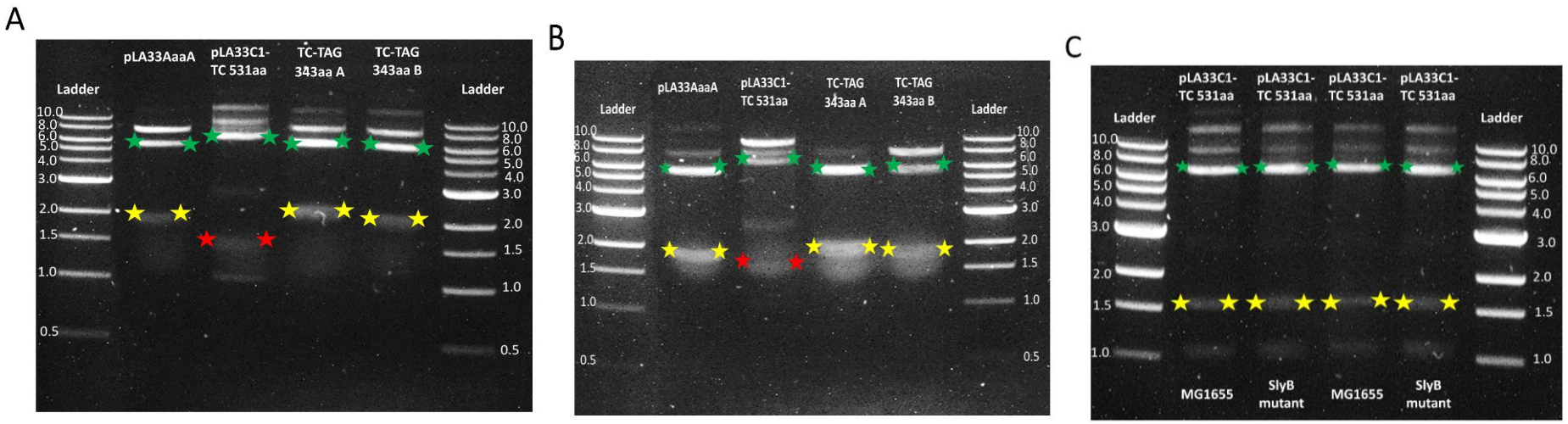

Supplementary Figure 4 : Parental MG1655 and the Δ*slyB* mutant containing native AaaA (pLA33AaaA), FL EspC FlAsH tag (pLA33C1-TC 531aa) and AaaA truncated version (pLA33AaaA-TC-TAG343aa) produced similar detectable AaaA and EspC protein in whole cell lysates. Plasmids pLA33AaaA, pLA33C1-TC 531aa and pLA33AaaA-TC-TAG343aa were transformed into MG1655 WT and the derived *ΔslyB* secretion accessory factor mutant. Transformation was confirmed by double digest with *BglII* and *SalI*. In FL EspC (pLA33C1-TC 531aa) ~1064 bp upstream portion of *espC* was separated from 5327 bp open pBAD33 vector as expected (Panel C). 2059bp native *aaaA* fragment from native *aaaA* (pLA33AaaA) and *aaaA* truncated version (pLA33AaaA-TC-TAG343aa) were separated from 5327 bp rest of the vector (Panel A & B).

Supplementary Table 1: list of Plasmids used in this study with description for expression and regulation of AaaA.

Plasmid	Description	Origin
PAO1 WT Mini CTX-Pkan-*lux*	Wild type strain plus the Mini CTX-Pkan-*lux* vector. TetR	Esteban Thesis,2014
PAO1Δ*aaaA* Mini CTX-Pkan-*lux*	In-frame *aaaA* deletion mutant plus the Mini CTX-Pkan-*lux* vector. TetR	Esteban Thesis ,2014
PAO1 ΔrpoN Mini CTX-Pkan-*lux*	In-frame *ΔrpoN* plus the Mini CTX-Pkan-*lux* vector. TetR	Spencer Thesis,2018
PAO1 ΔmvaU Mini CTX-Pkan-*lux*	In-frame *mvaU* deletion mutant plus the Mini CTX-Pkan-*lux* vector. TetR	Esteban Thesis ,2014
PAO1 ΔmvaT Mini CTX-Pkan-*lux*	In-frame *mvaT* deletion mutant plus the Mini CTX-Pkan-*lux* vector. TetR	Esteban Thesis ,2014
PAO1 Δsfa2 Mini CTX-Pkan-*lux*	In-frame *sfa2* deletion mutant plus the Mini CTX-Pkan-*lux* vector. TetR	Esteban Thesis ,2014
PAO1 Δsfa3 Mini CTX-Pkan-*lux*	In-frame *sfa3* deletion mutant plus the Mini CTX-Pkan-*lux* vector. TetR	Esteban Thesis ,2014
PAO1 ΔpqsE Mini CTX-Pkan-*lux*	In-frame *pqsE* deletion mutant plus the Mini CTX-Pkan-*lux* vector. TetR	Esteban Thesis, 2014
PAO1 ΔlasR Mini CTX-Pkan-*lux*	In-frame *lasR* deletion mutant plus the Mini CTX-Pkan-*lux* vector. TetR	Esteban Thesis, 2014
PAO1 ΔrhlR Mini CTX-Pkan-*lux*	In-frame *rhlR* deletion mutant plus the Mini CTX-Pkan-*lux* vector. TetR	Esteban Thesis, 2014
PAO1 Δrsal Mini CTX-Pkan-*lux*	In-frame *rsal* deletion mutant plus the Mini CTX-Pkan-*lux* vector. TetR	Esteban Thesis, 2014
PAO1 L ΔnirQ Mini CTX-Pkan-*lux*	In-frame *nirQ* deletion mutant plus the Mini CTX-Pkan-*lux* vector. TetR	In this study

Plasmid	Description	Origin
PA14 ΔargR Mini CTX-Pkan-*lux*	In-frame *argR* deletion mutant plus the Mini CTX-Pkan-*lux* vector. TetR	Esteban Thesis, 2014
PA14 Δsfa2 Mini CTX-Pkan-*lux*	In-frame *sfa2* deletion mutant plus the Mini CTX-Pkan-*lux* vector. TetR	In this study
PA14 ΔphhR Mini CTX-Pkan-*lux*	In-frame *phhR* deletion mutant plus the Mini CTX-Pkan-*lux* vector. TetR	In this study
PA14 ΔalgB Mini CTX-Pkan-*lux*	In-frame *algB* deletion mutant plus the Mini CTX-Pkan-*lux* vector. TetR	In this study
PA14 ΔPilR Mini CTX-Pkan-*lux*	In-frame *PilR* deletion mutant plus the Mini CTX-Pkan-*lux* vector. TetR	In this study
PA14 ΔdctD Mini CTX-Pkan-*lux*	In-frame *dctD* deletion mutant plus the Mini CTX-Pkan-*lux* vector. TetR	In this study
PA14 ΔfleQ Mini CTX-Pkan-*lux*	In-frame *fleQ* deletion mutant plus the Mini CTX-Pkan-*lux* vector. TetR	In this study
PA14 ΔmifR Mini CTX-Pkan-*lux*	In-frame *mifR* deletion mutant plus the Mini CTX-Pkan-*lux* vector. TetR	In this study
PA14 ΔntrC Mini CTX-Pkan-*lux*	In-frame *ntrC* deletion mutant plus the Mini CTX-Pkan-*lux* vector. TetR	In this study
PA14 ΔcbrB Mini CTX-Pkan-*lux*	In-frame *cbrB* deletion mutant plus the Mini CTX-Pkan-*lux* vector. TetR	In this study
PA14 ΔrtcR Mini CTX-Pkan-*lux*	In-frame *rtcR* deletion mutant plus the Mini CTX-Pkan-*lux* vector. TetR	In this study
PA14 ΔacoR Mini CTX-Pkan-*lux*	In-frame *acoR* deletion mutant plus the Mini CTX-Pkan-*lux* vector. TetR	In this study
PA14 ΔeatR Mini CTX-Pkan-*lux*	In-frame *eatR* deletion mutant plus the Mini CTX-Pkan-*lux* vector. TetR	In this study
PA14 Δ13000 Mini CTX-Pkan-*lux*	In-frame *13000* deletion mutant plus the Mini CTX-Pkan-*lux* vector. TetR	In this study
PA14 ΔNorR Mini CTX-Pkan-*lux*	In-frame *NorR* deletion mutant plus the Mini CTX-Pkan-*lux* vector. TetR	In this study
PA14 ΔgscR Mini CTX-Pkan-*lux*	In-frame *gscR* deletion mutant plus the Mini CTX-Pkan-*lux* vector. TetR	In this study
PA14 ΔSfa3 Mini CTX-Pkan-*lux*	In-frame *Sfa3* deletion mutant plus the Mini CTX-Pkan-*lux* vector. TetR	In this study
PA14 ΔhbcR Mini CTX-Pkan-*lux*	In-frame *hbcR* deletion mutant plus the Mini CTX-Pkan-*lux* vector. TetR	In this study
PA14 Δ39360 Mini CTX-Pkan-*lux*	In-frame *39360* deletion mutant plus the Mini CTX-Pkan-*lux* vector. TetR	In this study
PA14 ΔddaR Mini CTX-Pkan-*lux*	In-frame *ddaR* deletion mutant plus the Mini CTX-Pkan-*lux* vector. TetR	In this study
PA14 ΔfleR Mini CTX-Pkan-*lux*	In-frame *fleR* deletion mutant plus the Mini CTX-Pkan-*lux* vector. TetR	In this study

Plasmid	Description	Origin
PAO1 WT Mini CTX-P*aaaA*-*lux*	Wild type strain plus the Mini CTX-P*aaaA*-*lux* vector. TetR	Esteban Thesis ,2014
PAO1Δ*aaaA* Mini CTX-P*aaaA*-*lux*	In-frame *aaaA* deletion mutant plus the Mini CTX-P*aaaA*-lux vector. TetR	Esteban Thesis ,2014
PAO1 *ΔrpoN* miniCTX-*lux*::P*aaaA*	PAO1 *ΔrpoN* with miniCTX-*lux aaaA* promoter fusion	Spencer Thesis, 2018
PAO1 *ΔrpoN att Tn7:rpoN* + miniCTX-lux::P*aaaA*	Complemented *ΔrpoN* with miniCTX-*lux aaaA* promoter fusion	Spencer Thesis, 2018
PAO1 ΔmvaU Mini CTX-*lux*::P*aaaA*	In-frame *mvaU* deletion mutant plus the Mini CTX-P*aaaA*-lux vector. TetR	Esteban Thesis ,2014
PAO1 ΔmvaT Mini CTX-*lux*::P*aaaA*	In-frame *mvaT* deletion mutant plus the Mini CTX-P*aaaA*-lux vector. TetR	Esteban Thesis ,2014
PAO1 Δsfa2 Mini CTX-*lux*::P*aaaA*	In-frame *sfa2* deletion mutant plus the Mini CTX-P*aaaA*-lux vector. TetR	Esteban Thesis ,2014
PAO1 Δsfa3 Mini CTX-*lux*::P*aaaA*	In-frame *sfa3* deletion mutant plus the Mini CTX-P*aaaA*-lux vector. TetR	Esteban Thesis ,2014
PAO1 ΔpqsE Mini CTX-*lux*::P*aaaA*	In-frame *pqsE* deletion mutant plus the Mini CTX-P*aaaA*-lux vector.TetR	Esteban Thesis, 2014
PAO1 ΔlasR Mini CTX-*lux*::P*aaaA*	In-frame *lasR* deletion mutant plus the Mini CTX-P*aaaA*-lux vector. TetR	Esteban Thesis, 2014
PAO1 ΔrhlR Mini CTX-*lux*::P*aaaA*	In-frame *rhlR* deletion mutant plus the Mini CTX-P*aaaA*-lux vector. TetR	Esteban Thesis, 2014
PAO1 Δrsal Mini CTX-*lux*::P*aaaA*	In-frame *rsal* deletion mutant plus the Mini CTX-P*aaaA*-lux vector. TetR	Esteban Thesis, 2014
PAO1 ΔnirQ Mini CTX-*lux*::P*aaaA*	In-frame *nirQ* deletion mutant plus the Mini CTX-P*aaaA*-lux vector. TetR	In this study

Plasmid	Description	Origin
PA14 ΔargRMini CTX-*lux*::P*aaaA*	In-frame *argR* deletion mutant plus the Mini CTX-P*aaaA*-lux vector.TetR	Esteban Thesis, 2014
PA14 Δsfa2 Mini CTX-*lux*::P*aaaA*	In-frame *sfa2* deletion mutant plus the Mini CTX-P*aaaA*-lux vector. TetR	In this study
PA14 ΔphhR Mini CTX-*lux*::P*aaaA*	In-frame *phhR* deletion mutant plus the Mini CTX-P*aaaA*-lux vector.TetR	In this study
PA14 ΔalgB Mini CTX-*lux*::P*aaaA*	In-frame *algB* deletion mutant plus the Mini CTX-P*aaaA*-lux vector. TetR	In this study
PA14 ΔPilR Mini CTX-*lux*::P*aaaA*	In-frame *PilR* deletion mutant plus the Mini CTX-P*aaaA*-lux vector. TetR	In this study
PA14 ΔdctD Mini CTX-*lux*::P*aaaA*	In-frame *dctD* deletion mutant plus the Mini CTX-P*aaaA*-lux vector. TetR	In this study
PA14 ΔfleQ Mini CTX-*lux*::P*aaaA*	In-frame *fleQ* deletion mutant plus the Mini CTX-P*aaaA*-lux vector. TetR	In this study
PA14 ΔmifR Mini CTX-*lux*::P*aaaA*	In-frame *mifR* deletion mutant plus the Mini CTX-P*aaaA*-lux vector. TetR	In this study
PA14 ΔntrC Mini CTX-*lux*::P*aaaA*	In-frame *ntrC* deletion mutant plus the Mini CTX-P*aaaA*-lux vector. TetR	In this study
PA14 ΔcbrB Mini CTX-*lux*::P*aaaA*	In-frame *cbrB* deletion mutant plus the Mini CTX-P*aaaA*-lux vector. TetR	In this study
PA14 ΔrtcR Mini CTX-*lux*::P*aaaA*	In-frame *rtcR* deletion mutant plus the Mini CTX-P*aaaA*-lux vector. TetR	In this study
PA14 ΔacoR Mini CTX-*lux*::P*aaaA*	In-frame *acoR* deletion mutant plus the Mini CTX-P*aaaA*-lux vector. TetR	In this study
PA14 ΔeatR Mini CTX-*lux*::P*aaaA*	In-frame *eatR* deletion mutant plus the Mini CTX-P*aaaA*-lux vector. TetR	In this study
PA14 Δ13000 Mini CTX-*lux*::P*aaaA*	In-frame *13000* deletion mutant plus the Mini CTX-P*aaaA*-lux vector. TetR	In this study
PA14 ΔNorR Mini CTX-*lux*::P*aaaA*	In-frame *NorR* deletion mutant plus the Mini CTX-P*aaaA*-lux vector. TetR	In this study
PA14 ΔgscR Mini CTX-*lux*::P*aaaA*	In-frame *gscR* deletion mutant plus the Mini CTX-P*aaaA*-lux vector. TetR	In this study
PA14 ΔSfa3 Mini CTX-*lux*::P*aaaA*	In-frame *Sfa3* deletion mutant plus the Mini CTX-P*aaaA*-lux vector. TetR	In this study
PA14 ΔhbcR Mini CTX-*lux*::P*aaaA*	In-frame *hbcR* deletion mutant plus the Mini CTX-P*aaaA*-lux vector. TetR	In this study
PA14 Δ39360 Mini CTX-*lux*::P*aaaA*	In-frame *39360* deletion mutant plus the Mini CTX-P*aaaA*-lux vector. TetR	In this study
PA14 ΔddaR Mini CTX-*lux*::P*aaaA*	In-frame *ddaR* deletion mutant plus the Mini CTX-P*aaaA*-lux vector. TetR	In this study
PA14 ΔfleR Mini CTX-*lux*::P*aaaA*	In-frame *fleR* deletion mutant plus the Mini CTX-P*aaaA*-lux vector. TetR	In this study

Plasmid	Description	Origin
PAO1 WT PaaaA△rpoNmotif -lux	Wild type strain plus the Mini CTX- PaaaA△rpoNmotif -lux vector. TetR	In this study
PAO1ΔaaaA PaaaA△rpoNmotif -lux	In-frame aaaA deletion mutant plus the Mini CTX- PaaaA△rpoNmotif-lux vector. TetR	In this study
PAO1 ΔrpoN att Tn7:rpoN + PaaaA△rpoNmotif -lux	Complemented ΔrpoN with the Mini CTX- PaaaA△rpoNmotif -lux vector. TetR	In this study
PAO1 ΔmvaU PaaaA△rpoNmotif -lux	In-frame *mvaU* deletion mutant plus the Mini CTX- PaaaA△rpoNmotif-lux vector. TetR	In this study
PAO1 ΔmvaT PaaaA△rpoNmotif -lux	In-frame *mvaT* deletion mutant plus the Mini CTX- PaaaA△rpoNmotif-lux vector. TetR	In this study
PAO1 Δsfa2 PaaaA△rpoNmotif -lux	In-frame *sfa2* deletion mutant plus the Mini CTX- PaaaA△rpoNmotif-lux vector. TetR	In this study
PAO1 Δsfa3 PaaaA△rpoNmotif -lux	In-frame *sfa3* deletion mutant plus the Mini CTX- PaaaA△rpoNmotif-lux vector. TetR	In this study
PAO1 ΔpqsE PaaaA△rpoNmotif -lux	In-frame *pqsE* deletion mutant plus the Mini CTX- PaaaA△rpoNmotif-lux vector. TetR	In this study
PAO1 ΔlasR PaaaA△rpoNmotif -lux	In-frame *lasR* deletion mutant plus the Mini CTX- PaaaA△rpoNmotif-lux vector. TetR	In this study
PAO1 ΔrhlR PaaaA△rpoNmotif -lux	In-frame *rhlR* deletion mutant plus the Mini CTX- PaaaA△rpoNmotif-lux vector. TetR	In this study
PAO1 Δrsal PaaaA△rpoNmotif -lux	In-frame *rsal* deletion mutant plus the Mini CTX- PaaaA△rpoNmotif-lux vector. TetR	In this study
PAO1 ΔnirQ PaaaA△rpoNmotif -lux	In-frame *nirQ* deletion mutant plus the Mini CTX-PaaaA△rpoNmotif-lux vector.TetR	In this study

Plasmid	Description	Origin
PA14 ΔargR PaaaA△rpoNmotif -lux	In-frame *argR* deletion mutant plus the Mini CTX- PaaaA△rpoNmotif-lux vector. TetR	In this study
PA14 Δsfa2 PaaaA△rpoNmotif -lux	In-frame *sfa2* deletion mutant plus the Mini CTX- PaaaA△rpoNmotif-lux vector. TetR	In this study
PA14 Δ phhR PaaaA△rpoNmotif -lux	In-frame *phhR* deletion mutant plus the Mini CTX- PaaaA△rpoNmotif-lux vector. TetR	In this study
PA14 ΔalgB PaaaA△rpoNmotif -lux	In-frame *algB* deletion mutant plus the Mini CTX-PaaaA△rpoNmotif-lux vector. TetR	In this study
PA14 ΔPilR PaaaA△rpoNmotif -lux	In-frame *PilR* deletion mutant plus the Mini CTX-PaaaA△rpoNmotif-lux vector.TetR	In this study
PA14 ΔdctD PaaaA△rpoNmotif -lux	In-frame *dctD* deletion mutant plus the Mini CTX-PaaaA△rpoNmotif-lux vector. TetR	In this study
PA14 ΔfleQ PaaaA△rpoNmotif -lux	In-frame *fleQ* deletion mutant plus the Mini CTX-PaaaA△rpoNmotif-lux vector.TetR	In this study
PA14 ΔmifR PaaaA△rpoNmotif -lux	In-frame *mifR* deletion mutant plus the Mini CTX-PaaaA△rpoNmotif-lux vector. TetR	In this study
PA14 Δ13000PaaaA△rpoNmotif -lux	In-frame *13000* deletion mutant plus the Mini CTX-PaaaA△rpoNmotif-lux vector.TetR	In this study
PA14 ΔNorR PaaaA△rpoNmotif -lux	In-frame *NorR* deletion mutant plus the Mini CTX-PaaaA△rpoNmotif-lux vector. TetR	In this study
PA14 ΔgscR PaaaA△rpoNmotif -lux	In-frame *gscR* deletion mutant plus the Mini CTX-PaaaA△rpoNmotif-lux vector. TetR	In this study
PA14 ΔSfa3 PaaaA△rpoNmotif -lux	In-frame *Sfa3* deletion mutant plus the Mini CTX-PaaaA△rpoNmotif-lux vector. TetR	In this study
PA14 ΔhbcR PaaaA△rpoNmotif -lux	In-frame *hbcR* deletion mutant plus the Mini CTX-PaaaA△rpoNmotif-lux vector. TetR	In this study
PA14 Δ39360 PaaaA△rpoNmotif -lux	In-frame *39360* deletion mutant plus the Mini CTX-PaaaA△rpoNmotif-lux vector. TetR	In this study
PA14 ΔddaR PaaaA△rpoNmotif -lux	In-frame *ddaR* deletion mutant plus the Mini CTX-PaaaA△rpoNmotif-lux vector. TetR	In this study
PA14 ΔfleR PaaaA△rpoNmotif -lux	In-frame *fleR* deletion mutant plus the Mini CTX-PaaaA△rpoNmotif-lux vector. TetR	In this study

Supplementary Table 2: Bacterial strains used in this study

Strain Name	Description	Antibiotic resistance	Bacteria	Reference
MG1655Δ*nei*	defined, non-polar mutant in *nei* created by lambda red recombination	Chloramphenicol (CM)	*E. coli*	Stephenie Pommier,2012
MG1655Δ*proW*	defined, non-polar mutant in *proW* created by lambda red recombination	-------	*E. coli*	Stephenie Pommier,2012
MG1655Δ*SlyB*	defined, non-polar mutant in *SlyB* created by lambda red recombination	-------	*E. coli*	Stephenie Pommier,2012
MG1655Δ*sapA*	defined, non-polar mutant in *sapA* created by lambda red recombination	-------	*E. coli*	Stephenie Pommier,2012
MG1655Δ*ybgC*	defined, non-polar mutant in *ybgC* created by lambda red recombination	------	*E. coli*	Stephenie Pommier,2012
MG1655Δ*yqjE*	defined, non-polar mutant in *yqjE* created by lambda red recombination	------	*E. coli*	Stephenie Pommier,2012
MG1655Δ*abrB A*	defined, non-polar mutant in *abrB A* created by lambda red recombination	-------	*E. coli*	Stephenie Pommier,2012
MG1655	*F- λ- ilvG- rfb-50 rph-1.*	-------	*E. coli*	Mahmoud Ashawesh, 2016
DH5α	F'/*endA*1, *hsd*R17(R- M+), *supE*44, thi-1, recA1, gyrA, relA1, Δ(*lacZYA*-*argF*) U169, *deoR* [Φ80d *lac*Δ(*lacZ*) M15].	-------	*E. coli*	Mahmoud Ashawesh, 2016
S17-1 λpir	*E.coli* strain capable of conjugation into *P. aeruginosa*	-------	*E. coli*	Paredes, 2014

Strain Name	Description	Bacteria	Reference
PAO1 WT	Wild-type	*P. aeruginosa*	ATCC15692
PAO1 WT L	Wild-type	*P. aeruginosa*	Arat et al., 2015
PAO1 ΔaaaA	In-frame *aaaA* deletion mutant	*P. aeruginosa*	Luckett et al., 2012
PAO1 ΔrpoN (PA06358)	Deletion mutant of rpoN	*P. aeruginosa*	Heurlier et al (2003)
PAO1 *ΔrpoN att Tn7:rpoN+*	Complemented ΔrpoN	*P. aeruginosa*	Heurlier et al (2003)
PAO1 ΔmvaU	P. aeruginosa PAO1 mvaU deletion mutant	*P. aeruginosa*	Esteban Thesis ,2014
PAO1 ΔmvaT	P. aeruginosa PAO1 mvaT deletion mutant	*P. aeruginosa*	Esteban Thesis ,2014
PAO1 Δsfa2	sfa2 mutant of PAO1	*P. aeruginosa*	Esteban Thesis ,2014
PAO1 Δsfa3	Sfa3 mutant of PAO1	*P. aeruginosa*	Esteban Thesis ,2014
PAO1 ΔpqsE	P. aeruginosa PAO1 *pqsE* deletion mutant	*P. aeruginosa*	Steve Higgins's Thesis, 2014
PAO1 ΔlasR	P. aeruginosa PAO1 *lasR* deletion mutant	*P. aeruginosa*	Steve Higgins's Thesis, 2014
PAO1 ΔrhlR	P. aeruginosa PAO1 *rhlR* deletion mutant	*P. aeruginosa*	Steve Higgins's Thesis, 2014
PAO1 Δrsal	P. aeruginosa PAO1 *rsal* deletion mutant	*P. aeruginosa*	Steve Higgins's Thesis, 2014
PAO1 L ΔnirQ	P. aeruginosa PAO1 L *nirQ* deletion mutant	*P. aeruginosa*	Arat et al., 2015
pDM4:ΔAaaA	PAO1ΔaaaA CM R	*P. aeruginosa*	Owen Matthew Darch Thesis, 2014

Strain Name	Description	Bacteria	Reference
PA14 WT	Wild-type	*P. aeruginosa*	Dietrich *et al* (2013)
PA14 ΔargR	argR deletion mutant in P. aeruginosa PA14	*P. aeruginosa*	Esteban Thesis, 2014
PA14 Δsfa2	*Sfa2* deletion mutant in *P. aeruginosa* PA14	*P. aeruginosa*	Jacobs et al (2003)
PA14 ΔphhR	*phhR* mutant of PA14	*P. aeruginosa*	Held et al (2012)
PA14 ΔalgB	*algB* mutant of PA14	*P. aeruginosa*	Jacobs et al (2003)
PA14 ΔPilR	*PilR* mutant of PA14	*P. aeruginosa*	Held et al (2012)
PA14 ΔdctD	*dctD* mutant of PA14	*P. aeruginosa*	Jacobs et al (2003)
PA14 ΔfleQ	*fleQ* mutant of PA14	*P. aeruginosa*	Held et al (2012)
PA14 ΔmifR	*mifR* mutant of PA14	*P. aeruginosa*	Jacobs et al (2003)
PA14 ΔntrC	*ntrC* mutant of PA14	*P. aeruginosa*	Held et al (2012)
PA14 ΔcbrB	*cbrB* mutant of PA14	*P. aeruginosa*	Jacobs et al (2003)
PA14 ΔrtcR	*rtcR* mutant of PA14	*P. aeruginosa*	Held et al (2012)
PA14 ΔacoR	*acoR* mutant of PA14	*P. aeruginosa*	Jacobs et al (2003)
PA14 ΔeatR	eatR mutant of PA14	*P. aeruginosa*	Held et al (2012)
PA14 Δ13000	13000 mutant of PA14	*P. aeruginosa*	Jacobs et al (2003)
PA14 ΔNorR	*NorR* mutant of PA14	*P. aeruginosa*	Held et al (2012)
PA14 ΔgscR	*gscR* mutant of PA14	*P. aeruginosa*	Jacobs et al (2003)
PA14 ΔSfa3	*Sfa3* mutant of PA14	*P. aeruginosa*	Held et al (2012)
PA14 ΔhbcR	*hbcR* mutant of PA14	*P. aeruginosa*	Held et al (2012)
PA14 Δ39360	39360 mutant of PA14	*P. aeruginosa*	Held et al (2012)
PA14 ΔddaR	*ddaR* mutant of PA14	*P. aeruginosa*	Held et al (2012)
PA14 ΔfleR	*fleR* mutant of PA14	*P. aeruginosa*	Held et al (2012)